

Biofilm formation and virulence of
Streptococcus pneumoniae



THE UNIVERSITY
of ADELAIDE

Zarina Amin, B.Sc. (Hons), MSc.

A thesis submitted in fulfillment of the requirements for the
degree of
Doctor of Philosophy from the University of Adelaide

March 2017

Research Centre for Infectious Diseases
Department of Molecular and Cellular Biology
Faculty of Sciences
The University of Adelaide

Declaration

This work contains no material which has been accepted for the award of any other degree or diploma in any university or other tertiary institution and, to the best of my knowledge and belief, contains no material previously published or written by another person, except where due reference has been made in the text.

I give consent to this copy of my thesis, when deposited in the University Library, being made available for loan and photocopying, subject to the provisions of the Copyright Act 1968.

I also give permission for the digital version of my thesis to be made available on the web, via the University's digital research repository, the Library catalogue, and also through web search engines, unless permission has been granted by the University to restrict access for a period of time.

Zarina Amin

24 March 2017

Table of Contents

Abstract	vi
Abbreviations	viii
List of Figures	xi
List of Tables	xiv
Acknowledgements	xix
Chapter 1: INTRODUCTION	1
1.1 Burden of pneumococcal disease.....	1
1.2 Pneumococcal colonisation and disease.....	2
1.3 Transition from asymptomatic colonisation to disease.....	5
1.4 Mechanisms of pneumococcal colonisation and disease.....	5
1.4.1 Virulence factors.....	5
1.4.1.1 Capsular Polysaccharides (CPS).....	6
1.4.1.2 Pneumolysin.....	7
1.4.1.3 Pneumococcal surface protein A (PspA).....	7
1.4.1.4 Autolysin (LytA).....	8
1.4.1.5 Pneumococcal surface protein C (PspC).....	9
1.4.1.6 Pneumococcal surface antigen A (PsaA).....	9
1.4.1.7 Pneumococcal Iron Uptake A (PiuA) and Pneumococcal Iron Acquisition A (PiuA) lipoproteins.....	9
1.4.1.8 Neuraminidases.....	9
1.4.1.9 Hyaluronate lyase (Hyl).....	10
1.4.2 Phase variation.....	11
1.4.3 Host immune responses in colonisation and disease.....	14
1.4.4 Associations with viral infections.....	15
1.5 Genomic diversity of <i>S.pneumoniae</i>	16
1.6 Pneumococcal vaccines and serotype replacement.....	17
1.7 Bacterial biofilms.....	18
1.7.1 Industrial and environmental significance of biofilms.....	19
1.7.2 Clinical significance of biofilms.....	20
1.7.3 Stages of biofilm formation.....	23
1.7.3.1 Attachment and proliferation.....	23
1.7.3.2 Growth and maturation.....	24
1.7.3.3 Detachment.....	25
1.8 <i>S. pneumoniae</i> biofilms and virulence.....	25
1.8.1 Resistance of pneumococcal biofilms to host immune responses.....	26
1.8.2 Mechanisms of pneumococcal biofilm formation in colonisation and disease.....	27
1.8.3 Social interactions in pneumococcal biofilm formation and virulence.....	29
1.8.4 The LuxS-Autoinducer 2 QS system.....	31
1.8.4.1 The role of LuxS/AI-2 in <i>S.pneumoniae</i>	32

1.8.5 Role of iron in biofilm development in <i>S. pneumonia</i>	33
1.9 Project Hypothesis and Aims.....	33
Chapter 2: MATERIALS AND METHODS.....	35
2.1 Bacterial strains.....	35
2.2 Growth media and bacterial cultures.....	40
2.3 Oligonucleotide primers.....	40
2.4 Biofilm assay.....	42
2.4.1 Quantification of bacteria.....	42
2.4.2 Microscopic examination of biofilms.....	42
2.4.3 Quantitation of biofilm density.....	43
2.5 Growth curves of clinical isolates.....	43
2.6 SDS-PAGE and western blotting.....	43
2.6.1 SDS-PAGE.....	43
2.6.2 Western blotting.....	44
2.7 Quantitation of Pneumococcal Capsular Polysaccharide.....	45
2.7.1 CPS Preparation.....	45
2.7.2 Uronic Acid Assay.....	46
2.7.3 CPS ELISA.....	46
2.8 Manipulation and analysis of DNA.....	46
2.8.1 Preparation of genomic DNA.....	46
2.8.2 PCR and agarose gel electrophoresis.....	47
2.8.3 Multi locus sequence typing of isolates.....	47
2.8.4 Overlap-extension PCR.....	48
2.8.5 Transformation of <i>S. pneumonia</i>	48
2.9 RNA Extraction and analysis.....	48
2.9.1 RNA extraction.....	48
2.9.2 Quantitative real-time RT-PCR.....	49
2.10 Animal studies.....	49
2.10.1 Mouse infection model.....	49
2.10.2 <i>In vivo</i> competition experiments.....	50
2.10.3 FACS detection of Ly-6G and F4/80 positive cells in blood and bronchoalveolar lavage.....	51
2.10.4 Examination of lung tissue with HE staining or immunofluorescence labelling.....	52
2.11 Detroit 562 adherence and invasion assays.....	52
2.12 PCR Array analysis of host innate and adaptive immune responses.....	53
2.12.1 Tissue RNA isolation using TRIzol®.....	53
2.12.2 cDNA synthesis.....	53
2.12.3 RT ² Profiler Array.....	53
2.13 RNA sequencing.....	54

Chapter 3: <i>IN VITRO</i> CHARACTERISATION OF BIOFILM FORMATION BY <i>S.PNEUMONIAE</i> CLINICAL ISOLATES.....	56
3.1 Introduction.....	56
3.2 Results.....	58
3.2.1 Viable count(CFU/well) assays for influence of clinical isolate source, pH and Fe(III) availability biofilm formation.....	58
3.2.1.1 Serotype 3.....	58
3.2.1.2 Serogroup 6.....	61
3.2.1.3 Serotype 9.....	62
3.2.1.4 Serotype 14.....	64
3.2.1.5 Serogroup 19.....	67
3.2.2 Crystal violet biofilm assay.....	70
3.2.2.1 Serotype 3.....	70
3.2.2.2 Serogroup 6.....	71
3.2.2.3 Serotype 9.....	73
3.2.2.4 Serotype 14.....	74
3.2.2.5 Serogroup 19.....	76
3.2.3 Microscopic analysis of CV-stained biofilms of blood and ear isolates.....	77
3.2.3.1 Serotype 3.....	77
3.2.3.2 Serotype 6.....	79
3.2.3.3 Serotype 9.....	80
3.2.3.4 Serotype 14.....	81
3.2.3.5 Serogroup 19.....	82
3.2.4 MLST of clinical isolates.....	83
3.2.4.1 Serotype 3.....	84
3.2.4.2 Serotype 14.....	86
3.2.4.3 Serogroup 19.....	88
3.2.5 Pooled ST-typed isolate biofilm assay (CFU) analysis.....	90
3.2.5.1 Serotype 3.....	90
3.2.5.2 Serotype 14.....	93
3.3 Discussion.....	95
Chapter 4: INFLUENCE OF ISOLATE SOURCE ON VIRULENCE PHENOTYPE OF SEROTYPE 3 <i>S. PNEUMONIAE</i> CLINICAL ISOLATES.....	100
4.1 Introduction.....	100
4.2 Results.....	101
4.2.1 Influence of LuxS on serotype 3 biofilm formation.....	101
4.2.2 Investigation of <i>p<i>iu</i>A</i> expression in relation to Fe(III), pH and isolate source.....	105
4.2.3 Investigation of transformability of serotype 3 strains.....	106

4.2.4 Capsular polysaccharide production by serotype 3 strains.....	108
4.2.5 Virulence phenotypes of serotype 3 strains.....	109
4.3 Discussion.....	113
Chapter 5: INFLUENCE OF ISOLATE SOURCE ON VIRULENCE PHENOTYPE OF SEROTYPE 14 <i>S. PNEUMONIAE</i> CLINICAL ISOLATES.....	118
5.1 Introduction.....	118
5.2 Results.....	119
5.2.1 Effect of isolate source and ST type on expression of <i>luxS</i>	119
5.2.2 Virulence phenotype of ST130 blood and ear isolates.....	120
5.2.3 Virulence phenotype of ST15 blood and ear isolates.....	123
5.2.4 <i>In vivo</i> competition analysis of ST15 blood and ear isolates.....	126
5.2.5 <i>In vitro</i> adherence and invasion of ST15/9-47 (ear isolate) and ST15/4495 (blood isolate).....	129
5.2.6 Expression of host immune response genes in infected tissues.....	130
5.2.7 Cellular and histopathological responses to lung infection.....	133
5.3 Discussion.....	137
Chapter 6: TRANSCRIPTOMIC ANALYSIS OF CLONALLY RELATED BLOOD AND EAR ISOLATES OF SEROTYPES 3 AND 14.....	144
6.1 Introduction.....	144
6.2 Results.....	145
6.2.1 Transcriptomic analysis of serotype 14 ST15 clinical isolates.....	145
6.2.1.1 Transcriptomic analysis of ST15 blood and ear isolates.....	146
6.2.1.2 Validation of RNA-Seq data by qRT-PCR.....	156
6.2.2 Transcriptomic analysis of serotype 3 ST180 and ST232 clinical isolates.....	157
6.2.2.1 RNA-Seq data validation of ST180 and ST232 isolates by qRT-PCR....	159
6.3 Discussion.....	160
Chapter 7: FINAL DISCUSSION.....	166
7.1 Introduction.....	166
7.1.1 Biofilm formation of blood and ear clinical isolates of serotypes/serogroups 3,6,9,14 and 19.....	167
7.1.2 Influence of clinical isolate source on virulence profiles of ST-matched serotype 3 and 14 isolates.....	167
7.1.3 Early lung immune response of mice to infection with blood and ear isolates.....	168
7.1.4 Transcriptomic analysis of blood and ear isolate <i>in vitro</i>	168
7.2 Concluding remarks and future directions.....	169

References	171
Appendices	197
Appendix A: Published Journal Article in Infection and Immunity (2012) from Chapter 4.....	197
Appendix B: Published Journal Article in Infection and Immunity (2015) from Chapter 5.....	206
Appendix C: Significantly differentiated genes identified by DESeq analysis.....	216
Appendix D: 67 significantly differentiated genes identified by DESeq analysis.....	217
Appendix E: 7 significantly differentiated genes identified by DESeq analysis.....	219
Conference Presentation	220

Abstract

S. pneumoniae is a genetically diverse species which complicates attempts to associate a given clonal lineage or serotype with propensity to cause disease; as well as in the identification of specific molecular determinants of distinct virulence phenotypes. Formation of biofilms is an important step in pneumococcal pathogenesis, as they serve as reservoirs of infection and organisms within biofilms are resistant to antimicrobials and host immune defences.

The aim of this work was to extend our understanding of the correlation between biofilm formation in clinical isolates of *S. pneumoniae* and factors that could influence their invasive disease potential, namely isolate source, pH and Fe(III) supplementation. Firstly, the formation of biofilms of clinical isolates belonging to serotypes/groups 3, 6, 9, 14 and 19 isolated from blood and ear revealed marked inconsistencies in biofilm formation capacity. However, upon MLST typing distinct biofilm phenotypes were identified between blood and ear isolates belonging to the same serotype/group and ST type. Further *in vivo* investigations on blood and ear isolates of serotype 3 ST180, ST232, ST233 and serotype 14 ST15 revealed distinct pathogenic profiles, which clearly demonstrated the adaptation of the strains to the host niches from which they were isolated. The *in vivo* co-infection experiment of ST15 isolates further suggested the possibilities of induction of distinct host immune responses, or secretion of a virulence factor by the blood isolate, that prolonged survival of the ear isolate, which would otherwise have been cleared from the lung when challenged in isolation. Investigation of early immune response in the lungs of mice challenged by blood and ear isolates revealed strain-specific differences in gene expression and provided insight into how the immune response may vary from strain to strain, resulting in distinct patterns of infection from two closely related strains.

The observed consistent differences suggested the existence of fundamental genomic, methylomic, transcriptomic, proteomic or metabolomic differences between clonally-related blood and ear isolates, which allows them to adapt to, and survive in, distinct host niches. Nevertheless, transcriptomic analysis of the *in vitro* grown ST180, ST232 and ST15 strains using RNA-Sequencing did not identify any genes that were

consistently differentially expressed between the blood and ear isolates of a given ST. This suggests that there may be differences in expression patterns of key virulence-related genes between bacteria growing in different *in vivo* niches, as well as between *in vivo* niches and the *in vitro* cultures.

The findings of this study constitute a significant paradigm shift, in that we have found multiple examples of clonally-related strains that consistently and reproducibly exhibit distinct virulence phenotypes in mice that directly correlate with the original site of isolation from human patients (in this case, ear vs blood). Thus, strains within a clonal lineage can exhibit stable niche adaptation. Moreover, our data suggest differential capacity to trigger early host innate immune responses may underpin this adaptation and influence the course of disease. These findings provide a robust platform for future studies aimed at identifying critical bacterial and host determinants of pneumococcal virulence phenotype.

Abbreviations

°C	degrees Celsius
µg	microgram/s
µl	microlitre/s
µM	microMolar/s
ABC	ATP-binding cassette transporter
ATP	adenosine triphosphate
bp	base pairs
C+Y	casein hydrolysate medium with yeast
CFU	colony forming units
CV	crystal violet
DNA	deoxyribonucleic acid
DOC	deoxycholate citrate
ELISA	enzyme-linked immunosorbent assay
EDTA	ethylene diamine tetraacetic acid
ery	erythromycin
g	relative centrifugal force
h	hour/s
IgG	immunoglobulin G
kb	kilobase/s
kDa	kilodalton/s
kHz	kiloHertz
kg	kilogram/s

LB	Luria Bertani broth
M	molar
mg	milligram/s
min	minute/s
ml	millilitre/s
MLST	multi locus sequence typing
mM	millimolar
MOPS	3-(N-morpholino) propanesulphonic acid
ng	nanogram/s
Ni-NTA	nickel-nitrilotriacetic acid
nm	nanometres
OD600	optical density at 600 nm
PAGE	polyacrylamide gel electrophoresis
PBS	phosphate buffered saline
PCR	polymerase chain reaction
rRNA	ribosomal RNA
RT	room temperature
s	second/s
SDS	sodium dodecyl sulphate
spec	spectinomycin
sp	species
TBE	tris-borate EDTA buffer
tet	tetracycline
THY	Todd-Hewitt broth supplemented with 0.2% yeast extract

TTBS	Tween tris buffered saline
U	units
μ l	microlitre/s
V	volt
v/v	volume per volume
w/v	weight per volume
WT	wild-type

List of Figures

Figure 1.1	<i>S. pneumoniae</i> virulence proteins.....	11
Figure 1.2	Illustration of biofilm development.....	24
Figure 1.3	Activated methyl cycle.....	31
Figure 3.1	Biofilm formation of serotype 3 blood isolates by viable count (CFU/well).....	60
Figure 3.2	Biofilm formation of serotype 3 ear isolates by viable count (CFU/well).....	60
Figure 3.3	Biofilm formation of serogroup 6 blood and ear isolates by viable count (CFU/well).....	61
Figure 3.4	Biofilm formation of serogroup 9 blood and ear isolates by viable count (CFU/well).....	63
Figure 3.5	Biofilm formation of serogroup 14 blood isolates by viable count (CFU/well).....	65
Figure 3.6	Biofilm formation of serogroup 14 ear isolates by viable count (CFU/well).....	66
Figure 3.7	Biofilm formation of serogroup 19 blood isolates by viable count (CFU/well).....	68
Figure 3.8	Biofilm formation of serogroup 19 ear isolates by by viable count (CFU/well).....	69
Figure 3.9	Biofilm formation of serotype 3 blood isolates by CV staining.....	70
Figure 3.10	Biofilm formation of serotype 3 ear isolates by CV staining.....	71
Figure 3.11	Biofilm formation of serogroup 6 blood and ear isolates by CV staining.....	72
Figure 3.12	Biofilm formation of serogroup 9 blood and ear isolates by CV staining.....	73
Figure 3.13	Biofilm formation of serotype 14 blood isolates by CV staining.....	75
Figure 3.14	Biofilm formation of serotype 14 ear isolates by CV staining.....	76
Figure 3.15	Biofilm formation of serogroup 19 blood isolates by CV staining.....	76
Figure 3.16	Biofilm formation of serogroup 19 ear isolates by CV staining.....	77
Figure 3.17	Microscopic analysis of CV-stained 24-h biofilms of serotype 3 blood and ear isolates grown at pH 7.4 and 6.8 in C+Y or C+Y+Fe(III).....	78
Figure 3.18	Microscopic analysis of CV-stained 24-h biofilms of serogroup 6 blood and ear isolates grown at pH 7.4 and 6.8 in C+Y or C+Y+Fe(III).....	79

Figure 3.19	Microscopic analysis of CV-stained 24-h biofilms of serogroup 9 blood and ear isolates grown at pH 7.4 and 6.8 in C+Y or C+Y+Fe(III).....	80
Figure 3.20	Microscopic analysis of CV-stained 24-h biofilms of serotype 14 blood and ear isolates grown at pH 7.4 and 6.8 in C+Y or C+Y+Fe(III).....	81
Figure 3.21	Microscopic analysis of CV-stained 24-h biofilms of serogroup 19 blood and ear isolates grown at pH 7.4 and 6.8 in C+Y or C+Y+Fe(III).....	82
Figure 3.22	Biofilm formation by serotype 3 ST232, ST233 and ST180 blood and ear isolates at pH 7.4.....	91
Figure 3.23	Biofilm formation by serotype 3 ST232, ST233 and ST180 blood and ear isolates at pH 6.8.....	92
Figure 3.24	Biofilm formation by serotype 14 <i>S. pneumoniae</i> ST15 and ST130 at pH 7.4.....	93
Figure 3.25	Biofilm formation by serotype 14 <i>S. pneumoniae</i> ST15 and ST130 at pH 6.8.....	94
Figure 4.1	Expression of <i>luxS</i> relative to 16S rRNA in blood and ear isolates of ST180, ST233 and ST232.....	102
Figure 4.2	Effect of <i>luxS</i> mutation on biofilm formation by ear isolates, determined by viable count.....	103
Figure 4.3	Microscopic analysis of stained biofilms.....	104
Figure 4.4	Expression of <i>piuA</i> relative to 16S rRNA in blood and ear isolates of ST180, ST233 and ST232.....	105
Figure 4.5	Transformability of the reference invasive strain D39 and serotype 3 blood and ear isolates.....	107
Figure 4.6	CPS production by ST180, ST232 and ST233 blood and ear isolates at pH 7.4.....	108
Figure 4.7	CPS production by pooled blood and ear isolates at pH 7.4.....	109
Figure 4.8 A-C	Virulence phenotypes of blood and ear isolates.....	111
Figure 4.8 D-F	Virulence phenotypes of blood and ear isolates (Continued).....	112
Figure 5.1	Effect of isolate source and ST type on <i>luxS</i> expression.....	120
Figure 5.2	Comparative virulence of ST130 blood (ST130/4524) and ear (ST130/76547) isolates.....	122
Figure 5.3	Comparative virulence of ST15 blood (ST15/4495, ST15/4534 and ST15/4559) and ST15 ear (ST15/9-47 and ST15/51742) isolates.....	125
Figure 5.4	<i>In vivo</i> competition between ST15/9-47 (ear isolate) and ST15/4495 (blood isolate).....	128

Figure 5.5	Peripheral blood leukocyte counts.....	135
Figure 5.6	Lung histopathology.....	136
Figure 5.7	Neutrophil infiltration.....	137

List of Tables

Table 1.1	Partial list of human infections involving biofilms.....	22
Table 2.1	<i>S. pneumoniae</i> strains.....	35
Table 2.2	Oligonucleotide primers and plasmids.....	43
Table 3.1	Statistical analysis of biofilm formation by serogroup 6 isolates.....	62
Table 3.2	Statistical analysis of biofilm formation by serogroup 9 isolates.....	63
Table 3.3	Statistical analysis of serotype 14 blood isolates biofilm formation.....	65
Table 3.4	Statistical analysis of serotype 14 ear isolates biofilm formation.....	66
Table 3.5	Statistical analysis of serogroup 19 blood isolates biofilm formation.....	68
Table 3.6	Statistical analysis of serogroup 19 ear isolates biofilm formation.....	69
Table 3.7	Statistical analysis of biofilm formation by serogroup 6 isolates.....	72
Table 3.8	Statistical analysis of biofilm formation by serogroup 9 isolates.....	74
Table 3.9	STs and CCs of serotype 3 strains typed by MLST.....	84
Table 3.10	STs and CCs of serotype 14 strains typed by MLST.....	86
Table 3.11	STs and CCs of serogroup 19 strains typed by MLST.....	89
Table 5.1	Adherence to and invasion of Detroit 562 cells.....	130
Table 5.2	Genes differentially expressed in infected relative to sham-infected lungs.....	131
Table 5.3	Genes differentially induced after infection with ST15/9-47 versus ST15/4495.....	133
Table 6.1	Significantly differentiated genes identified by DESeq analysis of single blood and ear isolates.....	147
Table 6.2	Common differentially expressed genes in ear isolates ST15/9-47 and ST15/51742 relative to blood isolate ST15/4495.....	148
Table 6.3	Common differentially expressed genes in ear isolates ST15/9-47 and ST15/51742 relative to blood isolate ST15/4534.....	152
Table 6.4	Common differentially expressed genes in ear isolates ST15/9-47 and ST15/51742 relative to blood isolate	

	ST15/4559.....	155
Table 6.5	Validation of RNA-Seq data for <i>nanA</i> and <i>spxB</i> by qRT-PCR.....	157
Table 6.6	Genes commonly differentially expressed in blood isolates ST232/1 and 180/15 relative to ear isolate ST232/11.....	159
Table 6.7	qRT-PCR validation of RNA-Seq data for <i>trpF</i> and <i>trpG</i>	160

Acknowledgements

Syukur alhamdulillah. Firstly I would like to express my gratefulness to Allah SWT the Gracious and Merciful for the successful completion of this thesis. Through His power of love and mercy, everything difficult has been overcome and everything wonderful has been encountered, in the forms of friends and two supervisors who must have been sent to me from the heavens. I am truly humbled and grateful for these blessings.

Professor James C Paton; my principal supervisor. From the day I set foot in Adelaide; until today you have always been looking out for me in more ways than any supervisor should; with much love care and understanding you helped guide my research from start to finish; and from rough to polished despite all your constraints. Thank you James for everything; for taking me on as your student in Adelaide. As an academic and researcher as yourself you have truly set a precedent for me. I am eternally grateful.

To Dr. Claudia Trappetti, the one in a million co-supervisor. Words cannot express how thankful I am to you cara for your commitment, time and guidance for me. I will never forget the numerous times I came into your room (with your heater on forever of course even when it was warm) crying my eyes out when I had a problem with my extraction or technique; where you will without fail, say “What happened?”, and then helped me to make it right; how we always wanted to jump out from the window of our 5th Floor lab when our stuff didn’t work!! Thank you God for giving me such a beautiful angel to take care of me here in Adelaide. When times were especially hard, you always said it was going to be all right. You always believed I would do it, no matter how tough it was. Thank you cara for being a friend and family to me. Grazie mille. You are the world’s most precious gem. I am indebted. Truly.

May God always, always bless you both with the best everything this life has to offer, for you are the best supervisors in the world.

To my family – my beloved husband Fendi; thank you for your understanding and support throughout my life here as a student and for holding the fort at home during my absence. To my brave and lovely boys: Arian and Gagi; and Kakak Suri: thank you for being the solid support for me throughout these years; and for all of your sacrifices. For my siblings – Liz, Rudy, Amon, Kay and Iqbal thank you for your never ending support and love for me. Ngah Ti, Aruah Mak, Mak and Abah and the rest of my family: thank you for your words of wisdom and support for me throughout these times and beyond.

Where would I be without friends to help me along the way? A big huge thanks to Lauren for all of your help in helping me with my transcriptomic data and thesis. May you always be blessed with the best, Lauren! Everyone in the Paton Lab namely, Mel, Layla, Richard, Dan, Charlie, Adrienne, Hui and everyone else I know at the Uni; and...Luca my dearest friend and family!! My friends in Malaysia, my housemates in Kent Town. To everyone else that I may have missed out, thank you for helping beautify my journey here.

Lastly, I dedicate this thesis to my beloved parents Papa and Mama who always believed I was capable of anything excellent and taught me that knowledge is indeed the key to everything and the best way for me to better myself. This thesis is for you.

Chapter 1: Introduction

1.1 Burden of pneumococcal disease

Streptococcus pneumoniae (the pneumococcus) is a Gram positive, aerotolerant, facultatively anaerobic bacterium belonging to the pneumoniae-mitis-pseudopneumoniae cluster of the *Streptococcus* genus, along with *S. mitis*, *S. oralis*, *S. infantis* and *S. pseudopneumoniae* (Kilian *et al.*, 2008). Diseases caused by *S. pneumoniae* include localized infections such as otitis media (OM), sinusitis and focal pneumonia, as well as invasive diseases such as bacteraemic pneumonia, septicemia and meningitis. Individuals at increased risk of pneumococcal disease include children with immature immune responses, adults with immunodeficiency disorders (particularly HIV infection) and elderly people with waning immunity and other co-morbidities such as heart and lung problems (Naucler *et al.*, 2013; O'Brien *et al.*, 2009).

Despite significant reductions in child mortality between 2000 and 2012, the status of *S. pneumoniae* as the world's leading bacterial pathogen remains unchallenged. A 2007 World Health Organization (WHO) report estimated 1.6 million deaths occur annually due to pneumococcal disease. In 2000, global estimates of pneumococcal deaths were 826,000 in children between 1-59 months of age, of which 735,000 were HIV-negative (O'Brien *et al.*, 2009). In 2008, WHO reported approximately 500,000 pneumococcus-related deaths of children in this age group. From 2010-2011, 120 million episodes of pneumococcal pneumonia were estimated to have occurred, of which 14 million cases progressed to severe disease (Walker *et al.*, 2013). Of these, 1.3 million fatalities were reported, with 1 million deaths occurring in children under 2 years old (Walker *et al.*, 2013). In a study on global burden of pneumococcal diseases by O'Brien *et al.*, of the 735,000 deaths occurring in HIV-negative children, 61% occurred in ten African and Asian countries (India 27%, China 12%, Nigeria 5%, Pakistan 5%, Bangladesh 4%, Indonesia 3%, Ethiopia 3%, Congo 3%, Kenya 2%, and the Philippines

2%). Out of the estimated 14.5 million cases of pneumococcal disease, 95.6% were due to pneumonia, 3.7% non-pneumonia, non-meningitis invasive pneumococcal syndromes, and 0.7% meningitis (O' Brien *et al.*, 2009). In Australia, indigenous Aborigines show one of the highest invasive pneumococcal disease (IPD) burdens in the world (Torzillo *et al.*, 2007).

The World Health Organization (WHO) reported that the majority of deaths due to pneumococcal disease that occur in developing countries of Africa and South East Asia, is due to the limited availability of pneumococcal conjugate vaccines. While pneumococcal diseases are mainly treated by antibiotics in these regions where vaccines are not readily available, the flagrant use of antibiotics has resulted in the emergence of antibiotic resistant strains which further complicates treatment to pneumococcal diseases; (Rutebemberwa *et al.*, 2015; Kim *et al.*, 2012). As Africa and South East Asia also present the highest HIV incidences in the world, immunodeficiency is a further significant contributing factor to fatalities in these regions. Other related factors include poor hygiene, overcrowding and inadequate housing, which facilitate transmission of pneumococci. *S. pneumoniae* is also one of the major pathogens implicated in OM, a non-invasive but significant disease associated with hearing loss, social disadvantage and high medical costs. In the US, the total costs for OM treatment exceed USD 5 billion per year (Klein, 2000). Closer to home, the prevalence and severity of OM is highest amongst Australian Indigenous children. A study by Morris *et al* reported 91% of 914 participating Indigenous children were found to have OM (Morris *et al.*, 2005). OM in Indigenous Australians can be almost universal in some communities (Leach *et al.*, 1994).

1.2 Pneumococcal colonisation and disease

A paradoxical feature of *S. pneumoniae* is that despite its ability to cause life-threatening diseases, it is also a common commensal inhabitant of the human

nasopharynx. Indeed, humans are the primary reservoir for pneumococci, which resides particularly in the upper respiratory tract of small children. In general, global pneumococcal carriage was estimated to occur in 25 to 40% of healthy children and 10 to 15% adults at any given time without any symptoms of disease (Crook *et al.*, 2004).

The peak incidence of colonisation in the nasopharynx of children occurs around the age of 2-3 years, followed by a decrease where stable prevalence can be observed after the age of 10 years (reviewed by Bogaert *et al.* (2004)). Various other potentially pathogenic bacterial species also co-reside in the human nasopharynx, such as *Moraxella catarrhalis* and *Haemophilus influenzae*, and multiple serotypes/strains of *S. pneumoniae* may colonize the nasopharynx simultaneously (Shiri *et al.*, 2013; Xu & Pichichero, 2014). Spread or transmission of pneumococci to a new host primarily occurs via contaminated respiratory secretions (droplet infection), usually among close family contacts. Crowding that frequently occurs in child day care centers, hospitals and prisons facilitates spread (Hoge *et al.*, 1994; Mandigers *et al.*, 1994; Pessoa *et al.*, 2013). There are three possible outcomes of pneumococcal carriage: elimination of the pneumococci by host immune responses soon after acquisition, asymptomatic persistence for weeks or months in the nasopharynx, or invasion of the pneumococci into deeper tissues and progression to disease. Longitudinal studies (Weiser, 2010) have shown that although nasopharyngeal colonisation by itself is insufficient for progression to invasive disease, it is a necessary first step in pneumococcal pathogenesis.

Adherence of pneumococci to the epithelial cells lining the upper respiratory tract is the first important step for colonisation. The interactions between bacteria and host occur by specific binding of ligands (e.g. adhesins) to receptors, for example some members of the choline binding protein family of surface proteins (CBPs) adhere specifically to host cell glycoconjugates (Rosenow *et al.*, 1997). Colonisation is also facilitated by non-specific physico-chemical interactions (e.g. hydrophobic or surface charge interactions) between the bacterial cell and host mucosa (Swiatlo *et al.*, 2002). Several other factors reported to be important for colonisation include phosphorylcholine

(choP) present in the pneumococcal cell wall, which has affinity for the platelet activating factor receptor (rPAF) (Cundell *et al.*, 1995), while neuraminidase (NanA), β -galactosidase (BgaA) and β *N*-acetylglucosaminidase (SrtH) may unmask adhesin receptors by cleaving terminal sugars from human cell surface glycoconjugates (Kadioglu *et al.*, 2008). The capacity of pneumococci to switch between colony opacity phenotypes (“opaque” or “transparent”) also impacts on nasopharyngeal colonisation (discussed further in 1.2.2.2) (Weiser *et al.*, 1994).

Intraspecies competition between pneumococci has also been suggested to be an important driving factor in pneumococcal colonisation. Dawid *et al.* (2007) reported that the bacteriocins encoded by *blpM* and *blpN* genes of a type 6A strain inhibited the growth of a type 4 strain *in vitro*. Furthermore, when *blpMN* mutants were constructed in a type 19 background and used to challenge mice intranasally along with a type 4 strain or its wild type parent, the mutant strain was not able to compete with the parent type 19 strain or the type 4 strain (Dawid *et al.*, 2009).

Another important factor modulating bacterial adherence to host cells is the pneumococcal capsule. Capsule expression repels sialic acid contained in the mucus allowing access to epithelial surfaces (Nelson *et al.*, 2007). This is due to the net negative charge of the capsular polysaccharides (CPS) produced by the vast majority pneumococcal serotypes. They also demonstrated the important role of capsule in enhancing colonisation *in vivo* by showing that unencapsulated mutants were less able to stably colonize the mouse nasopharynx compared to the encapsulated strains (Nelson *et al.*, 2007). Levels of pneumococcal capsular expression was also shown to be differentially regulated in the first stages of pneumococcal infections. Using a lysine-ruthenium-red fixation procedure in conjunction with electron microscopy, Hammerschmidt *et al* visually demonstrated total loss of capsular material in pneumococci when they were in close proximity with A549 cells (type II pneumocytes) and HEp-2 epithelial cells and in the process of invasion. This study also went on to show a significant loss of capsular material in invasive pneumococci recovered from the host cells compared to their wild type (WT) counterparts; the occurrence of which possibly

further promotes adherence by exposure of other virulence factors located beneath the capsule layer (Hammerschmidt *et al.*, 2005).

1.3 Transition from asymptomatic colonisation to disease

The spectrum of diseases caused by the pneumococcus reflects its ability to survive in, and adapt to, distinct ecological niches within the human host (Weiser, 2010). Translocation of pneumococci from the nasopharynx to other tissues may follow various routes, and may result in distinct pathogenic outcomes. For example, spread that occurs from the nasopharynx to the middle ear cavity via the Eustachian tubes results in OM, while aspiration into the lungs may cause pneumonia (Bogaert *et al.*, 2004). Pneumococci can also spread from the lungs via the pleural cavity into the blood, resulting in septicemia. In some instances the pneumococcus then crosses the blood brain barrier to cause meningitis; alternatively it can invade the brain directly from the nasopharynx, via olfactory neurons (van Ginkel *et al.*, 2004). The transition from asymptomatic carriage to invasive or non-invasive disease has been a focal point of research for many decades. Studies have so far indicated that the transition event is multifactorial, involving a complex interplay of genetic and environmental elements of both bacterium and host. Although still poorly understood, some molecular mechanisms behind pneumococcal disease progression have been identified. These are briefly described below.

1.4 Mechanisms of pneumococcal colonisation and disease

1.4.1 Virulence factors

Virulence factors are molecules expressed by pathogenic bacteria that facilitate their ability to cause disease. *S. pneumoniae* produces a myriad of virulence factors, and for many of these their role in disease is only partly understood. Generally, pneumococcal virulence factors facilitate evasion of host defense mechanisms to allow for persistence and invasion of host tissues. Brief descriptions of some of the more important

pneumococcal virulence factors which have been identified as potential vaccine candidates (Kadioglu *et al.*, 2008) are provided below.

1.4.1.1 Capsular Polysaccharides (CPS)

The capsule is arguably the most important virulence factor of the pneumococcus. Initially reduced during colonisation, capsule expression significantly increases during invasive disease (Hammerschmidt *et al.*, 2005). The capsule facilitates evasion of phagocytosis and complement activity (Hyams *et al.*, 2010). It prevents complement factor C3b and the Fc portion of antibodies bound to deeper cell wall structures from interacting with surface receptors on phagocytic cells, as well as inhibiting complement-mediated adaptive immunity. CPS also has negative impact on the occurrence of spontaneous autolysis in stationary phase in an autolysin dependent manner (Fernebro *et al.*, 2004). This study also highlighted the role of CPS in reducing vancomycin- and penicillin-induced lysis in encapsulated strains.

Capsular serotype is known to influence disease type and severity, and the distinct CPS structures differ in anti-phagocytic efficacy (Kadioglu *et al.*, 2008). Although > 93 serotypes have been described, a relatively small subset of types accounts for the majority of disease. Certain serotypes (e.g. types 1, 4, 5, 7F and 14) have been found to have a high invasive capacity, as they are rarely isolated from asymptomatic carriers, but are frequent causes of invasive disease. Conversely, certain other serotypes (e.g. types 3, 6A and 19F) are more commonly isolated from carriers although they are also able to cause invasive disease (Sandgren *et al.*, 2004). Various factors influence the distribution of serotypes among disease-causing pneumococci, including age and immune status of the host, type of disease and geographical region. The incidence of pneumococcal disease is greatest in the young, the elderly, the poor and those living in institutional settings (Levine *et al.*, 1999; Pastor *et al.*, 1998; Takala *et al.*, 1995). Since children are more commonly colonized with pneumococci than adults, exposure to young children appears

to increase the risk of adults acquiring pneumococcal infection. A diagram showing cellular location of pneumococcal capsule is as depicted in Figure 1.1.

1.4.1.2 Pneumolysin

One of the earliest described protein virulence factors, pneumolysin (Ply) is a 53-kDa multifunctional cytotoxin that form pores in cells leading to tissue damage and cell death. It is a member of the cholesterol-dependent cytolysin (CDC) family of bacterial toxins (Gonzalez *et al.*, 2008), but it initially binds to target cell surfaces via glycan (particularly sialyl-LewisX) receptors, followed by interaction with membrane cholesterol, enabling the toxin to oligomerize and form membrane pores leading to lysis (Shewell *et al.*, 2014). The role of pneumolysin (Ply) in pathogenesis has been examined in many studies, which report that *ply* deficient pneumococci cause significantly reduced injury in the lungs compared to their isogenic wild type strains (Rubins *et al.*, 1995), increased survival times (Berry *et al.*, 1989), reduced bacterial recovery in the nasopharynx (Kadioglu *et al.*, 2008) and lungs (Rubins *et al.*, 1995), as well as significantly delayed bacteremia and lung damage (Canvin *et al.*, 1995). More recently it was demonstrated that circulating Ply is a potent inducer of cardiac tissue damage (Alhamdi *et al.*, 2015). A strong activator of the classic complement pathway (Mitchell *et al.*, 1991; Paton *et al.*, 1984; Yuste *et al.*, 2010), Ply also acts as a double-edged sword in the activation of immune responses, where it is involved in the bacterial activation of macrophage apoptosis (Bewley *et al.*, 2014). It also stimulates the production of tumor necrosis factor and interleukins by activating phagocytes, thereby facilitating bacterial clearance (Houldsworth *et al.*, 1994). A diagram showing cellular location of pneumolysin is depicted in Figure 1.1.

1.4.1.3 Pneumococcal surface protein A (PspA)

PspA is a member of the choline binding protein (CBP) family of surface proteins, which are non-covalently attached to phosphoryl choline moieties on the cell wall

teichoic acid and membrane lipoteichoic acid via a binding domain comprising roughly ten copies of a conserved 20 amino acid repeat sequence (Gosink *et al.*, 2000). There are roughly 12 distinct CBPs encoded on the pneumococcal genome with a diverse range of functions (Frolet *et al.*, 2010). PspA was one of the first CBPs to be characterized; it is a highly immunogenic (Ren *et al.*, 2003) virulence factor that provides protection against complement activation (Tu *et al.*, 1999) by preventing the attachment of C3 to the pneumococcal cell surface, as well as protecting against apolactoferrin, which is bactericidal towards pneumococci (Shaper *et al.*, 2004). A diagram showing cellular location of PspA is depicted in Figure 1.1.

1.4.1.4 Autolysin (LytA)

LytA, another CBP family member, is an amidase that breaks down the *N*-acetylmuramoyl-L-alanine bonds in the peptidoglycan backbone of *S. pneumoniae*, resulting in autolysis. This releases highly inflammatory cell wall degradation products, as well as cell-associated virulence factors such as Ply (Berry *et al.*, 1992; Canvin *et al.*, 1995; Mosser & Tomasz, 1970). LytA also mediates penicillin-induced lysis (Tomasz & Waks, 1975), and along with other CBPs with cell wall hydrolase activity (CbpD and LytC), plays an important role in the phenomenon of fratricide, whereby genetically competent pneumococci are able to lyse non-competent pneumococci in their immediate environment (Eldholm *et al.*, 2009). A diagram showing cellular location of LytA is depicted in Figure 1.1.

1.4.1.5 Pneumococcal surface protein C (PspC)

PspC (also known as CbpA and SpsA) is another CBP whose functions include specifically binding to the complement regulatory protein factor H, contributing to protection against complement action and opsonophagocytosis (Dave *et al.*, 2004a; Dave *et al.*, 2004b). It also is able to bind to the secretory component of secretory IgA (Hammerschmidt *et al.*, 1997) and thereby mediates binding to the polymeric immunoglobulin receptor on the surface of respiratory epithelial cells, triggering

internalization of pneumococci (Zhang *et al.*, 2000). A separate domain of PspC mediates binding to the laminin receptor on endothelial cells, triggering translocation across the blood brain barrier to cause meningitis (Orihuela *et al.*, 2009). A diagram showing cellular location of virulence factor PspC is depicted in Figure 1.1.

1.4.1.6 Pneumococcal surface antigen A (PsaA)

PsaA is a lipoprotein tethered to the outer face of the pneumococcal cell membrane. Although originally thought to function as an adhesin, it is actually the solute binding protein (SBP) component of the highly conserved ABC transport system essential for uptake of Mn^{2+} by *S. pneumoniae*. Capacity to scavenge Mn^{2+} is essential for survival of the pneumococcus in host tissues, as it is a cofactor for numerous important cellular proteins, including Mn-superoxide dismutase, which mediates resistance to oxidative killing mechanisms of the host (McAllister *et al.*, 2004; Rajam *et al.*, 2008). A diagram showing cellular location of PsaA is depicted in Figure 1.1.

1.4.1.7 Pneumococcal Iron Uptake A (PiuA) and Pneumococcal Iron Acquisition A (PiaA) lipoproteins

PiuA and PiaA are the solute binding protein (SBP) components of two distinct ABC transporters deployed by the pneumococcus to scavenge iron in the host environment. The PiaA system is responsible for the transport of hydroxamate siderophores such as ferrichrome and ferrioxamine B, whereas the PiuA system is responsible for uptake of heme from hemoglobin (Whalan *et al.*, 2006). A diagram showing cellular location of PiuA and PiaA is depicted in Figure 1.1.

1.4.1.8 Neuraminidases

Pneumococci produce up to three neuraminidases (NanA, NanB and NanC) capable of cleaving the terminal sialic acid residues from host glycoconjugates (Taylor, 1996; Lock *et al.*, 1988; Camara *et al.*, 1994; Berry *et al.*, 1996). Neuraminidases promote virulence by altering the function of host glycoproteins including immune

defense proteins (King *et al.*, 2004) and unmask potential binding receptors for adherence (Andersson *et al.*, 1983; Linder *et al.*, 1994; McCullers & Bartmess, 2003). Sialic acid released by neuraminidases from host mucosal glycoconjugates can also be taken up and metabolized by pneumococci (Burnaugh *et al.*, 2008; King *et al.*, 2006). Of the three neuraminidases, NanA is the most highly expressed at the transcriptional level (Manco *et al.*, 2006) and is most highly conserved in all strains (King *et al.*, 2005; Pettigrew *et al.*, 2006). Mutational studies have shown the importance of NanA in nasopharyngeal colonisation and middle ear infection in a chinchilla model, where mutation of *nana* significantly reduced persistence of *S. pneumoniae* in the tracheal epithelia, as well as enhanced clearance from the middle ear of infected chinchillas (Tong *et al.*, 2000; Tong *et al.*, 2002). A diagram showing cellular location of neuraminidases is depicted in Figure 1.1.

1.4.1.9 Hyaluronate lyase (Hyl)

Hyaluronate lyase (Hyl) is another sortase-dependent surface protein, which may contribute to virulence by breaking down hyaluronan, a ubiquitous host extracellular matrix component, potentially enhancing access to host cell surfaces. It also enables the pneumococcus to utilize hyaluronan, which is present in the upper respiratory tract, as a carbon source (Marion *et al.*, 2012). Mutagenesis of the *hyl* gene in *S. pneumoniae* D39 did not have a significant impact on virulence on its own, but resulted in significant additional attenuation of a *ply* deletion derivative of D39 (Berry & Paton, 2000). A diagram showing cellular location of Hyl is depicted in Figure 1.1.

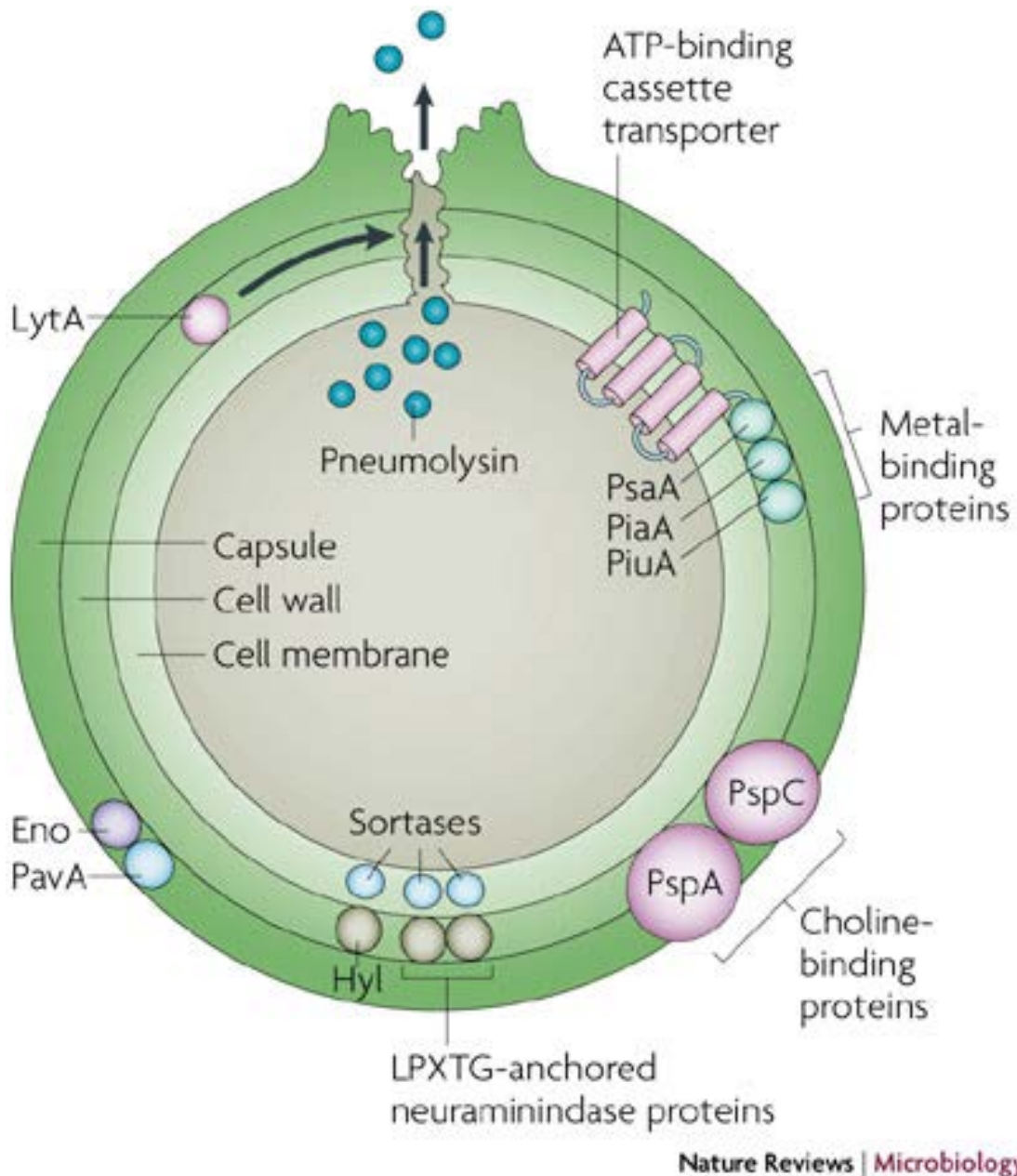


Figure 1.1: Diagram showing cellular location of selected *S. pneumoniae* virulence proteins: Taken from Kadioglu *et al.* (2008).

1.4.2 Phase variation

In 1994, Weiser and colleagues observed distinct colonial morphologies in isolates of *S. pneumoniae* based on opacity when viewed on a transparent agar surface under oblique, transmitted light, referred to as “transparent” and “opaque” (Weiser *et al.*, 1994). Isolates were able to spontaneously and reversibly switch between these

phenotypes at frequencies between 10^{-3} and 10^{-6} per generation, depending on the strain. Such a phenomenon, termed phase variation, has previously been described in other pathogenic bacteria (Swanson, 1982; Weiser *et al.*, 1990). Analyses by Weiser and others revealed marked distinctions between the opaque and transparent phenotypes. When compared with the opaque variant, electron micrographs of the transparent variant showed less well-defined surface structures, cytoplasm separation from the cell and the presence of extracellular debris, suggesting that it was more prone to autolysis. The transparent variant was also found to show reduced levels of PspA and CPS. Conversely, the opaque variants showed decreased teichoic acid (a component of the cell wall) but increased amounts of CPS and PspA (Kim & Weiser, 1998; Weiser *et al.*, 1994). By sandwich ELISA, the CPS content of the opaque phenotype was up to 5.6-fold higher than the transparent variant. Conversely, the teichoic acid content of the transparent strain was up to 3.8-fold higher than the opaque phenotype.

In vivo studies also revealed distinct differences in virulence phenotype between the two variants (Weiser *et al.*, 1994). When equal doses of transparent and opaque variants were separately introduced into the nasopharynx of infant rats, the transparent variant displayed higher levels of colonisation at all time points (days 1, 3, and 7) compared to the opaque variant. By day 7, no opaque colonies were identified from nasal washes of animals given the opaque phenotype. Transparent variants were also found to show greater adherence to buccal epithelial cells *in vitro* (Cundell *et al.*, 1995). When the two phenotypes of the type 2 strain D39 were compared in an intraperitoneal mouse challenge model (which bypassed the nasopharynx), the opaque phenotype showed significantly higher mortality rates than their transparent counterparts (Kim & Weiser, 1998). In an analysis of 304 pneumococcal clinical isolates from cases of invasive disease belonging to over 10 serotypes, Serrano *et al.* (2006) found that 52% of the isolates were of the opaque phenotype, while only 26% were transparent. The remaining 22% comprised either mixtures of different phenotypes or an intermediate phenotype. This study also confirmed the animal model predictions that isolates recovered from human

invasive infections predominantly display the opaque phenotype, but also demonstrated that the recovery frequencies of each phase variant was heterogeneous between serotypes and further suggested that distinct variant phenotypes may be preferentially expressed by some serotypes. The differential prevalence of the transparent and opaque variants in the nasopharynx versus invasive sites highlights the importance of phase variation in pneumococcal pathogenesis, as both variants reflect adaptations to distinct host niches that the pneumococcus is exposed to during the transition from carriage to disease. Increased CPS expression in the opaque variants confers higher resistance to complement-mediated opsonophagocytosis, as described in Section 1.4.1.1 above. In contrast, transparent variants with higher teichoic acid content are better able to adhere to the nasopharyngeal mucosa. Teichoic acid, a major component of the pneumococcal cell wall is decorated with phosphorylcholine (choP), which mediates bacterial attachment to the receptor for platelet activating factor on respiratory epithelial cells (Kadioglu *et al.*, 2008).

The precise molecular basis for pneumococcal phase variation remains poorly understood. Weiser *et al.* reported that differences in colony opacity were not directly attributable to either environmental conditions, expression and type of CPS, or differences in the function or expression of the major amidase *lytA* (Weiser *et al.*, 1996). Repetitive intergenic box elements A and C, which were located immediately 3' to the *glpF* termination codon, were later identified by Weiser's group to be important for a high frequency of phase switching, but not for the opacity phenotype itself (Saluja & Weiser, 1995). Recently it was demonstrated that pneumococcal opacity phenotype was influenced by a Type I restriction-modification (RM) system (SpnD39III). Spontaneous genetic rearrangements at the SpnD39III locus generate six alternative sequence target specificities resulting in distinct genome-wide DNA methylation patterns, as determined by single-molecule, real-time (SMRT) methylomics (Manso *et al.*, 2014). A series of mutants that were each locked in one of the six alternative SpnD39III arrangements exhibited marked differences in expression of several virulence-associated genes

including *luxS* and the *cps* operon (encodes CPS biosynthesis). This was associated with differences in colony opacity *in vitro*, as well as virulence in mouse models. However, such SpnD39III-locked strains do not exist in nature. Rather, the rate of SpnD39III switching *in vivo* is sufficiently high that pneumococci exist as mixed populations with heterogeneous genomic methylation patterns. In parallel with the observations relating to selection for opaque vs. transparent phase variants in one host niche vs. another, changes in SpnD39III allele frequencies were observed during the course of experimental pneumococcal infection, and between host niches (Manso *et al.*, 2014).

1.4.3 Host immune responses in colonisation and disease

Defense of a eukaryotic host against pathogen invasion is achieved via a combination of physico-chemical barriers such as skin or chemical secretions, innate immunity which involves the response of a defined population of cells in a non-specific manner, and adaptive immunity which is mediated by B- and T- lymphocytes following exposure to a specific antigen, and is characterized by immunological memory. Upon breaching physical barriers, innate immunity firstly comes into play against the pneumococcus by recognition of a variety of pneumococcal surface structures and virulence factors, via the host's pattern recognition receptors (PRRs). PRRs include the transmembrane Toll-like receptors (TLRs), the cytosolic NOD-like receptors (NLRs) and DNA sensors; these are critical for pneumococcal clearance as they initiate and control a range of host defense mechanisms. This includes inflammatory response molecules such as TNF α and IL-1 β , which mediate migration of immune cells such as macrophages and neutrophils to the site of infection and initiate the adaptive immune response (reviewed by Opitz *et al.* (2010)). The importance of these PRRs has been demonstrated in a number of studies in which mutation and genetic defects in various types of TLR resulted in increased susceptibility to bacteremia (Currie *et al.*, 2004) and reduced survival in mice even after low-dose challenge (Branger *et al.*, 2004).

The complement system is critical for immunity against pneumococcal infections, as activation of one or more of the 3 major pathways: the classical, alternative and

mannan-binding pathways mediates bacterial clearance. The classical complement pathway is activated by antibody-mediated opsonisation and is thought to be the most important means of host protection against pneumococcal infections. Brown *et al.*, used a variety of complement-deficient mice to demonstrate the importance of the classical pathway of complement activation, loss of which significantly increased disease severity (Brown *et al.*, 2002). The importance of complement mediated immunity is also reflected in the vast numbers of factors produced by *S. pneumoniae* to resist or evade complement activity, including CPS, Ply, PspA and CbpA, as discussed above, as well as the surface exoglycosidases NanA, BgaA (a beta-galactosidase gene encoding a putative 2,235-amino-acid protein) and StrH (a β -N-acetylglucosaminidase required to process the termini of host complex N-linked glycans) (Dalia *et al.*, 2010; Hyams *et al.*, 2010; Yuste *et al.*, 2005).

1.4.4 Associations with viral infections

The lethal synergy between influenza A viruses (IVA) and pneumococci was identified as early as 1918, with a significant proportion of the 50 million deaths during the Spanish influenza pandemic attributable to secondary bacterial infections, predominantly with *S. pneumoniae* (Morens *et al.*, 2008). Analyses by Shrestha *et al.* (2013) indicated a 100-fold higher risk of pneumococcal pneumonia following influenza infection. Given the morbidity and mortality associated with recent major influenza outbreaks around the world, as well as 4 pandemics over the last 120 years, much attention has been focused on understanding mechanisms of co-pathogenesis between respiratory viruses and pneumococci. These studies have revealed a complex and multifactorial synergy between both pathogen classes and host. For example, viral-induced epithelial cell damage brought about by the host immune response (i.e. inflammation) allows better access of bacteria to underlying sterile sites. Such damage also causes surface sloughing, resulting in exposure of additional host sites for adherence of pneumococci, mediated by various virulence factors such as PspA, CbpA and pneumococcal serine-rich repeat protein (PsrP). These virulence proteins can bind to the

basement membrane or elements of the extracellular matrix such as fibrin, fibrinogen and collagen (reviewed by McCullers & Tuomanen (2001)). The production of viral proteins such as the influenza virus non-structural protein 1 (NS1) was also found to hamper early host immune responses (Hale *et al.*, 2008) allowing easier access of the pneumococci to the host. Furthermore, the cleaving of host terminal sialic acid residues by the influenza virus increases sialic acid availability for bacterial metabolism, thereby facilitating pneumococcal proliferation in the host (Siegel *et al.*, 2014).

1.5 Genomic diversity of *S. pneumoniae*

S. pneumoniae is naturally competent, in that it has the ability to take up genetic material from the environment and incorporate it into its chromosome. Such horizontal gene transfer (HGT) is the backbone of its genetic diversity (Gogarten & Townsend, 2005). HGT occurs through interactions and competition between neighboring populations of bacteria from the same or other species. Active DNA uptake by the natural process of transformation is common in pneumococcal biofilms, facilitated by “fratricide” in which genetically competent *S. pneumoniae* cells are able to take up DNA by the induction of cell lysis in non-competent neighboring cells (Hall-Stoodley *et al.*, 2008). Hiller *et al.* (2010) have also reported the generation of genetic diversity by HGT in pneumococcal isolates during chronic polyclonal pediatric infection. Novel DNA acquisition due to recombination has resulted in a species-level supragenome (pan-genome) in pneumococci wherein between 46% (Hiller *et al.*, 2007) and 74% (Donati *et al.*, 2010) of genes in the genome are conserved in all strains.

Genomic diversity of *S. pneumoniae* is reflected by the 93 distinct CPS serotypes recognized to date, superimposed on >5,000 clonal lineages or sequence types (ST) distinguished on the basis of multi-locus sequence typing of seven house-keeping genes (Enright & Spratt, 1998). Additional genomic differences also occur within a given serotype and ST (Silva *et al.*, 2006). Genetic diversity facilitates host niche adaptation strategies and antibiotic resistance, and presumably determines invasive disease potential. *S. pneumoniae* isolates exhibit diverse virulence phenotypes within as well as across

capsular serotypes (McAllister *et al.*, 2011). Of the 93 known CPS serotypes, 20 types account for roughly 85% of pneumococcal disease, while some STs are more associated with invasive disease than others (Sjostrom *et al.*, 2006). Marked serotype-independent variation in complement activation, a critical factor mediating bacterial clearance, was also observed in genetically distinct *S. pneumoniae* strains (Hyams *et al.*, 2011), further supporting the contribution of genetic diversity towards differences in invasive disease potential (Hiller *et al.*, 2010; McAllister *et al.*, 2011).

1.6 Pneumococcal vaccines and serotype replacement

In order to combat the serious burden of pneumococcal disease, polyvalent vaccines have been developed based on the CPS, either alone or conjugated to protein carriers. Purified CPS vaccines were the first to be licensed for general use in about 1980. The initial formulation (Pneumovax®) was 14-valent, with coverage expanded to 23 serotypes a few years later (White, 1988). However these CPS vaccines are T-cell independent and were poorly immunogenic in young children – a principal high-risk group (Douglas *et al.*, 1983). This prompted development of more immunogenic polysaccharide-protein conjugate vaccines, which elicit strong, T-cell dependent antibody responses and immunological memory, even in infants. A 7-valent conjugate vaccine (PCV7) (Pevnar®, Wyeth), first licensed in 2000, included the seven serotypes known to be the most prevalent causes of invasive pneumococcal disease in USA at the time (serotypes 4, 6B, 9V, 14, 18C, 19F and 23F).

The widespread use of the PCV7 vaccine in young children in USA led to a significant decrease in nasopharyngeal carriage and invasive pneumococcal disease due to the 7 “vaccine types” (VT) in vaccine recipients, as well as a marked herd immunity effect in non-recipients, particularly the elderly (Miller *et al.*, 2011). However, it also introduced strong selection for the emergence of non-vaccine types (NVT) resulting in “serotype replacement” in both carriage and disease. This was unsurprising, as the phenomenon of serotype replacement was observed in one of the earliest clinical trials of

PCVs conducted in Gambia (Obaro *et al.*, 1996), and has since been observed to varying extents in virtually all regions where PCVs have been deployed (Weinberger *et al.*, 2011). Serotype replacement can result from two distinct scenarios. Firstly, NVT pneumococci already present in a vaccine recipient in low numbers, or in the vaccinated community at large at lower frequency, are able to expand in number once competition from more “successful” VT strains is eliminated by the PCV. The second, and perhaps more concerning scenario involves “capsule switching” whereby one of the more “successful” VT strains may acquire a NVT *cps* locus by genetic recombination with a NVT strain co-occupying the nasopharynx. The retention of the “successful” genetic background in such “vaccine escape mutants” may confer higher virulence, and/or transmissibility and/or drug-resistance on a previously “less successful” serotype.

Regardless of scenario, increased NVT levels in the nasopharynx increase the likelihood of progression to disease, as well as the rate of transmission of NVT pneumococci in the community. In a study of Aboriginal people in Western Australia it was found that although a significant decrease in IPD incidence in young children and the elderly was observed with PCV7, a marked increase in incidence of NVT IPD was also observed in young adults (Lehmann *et al.*, 2010). In non-invasive pneumococcal diseases such as otitis media, NVT serotype 3 otitis media involving the ST180 complex was reported to increase from 3% of total cases in 1999 to 11% in 2002 (McEllistrem *et al.*, 2005). A 13-valent vaccine (PCV13) covering all serotypes in PCV7 as well as serotypes 1, 3, 5, 6A, 7F and 19A is now replacing PCV7 in an attempt to address serotype replacement (Gaviria-Agudelo *et al.*, 2016).

1.7 Bacterial biofilms

Bacteria had long been assumed to exist principally as individual organisms, which adopt a strictly unicellular, independent lifestyle. However, bacteria exhibit an alternative mode of growth similar to eukaryotic organisms, as organised communities (biofilms) that are either single species, or more commonly, multispecies in nature (Costerton, 1999). The occurrence of heterogeneous, sessile bacterial populations, as

opposed to independent planktonic organisms, has since been recognized to be a predominant feature of bacterial growth in various natural, clinical and industrial environments (Costerton *et al.*, 1995). Biofilms, which occur in both bacteria and fungi, can be defined as highly structured and intricate microbial populations, which are densely aggregated and adhere to various biological or inert surfaces, or each other. Biofilm-forming bacteria extrude and become embedded in an extracellular matrix comprising polysaccharides, DNA and proteins, which is responsible for the cohesion and three dimensional structure of biofilms (Costerton *et al.*, 2003; Domenech *et al.*, 2013; Moscoso *et al.*, 2009).

Bacteria in biofilms engage in activities and respond as single or multispecies populations and biofilm formation is an adaptation strategy for survival in hostile environments (Hall-Stoodley *et al.*, 2004). Bacterial biofilms have been shown to be phenotypically distinct from their homogenous planktonic counterparts with regard to growth rate and gene transcription (Costerton *et al.*, 2003; Fux *et al.*, 2003). This distinction has been brought about by the exposure to different microenvironments as a consequence of living in dense populations. The modified microenvironments involve, among other parameters, nutrient limitation, higher cell density and high osmolarity conditions. Other significant features of bacterial biofilms include increased resistance to desiccation, biocides and radiation, which facilitate persistence in adverse environments (Hall-Stoodley & Stoodley, 2002).

1.7.1 Industrial and environmental significance of biofilms

Biofilms were first reported over 70 years ago, when bacteria from sea water were observed to grow tenaciously on solid surfaces (Zobell, 1943). Although biofilms may be beneficial in applications such as bioremediation of contaminated soil, wastewater treatment and microbial leaching for recovery of metals, they are still a major cause of concern across a variety of sectors, particularly in industry, medicine and the environment (Maukonen *et al.*, 2003; Sihorkar & Vyas 2001).

In the dairy industry, biofilm development on equipment leads to contamination

and spoilage of milk and other dairy products due to the resistance to cleaning agents and disinfectants (Gibson *et al.*, 1999). Metal corrosion has also been shown to occur as a result of bacterial biofilms via the catalysis of chemical and biological reactions, leading to billions of dollars' worth of damage annually for the replacement of parts in piping systems, etc. Sulphate reducing bacteria (SRB) such as *Desulfovibrio gigas* have been implicated in the corrosion of ferrous metals in various aquatic and terrestrial habitats. The key mechanisms of SRB-influenced metal corrosion involve dehydrogenase enzymes and the presence of iron sulphide bacteria.

1.7.2 Clinical significance of biofilms

The adaptability of bacteria in biofilms to harsh environments poses significant challenges in clinical and hospital settings, particularly their inherent resistance to antimicrobial agents, and as well as their capacity to evade host immune defense mechanisms. Biofilms act as infection reservoirs (Fux *et al.*, 2003) and facilitate colonisation of new niches by various dispersal mechanisms (Hall-Stoodley & Stoodley 2005; Mai-Prochnow *et al.*, 2008). According to estimates by the Centers for Disease Control and Prevention (Costerton *et al.*, 1999), approximately 65% of all human bacterial infections involve biofilm growth by pathogens, including *Pseudomonas* sp, *Haemophilus* sp, staphylococci and streptococci. Clinical diagnosis of biofilm infections is complicated by the replicative inactivity of bacteria within biofilms, which may delay or inhibit growth in diagnostic cultures. Biofilms are also the preferred bacterial phenotype adopted for chronic persistence (Ehrlich *et al.*, 2002). They facilitate the growth and spread of microorganisms by providing a stable protective environment for persistence (Post *et al.*, 2004).

The use of antibiotics is currently the mainstay of treatment for bacterial diseases, especially for the management of acute infections. Single or combinatorial antibiotic therapy has been found to be effective against many pathogenic bacteria such as *P. aeruginosa* and *S. pneumoniae*, but resistance is not uncommon. Generally the clearance of bacteria by antibiotics is achieved more efficiently when the bacteria are in planktonic

form and exponentially growing. Biofilm infections are a bane to resolve, as combinations of increased doses and prolonged courses of antibiotics are usually required to eradicate them. Several hypotheses have been postulated to explain enhanced antimicrobial resistance in biofilms. Biofilms are sessile communities and the bacteria therein exhibit stationary phase characteristics (Anderl *et al.*, 2003; Xu *et al.*, 2001) with MBC (minimal bactericidal concentration) values three to four logs higher than those of exponentially growing planktonic cells (Anderl *et al.*, 2000; Ceri *et al.*, 1999). Given the nature of biofilms as clusters of bacteria embedded in extracellular matrix, it has been hypothesized that antibiotic resistance in biofilms is directly attributable to the restricted penetration of these agents. In *P. aeruginosa* biofilms, penetration of positively charged aminoglycosides was significantly hindered by binding of these antibiotics to the negatively charged matrix polymers (Walters *et al.*, 2003). The production of extracellular slime in coagulase-negative staphylococci was also observed to reduce glycopeptide activity even in planktonic cultures (Konig *et al.*, 2001; Souli & Giamarellou 1998).

Starvation-induced stationary phase in biofilm bacteria is another contributor to resistance. Due to the high number of cells in the population, bacteria in biofilms are constantly exposed to nutrient limitation, which along with waste product accumulation, may result in dormant metabolic and reproductive activity in biofilm bacteria. Nutritional starvation has been documented in deep layers of endocarditis vegetations by means of radiolabeled amino acids (Durack & Beeson, 1972). Antimicrobial action has been found to be more effective against exponentially growing cells as opposed to those in the stationary phase. Indeed for β -lactams such as penicillin and ampicillin, cell growth is a prerequisite for effective bactericidal action (Eng *et al.*, 1991). When mechanically dispersed from biofilms and transferred to fresh medium (Williams *et al.*, 1997), bacteria will then regain nutrients initially accessible only to bacteria at surface layers and thus will also become antibiotic susceptible due to their switch from stationary to exponential growth phase. This observation shows that antibiotic resistance within biofilms is an important survival mechanism, which is not obtained through mutation.

The ability of bacterial biofilms to escape elimination by host immune defenses is increasingly being identified as another key factor behind the persistence of many chronic infections. Polymorphonuclear leucocytes (PMNs) have been identified to be the most prominent immune cells encountered by bacterial biofilms as evident in studies of infections in cystic fibrosis patients caused by *P. aeruginosa*. The interaction between neutrophils and *P. aeruginosa* biofilms explored *in vitro* via scanning electron microscopy (SEM) and confocal scanning laser microscopy (CSLM) analysis revealed unstimulated neutrophil morphology (Jesaitis *et al.*, 2003). *P. aeruginosa* biofilms were also found to down-modulate leukocyte functions, with elastase observed to inhibit human monocyte function (Kharazmi & Nielsen 1991). The activation of complement is a typical host response against many Gram positive and negative bacteria. However, complement activation analyses carried out in *P. aeruginosa* biofilms exhibited less complement activation than their planktonic counterparts (Jensen *et al.*, 1993). Some examples of bacterial biofilm-associated diseases are listed in Table 1.

Table 1.1 Partial list of human infections involving biofilms (adapted from (Costerton, JW, Stewart & Greenberg 1999))

Infection or disease	Common biofilm bacterial species
Dental caries	Acidogenic Gram-positive cocci
Periodontitis	Gram-negative anaerobic oral bacteria
Otitis media	<i>S. pneumoniae</i> , Nontypable strains of <i>H. influenzae</i> , <i>M. catarrhalis</i> , etc.
Musculoskeletal infections	Gram-positive cocci (e.g. staphylococci)
Necrotizing fasciitis	Group A streptococci
Biliary tract infections	Enteric bacteria (e.g. <i>Escherichia coli</i>)
Osteomyelitis	Mixed bacterial and fungal species
Bacterial prostatitis	<i>E. coli</i> and other Gram-negative bacteria
Native valve endocarditis	Viridans group streptococci

Cystic fibrosis pneumonia	<i>Burkholderia cepacia</i> and <i>P. aeruginosa</i>
Melioidosis	<i>Pseudomonas pseudomallei</i>
Nosocomial infections:	
ICU pneumonia	Gram negative rods
Sutures	<i>S. epidermidis</i> and <i>S.aureus</i>
Exit sites	<i>S. epidermidis</i> and <i>S.aureus</i>
Arteriovenous shunts	<i>S. epidermidis</i> and <i>S.aureus</i>
Endovascular catheter infections	Staphylococci
Intra Uterine Devices (IUDs)	<i>Actinomycetes israelii</i> and others

1.7.3 Stages of biofilm formation

The formation of biofilms can be divided into distinct stages comprising attachment, growth and maturation, and detachment, and represents a survival strategy where microorganisms can form mature, single or multiple species biofilms, and then disseminate to new surfaces (Hall-Stoodley & Stoodley 2005).

1.7.3.1 Attachment and proliferation

Biofilm formation is a dynamic process that begins with weak and reversible attachment of a small number of bacteria to either each other, or onto a surface, primarily by Van der Waals forces. When sufficient numbers of bacteria have attached, bacterial signaling or 'quorum sensing' (QS) is then initiated. This leads to a cascade of changes in gene expression, including those encoding species-specific adhesins, as well as other proteins and polysaccharides, which firmly attach the cells to the substratum and to each other as they undergo exponential binary division (Vandecasteele *et al.*, 2003). Upon cell division, spread of the daughter cells occurs outward and upward from the attachment point, forming cell clusters. Exopolysaccharides (EPS) or "slime" are produced, which embeds the aggregating cells to form microcolonies, which are typically composed of 10% to 25% cells and 75% to 90% EPS matrix, with a consistency similar to a viscous polymer hydrogel (Costerton, W *et al.*, 2003) (see Figure 1.2).

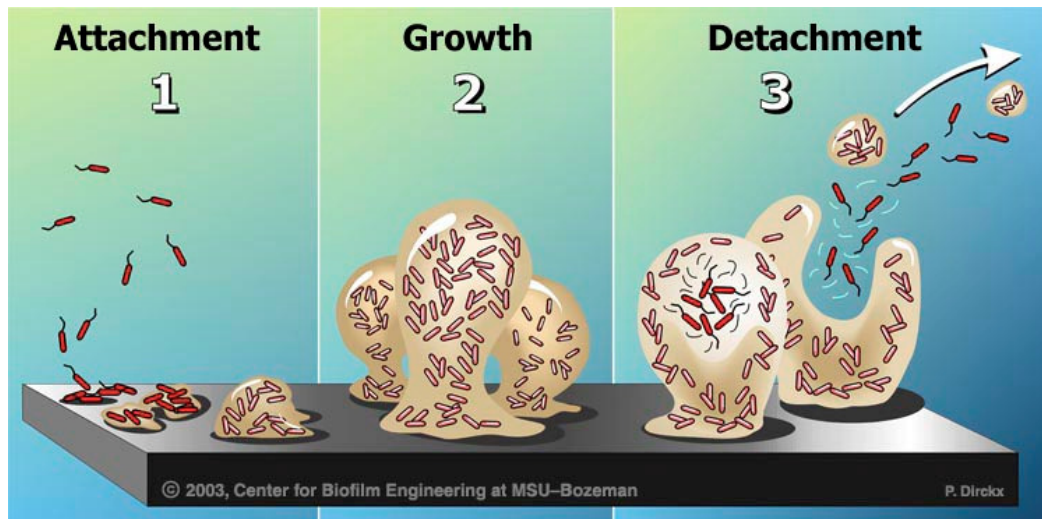


Figure 1.2. Illustration of biofilm development, including initial attachment, the growth and maturation, and detachment events, seeding dispersal either via clumps or individual planktonic bacteria (Image credit : P. Dirckx; Adapted from Hall-Stoodley *et al.*; 2004).

1.7.3.2 Growth and maturation

Biofilms continue to form according to the biochemical and hydrodynamic conditions, as well as the availability of nutrients in the immediate environment (Cappelli *et al.*, 2005). The hormone-like regulatory QS signals produced by the biofilm cells themselves influence structural organization in reaction to growth conditions. QS allows for communication among the cells, not only controlling colony formation, but also regulation of growth rate, species interactions, toxin production, invasive properties, etc. (Costerton, 1999). There is structural and metabolic heterogeneity in the cell clusters and both aerobic and anaerobic processes occur simultaneously in different parts of the multicellular community. Depending on the species and local environmental conditions, increases in cell density lead to the formation of complex 3-D structures, such as tower- and mushroom-shaped cell clusters within 1-2 weeks of growth, with aqueous channels that connect adjacent microcolonies and serve as a primitive circulatory system for delivery of nutrients and removal of wastes. Biofilm thickness varies (between 13-60 μm) depending on the balance between growth of the biofilm and detachment of cells (see Figure 1.2).

1.7.3.3 Detachment

Detachment and dissemination is a critical step for colonisation of new surfaces and to prevent density-mediated starvation within the mature biofilm, and is accomplished by shedding, detachment, or shearing. Shedding occurs when increased cell density induces cell-cell signaling to direct chemical degradation of the EPS, releasing bacteria from cell clusters and sending clumps of biofilm into the circulation (Donlan, 2002). Detached biofilm clumps contain thousands of cells and leave behind an adherent layer of bacteria on the surface for the biofilm to be regenerated (Fux *et al.*, 2004). Biofilm cells, which disseminate into the systemic circulation may result in bloodstream infection. Antimicrobial therapy and/or the host's immune system may eliminate shedded single cells, as they are more susceptible to antibiotics. However, the released clumps of biofilm can still retain resistance to antibiotics and immune clearance (see Figure 1.2).

1.8 *S. pneumoniae* biofilms and virulence

In *S. pneumoniae*, all invasive isolates and commensal strains investigated to date have been found to be capable of producing biofilms *in vitro*, using static or continuous cultures, albeit to varying extents (Allegrucci *et al.*, 2006). In a study by Reid *et al.* (2009), bacterial biofilms were detected in the middle ear of infected chinchillas. The presence of structures resembling biofilms in the lungs, trachea, and nasopharynx of mice infected with *S. pneumoniae* has also been reported (Sanchez *et al.*, 2010). Bacterial biofilms have also been demonstrated on the middle ear mucosa of children with chronic OM (Hall-Stoodley & Stoodley, 2005).

Microscopic evidence of pneumococcal biofilms in children (Hall-Stoodley *et al.*, 2006) and animal models (Reid *et al.*, 2009) suggests a complex role for biofilms in pneumococcal disease pathogenesis. Associations between biofilm phenotype in clinical isolates of different origin, or site of isolation, and a specific clinical outcome have also been reported (Garcia-Castillo *et al.*, 2007; Oggioni *et al.*, 2006; Tapiainen *et al.*, 2010). In a study by Garcia-Castillo, biofilm formation and increased antimicrobial resistance

was found to occur significantly more frequently in pneumococcal isolates from cystic fibrosis bronchial secretions than non-cystic fibrosis blood isolates (Garcia-Castillo *et al.*, 2007). Oggioni and colleagues reported that pneumococci resemble planktonic growth during bacteremia, while during tissue infection, such as pneumonia or meningitis, pneumococci are in a biofilm-like state (Oggioni *et al.*, 2006). However, Tapiainen *et al.* (2010) did not find any observable differences in biofilm formation capacity between isolate source for 204 nasopharyngeal, middle ear effusion and blood isolates.

To date many investigations have been carried out on pneumococcal biofilm formation in clinical isolates, particularly with respect to antimicrobial resistance and examination of any link between high biofilm formation, serotype and source of clinical isolate. A higher degree of antimicrobial resistance has been detected in biofilm versus planktonic cells (Hoyle & Costerton, 1991), perhaps due to close proximity of cells facilitating horizontal transfer of resistance genes. However, a study into links between high biofilm formation and isolate source or serotype has revealed marked inter-strain variations (Camilli *et al.*, 2011; Tapiainen *et al.*, 2010).

1.8.1 Resistance of pneumococcal biofilms to host immune responses

Resistance of pneumococcal biofilms to specific immune responses has only recently been investigated. By means of flow cytometry and confocal laser scanning microscopy, Domenech *et al.* (2012) demonstrated that the deposition of C3b, the key component in complement-mediated innate immunity, was impaired on *S. pneumoniae* biofilms. In addition, binding of C-reactive protein and the complement component C1q to the pneumococcal surface was reduced in biofilm bacteria, indicating that pneumococcal biofilms can resist activation of the classical complement pathway (Sanchez *et al.*, 2010). Recruitment of factor H, a down-regulator of the alternative pathway, was also enhanced in *S. pneumoniae* growing as a biofilm. These results also show that biofilm formation attenuates alternative complement pathway activation by a PspC-mediated mechanism (Sanchez *et al.*, 2010). Phagocytosis of pneumococci in biofilms was also impaired. The study cited above also confirms that biofilm formation

by *S. pneumoniae* is an efficient means of evading both the classical and the PspC-dependent alternative complement pathways of the host innate immune system. Sanchez *et al.* (2011) also reported that planktonic pneumococci elicited stronger adaptive immune responses during invasive disease compared to cells growing in biofilms, which showed weaker antibody responses against planktonic cell lysates and did not confer protection against virulent pneumococci belonging to another serotype.

1.8.2 Mechanisms of pneumococcal biofilm formation in colonisation and disease

The presence of pneumococcal biofilms has been reported in disease states (Hoa *et al.*, 2010; Reid *et al.*, 2009) and more recently in asymptomatic colonisation of the murine nasopharynx (Blanchette-Cain *et al.*, 2013; Marks *et al.*, 2012). Several proteins and sugars such as LytA, LytC (lysozyme), LytB (glucosaminidase), CbpA, PcpA (a putative adhesion) (Moscoso *et al.*, 2006), NanA (Parker *et al.*, 2009) and sialic acid (Trappetti *et al.*, 2009), as well as the cellular processes associated with iron-dependent competence and fratricide (Trappetti *et al.*, 2011c) have been implicated in biofilm formation.

A recent study which compared the gene expression profiles in early biofilms of *S. pneumoniae* with that in planktonic cells via cDNA microarray analysis (and subsequently confirmed by RT-PCR) reported that 89 genes were significantly differentially expressed in biofilm versus planktonic cells (Yadav *et al.*, 2012). Genes that were preferentially expressed in biofilms included those involved in cell wall and isoprenoid biosynthesis, cell wall biosynthesis, translation and purine and pyrimidine nucleotide metabolic pathways. For planktonic cells, the transcriptional regulator genes *ccpA*, *rr13* and *marR* were exclusively upregulated. Differences in gene expression and virulence determinant production between planktonic and biofilm bacteria reported in other studies include pneumococcal serine-rich repeat protein (PsrP), CbpA, Ply and PspA, indicating growth mode-dependent alterations in the antigenic profile of pneumococci (Moscoso *et al.*, 2006; Oggioni *et al.*, 2006; Orihuela *et al.*, 2009; Sanchez *et al.*, 2010). Microarray analysis of planktonic and sessile pneumococci by Trappetti *et*

al demonstrated the role of the two-component system CiaRH in the formation of extracellular matrix, a characteristic feature of biofilms (Trappetti *et al.*, 2011b). In a study by Blanchette-Cain *et al.* (2013), biofilm formation was investigated in nasal septa of the murine nasopharynx, which also showed that the two-component system CiaR/H responsible for competence and virulence was critical for colonisation of mice and biofilm formation.

Ply, the pneumococcal pore-forming toxin, was also revealed to play a novel role in biofilm formation (Shak *et al.*, 2013), independent of its haemolytic activity; *ply* knockout mutants in D39 and TIGR4 strains produced significantly lesser biofilm biomass than their wild-type counterparts. These findings contradicted those of Lizcano *et al.* (2010), which revealed that *ply* knockout mutants were able to form biofilms normally like the wild type. These differences in findings may be related to differences in culture conditions. Furthermore, different strains have been used between these studies; therefore resulting in differences in biofilm phenotypic observations.

The last five years have seen an increase in investigations of pneumococcal biofilms at the structural and genetic level (Domenech *et al.*, 2012), facilitated by technological advances, such as Real-Time PCR and next generation sequencing. However the role of biofilm formation in disease pathogenesis is still incompletely understood. A recent study by Pettigrew *et al.* (2014) found significant differences in transcriptomic profiles between planktonic bacteria and bacteria dispersed from biofilms.

Hyaluronic acid (HA), an important component of the extracellular matrix of host epithelial cell apical surfaces, has also been recently recognized to play a role in biofilm formation (Yadav *et al.*, 2013). This study reported hyaluronic acid derived from *Streptococcus equi* gave rise to enhanced biofilm formation in *S. pneumoniae*. Biofilm biomass was higher compared to controls when cultures were stained with crystal violet. Subsequent SEM analysis also showed biofilms grown in HA-supplemented Yeast Extract (YE) medium as adherent cells which were interconnected in thick organized structures, as opposed to non-supplemented YE medium which showed no detectable

biofilm formation. Gene expression in planktonic cells and biofilms grown in HA was also assessed and it was found that *luxS*, *nanA*, *ugl*, *hysA* and PTS-EIIA encoding genes (genes implicated in HA degradation) were significantly up-regulated at least 2-fold in biofilms. This study indicated that HA supports pneumococcal biofilm growth and up-regulated some virulence and biofilm-related genes.

Colony opacity phenotypic (phase) variation has also been reported to influence biofilm formation. In a 4 day static biofilm assay of opaque and transparent variants of a serogroup 19F clinical isolate, Trappetti *et al.* (2011b) observed the presence of extracellular matrix, a characteristic feature of biofilms, on opaque variants but not on transparent variants. This study went on to show that opaque bacteria were able to translocate from the nasopharynx to the lungs and brains of mice; as well as an observed 100-fold greater *in vitro* adherence to A549 cells than the transparent counterpart. Differential gene expression of the *ciaRH* two-component system and the choline uptake *lic* operon between the two phenotypes was confirmed via microarray analysis. It was proposed that the production of extracellular matrix by the opaque phase variants enhanced the ability of pneumococci to cause invasive disease.

1.8.3 Social interactions in pneumococcal biofilm formation and virulence

Various signalling pathways have been shown to be involved in the switch from the planktonic mode of growth to the biofilm state. The term ‘quorum sensing’ (QS) was first coined by Tomasz *et al.* (1964) to describe intercellular concentration-dependent microbial communication in microorganisms. QS is a widespread phenomenon and is a social networking channel for both Gram-positive and Gram-negative bacteria. It involves the production, secretion and detection of diffusible chemical signals when cell density reaches a threshold. The term ‘signal’ indicates the chemical compound is produced explicitly to invoke a response from other organisms (or itself) to coordinate activities between signal producers and the responder (Platt & Fuqua 2010). This mechanism enables bacteria to ‘count’ their local population and monitor external environmental

parameters such as pH, osmolarity and nutrient availability. Once a quorum is reached, bacteria are able to modify their group behavior through changes in gene expression.

The most common QS system found among Gram-negative bacteria such as *P. aeruginosa*, *E. coli* and *Vibrio* spp. employs acylated homoserine lactones as autoinducers, while in Gram-positive bacteria processed oligopeptides are used (Miller & Bassler, 2001). In Gram positive bacteria including streptococci, QS systems comprise three components: a peptide signal, and a two component regulatory system comprising a histidine kinase sensor (HK) and an intracellular response regulator (RR) (Cvitkovitch *et al.*, 2003). In *S. pneumoniae*, the QS signalling molecule is a 17-amino acid (aa) competence-stimulating peptide (CSP) processed from a 41-amino acid precursor (Havarstein *et al.*, 1995).

Biofilm formation is one of many physiological processes or phenotypes regulated through the QS mechanism, with others including luminescence, swarming motility, antibiotic and virulence factor production, pigment production, plant-microbe interactions and motility. The involvement of QS in biofilm formation by streptococci was first shown by Loo *et al.* (2000), who recovered a biofilm defective mutant of *S. gordonii* following transposon mutagenesis which had inactivated the *comD* gene encoding the HK receptor that detected the QS autoinducer peptide. Gilmore *et al.* (2003), later demonstrated that two *S. gordonii* genes, *comD* and *comE* encoding the HK and RR of the QS two-component signal transduction system were upregulated in the biofilm phase.

In *S. pneumoniae* biofilm formation involves a variety of factors, including QS peptides (Costerton *et al.*, 2003). Oggioni *et al.* (2006) revealed a relationship between biofilm formation and the *S. pneumoniae* CSP QS system that mediates genetic competence. Biofilm formation was dependent on CSP, and CSP receptor (*comD*) mutants could not form biofilms. They went on to show that CSP induced *in vitro* biofilm formation, and increased virulence in pneumonia and meningitis models in mice. They also showed that a *comD* receptor mutant that did not form biofilms showed decreased virulence in mice.

1.8.4 The LuxS – Autoinducer 2 QS system

An additional QS system used by both Gram-positive and Gram-negative bacteria has been identified, which represents a “universal language”. This involves synthesis of a signaling molecule called autoinducer-2 (AI-2) by the metabolic enzyme LuxS (S-ribosylhomocysteine lyase), as a by-product of the activated methyl cycle (see Fig. 1.3).

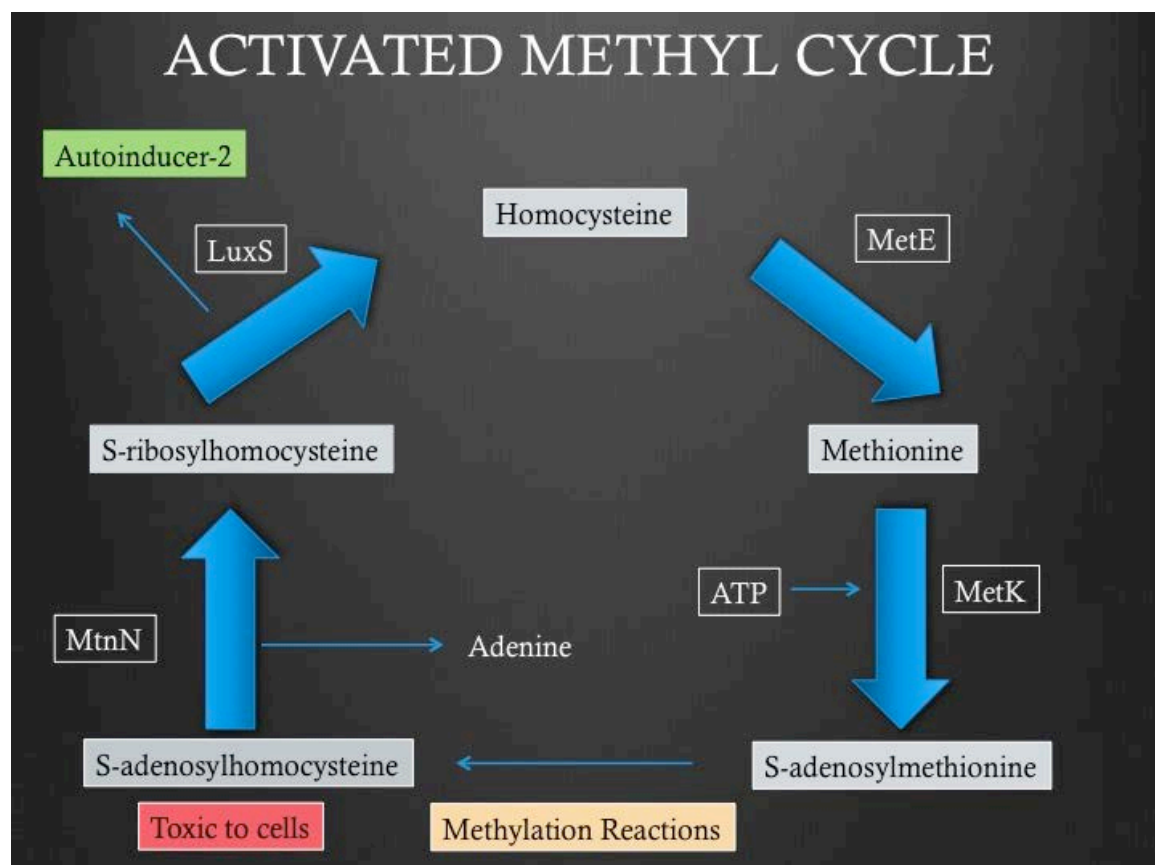


Figure 1.3 Activated methyl cycle. In the first instance, methylation reactions result in conversion of S-adenosylmethionine (SAM) to a toxic intermediate S-adenosylhomocysteine, which is then catalyzed by MtnN to form S-ribosylhomocysteine (SRH). *LuxS* then converts SRH to homocysteine and 4,5-dihydroxy 2,3-pentanedione (DPD). DPD is the precursor to AI-2, an unstable compound that spontaneously cyclises to form several furanone ring formations including AI-2. [Credit image: A. Potter]

Homologues of LuxS have been found in almost all bacterial species, suggesting a key role in interspecies communication. In *Vibrio* species, AI-2 binds to the periplasmic protein LuxP forming a complex that interacts with LuxQ, a membrane bound histidine kinase, and the signal is transduced inside the cell (Freeman & Bassler 1999; Reading &

Sperandio 2006). Other bacterial species lack LuxPQ homologues and sense AI-2 in a different manner. In *Salmonella* and *Escherichia coli* the ABC transporter encoded by the Lsr operon (LuxS regulated) is responsible for AI-2 uptake into the cell. AI-2 is then phosphorylated inside the cell and interacts with the LsrR regulator (Taga et al., 2001; Xavier & Bassler, 2005). The actual structure of AI-2 was determined by co-crystallization with its receptor LuxP (a periplasmic protein that resembles the ribose-binding protein RbsB). Using electron density analysis the AI-2 structure was identified as a furanosyl-borate diester with a molecular mass of 192.9 Da (Chen *et al.*, 2002).

The involvement of LuxS in biofilm formation has been demonstrated by mutational analysis in many Gram-negative bacteria such as *Shewanella oneidensis* (Bodor *et al.*, 2011), *Klebsiella pneumoniae* (De Araujo *et al.*, 2010) and *P. aeruginosa* (Parveen *et al.*, 2001), as well Gram positive bacteria such as *Staphylococcus epidermidis* (Lin-Xu *et al.*, 2005), *S. mutans* (Merritt *et al.*, 2005) and *S. suis* (Wang *et al.*, 2011).

1.8.4.1 The role of LuxS/AI-2 QS in *S. pneumoniae*

Initial studies of the role of the LuxS/AI-2-mediated QS in *S. pneumoniae* focused on its contribution to disease pathogenesis. Stroehler *et al.* (2003) reported that a *luxS* mutation significantly reduced virulence in a mouse sepsis model, and also resulted in multiple changes in protein expression patterns. In a separate study, LuxS was also shown to be necessary for persistent carriage and expression of virulence-associated genes such as *ply*, as well as other cellular processes (Joyce *et al.*, 2004). More recent studies have focused on the role of LuxS/AI-2 QS in biofilm development. Trappetti *et al.* (2011c) showed that a *luxS*-deficient mutant of *S. pneumoniae* D39 failed to form a biofilm. Interestingly, genetic competence and fratricide, functions known to be regulated by the CSP QS system, were also massively impacted. Thus, the two QS systems in *S. pneumoniae* interact, resulting in close linkage of several critical pathophysiological parameters, with *luxS* proposed as a central regulator (Trappetti *et al.*, 2011c). A study by Vidal *et al.* also demonstrated a role for the *luxS* system in regulating *S. pneumoniae* biofilms, where at 24 h post-inoculation, two different D39 Δ *luxS* mutants produced

~80% less biofilm biomass than the wild-type (WT) strain. When these strains were complemented with *luxS*, either on a plasmid or integrated as a single copy in the chromosome, their biofilm formation capacity was restored to that of the WT. Supplementation with a soluble factor secreted by WT D39 or purified AI-2 restored the biofilm phenotype of D39 Δ *luxS*. Thus, the LuxS/AI-2 QS system is a key regulator of biofilm formation by *S. pneumoniae* (Vidal *et al.*, 2011).

1.8.5 Role of iron in biofilm development in *S. pneumoniae*

S. pneumoniae utilizes a high-affinity iron uptake mechanism to overcome iron restriction in the host environment. ABC transporter systems Pia (pneumococcal iron acquisition) and Piu (pneumococcal iron uptake) have been shown to mediate iron uptake in *S. pneumoniae* (Brown *et al.*, 2001) and are necessary for full virulence of *S. pneumoniae*. Trappetti *et al.* (2011c) established a positive association between iron (Fe[III]) concentration in the growth medium, *luxS* expression and biofilm development in *S. pneumoniae* D39.

1.9 Project Hypothesis and Aims

From the aforementioned studies, it is clear that *S. pneumoniae* is a genetically diverse bacterium capable of causing a broad spectrum of infections, spanning asymptomatic carriage, localized infections and life-threatening invasive disease. Biofilm formation also appears to be an important component of pneumococcal disease pathogenesis. Our central hypothesis is that differences in virulence phenotype between *S. pneumoniae* strains belonging to diverse serotypes and STs will be related in some way to biofilm formation capacity. Thus, the overall aim of this research project is to identify any correlation between biofilm formation in clinical isolates of *S. pneumoniae* and factors that would influence their invasive disease potential. Specific research objectives are as follows:

Aim 1. Investigate the biofilm formation capacity of a collection of clinical isolates of *S. pneumoniae* belonging to serotypes/serogroups 3, 6, 9, 14 and 19 in relation to site of isolation (clinical isolate source) and environmental factors including medium pH and Fe(III) supplementation.

Aim 2. Examine the virulence profiles of clonally-related blood and ear isolates exhibiting distinct *in vitro* biofilm phenotypes.

Aim 3. Examine differences in host immune responses to infection with *S. pneumoniae* isolates with distinct virulence profiles.

Aim 4. Identify transcriptomic differences between closely-related *S. pneumoniae* strains that exhibit distinct biofilm and/or virulence phenotypes.

Chapter 2: Materials and Methods

2.1 Bacterial strains

The *S. pneumoniae* strains used in this study are listed in Table 2.1.

Table 2.1 *S. pneumoniae* strains

Strain	Description	Source
4482	Capsular serotype 3 blood isolate	Women's and Children's Hospital, Adelaide (WCH)
4499	Capsular serotype 3 blood isolate	WCH
4522	Capsular serotype 3 blood isolate	WCH
4529	Capsular serotype 3 blood isolate	WCH
5065	Capsular serotype 3 blood isolate	WCH
5234	Capsular serotype 3 blood isolate	WCH
5258	Capsular serotype 3 blood isolate	WCH
5267	Capsular serotype 3 blood isolate	WCH
4483	Capsular serotype 3 blood isolate	WCH
4521	Capsular serotype 3 blood isolate	WCH
5272	Capsular serotype 3 blood isolate	WCH
5060	Capsular serotype 3 blood isolate	WCH
9706840	Capsular serotype 3 ear isolate	WCH

61887	Capsular serotype 3 ear isolate	WCH
22318	Capsular serotype 3 ear isolate	WCH
54833	Capsular serotype 3 ear isolate	WCH
57934	Capsular serotype 3 ear isolate	WCH
68872	Capsular serotype 3 ear isolate	WCH
62139	Capsular serotype 3 ear isolate	WCH
75100	Capsular serotype 3 ear isolate	WCH
58497	Capsular serotype 3 ear isolate	WCH
53203	Capsular serotype 3 ear isolate	WCH
79725	Capsular serotype 3 ear isolate	WCH
5069	Capsular serotype 3 ear isolate	WCH
5268	Capsular serotype 3 ear isolate	WCH
4501	Capsular serogroup 6 blood isolate	WCH
4519	Capsular serogroup 6 blood isolate	WCH
4526	Capsular serogroup 6 blood isolate	WCH
4550	Capsular serogroup 6 blood isolate	WCH
53034	Capsular serogroup 6 ear isolate	WCH

61888	Capsular serogroup 6 ear isolate	WCH
87765	Capsular serogroup 6 ear isolate	WCH
50397	Capsular serogroup 6 ear isolate	WCH
4531	Capsular serogroup 9 blood isolate	WCH
4539	Capsular serogroup 9 blood isolate	WCH
5055	Capsular serogroup 9 blood isolate	WCH
62195	Capsular serogroup 9 ear isolate	WCH
66919	Capsular serogroup 9 ear isolate	WCH
9723173	Capsular serogroup 9 ear isolate	WCH
40502	Capsular serogroup 9 ear isolate	WCH
4484	Capsular serotype 14 blood isolate	WCH
4495	Capsular serotype 14 blood isolate	WCH
4524	Capsular serotype 14 blood isolate	WCH
4534	Capsular serotype 14 blood isolate	WCH
4511	Capsular serotype 14 blood isolate	WCH
4538	Capsular serotype 14 blood isolate	WCH
4545	Capsular serotype 14 blood isolate	WCH

4549	Capsular serotype 14 blood isolate	WCH
4559	Capsular serotype 14 blood isolate	WCH
51742	Capsular serotype 14 ear isolate	WCH
53705	Capsular serotype 14 ear isolate	WCH
67456	Capsular serotype 14 ear isolate	WCH
73363	Capsular serotype 14 ear isolate	WCH
9725201	Capsular serotype 14 ear isolate	WCH
50582	Capsular serotype 14 ear isolate	WCH
76547	Capsular serotype 14 ear isolate	WCH
9-47	Capsular serotype 14 ear isolate	WCH
9-5133	Capsular serotype 14 ear isolate	WCH
5210	Capsular serogroup 19 blood isolate	WCH
5219	Capsular serogroup 19 blood isolate	WCH
5239	Capsular serogroup 19 blood isolate	WCH
5221	Capsular serogroup 19 blood isolate	WCH
4507	Capsular serogroup 19 blood isolate	WCH
5027	Capsular serogroup 19 blood isolate	WCH

5058	Capsular serogroup 19 blood isolate	WCH
5074	Capsular serogroup 19 blood isolate	WCH
5030	Capsular serogroup 19 blood isolate	WCH
5054	Capsular serogroup 19 blood isolate	WCH
24190	Capsular serogroup 19 ear isolate	WCH
51862	Capsular serogroup 19 ear isolate	WCH
53685	Capsular serogroup 19 ear isolate	WCH
48498	Capsular serogroup 19 ear isolate	WCH
61884	Capsular serogroup 19 ear isolate	WCH
63748	Capsular serogroup 19 ear isolate	WCH
64051	Capsular serogroup 19 ear isolate	WCH
74434	Capsular serogroup 19 ear isolate	WCH
74951	Capsular serogroup 19 ear isolate	WCH
79213	Capsular serogroup 19 ear isolate	WCH

2.2 Growth Media and Bacterial Cultures

S. pneumoniae strains were routinely grown in a semisynthetic casein hydrolysate medium with 0.5% yeast extract (C+Y) according to the recipe of Lacks and Hotchkiss (1960), Todd–Hewitt broth (Oxoid, Hampshire, UK) with 1% Bacto yeast extract (Becton, Dickinson and Company (BD), New Jersey, USA) (THY), on blood agar (BA) (39 g/l Columbia base agar [Oxoid], 5% (v/v) defibrinated horse blood), or for challenge of mice, in serum broth (SB) (10% [v/v] heat-inactivated horse serum [Gibco®, Auckland, New Zealand], 10 g/l peptone [Oxoid], 10 g/l Lab Lemco powder [Oxoid] and 5 g/l NaCl).

BA was routinely supplemented with gentamicin (5 µg/ml) to inhibit background bacteria from *in vivo* samples, or with erythromycin (0.2 µg/ml), for the selection of suitable transformants for competitive index experiments in ST15/4495 blood and ST15/9-47 ear isolates.

For examination of colony opacity phenotype (opaque vs transparent), strains were grown on THY agar (THY with 1.5 % (w/v) agar [Merck, Darmstadt, Germany]) supplemented with 200 U/ml catalase (Sigma, NSW, Australia). After incubation at 37°C with 5% CO₂ overnight, the colony phenotype was viewed under oblique transmitted light, as described by Weiser *et al.* (1994). For storage of pneumococci, opaque colonies selected from THY/catalase plates were grown in C+Y medium to a final A₆₀₀ of 0.4, 20% (v/v) glycerol was then added and the culture was stored at –80°C until use. Opaque colonies were used in all experiments.

2.3 Oligonucleotide primers

The oligonucleotide primers and plasmids used in this study are listed in Table 2.2.

Table 2.2: Oligonucleotide primers and plasmids

Target gene and primer/plasmid name	Sequence (5'-3')	Purpose (reference)
recP (transketolase) <i>recP</i> F (forward)	GCCAACTCAGGTCATCCAGG	MLST typing (Enright & Spratt, 1998)
<i>recP</i> R (reverse)	TGCAACCGTAGCATTGTAAC	MLST typing (Enright & Spratt, 1998)
aroE (shikimate dehydrogenase) <i>aroE</i> F	GCCTTTGAGGCGACAGC	MLST typing (Enright & Spratt, 1998)
<i>aroE</i> R	TGCAGTTCA(G/A)AAACAT(A/T)TTCTAA	MLST typing (Enright & Spratt, 1998)
ddl (D-alanine ligase) <i>ddl</i> F	TGC(C/T)CAAGTTCCTTATGTGG	MLST typing (Enright & Spratt, 1998)
<i>ddl</i> R	CACTGGGT(G/A)AAACC(A/T)GGCAT	MLST typing (Enright & Spratt, 1998)
gdh (glucose-6-phosphate dehydrogenase) <i>gdh</i> F	ATGGACAAACCAGC(G/A/T/C)AG(C/T)TT	MLST typing (Enright & Spratt, 1998)
<i>gdh</i> R	GCTTGAGGTCCCAT(G/A)CT(G/A/T/C)CC	MLST typing (Enright & Spratt, 1998)
gki (glucokinase) <i>gki</i> F	GGCATTGGAATGGGATCACC	MLST typing (Enright & Spratt, 1998)
<i>gki</i> R	TCTCCCGCAGCTGACAC	MLST typing (Enright & Spratt, 1998)
spi (signal peptidase I) <i>spi</i> F	TTATTCTCCTGATTCTGTC	MLST typing (Enright & Spratt, 1998)
<i>spi</i> R	GTGATTGGCCAGAAGCGGAA	MLST typing (Enright & Spratt, 1998)
xpt (xanthine phospho-ribosyltransferase) <i>xpt</i> F	TTATTAGAAGAGCGCATCCT	MLST typing (Enright & Spratt, 1998)
<i>xpt</i> R	AGATCTGCCTCCTTAAATAC	MLST typing (Enright & Spratt, 1998)
<i>16S</i> rRNA F	CATGCAAGTAGAACGCTGAA	Q-PCR for <i>16S</i> rRNA
<i>16S</i> rRNA R	TGTCATGCAACATCCACTCT	Q-PCR for <i>16S</i> rRNA
<i>luxS</i> F	CCCTATGTTGCTTATTGGGG	Q-PCR for <i>luxS</i>
<i>luxS</i> R	AGTCAATCATGCCGTCAATGCG	Q-PCR for <i>luxS</i>
<i>trpF</i> F	GGCTGTGCAGGTAGATGGAA	Q-PCR for <i>trpF</i>
<i>trpF</i> R	TTCATTAAGGCCACCTGCGA	Q-PCR for <i>trpF</i>
<i>trpG</i> F	GCGGTCATGCGTTATCACAG	Q-PCR for <i>trpG</i>
<i>trpG</i> R	TCTGGCGTTCCAATGCTCTC	Q-PCR for <i>trpG</i>
<i>nanA</i> F	CGGAGAGCGCCTCAAGATATTACTC	Q-PCR for <i>nanA</i>
<i>nanA</i> R	GCCCATTCCGAAGTACAATTCC	Q-PCR for <i>nanA</i>
<i>spxB</i> F	CAACATGTGCTACCCAGACG	Q-PCR for <i>spxB</i>
<i>spxB</i> R	CGAGCATCGATGACAACAGT	Q-PCR for <i>spxB</i>
pAL2 plasmid	pAL2 plasmid containing erythromycin resistance gene	(Biswas <i>et al.</i> , 2008)

2.4. Biofilm assay

Frozen stocks of opaque isolates were firstly grown on BA overnight at 37°C in 5% CO₂ and pre-cultured in 1.0 ml C+Y medium at pH 7.4 or pH 6.8 to a final A₆₀₀ of 0.3. The cultures were then diluted 1/100 in fresh C+Y medium and two-fold dilutions of the suspensions were transferred into consecutive wells of a flat-bottomed 96 well microtitre plate (Costar, Corning Corporation), with or without 100 µM Fe(III). Assays were carried out in triplicate and repeated for three biological replicates.

2.4.1 Quantification of bacteria

For the quantification of attached bacteria, the incubated microtitre plates were washed in Luria Bertani (LB) medium three times. A volume of 100 µl of fresh LB medium was then added to the wells. The plates were then sealed with parafilm and sonicated at 35 kHz for 3 sec in a Transonic 460/H sonicating water bath. The dispersed biofilm-derived bacterial suspension was then serially diluted two-fold before being plated on to BA plates and incubated at 37°C in 5% CO₂ overnight. Total CFU counts emanating from the biofilm for each well were then calculated.

2.4.2 Microscopic examination of biofilms

For microscopic examination of biofilms, wells of microtitre plates were washed three times in LB medium to remove planktonic bacteria. The wells were dried at 37°C for 30 min and stained with 0.5 % crystal violet (w/v) for 30 min at 37°C. Crystal violet was then removed from each well and the plate was left at room temperature for 10 min. The wells were then washed three times in phosphate-buffered saline (PBS) pH 7.4 and observed under transmitted light using an AMG Evos inverted microscope with a 40 × objective.

2.4.3 Quantitation of biofilm density

For quantitation of biofilm density, 50 μ l absolute ethanol was dispensed into the wells of the crystal violet-stained microtitre plates and Absorbance at 570nm was measured using a Spectramax M2 Microplate Reader (Molecular Devices). All assays were performed in duplicate and repeated for three biological replicates.

2.5 Growth curves of clinical isolates

Strains were grown overnight on BA at 37°C in 5% CO₂ and then grown in C+Y medium (pH 7.4) from an initial inoculum of $A_{600} = 0.05$ to a final $A_{600} = 0.2$. Cultures were then diluted 1/100 in C+Y and 180 μ l of bacterial suspension was then added to each well of a 96 well flat bottom microtitre plate (Costar, Corning Corporation) with a minimum of three replicates per sample. A breathable film cover was then placed over the plate. A_{600} was measured every 30 min for 18h, at 37°C in a Spectramax M2 Microplate Reader (Molecular Devices, California, USA). Data obtained were analysed using Softmax Pro® software v 4.6 (Molecular Devices).

2.6 SDS-PAGE and Western blotting

2.6.1 SDS-PAGE

Selected clinical isolates were grown to $A_{600} = 0.15$ and 0.3 at 37°C in C+Y (pH 7.4 or pH 6.8), with or without additional 100 μ M Fe(III). 1 ml of the culture was then placed in a centrifuge tube and spun for 5 min at 8,000 \times g. The pellet was then resuspended in 50 μ l PBS and lysed in 0.1% (w/v) sodium deoxycholate (DOC) at 37°C for 30 min. The protein concentrations of the lysates were then measured using the Pierce™ BCA Protein Assay Kit according to the manufacturer's instructions. Samples containing approximately 30 μ g of protein solubilised in LUG buffer (5% [v/v] β -

mercaptoethanol, 62.5 mM Tris-HCl, 2% [w/v] sodium dodecyl sulphate [SDS], 10% [v/v] glycerol and 0.05% [w/v] bromophenol blue, pH 6.8), together with a Benchmark™ prestained protein ladder (Thermo Fisher Scientific), were separated by SDS-polyacrylamide gel electrophoresis (SDS-PAGE) at 200V for 20 min using a 12% NuPage Bis-Tris mini gel (Invitrogen).

2.6.2 Western Blotting

Upon completion of electrophoresis, separated proteins were electrophoretically transferred onto a nitrocellulose membrane using an iBlot Dry Blotting System (Invitrogen) according to the manufacturer's instructions. The membrane was blocked by incubation in Tris-buffered saline containing 0.02% Tween 20 (TTBS) and 1% skim milk powder, at room temperature (RT) for 30 min and washed twice for 5 min in TTBS. The proteins were then labeled with the appropriate primary polyclonal mouse antiserum overnight at 4°C at a dilution of 1:1000 in TTBS supplemented with 0.05% (w/v) skim milk powder. The membrane was then washed three times for 5 min in TTBS and incubated with secondary antibody (IRDye800-labeled anti-mouse IgG [LI-COR Biosciences, Nebraska, USA]) diluted 1:50,000 in TTBS for 60 min at RT in the dark. Finally the membrane was washed three times for 5 min in TTBS and once in PBS for 5 min. Blots were dried at 37°C and scanned using an Odyssey Infrared Imaging System (LI-COR Biosciences). Relative quantification of protein expression between the strains was determined by the Odyssey Infrared Imaging System application software v 3.0.21 by comparing units of fluorescence (LI-COR Biosciences).

2.7 Quantitation of Pneumococcal Capsular Polysaccharide

2.7.1 Capsular Polysaccharide (CPS) Preparation

Pneumococci were grown overnight on BA at 37°C in 5% CO₂ and then harvested and suspended in 20 ml PBS to $A_{600} = 0.5$. A 10 ml aliquot was pelleted via centrifugation at $3,000 \times g$ for 30 min. Pellets were resuspended in Eppendorf tubes containing 500 μ l 150 mM Tris-HCl (pH 7.0), 1 mM MgSO₄. Five μ l 10% (w/v) DOC was then added and the tubes were incubated for 30 min at 37°C. 100 U of mutanolysin, 50 U DNase I and 50 μ g RNase A were added to each tube and incubated at 37°C overnight. After incubation, 100 μ g Proteinase K was added to each tube and tubes were then incubated at 56°C for 4 h. The CPS preparation was then spun briefly in a microfuge to pellet debris and stored at -20°C until use.

2.7.2 Uronic Acid Assay

CPS serotypes containing glucuronic acid in the repeat units were quantitated by uronic acid assay, as described by Morona *et al.* (2006). CPS samples were diluted two-fold, in duplicate, to a final volume of 100 μ l in ultrapure H₂O in Eppendorf tubes, including blanks comprising 100 μ l ultrapure H₂O. The samples were then cooled on ice. 600 μ l H₂SO₄ / 0.0125 M Na₂B₄O₄ was added, vortexed and heated at 100°C for 5 min before being cooled on ice. 10 μ l of 3-phenylphenol solution (0.15% (w/v) 3-phenylphenol in 0.5% (w/v) NaOH) was added to one sample tube, while 10 μ l 0.5% NaOH was added to the respective duplicate control tube. The tubes were mixed and 200 μ l of each sample and control were then transferred into wells of a 96-well flat-bottomed microtitre plate (Costar, Corning) and A_{520} was read within 5 min in a SpectraMax M2 Microplate Reader. The difference in the amount of uronic acid was determined by subtracting the NaOH-only control A_{520} from that for the respective test sample.

2.7.3 CPS ELISA

For *S. pneumoniae* serotype 14 (and other serotypes that do not contain uronic acid in the CPS repeat unit), CPS was quantitated by ELISA using a modification of the method described by Trappetti *et al.* (2011). Serial two-fold dilutions in sterile normal saline of either purified CPS standard (American Type Culture Collection, USA) (starting concentration 10 µg/ml) or CPS preparations (Section 2.12.1) were used to coat poly-L-lysine-treated Nunc MaxiSorp® flat-bottom 96-well plates overnight at 4°C. After blocking with 1% foetal calf serum (FCS) for 1 h at room temperature, the samples were reacted with a 1:10,000 dilution of serotype 14 pneumococcal typing serum (Statens Seruminstitut, Copenhagen, Denmark) for 4 h. The plates were washed five times (0.05% Tween in PBS) and then reacted with a 1:20,000 dilution of goat anti-rabbit IgG alkaline phosphatase conjugate (Sigma-Aldrich) overnight at 4°C. The plates were then developed using alkaline phosphatase substrate (p-nitrophenyl phosphate solution (PNPP) (Sigma)) (1mg/ml) in diethanolamine buffer (1.0 M diethanolamine with 0.5 mM MgCl₂), and the absorbance at 405 nm was read in a Spectramax M2 spectrometer (Molecular Devices, California, USA).

2.8 Manipulation and analysis of DNA

2.8.1 Preparation of genomic DNA

To obtain genomic DNA for use in PCR for MLST typing and other investigations, strains were grown overnight on BA at 37°C in 5% CO₂ and then harvested and suspended in an Eppendorf tube containing 1 ml sterile PBS to an A₆₀₀ of 0.2. The suspension was then microfuged for 5 min at 8,000 × g and the supernatant was removed. The bacterial pellet was then resuspended in 300 µl 0.1% DOC in PBS and incubated at 37°C for 30 min. The suspension was then microfuged for 3 min and the

supernatant was then transferred to a new Eppendorf 1.5 ml tube. Purification of DNA was then carried out using the QIAGEN DNeasy Blood and Tissue Kit according to the manufacturer's instructions. DNA was then quantitated by A_{260}/A_{280} using a Nanodrop spectrophotometer (Thermo Scientific).

2.8.2 PCR, agarose gel electrophoresis and DNA sequencing

PCR was performed using Phusion Flash High Fidelity PCR Master Mix (Thermo Fisher) according to the manufacturers' instructions. For overlap PCR in which one large product was to be amplified from multiple smaller fragments, equimolar amounts of each fragment were used as template, with approximately 100 ng of template DNA used in total.

Agarose gel electrophoresis was performed using gels composed of 0.8 - 1.5% (w/v) agarose dissolved in TBE (44.5 mM Tris, 44.5 mM boric acid, 1.25 mM EDTA, pH 8.4). These were immersed in TBE and electrophoresed at 180 V. DNA samples were mixed with 1/10th volume of loading buffer (15% [w/v] Ficoll, 0.1% [w/v] bromophenol blue, 100 ng/ml RNase A) prior to loading. Staining was performed using GelRed™ (Biotium, California, USA) according to the manufacturer's instructions and DNA was visualised by trans illumination with short wavelength ultraviolet light using the Gel Doc XR system (Bio-Rad, NSW, Australia).

For sequencing, DNA was purified from PCR reactions using a QIAquick PCR purification kit (Qiagen) according to the manufacturer's instructions. Purified DNA was submitted to the Australian Genome Research Facility for sequencing.

2.8.3 Multi Locus Sequence Typing of clinical isolates

MLST typing involved PCR amplification and sequence analyses of portions of the conserved but polymorphic housekeeping genes *aroE*, *gdh*, *gki*, *recP*, *spi*, *xpt* and *ddl*, using primers listed in Table 2.2. Sequencing of PCR products was carried out as

described in Sections 2.7.1 and 2.7.2 above. Sequence data for the 7 genes were then compared against the MLST database (<http://www.pubmlst.org>) and sequence type (ST) was assigned on the basis of allelic profile.

2.8.4 Overlap-extension PCR

Site-directed mutagenesis of target genes was carried out using overlap-extension polymerase chain reaction (OE-PCR) (Ho *et al.*, 1989) to amplify the products required for *S. pneumoniae* transformation. Primers used to amplify the respective fragments are specified in Table 2.2.

2.8.5 Transformation of *S. pneumoniae*

S. pneumoniae strains were grown overnight on BA at 37°C in 5% CO₂, and then inoculated into 1 ml C+Y medium at an initial A₆₀₀ = 0.05 and then incubated at 37°C to a final A₆₀₀ = 0.2. The cultures were then diluted 1/10 in fresh C+Y medium in a total volume of 1.0 ml. Competence was induced by addition of 50 ng of competence stimulating peptides CSP1 or CSP2 and incubation at 37°C for 15 min, followed by addition of 1 µg donor DNA and incubation for 2-3 h at 37°C. The culture was then microfuged for 1 min, 950 µl of the supernatant was removed, and then the pellet was resuspended and plated on BA supplemented with 0.2 µg/ml erythromycin and incubated overnight at 37°C in 5% CO₂.

2.9 RNA extraction and analysis

2.9.1 RNA Extraction

Strains were grown in 5 ml C+Y medium at pH 7.4 or 6.8, with or without 100 µM Fe(III), or in serum broth, until A₆₀₀ = 0.2. Using RNase-free Eppendorf tubes, 2 volumes of RNAProtect reagent (Qiagen) was added to 1 volume of bacterial culture,

mixed and left to stand for 5 min at room temperature. The culture was then microfuged at $8,000 \times g$ for 5 min and the supernatant was discarded. RNA was then extracted from the bacterial pellet using the Qiagen RNeasy Mini Kit, according to the manufacturer's instructions (Qiagen RNAprotect Bacteria Reagent Handbook).

2.9.2 Quantitative real-time RT-PCR

Real-time RT-PCR was performed using the Invitrogen Superscript III Platinum SYBR green one-step qRT-PCR kit (Invitrogen). A primer pair specific for 16S rRNA was used as an internal control and diluted 1/200 in RNase-free water (Table 2.2). A standard 20 μ l reaction mix was prepared for all the samples (10 μ l 2 \times Phusion Flash PCR Mix [Phusion Flash II DNA Polymerase, 2X reaction buffer, dNTPs, and MgCl₂] [Thermo-Fisher Scientific], 7 μ l ultrapure MilliQ water, 1 μ l forward primer, 1 μ l reverse primer [Table 2.2]); followed by 1 μ l of template or 16S rRNA diluted internal control. Amplification was performed using a Light Cycler 480 instrument (Roche) with the following program conditions: reverse transcription cycle at 50°C for 15 min, followed by 35 amplification cycles comprising denaturation at 95°C for 15 sec, annealing at 60°C for 30 sec and extension at 72°C for 30 sec. The relative gene expression was calculated by the comparative critical threshold ($2^{-\Delta\Delta CT}$) method (Livak & Schmittgen, 2001), whereby the amount of target mRNA in one sample was compared with the amount of the same target mRNA in another sample, which was normalised to the 16S rRNA internal control concentration. Alternatively, the amount of target mRNA relative to the amount of the 16S rRNA was also determined in some instances.

2.10 Animal studies

2.10.1 Mouse infection model

Animal experimentation was approved by the University of Adelaide Animal Ethics Committee. Groups of 5 week old outbred Swiss (CD-1) mice were first anaesthetized by intraperitoneal injection with sodium pentobarbitol (Nembutal [Rhone-Merieux]) at a dose of 66 $\mu\text{g/g}$ body weight. Mice were then challenged intranasally with a 40 μl volume containing 1×10^8 CFU of the respective clinical isolate grown to early exponential phase ($A_{600} = 0.2$) in SB. The mice were monitored frequently for signs of disease (e.g. lethargy, ruffled coat, etc.). At specified time points, the mice were euthanized by CO_2 asphyxiation. Blood was collected from the superior vena cava and after perfusion via the left ventricle with sterile saline, lung, brain, nasopharynx and ear tissues were harvested into tubes containing 2.8 mm diameter ceramic beads and 1 ml PBS and homogenized with a Precellys® 24 tissue homogeniser (Bertin Technologies). The samples were then serially diluted in serum broth and plated onto BA supplemented with gentamicin (to inhibit background bacteria). Plates were then incubated at 37°C in 5% CO_2 overnight and bacterial counts were determined.

2.10.2 *In vivo* competition experiments.

Two groups of mice were challenged with equal numbers of ST15/4495 blood isolate and ST15/9-47 ear isolate. In order to distinguish the strains, erythromycin-resistant derivatives of each strain (ST15/4495:pAL2 and ST15/9-47:pAL2) were constructed by transformation with the plasmid pAL2, as described in Section 2.8. Two competition experiments were performed with 5 mice per group for each time point of 24 h and 72 h. In one experiment, mice were challenged intranasally with a mixed inoculum comprising equal numbers of ST15/4495 and ST15/9-47:pAL2 (approximately 5×10^7 CFU of each strain), in a modified protocol previously described by Harvey *et al.* (2011).

In another experiment, mice were challenged with equal numbers of ST15/4495:pAL2 and ST15/9-47 (approximately 5×10^7 CFU of each strain). Tissue samples were plated on BA or BA + erythromycin to determine the numbers of sensitive and resistant organisms. The competitive index (CI) within nasopharyngeal, ear, lung and brain samples was determined at 24 h and 72 h post-challenge by calculating the ratio of sensitive to resistant organisms, relative to the input ratio (the ratio of sensitive to resistant organisms in the original inoculum). As the CI values were log transformed, a value close to 0 is expected if strains compete equally. For the purposes of CI calculation, when a given strain was not detected in a particular niche, it was assigned a CFU value equivalent to 50% of the detection threshold.

2.10.3 FACS detection of Ly-6G and F4/80 positive cells in blood and bronchoalveolar lavage

Blood was collected from infected and uninfected mice by cardiac puncture into heparin tubes. Blood leukocytes were isolated by lysing the red blood cells with a hypotonic shock. Bronchoalveolar lavage (BAL) was performed using 1 ml of ice cold PBS. The blood leukocytes or BAL cells were washed in ice cold PBS and fixed in 1% paraformaldehyde in PBS overnight at 4°C. Before immunofluorescence labelling, the leukocytes were washed with PBS and permeabilised with 0.1 ml of 0.1% Triton X100 in PBS for 30 sec. The cells were then washed again with PBS and were then incubated with monoclonal rat anti-mouse Ly-6G (BD Biosciences) or monoclonal rat anti-mouse F4/80 (Santa Cruz Biotechnology) at room temperature for 1 h. Ly-6G (neutrophil marker) or F4/80 (monocyte/macrophage marker) was detected by incubation with Alexa 488-conjugated donkey anti-rat Ig (Invitrogen) at RT for 1 h. Fluorescence data were acquired with a BD FACSCanto (Becton-Dickinson) or BD LSR II with high-throughput sampler plus BD FACSDiva Software (version 5.0.3) and analyzed with

WEASLE v2.6 software. The fluorescence intensity of Alexa-488 is proportional to the expression level of Ly-6G or F4/80. The data are reported as the product of geometric mean fluorescence intensity and the total number of Ly-6G or F4/80 positive cells. The data are presented as means \pm standard errors (SE), and differences were analyzed using Student's *t* test.

2.10.4 Examination of lung tissue with HE staining or immunofluorescence labelling

After the blood and BAL were collected, the lungs of infected and uninfected mice were removed and fixed in 4% formaldehyde overnight at 4°C, embedded in paraffin, sectioned, stained with hematoxylin-eosin (HE), and examined by light microscopy. Alternatively, sections were labelled with rat anti-mouse Ly-6G or F4/80, followed by Alexa 488-conjugated anti-rat IgG and examined by fluorescence microscopy (AX 70; Olympus).

2.11 Detroit 562 adherence and invasion assays

Detroit 562 (human nasopharyngeal carcinoma) cells were grown in a 1:1 mix of Dulbecco's Modified Eagle Medium (Gibco) and Ham's F-12 Nutrient Mixture (Gibco), supplemented with 5% fetal bovine serum, 2 mM L-glutamine, 50 IU of penicillin and 50 μ g/ml streptomycin. Confluent monolayers in 24-well plates were washed with PBS and infected with pneumococci (approximately 5×10^5 CFU per well) in 1:1 mixture of the above culture medium (without antibiotics) and C+Y, pH 7.4. Plates were centrifuged at $500 \times g$ for 5 min, and then incubated at 37°C in 5% CO₂ for 2.5 h. Monolayers were washed 3 times in PBS, and adherent bacteria were released by treatment with 100 μ l trypsin/EDTA, followed by 400 μ l 0.025% Triton X-100. Lysates were serially diluted and plated on BA to enumerate adherent bacteria. Invasion assays were carried out essentially as above, except that after the post-adherence washing step, cultures were

incubated for 1 h in fresh medium supplemented with 200 µg gentamicin and 10 µg benzyl penicillin per ml to kill extracellular bacteria, after which monolayers were again washed, lysed, serially diluted and plated on BA, as above.

2.12 PCR Array analysis of host innate and adaptive immune responses

2.12.1 Tissue RNA isolation using TRIzol®

Infected mouse tissues harvested in 1 ml TRIzol® Reagent (Ambion, Life Technologies) were first homogenized with 1 ml PBS in tubes containing 2.8 mm diameter ceramic beads tubes with a Precellys® 24 homogenizer (Bertin Technologies, France). The homogenate was then transferred to RNase-free tubes and incubated at room temperature for 5 min (or stored at -80°C). Chloroform (200 µl per tube) was then added and the tubes were shaken vigorously. The tubes were then incubated at room temperature for 3 min and centrifuged at 13,000 × g for 15 min at 4°C. The aqueous phase was then added to 500 µl isopropanol, inverted gently to mix, and then incubated at room temperature for 10 min before being centrifuged at 13,000 × g for 10 min at 4°C. The supernatant was then discarded and the pellet washed with 1 ml 75% (v/v) ethanol, vortexed and centrifuged at 10,000 × g for 5 min at 4°C. Ethanol was then removed and the resultant pellet was air dried and redissolved in 100 µl RNase-free water. RNA purification and clean up was carried out using the RNeasy kit (Qiagen), according to the manufacturer's instructions.

2.12.2 cDNA Synthesis

cDNA was synthesised from RNA samples using the RT² First Strand Kit (Qiagen). RNA samples were firstly treated with RNase-free DNase to remove

contaminating genomic DNA and then reverse-transcribed to cDNA according to the manufacturer's protocols.

2.12.3 RT² Profiler Array

Mouse innate and adaptive immune responses to *S. pneumoniae* infection were examined using the Mouse Innate & Adaptive Immune Responses RT² Profiler PCR Array [Qiagen] according to manufacturer's instructions. Briefly, a PCR components mix (2× RT² SYBR Green MasterMix, cDNA synthesis reaction and RNase-free water) was firstly prepared according to manufacturer's instructions. The mix was then dispensed into the RT² Profiler PCR Array plate, sealed tightly with optical adhesive film and centrifuged for 1 min at 1000 × *g* at RT. The array plate was then analysed for gene expression by quantitative reverse transcription-PCR (qRT-PCR) on a Roche LightCycler 480 II system using the following program settings: hot-start cycle (1 cycle at 95°C for 10 min), 45 amplification cycles (95°C for 15 sec, 60°C for 1 min) and a melt curve cycle (95°C for 1 min, 65°C for 2 min and 95°C continuously thereafter). Five (5) housekeeping genes (*Actb*, *B2m*, *Gapdh*, *Gusb*, *Hsp90ab1*) were included in the array to normalize PCR array data. In addition, genomic DNA control primer set was included to detect nontranscribed genomic DNA contamination, along with reverse transcription controls (RTC) to determine cDNA synthesis efficiency. Positive PCR controls (PPC) were also included to test the efficiency of the PCR itself; while the latter two controls (RTC and PPC) also tested for interwell and intraplate efficiency. Data were then analyzed using a PCR Array Data Analysis Software provided by the manufacturer.

2.13 RNA Sequencing

Strains were grown in serum broth at 37°C to A₆₀₀ = 0.2. RNAProtect reagent (Qiagen) was then added and the bacterial culture was centrifuged at 3000 × *g* for 30 min.

RNA was extracted from the pellet and purified using the Qiagen RNeasy Mini Kit according to the manufacturer's instructions (Qiagen RNAProtect Bacteria Reagent Handbook). The purified RNA was then quantitated using the Nanodrop spectrophotometer (Thermo Scientific) and the integrity of the RNA (RIN number) determined using an Agilent 2100 Bioanalyzer, according to the manufacturer's instructions (Agilent). RNA samples with a RIN integrity of ≥ 8.0 and total yield of ≥ 3 ng were then sent to the Australian Genome Research Facility (AGRF) for ribosomal RNA removal, cDNA library preparation and RNA-sequencing using the Illumina Next-Gen Sequencing platform. Initial analysis to compare the isolates' transcriptomes was carried out by AGRF using the EDGE-pro (Estimated Degree of Gene Expression in PROkaryotes) pipeline, as described by Magoc *et al.* (2013) and R/Bioconductor-based voom and limma packages, as described by Ritchie *et al.* (2015). In addition to AGRF's data analyses, differential gene expression analysis was also carried out using the R/Bioconductor DESeq (v.3.2) package, as described by Anders *et al.* (2010) to validate AGRF's analysis, as well as to examine differential gene expression analysis between single isolates. Firstly, sequenced reads were aligned to the CGSP14 and SPNOXC reference genomes using Bowtie2 (v2.0.0.0-beta6), as described by Langmead *et al.* (2012). SAMtools (v 0.0.18) (Li *et al.*, 2009) and BEDTools (v2.24.0) (Quinlan *et al.*, 2010) were then used to obtain read counts for each transcript. DESeq analysis was subsequently performed using these data. The Basic Local Alignment Search Tool (BLAST) (Altschul *et al.*, 1990) and the Kyoto Encyclopedia of Genes and Genomes (KEGG) database resource (<http://www.genome.jp/kegg/genes.html>) were used as appropriate.

Chapter 3: *In vitro* characterization of biofilm formation by *S. pneumoniae* clinical isolates.

3.1 Introduction

The studies of infectious diseases initiated by Koch and colleagues over 150 years ago were essentially based on the development of pure culture techniques for growth and isolation of planktonic, individual bacterial cells (Koch, 1880). More recent studies have shown instead that bacteria predominantly exist in biofilms, as a preferred lifestyle in many natural environments (Fux *et al.*, 2003). Analysis of human biopsy samples and studies in animal models have highlighted the potential importance of biofilm formation by *S. pneumoniae* during the early stages of colonisation and invasion (Hall-Stoodley *et al.*, 2006; Reid *et al.*, 2009; Sanchez *et al.*, 2010).

A large number of bacterial factors have been implicated in pneumococcal biofilm formation in previous studies, including the competence stimulating peptide (CSP) and LuxS quorum sensing systems, as well as various pneumococcal surface structures and virulence factors (Blanchette-Cain *et al.*, 2013; Hall-Stoodley *et al.*, 2008; Marks *et al.*, 2012; Moscoso *et al.*, 2006; Oggioni *et al.*, 2006; Parker *et al.*, 2009; Pettigrew *et al.*, 2014; Sanchez *et al.*, 2011; Sanchez *et al.*, 2010; Shak *et al.*, 2013; Talekar *et al.*, 2014; Trappetti *et al.*, 2009; Trappetti *et al.*, 2011c; Vidal *et al.*, 2011; Yadav *et al.*, 2013). However, the link between biofilms and disease has been less well defined. While some studies described the importance of biofilms in invasive disease (Trappetti *et al.*, 2011b), others have observed that the production of biofilms attenuated disease (Blanchette-Cain *et al.*, 2013; Chao *et al.*, 2014; Sanchez, Kumar, *et al.*, 2011). These differences may have been attributable to the type of experimental models used (Shak *et al.*, 2013; Trappetti *et al.*, 2011a).

Many studies involving different *in vitro* models have shown that biofilm formation is significantly affected by the growth medium and other environmental factors, including pH, temperature and osmolarity (Moscoso *et al.*, 2006; Oggioni *et al.*, 2006; Trappetti *et al.*, 2009). Moscoso *et al.* (2006) observed optimal pneumococcal biofilm development when the starting cultures were grown in a semisynthetic (C)

medium with pH adjusted in the range 7.0 - 8.0. A drop in pH to below 6.0 was shown to inhibit the activity of the major autolysin LytA, an important determinant of biofilm formation (Lopez *et al.*, 1976; Moscoso *et al.*, 2006).

Despite the abundant literature on pneumococcal biofilm formation in clinical isolates, studies on the influence of clinical isolate source and iron availability on biofilm formation have been very limited. These studies include that of Trappetti *et al.* (2011c) which reported that pneumococcal biofilm formation was significantly enhanced in D39 strains in media supplemented with 50 μ M Fe(III), while Garcia-Castillo *et al.* (2007) reported that biofilm formation occurred more frequently from cystic fibrosis (CF) respiratory samples than among non-CF blood culture isolates.

Certain serotypes and ST types of *S. pneumoniae* have been reported to show a greater potential to cause invasive disease in humans than others; likewise strains differ in their propensity to cause otitis media (OM) (Forbes *et al.*, 2008; Hanage *et al.*, 2005). This suggests that strains may differ in their capacity to adapt to and survive or proliferate within distinct host microenvironments. This further implies that clinical isolates from cases of OM may exhibit distinct *in vitro* and *in vivo* phenotypes from blood isolates. Two conditions that vary significantly between different niches of the human body are metal ion concentrations (McDevitt *et al.*, 2011) and pH; the pH of the blood is typically around 7.4, while in the (uninfected) ear cavity pH is in the range of 6.5 - 6.8 (Jahn, 2001). The aim of the work described in this chapter was to investigate the influence of isolate source, pH and Fe(III) concentration on biofilm formation by clinical isolates belonging to five distinct capsular serotypes/groups: 3, 6, 9, 14 and 19. The strains were grown in C+Y medium with or without 100 μ M Fe(III) supplementation, at either pH 7.4 or 6.8, which corresponds to the environmental pH of the blood and ear cavity, respectively, in human hosts (Jahn, 2001).

3.2 Results

3.2.1 Viable count (CFU/well) assays for influence of clinical isolate source, pH and Fe(III) availability on biofilm formation.

A total of 78 blood and OM isolates belonging to serotypes/groups 3 (n=25), 6 (n=8), 9 (n=7), 14 (n=18) and 19 (n=20) were selected (see Section 2.1) and grown accordingly (see Section 2.2). Two assays were carried out in parallel. The viable count assay quantitated colony forming units (CFU) of bacterial biofilms dispersed by brief sonication after 24 h incubation (detection limit of 40 CFU/well). The assays were performed in four different media: C+Y pH 7.4, C+Y pH 6.8, C+Y+Fe(III) pH 7.4 and C+Y+Fe(III) pH 6.8. The crystal violet assay quantitated the biofilm biomass and matrix by measuring the A_{570} of stained pneumococcal biofilms after 24 h incubation (see Section 2.4.1) (detection limit of $A_{570} = 0.05$, which corresponds to the Absorbance after staining of blank wells incubated with C+Y media without bacteria). Statistical comparisons were performed only for isolates which showed biofilm formation in all tested media conditions. Firstly, as shown in Figures 3.1 – 3.8, the viable count biofilm assays revealed markedly variable biofilm formation capacity of the strains within a clinical isolate source in response to pH and the presence of Fe(III), as discussed below.

3.2.1.1 Serotype 3

For the viable count biofilm assay of serotype 3 strains, a total of 12 blood (Figure 3.1) and 13 ear isolates (Figure 3.2) were investigated in 4 media conditions, as described above. Biofilm CFU counts for blood and ear isolates that formed detectable biofilms were low compared to those for the other serotypes/groups tested, and ranged between 5×10^1 and 10^3 CFU per well (Figure 3.1 and 3.2). For the blood isolates, two strains (5267 and 5272) did not form biofilms under any condition tested, while biofilm formation for 5258 was only evident in C+Y pH 7.4, and that was at a low level. Two strains (4529 and 5060) formed biofilms in all 4 media. 5065, 4482, 4499, 5234, 4483, formed biofilms in both C+Y and C+Y+Fe(III) at pH 7.4, but at pH 6.8, biofilm

formation was evident for only one of these strains (5065) and only when Fe(III) was supplemented. 4521 formed biofilms at both pHs when there was no Fe(III) supplementation. 4522 formed biofilms in C+Y+Fe(III) pH 7.4 and C+Y pH 6.8. The biofilm assay suggested better overall biofilm formation of the blood isolates at pH 7.4 compared to pH 6.8, particularly in the presence of Fe(III). Nevertheless, when statistical analysis was performed using the 2-tailed Student's *t*-test to investigate the influence of pH (i.e. C+Y pH 6.8 vs. C+Y pH 7.4 and C+Y+Fe(III) pH 6.8 vs. C+Y+Fe(III) pH7.4) and Fe(III) supplementation (i.e. C+Y pH 6.8 vs. C+Y+Fe(III) pH 6.8 and C+Y pH 7.4 vs. C+Y+Fe(III) pH7.4) on biofilm formation on all 12 isolates, no significant differences were detected.

For ear isolates, 6 strains (54833, 57934, 9706840, 61887, 22318, 58497) formed low level ($<10^2$ CFU) or no biofilms in C+Y pH 7.4, but exhibited greater biofilm formation at pH 6.8 with significant increases in three isolates (54833, 61887 and 58497) ($P < 0.01$). Four of the remaining strains (75100, 68872, 53203 and 79275) formed biofilms at densities $> 10^2$ CFU/well in both in C+Y pH 7.4 and C+Y pH 6.8, while two strains (5069 and 5268) formed little or no biofilms ($< 10^2$ CFU/well) under all conditions tested. Fe(III) had no consistent effect on biofilm formation at pH 7.4, but at pH 6.8, Fe(III) was inhibitory for 7 biofilm-forming strains ($P < 0.01$) except 57934, 9706840, 62139 and 75100 which showed inhibition but was not significantly different.

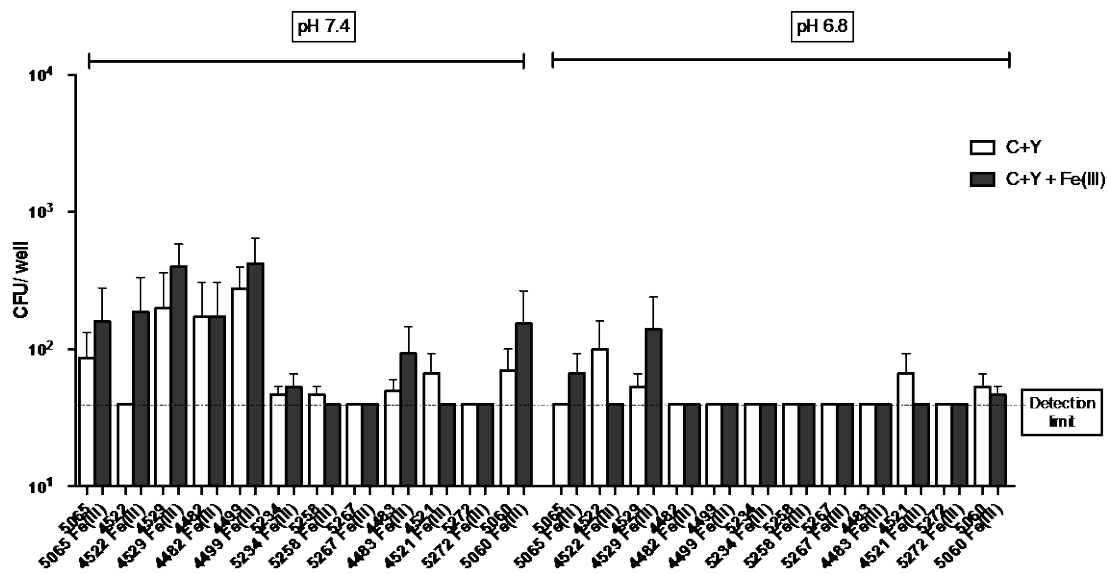


Figure 3.1. Biofilm formation of serotype 3 blood isolates assessed by viable count (CFU/well). Biofilm formation by serotype 3 blood isolates after 24 h of growth in C+Y medium at either pH 7.4 or 6.8, with (shaded columns) or without (open columns) 100 μM Fe(III), determined by viable count (CFU/well). Data are the means ± SEM for three independent experiments.

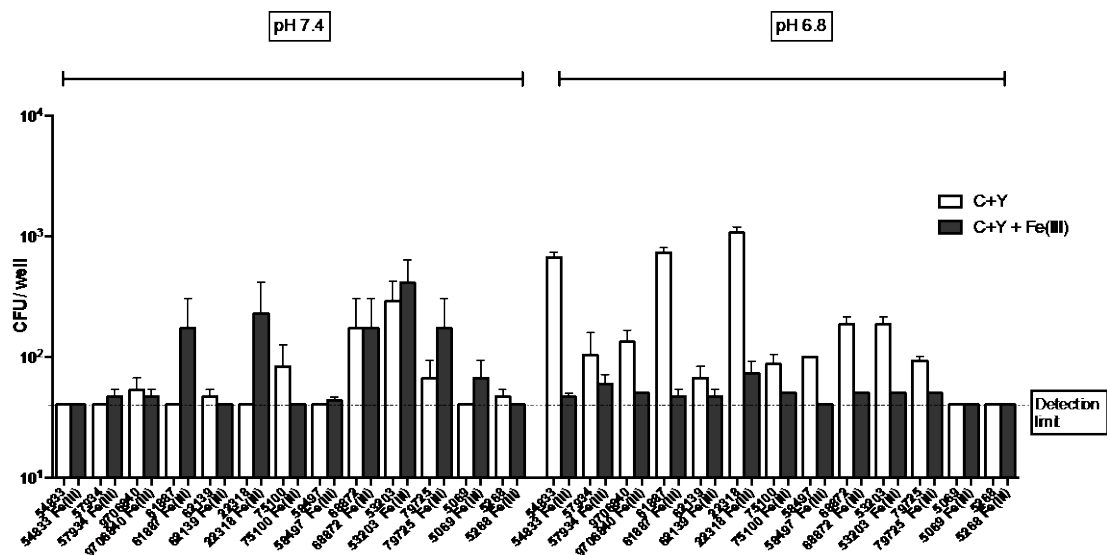


Figure 3.2. Biofilm formation of serotype 3 ear isolates by viable count (CFU/well). Biofilm formation by serotype 3 ear isolates after 24 h of growth in C+Y medium at either pH 7.4 or 6.8, with (shaded columns) or without (open columns) 100 μM Fe(III), determined by viable count (CFU/well). Data are the means ± SEM for three independent experiments.

3.2.1.2 Serogroup 6

For the viable count biofilm assay of serogroup 6 strains, a total of 4 blood (4501, 4519, 4526 and 4550) and 4 ear isolates (53034, 61888, 87765 and 50397) were investigated. CFU counts in isolates that formed biofilms ranged between 10^2 and 10^5 CFU (Figure 3.3). 4501 did not form a biofilm in any of the conditions tested, while 4519 formed a biofilm $>10^2$ CFU/well only in C+Y pH 7.4 with Fe(III) supplementation. The remaining two blood and four ear isolates formed measurable biofilms in all conditions tested. Whilst statistical analysis identified a number of significant differences in biofilm formation by individual strains between growth conditions (see Table 3.1), there was no consistent statistically significant effect of isolate source, pH or Fe(III) on biofilm formation across all strains. However, at pH 7.4, there was a consistent stimulatory effect of Fe(III) on biofilm formation for 7 of the 8 strains, which was significantly different in 3 strains (4550 and 50397 ($P < 0.05$) and 4519 ($P < 0.01$)).

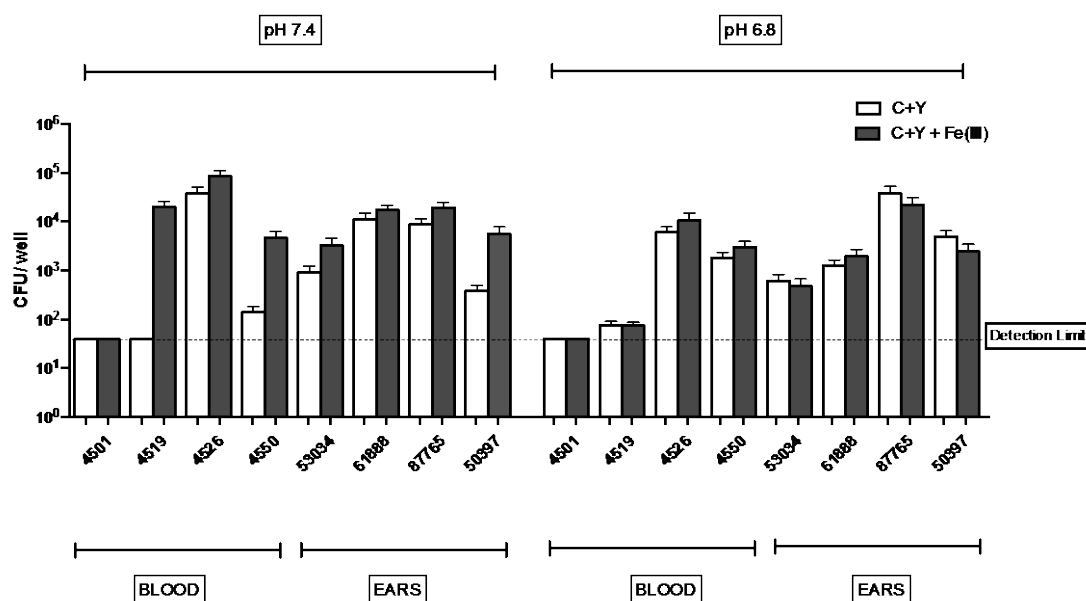


Figure 3.3. Biofilm formation by serogroup 6 blood and ear isolates by viable count (CFU/well). Biofilm formation by serogroup 6 blood and ear isolates after 24 h of growth in C+Y medium at either pH 7.4 or 6.8, with (shaded columns) or without (open columns) 100 μ M Fe(III), determined by viable count (CFU/well). Data are the means \pm SEM for three independent experiments.

Table 3.1. Statistical analysis of biofilm formation by serogroup 6 isolates.^a

Isolates	C+Y+Fe(III) vs. C+Y		pH 7.4 vs. 6.8	
	at pH 7.4	at pH 6.8	C+Y+Fe(III)	C+Y
4501	NS	NS	NS	NS
4519	<i>P</i> < 0.01	NS	<i>P</i> < 0.01	<i>P</i> < 0.05
4526	NS	NS	<i>P</i> < 0.05	<i>P</i> < 0.05
4550	<i>P</i> < 0.05	NS	NS	<i>P</i> < 0.05
53034	NS	NS	NS	NS
61888	NS	NS	<i>P</i> < 0.01	<i>P</i> < 0.05
87765	NS	NS	NS	NS
50397	<i>P</i> < 0.05	NS	NS	<i>P</i> < 0.05

^a Differences in biofilm formation by individual strains under the indicated growth conditions were analysed using 2-tailed Student *t*-tests. NS denotes not significantly different. Significant increases and decreases are denoted in **bold** and normal type, respectively.

3.2.1.3 Serogroup 9

For the viable count biofilm assay of serogroup 9, a total of 3 blood (4531, 4539, 5055) and 4 ear isolates (9723173, 40502, 66919 and 62195) were investigated. CFU counts in isolates that formed biofilms ranged between 10^3 and 10^5 CFU (see Figure 3.4). For blood isolates, 4531 and 4539 formed biofilms only at pH 7.4, and was significantly enhanced by Fe(III) supplementation for 4539 ($P < 0.05$). 5055 formed biofilms in all media conditions and was significantly enhanced at pH 7.4 in C+Y+Fe(III). Enhanced biofilm formation was also observed for 5055 in C+Y pH 6.8 compared to pH 7.4 ($P < 0.05$). For ear isolates, 9723173 did not form a biofilm at either pH, while 40502 and 62195 formed biofilms similarly at both pH 7.4 and pH 6.8. 66919 formed a biofilm only at pH 7.4, especially with Fe(III) supplementation. Similar to serogroup 6, there was no consistent effect of pH, Fe(III) or isolate source on biofilm formation across all strains, except for the consistent stimulatory effect of Fe(III) supplementation at pH 7.4 ($P < 0.05$).

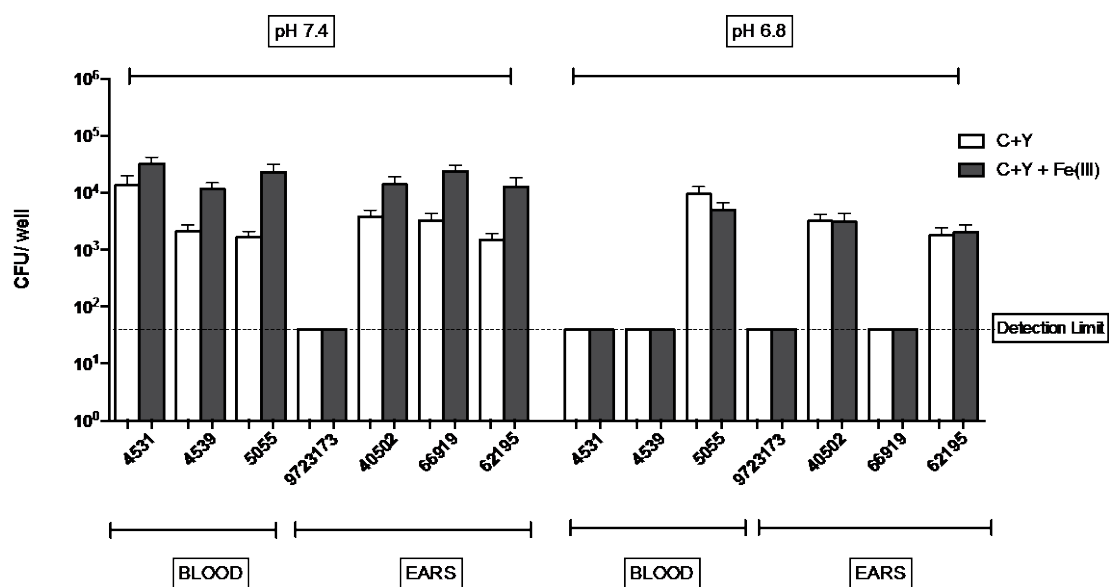


Figure 3.4 Biofilm formation by serogroup 9 blood and ear isolates by viable count (CFU/well). Biofilm formation by serogroup 9 blood and ear isolates after 24 h of growth in C+Y medium at either pH 7.4 or 6.8, with (shaded columns) or without (open columns) 100 μ M Fe(III), determined by viable count (CFU/well). Data are the means \pm SEM for three independent experiments.

Table 3.2. Statistical analysis of biofilm formation by serogroup 9 isolates.^a

Isolate	C+Y+Fe(III) vs. C+Y		pH 7.4 vs. 6.8	
	at pH 7.4	at pH 6.8	C+Y + Fe(III)	C+Y
4531	NS	NS	<i>P</i> < 0.01	<i>P</i> < 0.05
4539	<i>P</i> < 0.01	NS	<i>P</i> < 0.01	<i>P</i> < 0.01
5055	<i>P</i> < 0.05	NS	NS	<i>P</i> < 0.05
9723173	NS	NS	NS	NS
40502	NS	NS	NS	NS
66919	<i>P</i> < 0.05	NS	<i>P</i> < 0.01	<i>P</i> < 0.01
62195	NS	NS	NS	NS

^a Differences in biofilm formation by individual strains under the indicated growth conditions were analysed using 2-tailed Student *t*-tests. NS denotes not significantly different. Significant increases and decreases are denoted in **bold** and normal type, respectively.

3.2.1.4 Serotype 14

For the viable count biofilm assay of serotype 14, a total of 9 blood (Figure 3.5) and 9 ear isolates (Figure 3.6) were investigated. From both figures it can be seen that serotype 14 isolates showed the highest biofilm formation capacity when compared to other serotypes, with all isolates forming detectable biofilms. For the blood isolates, although actual level of biofilm formation by individual strains varied between approximately 2×10^2 and 10^6 CFU/well, there was close agreement within a strain between biofilm formation at pH 7.4 vs pH 6.8. Statistical analysis of biofilm data for individual strains (Table 3.3) showed a significant stimulatory effect of Fe(III) for strains 4524, 4534, 4511 and 4545 at pH 7.4, and for strain 4511 at pH 6.8 as well. Three of the blood isolates (4524, 4545 and 4549) also exhibited significantly higher biofilm formation at pH 7.4 vs pH 6.8. However, there was no significant overall effect for either parameter.

For the type 14 ear isolates, the level of biofilm formation by individual strains varied between approximately 5×10^2 and 10^6 CFU/well, but there was less agreement within a strain between biofilm formation at pH 7.4 vs pH 6.8. Statistical analysis of biofilm data for individual strains (Table 3.4) showed a significant stimulatory effect of Fe(III) for all strains except 9-47 at pH 7.4 ($P < 0.05$). Interestingly, the outlier 9-47 was the only strain showing a significant stimulatory effect of Fe(III) at pH 6.8. Individual strains also exhibited significant differences in biofilm formation at pH 7.4 vs pH 6.8 (Table 3.3), although the direction of change (i.e. higher or lower) was inconsistent between strains, with no overall significant effect.

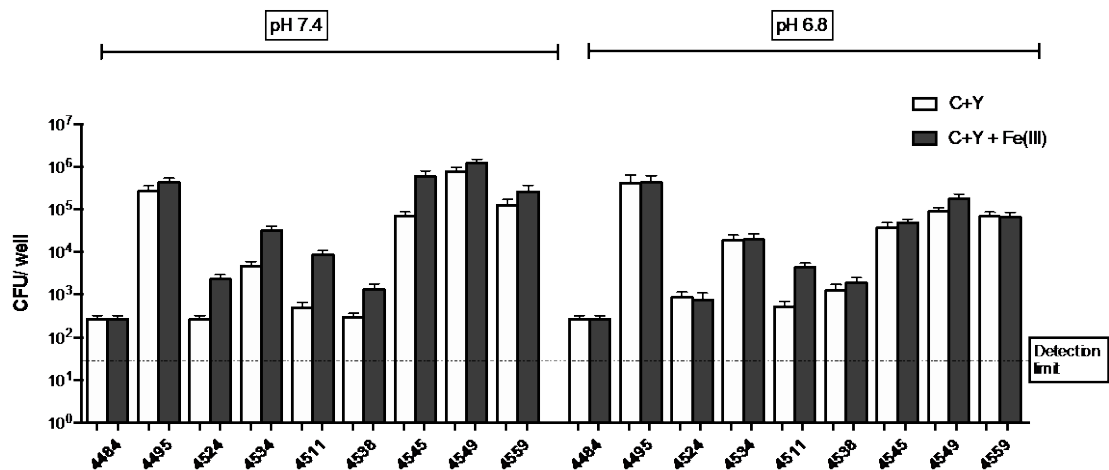


Figure 3.5. Biofilm formation by serotype 14 blood isolates viable count (CFU/well). Biofilm formation by serotype 14 blood isolates after 24 h of growth in C+Y medium at either pH 7.4 or 6.8, with (shaded columns) or without (open columns) 100 μ M Fe(III), determined by viable count (CFU/well). Data are the means \pm SEM for three independent experiments.

Table 3.3. Statistical analysis of serotype 14 blood isolate biofilm formation.^a

Isolate	C+Y+Fe(III) vs. C+Y		pH 7.4 vs. 6.8	
	at pH 7.4	at pH 6.8	C+Y + Fe(III)	C+Y
4484	NS	NS	NS	NS
4495	NS	NS	NS	NS
4524	<i>P</i> < 0.01	NS	<i>P</i> < 0.05	NS
4534	<i>P</i> < 0.01	NS	NS	<i>P</i> < 0.05
4511	<i>P</i> < 0.01	<i>P</i> < 0.01	NS	NS
4538	NS	NS	NS	NS
4545	<i>P</i> < 0.05	NS	<i>P</i> < 0.05	NS
4549	NS	NS	<i>P</i> < 0.01	<i>P</i> < 0.01
4559	NS	NS	NS	NS

^a Differences in biofilm formation by individual strains under the indicated growth conditions were analysed using 2-tailed Student's *t*-tests; NS denotes not significantly different. Significant increases and decreases are denoted in **bold** and normal type respectively.

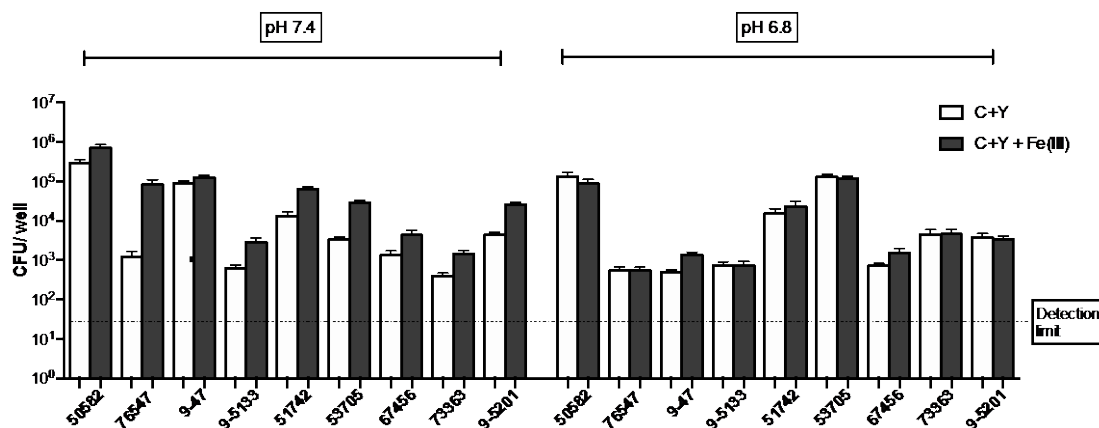


Figure 3.6. Biofilm formation by serotype 14 ear isolates by viable count (CFU/well). Biofilm formation of serotype 14 ear isolates after 24 h of growth in C+Y medium at either pH 7.4 or 6.8, with (light gray columns) or without (open columns) 100 μ M Fe(III), determined by viable count (CFU/well). Data are the means \pm SEM for three independent experiments.

Table 3.4. Statistical analysis of serotype 14 ear isolates biofilm formation.^a

Isolates	C+Y+Fe(III) vs C+Y		pH 7.4 vs. 6.8	
	at pH 7.4	at pH 6.8	C+Y + Fe(III)	C+Y
50582	<i>P</i> < 0.05	NS	<i>P</i> < 0.005	<i>P</i> < 0.05
76547	<i>P</i> < 0.01	NS	<i>P</i> < 0.01	NS
9-47	NS	<i>P</i> < 0.01	<i>P</i> < 0.0005	<i>P</i> < 0.0005
9-5133	<i>P</i> < 0.05	NS	<i>P</i> < 0.05	NS
51742	<i>P</i> < 0.005	NS	<i>P</i> < 0.01	NS
53705	<i>P</i> < 0.0005	NS	<i>P</i> < 0.005	<i>P</i> < 0.005
67456	<i>P</i> < 0.05	NS	<i>P</i> < 0.05	NS
73363	<i>P</i> < 0.05	NS	NS	<i>P</i> < 0.05
9-5201	<i>P</i> < 0.005	NS	<i>P</i> < 0.005	NS

^a Differences in biofilm formation by individual strains under the indicated growth conditions were analysed using 2-tailed Student's *t*-tests; NS denotes not significantly different. Significant increases and decreases are denoted in **bold** and normal type, respectively.

3.2.1.5 Serogroup 19

A total of 10 blood (Figure 3.7) and 10 ear (Figure 3.8) serogroup 19 isolates were investigated. All isolates formed biofilms with counts ranging between 10^2 and 10^5 CFU/well. For the blood isolates, Fe(III) supplementation had no significant impact on biofilm formation at either pH 7.4 or pH 6.8. However, three strains (5219, 5239 and 5027) formed significantly greater biofilms at pH 7.4 than pH 6.8, with or without Fe(III) supplementation, while 5058 showed significantly greater biofilms at pH 7.4 than pH 6.8 in C+Y+Fe(III) (Table 3.5).

For serogroup 19 ear isolates (Figure 3.8), six strains (24190, 51862, 53685, 64051, 74434 and 79213) formed biofilms similarly in all conditions tested. Biofilm formation was significantly greater for 48498 in both C+Y and C+Y+Fe(III) at pH 7.4 than at pH 6.8 (see Table 3.6). In contrast, 61884 and 74951 formed significantly greater biofilms at pH 6.8 in both C+Y and C+Y+Fe(III) than at pH 7.4, while 63748 formed significantly better biofilms at pH 6.8 than pH 7.4 only in C+Y+Fe(III). Fe(III) supplementation did not significantly impact biofilm formation of any isolate at either pH.

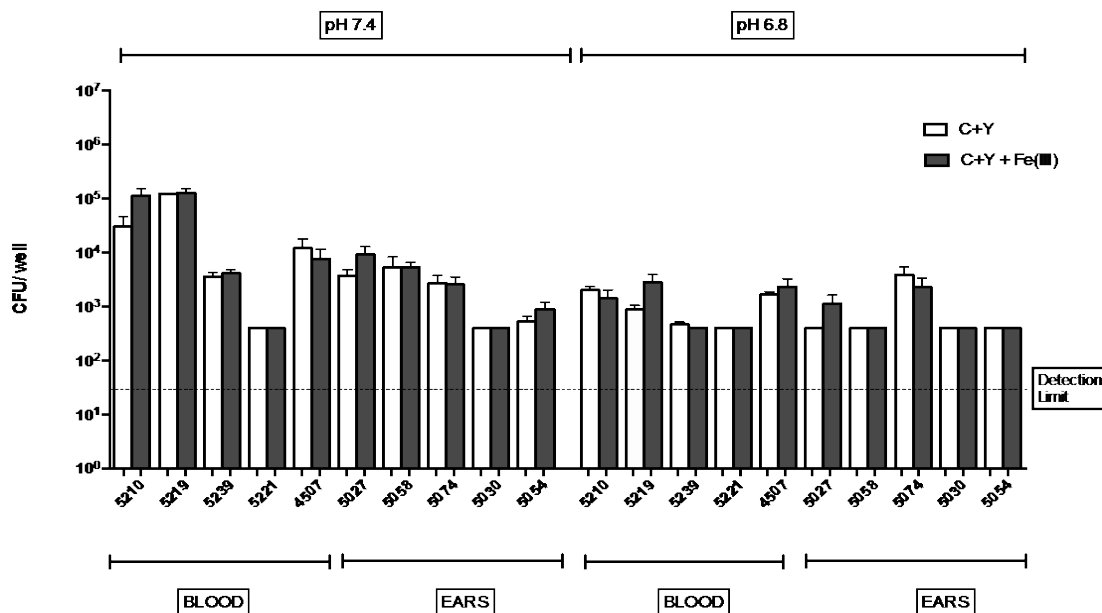


Figure 3.7 Biofilm formation by serogroup 19 blood isolates by viable count (CFU/well). Biofilm formation by serogroup 19 blood isolates after 24 h of growth in C+Y medium at either pH 7.4 or 6.8, with (shaded columns) or without (open columns) 100 μ M Fe(III), determined by viable count (CFU/well). Data are the means \pm SEM for three independent experiments.

Table 3.5. Statistical analysis of serogroup 19 blood isolates biofilm formation.^a

Isolates	C+Y+Fe(III) vs. C+Y		pH 7.4 vs. 6.8	
	at pH 7.4	at pH 6.8	C+Y + Fe(III)	C+Y
5210	NS	NS	NS	NS
5219	NS	NS	$P < 0.05$	$P < 0.0005$
5239	NS	NS	$P < 0.005$	$P < 0.005$
5221	NS	NS	NS	NS
4507	NS	NS	NS	NS
5027	NS	NS	$P < 0.05$	$P < 0.05$
5058	NS	NS	$P < 0.01$	NS
5074	NS	NS	NS	NS
5030	NS	NS	NS	NS
5054	NS	NS	NS	NS

^a Differences in biofilm formation by individual strains under the indicated growth conditions were analysed using 2-tailed Student's *t*-tests; NS denotes not significantly different. Significant increases and decreases are denoted in bold and normal type, respectively.

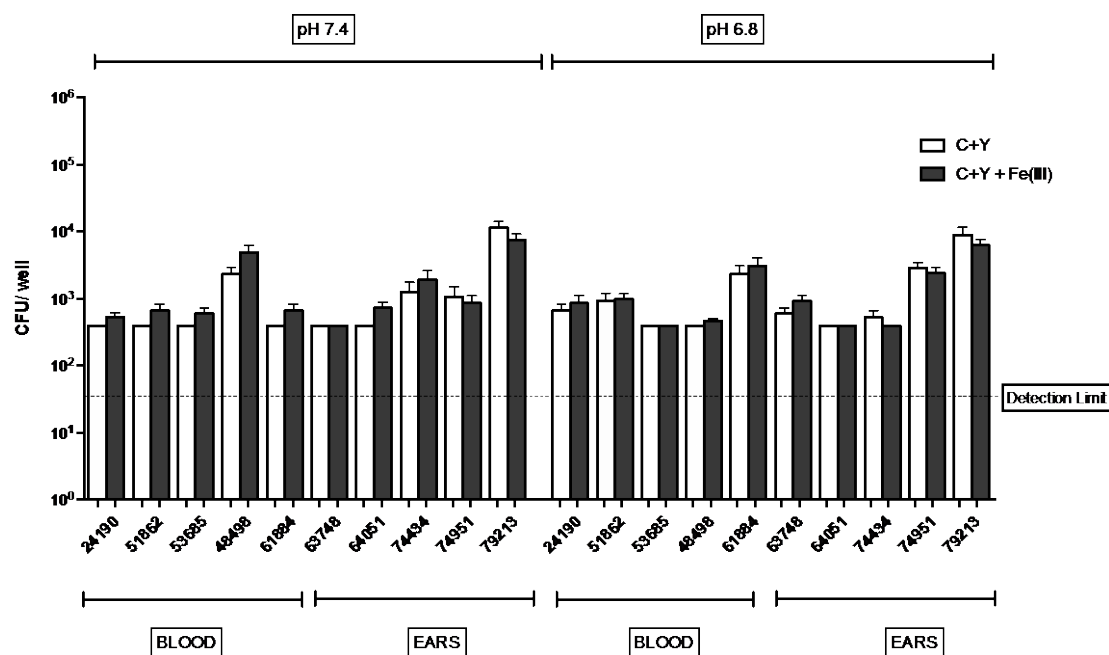


Figure 3.8. Biofilm formation by serogroup 19 ear isolates by viable count. Biofilm formation by serogroup 19 ear isolates after 24 h of growth in C+Y medium at either pH 7.4 or 6.8, with (shaded columns) or without (open columns) 100 μ M Fe(III), determined by viable count (CFU/well). Data are the means \pm SEM for three independent experiments.

Table 3.6. Statistical analysis of serogroup 19 ear isolates biofilm formation.^a

Isolates	C+Y+Fe(III) vs. C+Y		pH 7.4 vs. 6.8	
	at pH 7.4	at pH 6.8	C+Y + Fe(III)	C+Y
24190	NS	NS	NS	NS
51862	NS	NS	NS	NS
53685	NS	NS	NS	NS
48498	NS	NS	<i>P</i> < 0.01	<i>P</i> < 0.05
61884	NS	NS	<i>P</i> < 0.05	<i>P</i> < 0.05
63478	NS	NS	<i>P</i> < 0.05	NS
64051	NS	NS	NS	NS
74434	NS	NS	NS	NS
74951	NS	NS	<i>P</i> < 0.05	<i>P</i> < 0.05
79213	NS	NS	NS	NS

^a Differences in biofilm formation by individual strains under the indicated growth conditions were analysed using 2-tailed Student's *t*-tests; NS denotes not significantly different. Significant increases and decreases are denoted in **bold** and normal type, respectively.

3.2.2 Crystal Violet biofilm assay.

Biofilm formation by the various serotype/group blood and ear isolates was also assessed using Crystal Violet (CV) staining assays as independent confirmation of the CFU assays described above.

3.2.2.1 Serotype 3

Similar to the CFU data, CV assays of serotype 3 blood isolates (Figure 3.9) showed strain-strain variation in biofilm formation in response to pH and Fe(III) with the maximum observed A_{570} of 2, which was the highest compared to all other serotypes/groups. Ten of the twelve blood isolates formed biofilms similarly in all media conditions. However, 5234 formed significantly lesser biofilms in C+Y+Fe(III) at pH 7.4 than at pH 6.8 ($P < 0.05$), while 5267 formed greater biofilms at pH 7.4 than pH 6.8, regardless of Fe(III) supplementation ($P < 0.05$ in both cases). Indeed, supplementation with Fe(III) did not significantly influence biofilm formation of any strain at either pH.

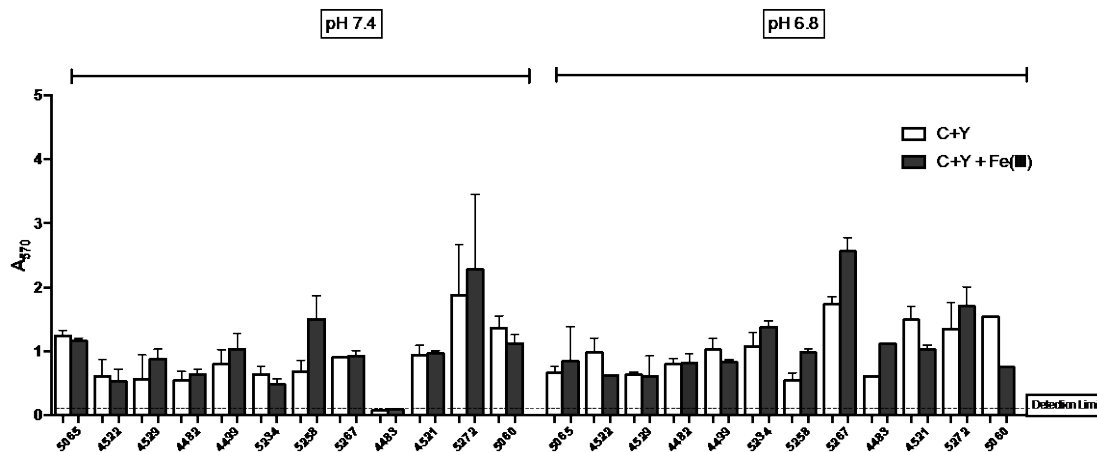


Figure 3.9. Biofilm formation by serotype 3 blood isolates assessed by CV staining. Biofilm formation by serotype 3 blood isolates after 24 h of growth at either pH 7.4 or 6.8, with or without 100 μ M Fe(III), was assayed by CV staining and A_{570} . Data are the means \pm SEM for three independent experiments.

CV assay of the 13 serotype 3 ear isolates (Figure 3.10) indicated generally stronger biofilm formation at pH 6.8 than at pH 7.4. However, between assay variability resulted in the differences only being statistically significant for strains 75100 and 58497, with or without Fe(III) supplementation ($P < 0.05$ in all cases). At pH 6.8, 75100 also showed significantly greater biofilm formation the presence of Fe(III) ($P < 0.05$).

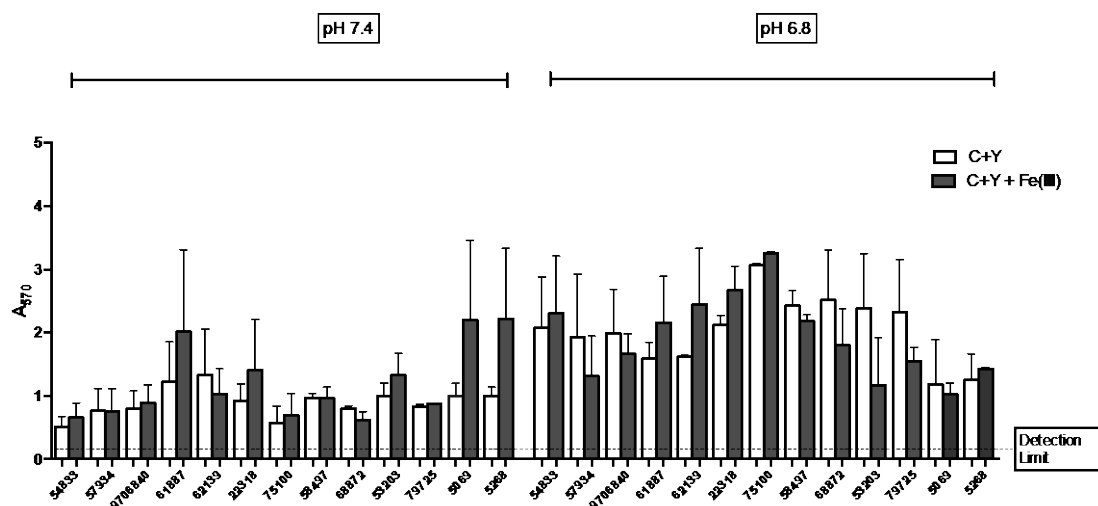


Figure 3.10. Biofilm formation by serotype 3 ear isolates assessed by CV staining. Biofilm formation by serotype 3 ear isolates after 24 h of growth at either pH 7.4 or 6.8, with or without 100 μ M Fe(III), was assayed by CV staining and A_{570} . Data are the means \pm SEM for three independent experiments.

3.2.2.2 Serogroup 6

CV assays of serogroup 6 blood and ear isolates (Figure 3.11) showed variable biofilm formation capacity of the isolates, with a maximum A_{570} of 0.4, generally well below that observed for serotype 3 strains. For blood isolates, 4501 and 4526 formed biofilms similarly in all tested conditions. At pH 7.4, supplementation with Fe(III) significantly increased biofilm formation by 4519, while Fe(III) significantly increased biofilm formation by 4550 at pH 6.8 (see Table 3.7). For ear isolates, biofilm formation was significantly greater for 53034 and 87765 at pH 7.4 than at pH 6.8, with or without Fe(III). 50397 and 61888 also formed greater biofilms at pH 7.4 than at pH 6.8 in C+Y+Fe(III) and C+Y, respectively (Table 3.7).

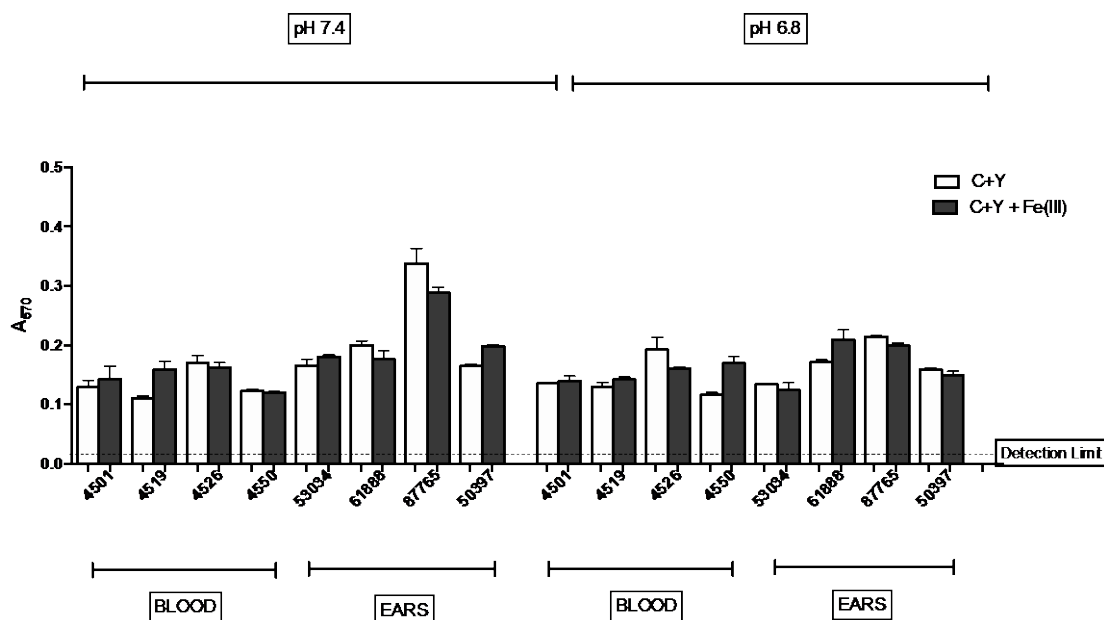


Figure 3.11. Biofilm formation by serogroup 6 blood and ear isolates assessed by CV staining. Biofilm formation by serogroup 6 blood and ear isolates after 24 h of growth at either pH 7.4 or 6.8, with or without 100 μ M Fe(III), was assayed by CV staining and A_{570} . Data are the means \pm SEM for three independent experiments.

Table 3.7. Statistical analysis of serogroup 6 biofilm formation.^a

Isolates	C+Y+Fe(III) vs. C+Y		pH 7.4 vs. 6.8	
	at pH 7.4	at pH 6.8	C+Y + Fe(III)	C+Y
4501	NS	NS	NS	NS
4519	<i>P</i> < 0.05	NS	NS	NS
4526	NS	NS	NS	NS
4550	NS	<i>P</i> < 0.01	NS	NS
53034	NS	NS	<i>P</i> < 0.01	<i>P</i> < 0.05
61888	NS	NS	NS	<i>P</i> < 0.05
87765	NS	<i>P</i> < 0.05	<i>P</i> < 0.005	<i>P</i> < 0.01
50397	<i>P</i> < 0.005	NS	<i>P</i> < 0.01	NS

^a Differences in biofilm formation by individual strains under the indicated growth conditions were analysed using 2-tailed Student's *t*-tests; NS denotes not significantly different. Significant increases and decreases are denoted in bold and normal type, respectively.

3.2.2.3 Serogroup 9

CV biofilm assays of serogroup 9 blood and ear isolates (Figure 3.12) showed a maximum A_{570} of 0.33. In the presence of Fe(III) blood isolates 4531, 4539 and 5055 formed significantly greater biofilms at pH 7.4 than at pH 6.8; 4531 biofilms in C+Y were also greater at pH 7.4 than at pH 6.8 (Table 3.8). For the ear isolates, 40502 formed biofilms similarly in all conditions tested. In C+Y, 9723173 and 66919 formed significantly greater biofilms at pH 7.4 than at pH 6.8, while the opposite was true for 62195 (Table 3.8).

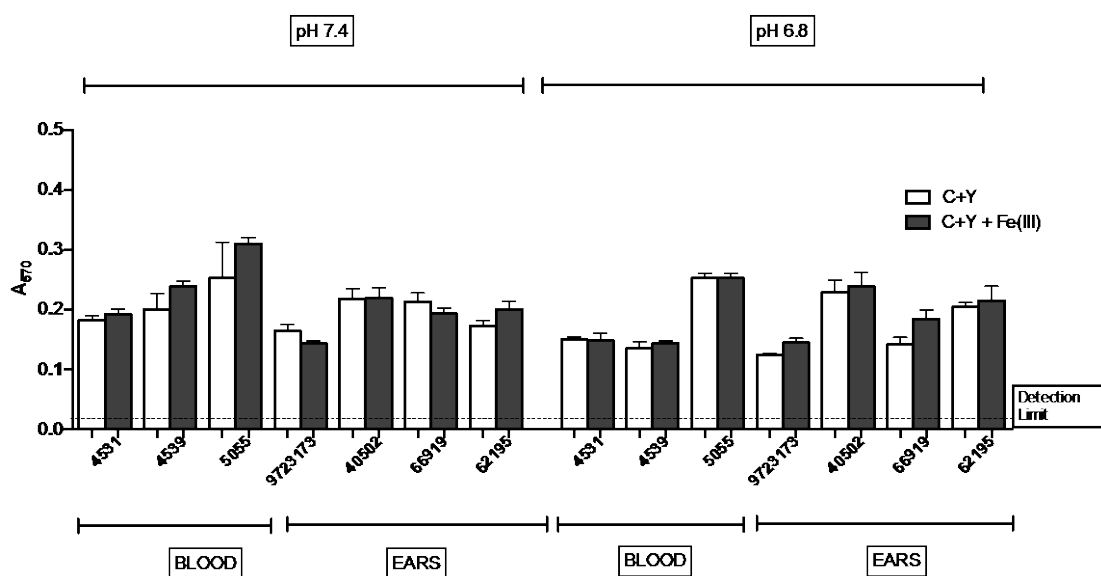


Figure 3.12. Biofilm formation by serogroup 9 blood and ear isolates assessed by CV staining. Biofilm formation by serogroup 9 blood and ear isolates after 24 h of growth at either pH 7.4 or 6.8, with or without 100 μ M Fe(III), was assayed by CV staining and A_{570} . Data are the means \pm SEM for three independent experiments.

Table 3.8. Statistical analysis of serogroup 9 biofilm formation.^a

Isolates	C+Y+Fe(III) vs. C+Y ^a		pH 7.4 vs. 6.8 ^b	
	at pH 7.4	at pH 6.8	C+Y + Fe(III)	C+Y
4531	NS	NS	<i>P</i> < 0.05	<i>P</i> < 0.05
4539	NS	NS	<i>P</i> < 0.005	NS
5055	NS	NS	<i>P</i> < 0.05	NS
9723173	NS	NS	NS	<i>P</i> < 0.05
40502	NS	NS	NS	NS
66919	NS	NS	NS	<i>P</i> < 0.05
62195	NS	NS	NS	<i>P</i> < 0.05

^a Differences in biofilm formation by individual strains under the indicated growth conditions were analysed using 2-tailed Student's *t*-tests; NS denotes not significantly different. Significant increases and decreases are denoted in bold and normal type, respectively.

3.2.2.4 Serotype 14

CV biofilm assays of serotype 14 blood isolates (Figure 3.13) also showed strain variation in biofilm formation in response to pH and Fe(III). Despite high biofilm CFU counts of serotype 14 isolates in the CFU assay (Figure 3.5), the maximum A_{570} for the strains in the CV assay was 0.4. There were no significant effects of Fe(III) or pH on biofilm formation for any of the serotype 14 blood isolates, except for 4549 which formed significantly greater biofilms in C+Y at pH 7.4 than at pH 6.8 ($P < 0.05$).

CV biofilm assays of serotype 14 ear isolates (Figure 3.14) also showed strain variation in biofilm formation with a maximum A_{570} of 0.4. Fe(III) or pH did not significantly affect biofilm formation for any of the strains, except for 76547 which formed significantly more biofilms at pH 6.8 than pH 7.4 in C+Y ($P < 0.05$), and 73363 and 9-5201 which also formed greater biofilms at pH 6.8 than at pH 7.4 in C+Y+Fe(III) ($P < 0.01$ and $P < 0.05$, respectively).

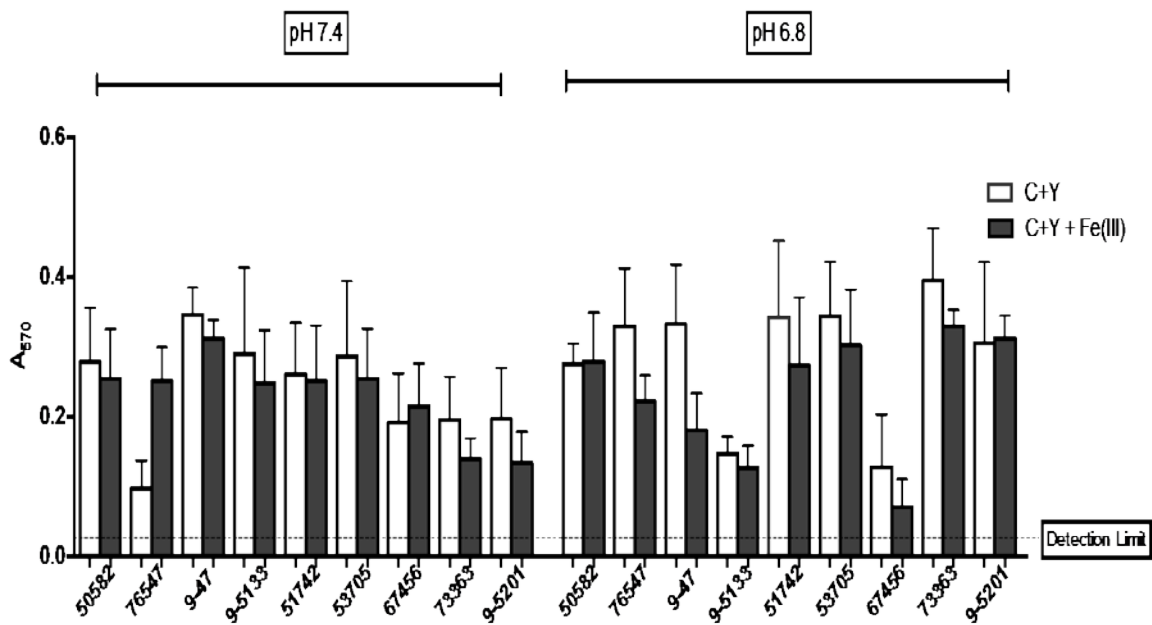


Figure 3.13. Biofilm formation by serotype 14 blood isolates assessed by CV staining. Biofilm formation by serotype 14 blood isolates after 24 h of growth at either pH 7.4 or 6.8, with or without 100 μ M Fe(III), was assayed by CV staining and A_{570} . Data are the means \pm SEM for three independent experiments.

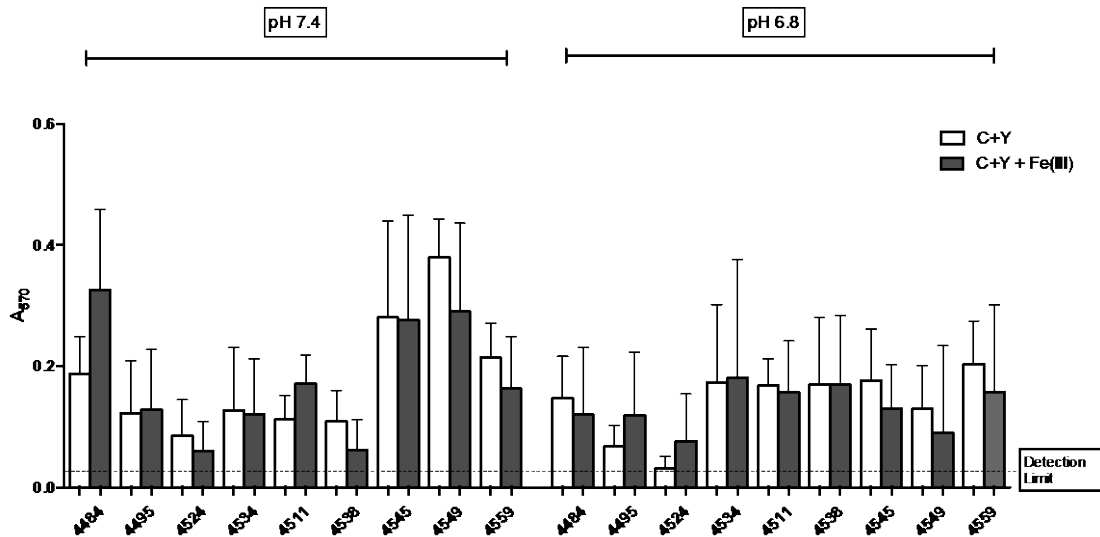


Figure 3.14. Biofilm formation by serotype 14 ear isolates assessed by CV staining. Biofilm formation by serotype 14 ear isolates after 24 h of growth at either pH 7.4 or 6.8, with or without 100 μ M Fe(III), was assayed by CV staining and A_{570} . Data are the means \pm SEM for three independent experiments.

3.2.2.5 Serogroup 19

CV biofilm assays of serogroup 19 blood (Figure 3.15) and ear isolates (Figure 3.16) showed no significant effects of either Fe(III) or pH on biofilm formation by any of the strains.

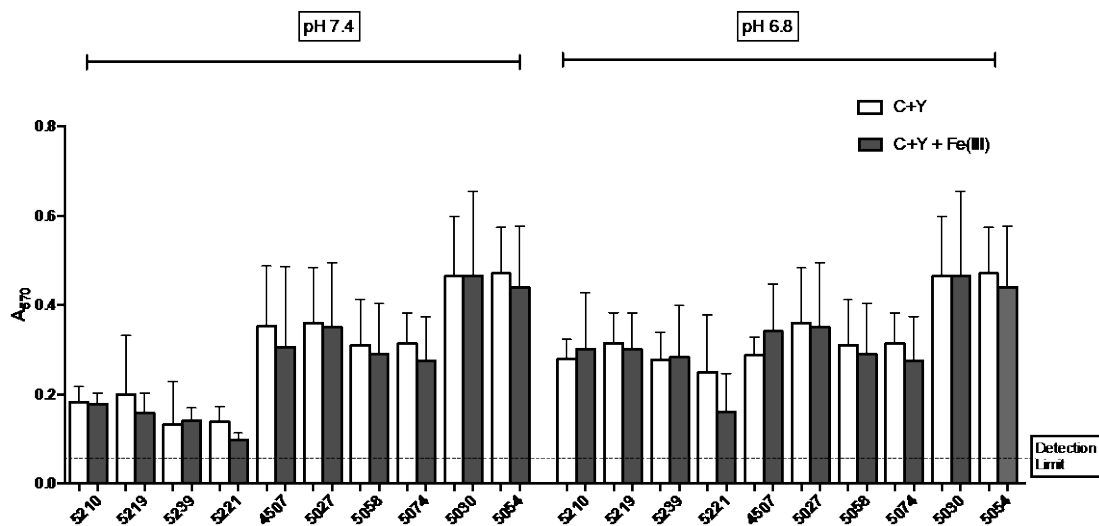


Figure 3.15. Biofilm formation by serogroup 19 blood isolates assessed by CV staining. Biofilm formation by serogroup 19 blood isolates after 24 h of growth at either pH 7.4 or 6.8, with or without 100 μ M Fe(III), was assayed by CV staining and A_{570} . Data are the means \pm SEM for three independent experiments.

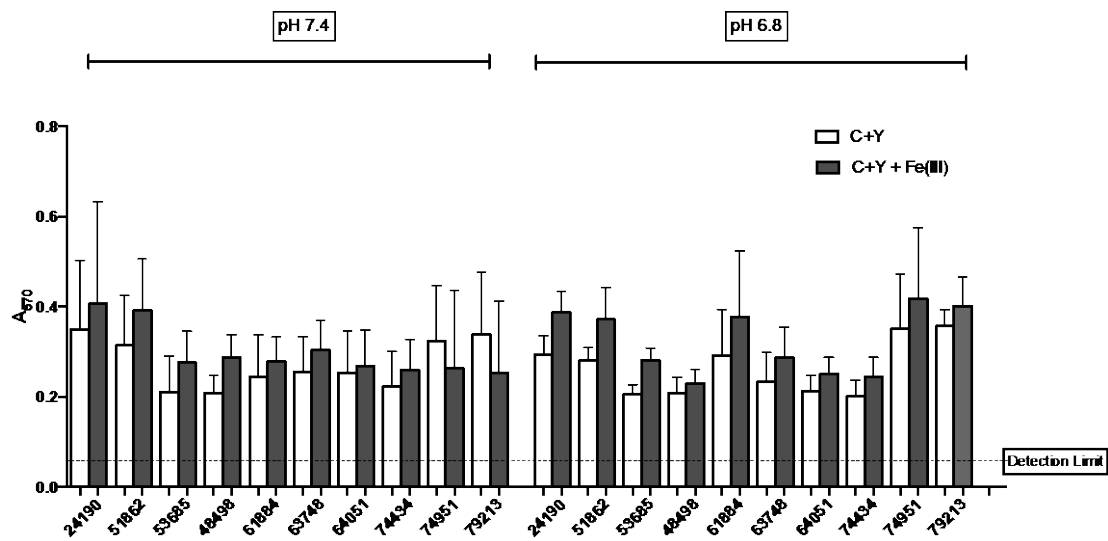


Figure 3.16. Biofilm formation by serogroup 19 ear isolates assessed by CV staining. Biofilm formation by serogroup 19 ear isolates after 24 h of growth at either pH 7.4 or 6.8, with or without 100 μM Fe(III), was assayed by CV staining and A_{570} . Data are the means \pm SEM for three independent experiments.

3.2.3 Microscopic analysis of CV-stained biofilms of blood and ear isolates.

Both viable count and CV assays revealed varied responses of blood and ear isolates in terms of the effects of pH and Fe(III) supplementation on biofilm formation. Unsurprisingly, data obtained using the separate biofilm assays did not show a close correlation for individual strains or serotypes/groups as a whole, as they were measuring distinct parameters (bacterial viability vs total biomass/matrix). To further explore this, microscopic analysis of CV-stained 24 h biofilms of a high biofilm forming blood and ear isolate from each serotype/group was carried out after growth in C+Y at pH 7.4 and pH 6.8, with or without 100 μM Fe(III) supplementation (see Section 2.4.2).

3.2.3.1 Serotype 3

Microscopic analysis of serotype 3 blood isolate 4529 grown at pH 7.4 with Fe(III) supplementation showed marked bacterial aggregation (Figure 3.17(ii)) compared to without Fe(III) (i). At pH 6.8, in C+Y (iii) and C+Y+Fe(III) (iv) the strain showed less aggregation than at pH 7.4 with or without Fe(III). Conversely, biofilm formation of ear isolate 9706840 was enhanced at pH 6.8 (Figure 3.17 (vii)) relative to pH 7.4 (v) and the presence of Fe(III) enhanced biofilm formation at pH 7.4 (vi).

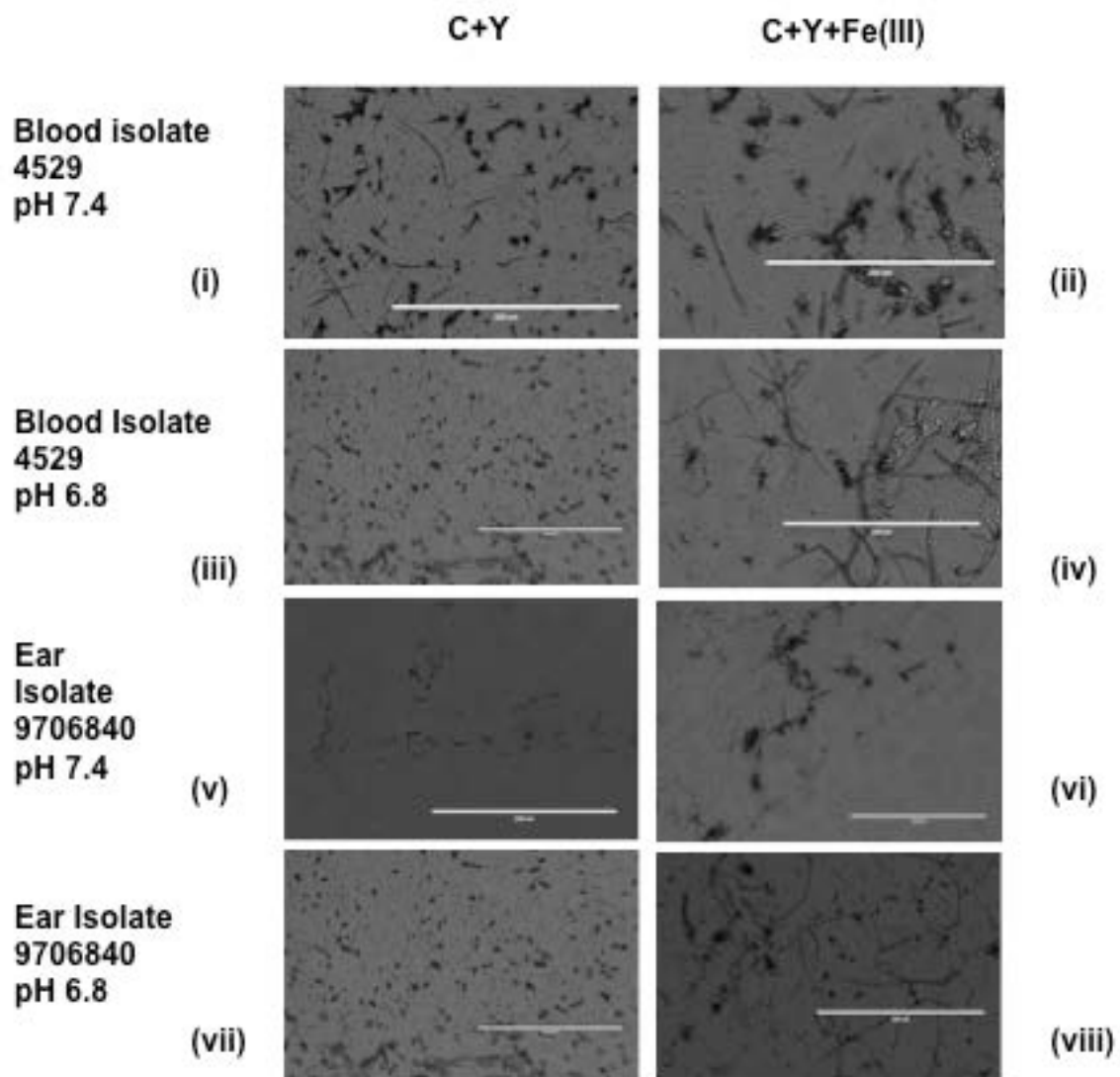


Figure 3.17. Microscopic analysis of CV-stained 24-h biofilms of serotype 3 blood and ear isolates grown at pH 7.4 and 6.8 in C+Y or C+Y+Fe(III). Scale bar = 0.2 mm.

3.2.3.2 Serogroup 6

As seen in Figure 3.18 panels (i) and (ii), serogroup 6 blood isolate 4526 in C+Y at pH 7.4 showed more marked aggregation of bacteria than at pH 6.8 (iii). At both pHs, the strains formed more robust biofilms in the presence of Fe(III), with increased aggregation at pH 7.4 ((ii) and (iv)). Ear isolate 87765 grown in C+Y formed biofilms similarly at both pHs ((v) and (vii)). However, the presence of Fe(III) at pH 6.8 appeared to reduce biofilm formation, as seen in Figure 3.18 (viii).

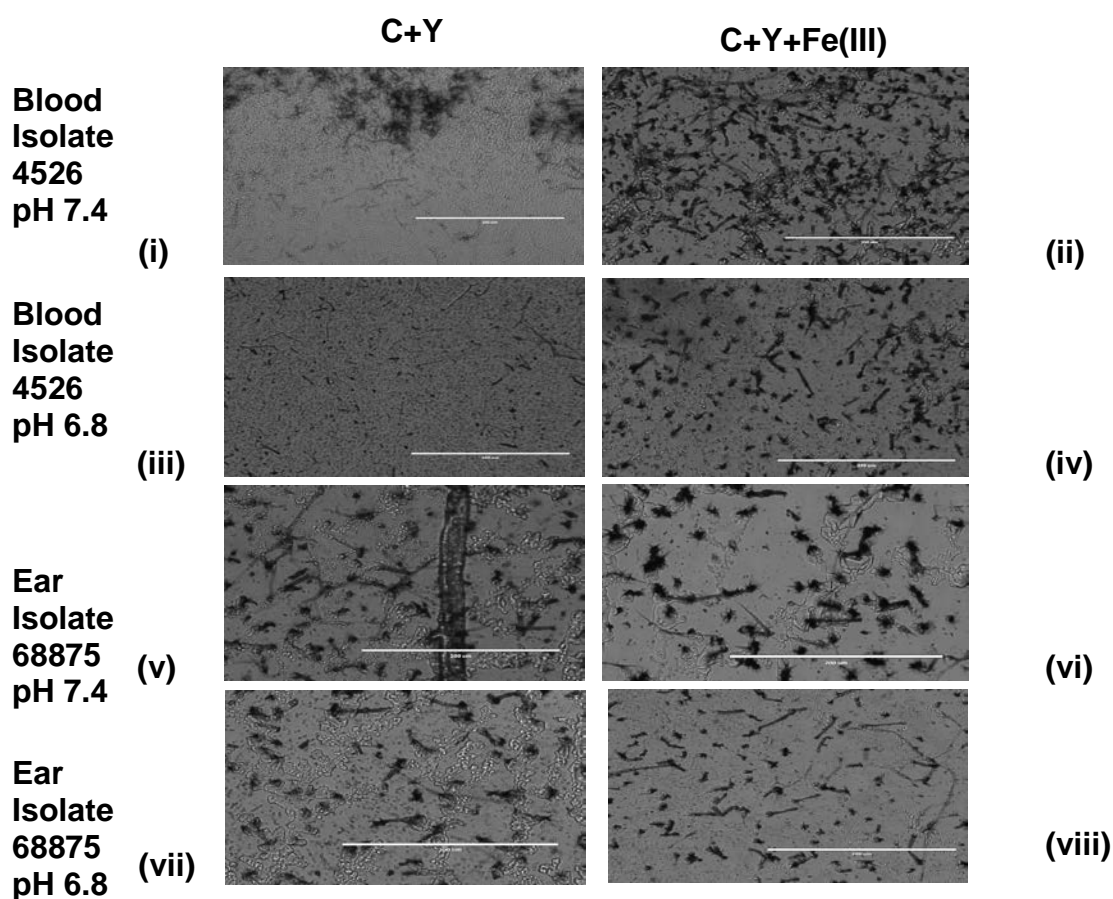


Figure 3.18. Microscopic analysis of crystal violet-stained 24-h biofilms of serogroup 6 blood and ear isolates grown at pH 7.4 and 6.8 in C+Y or C+Y+Fe(III). Scale bar = 0.2 mm.

3.2.3.3 Serogroup 9

Microscopic images of crystal violet stained serogroup 9 blood isolate 5055 in C+Y as seen in Figure 3.19 (i) appeared to show enhanced bacterial aggregation at pH 7.4 than at pH 6.8 (iii). The presence of Fe(III) did not appear to enhance bacterial aggregation of the blood isolates at either pH (Figure 3.19 (ii) and (iv)). Serotype 9 ear isolate 66919 in C+Y appeared to show similar biofilm formation at both pHs (Figure 3.19(v) and (vii)), but aggregation appeared to be slightly increased in the presence of Fe(III) at both pH ((vi) and (viii)).

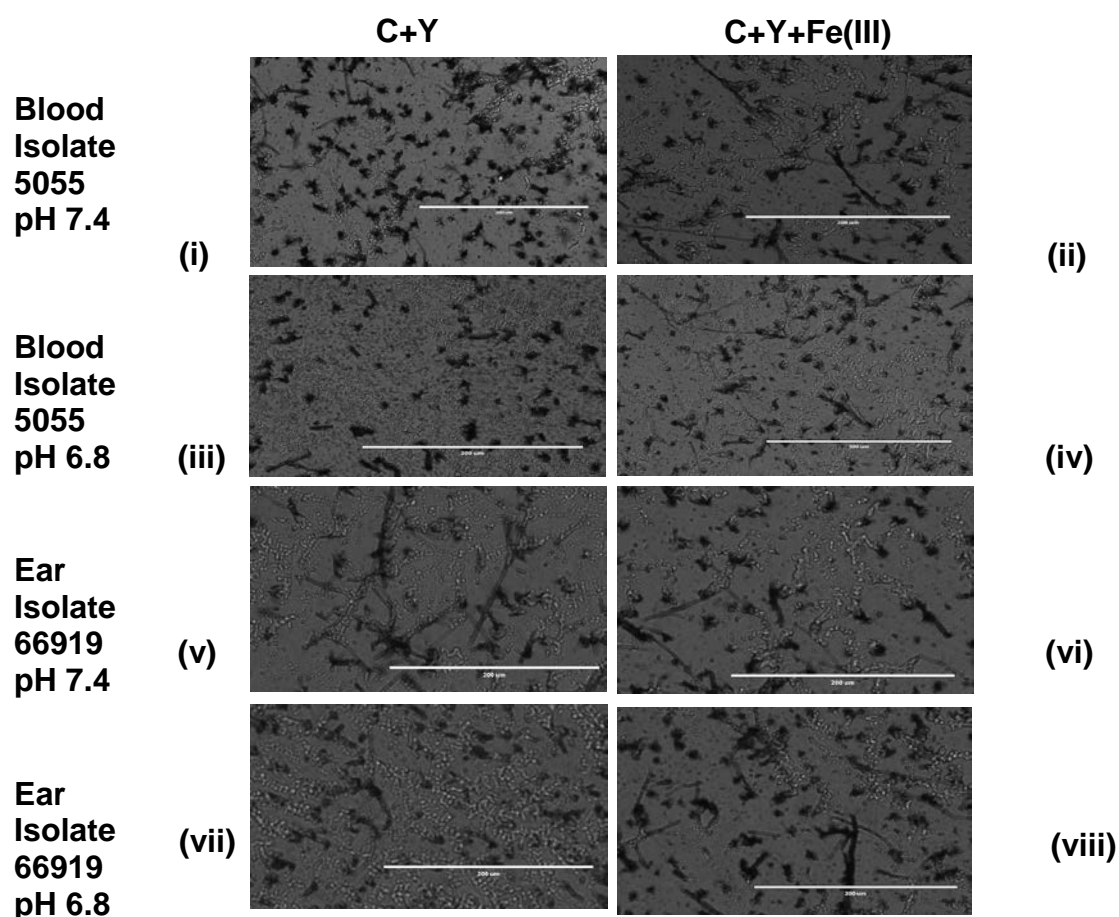


Figure 3.19 Microscopic analysis of crystal violet-stained 24-h biofilms of serogroup 9 blood and ear isolates grown at pH 7.4 and 6.8 in C+Y or C+Y+Fe(III). Scale bar = 0.2 mm.

3.2.3.4 Serotype 14

For serotype 14 blood isolate 4529, microscopic analysis showed the most robust biofilms compared to all other serotypes (Figure 3.20(i)-(iii)). Biofilm formation was enhanced at pH 7.4 (i) than at pH 6.8 (iii), especially in the presence of Fe(III) (ii). Fe(III) supplementation at pH 6.8 appeared to markedly inhibit biofilm formation of the blood isolate (Figure 3.20 (iv)). Ear isolate 9-5201 in C+Y at pH 6.8 (Figure 3.20(vii)) formed better biofilms than at pH 7.4 (v), while the presence of Fe(III) did not appear to positively influence biofilm formation at either pH (Figure 3.20(vi) and (viii)).

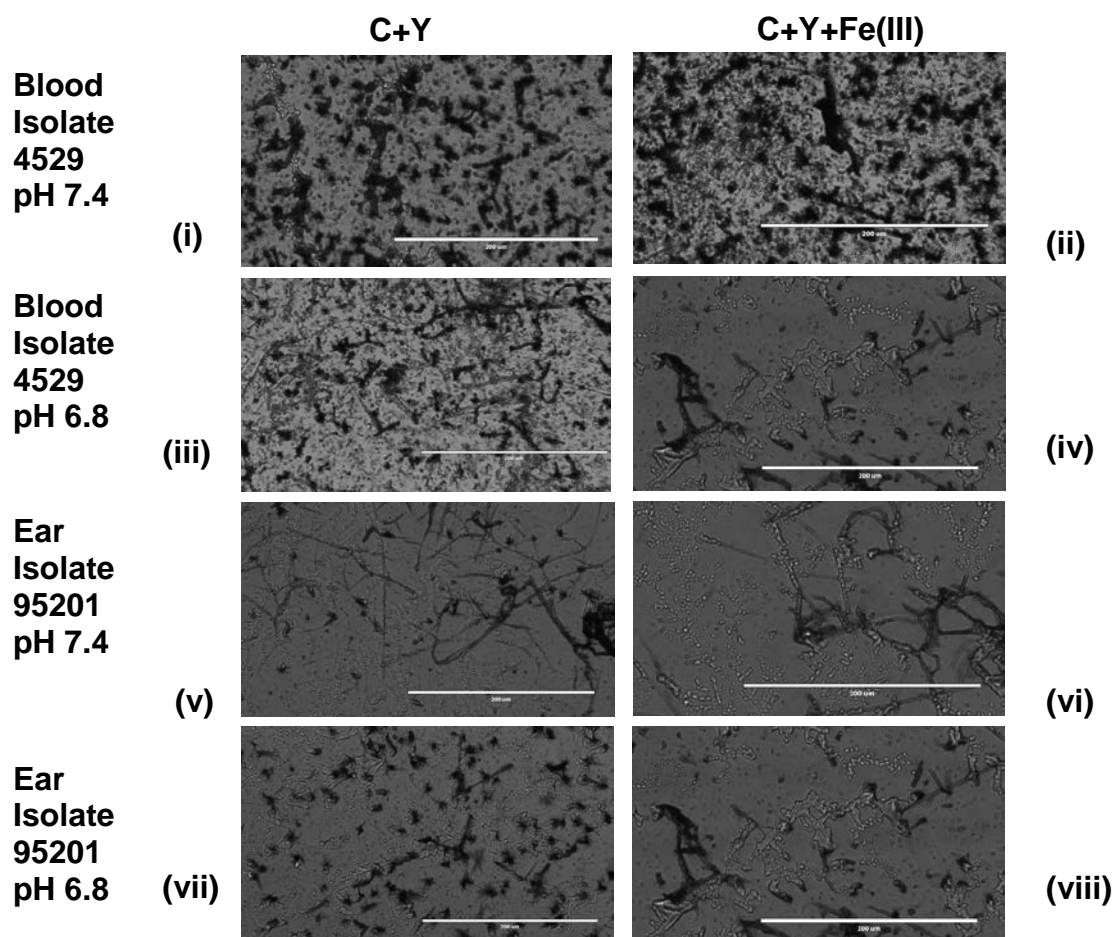


Figure 3.20. Microscopic analysis of crystal violet-stained 24-h biofilms of serotype 14 blood and ear isolates grown at pH 7.4 and 6.8 in C+Y or C+Y+Fe(III). Scale bar = 0.2 mm.

3.2.3.5 Serogroup 19

Microscopic images of serogroup 19 blood isolate 5210 in C+Y appeared to show more marked bacterial aggregation at pH 7.4 (Figure 3.21(i)) than at pH 6.8 (iii), while supplementation with Fe(III) increased bacterial aggregation at only pH 6.8 (iv). At pH 7.4, ear isolate 24190 appeared to show increased biofilm formation in the presence of Fe(III) (Figure 21(vi)) compared to without Fe(III) (v). When grown in C+Y+Fe(III) at pH 6.8 (viii) the strain also displayed visibly reduced aggregation compared to pH 7.4 (vi).

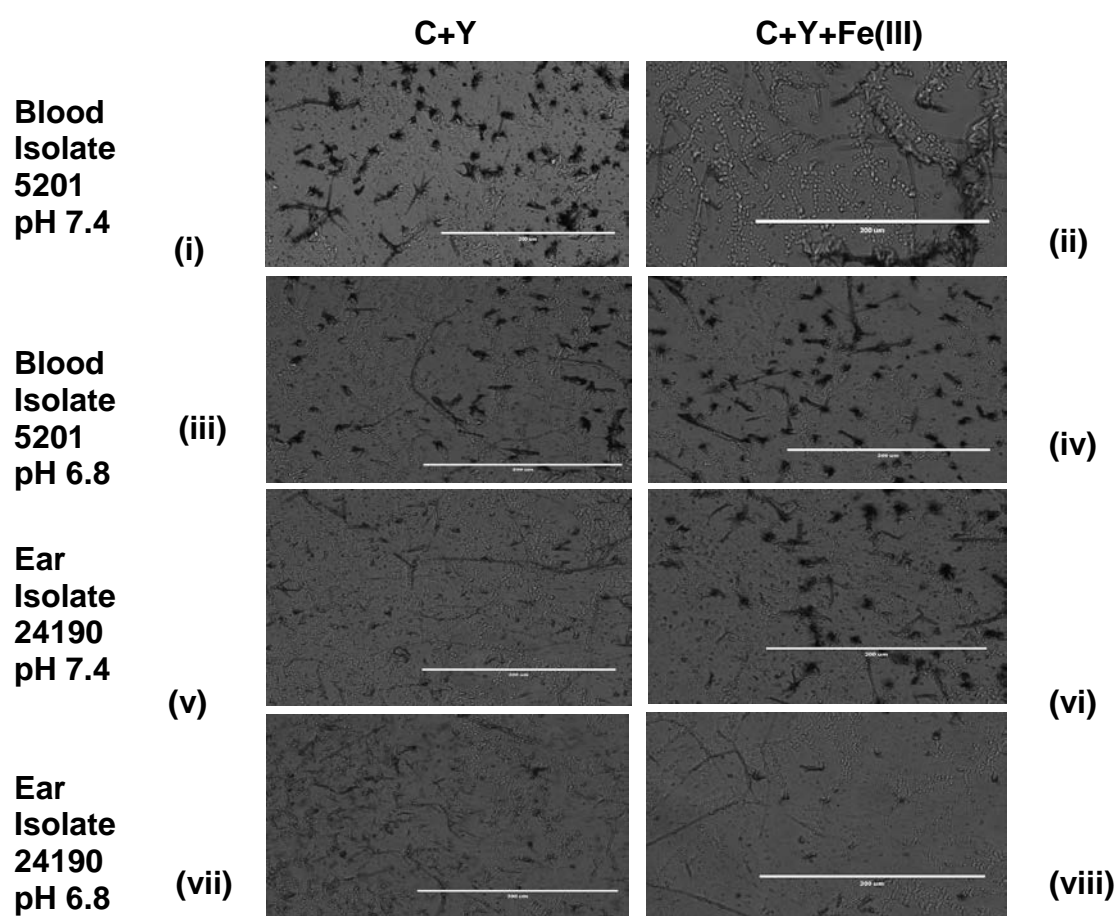


Figure 3.21. Microscopic analysis of crystal violet-stained 24-h biofilms of serogroup 19 blood and ear isolates grown at pH 7.4 and 6.8 in C+Y or C+Y+Fe(III). Scale bar = 0.2 mm.

Although microscopic images of the biofilms were variable across all serotypes, a general trend of increased bacterial aggregation was observed in the blood isolates primarily at pH 7.4, regardless of Fe(III) supplementation. Ear isolates showed an enhanced aggregation at pH 6.8 and the presence of Fe(III) reduced biofilm formation in most of these isolate types.

3.2.4 MLST typing of clinical isolates.

The highly variable biofilm phenotypes seen across all serotypes/groups indicated that non-capsular factors may be having a significant impact. Therefore, strains of serotypes/groups 3, 14 and 19, for which there were higher numbers of blood and ear isolates in our collection, were selected for MLST typing (see Section 2.7.2) to further investigate the genetic diversity of the isolates. Briefly, this involved DNA sequencing of internal fragments of 7 conserved, but polymorphic, pneumococcal house-keeping genes (*aroE*, *gdh*, *gki*, *recP*, *xpt*, *spi* and *ddl*) (Enright & Spratt 1998, 1999). The sequences were then compared with previously known sequence variants (alleles) and assigned an allele number for each of the 7 loci. The combination of 7 allele numbers represents an allelic profile for the strain, allowing it to be assigned to a sequence type (ST) derived from the *S. pneumoniae* MLST database <http://pubmlst.net>. Characterization of isolates by MLST enables strain comparisons independently of serotyping, and at a much higher resolution. It also may provide a more accurate picture of strain phylogeny, particularly since unrelated *S. pneumoniae* strains are known to be able to exchange capsule biosynthesis loci by natural recombination (Coffey *et al.*, 1998). ST typed strains may be part of a larger clonal complex (CC) comprising strains with 5-6 matching loci, denoting a degree of genetic relatedness (Tyrrell, 2011). Strains of the same CC or indeed ST may belong to different serotypes. The observed variation in biofilm formation among the strains of the same serotype/group seen in viable count and CV-staining assays presented in this chapter may be due to the presence of multiple STs, which may or may not form part of a CC, and indicate major genetic differences between the strains.

3.2.4.1 Serotype 3

A total of 23 blood and ear isolates (12 blood and 13 ear) from the serotype 3 collection were selected for MLST typing. As seen in Table 3.9, serotype 3 isolates comprised 4 STs, which were predominated by ST180 (7 blood and 6 ear isolates), ST232 (3 blood and 4 ear isolates) and ST233 (2 blood and 1 ear isolate) while ST458 comprised 2 blood isolates. Further detailed analysis using http://pubmlst.org/perl/bigdb/bigdb.pl?db=pubmlst_spneumoniae_seqdef&page=downloadProfiles&scheme_id=1 and the eBURST v3 software available from <http://spneumoniae.mlst.net/sql/burstspadvanced.asp> (Feil *et al.*, 2004) showed that ST232 and ST233 belonged to clonal complex CC378, while ST180 and ST458 belonged to CC180 and CC458, respectively. The allelic profiles of each ST are as described below.

Table 3.9. STs and CCs of serotype 3 strains typed by MLST.

Serotype 3 strain	Source	ST (CC)	New strain name
5065	Blood	ST232 (CC378) Allelic profile: <i>aroE</i> 13; <i>gdh</i> 9; <i>gki</i> 15; <i>recP</i> 14; <i>spi</i> 10; <i>xpt</i> 16; <i>ddl</i> 1	ST232/1
4522	Blood	ST233 (CC378) Allelic profile: <i>aroE</i> 13; <i>gdh</i> 9; <i>gki</i> 15; <i>recP</i> 14; <i>spi</i> 10; <i>xpt</i> 16; <i>ddl</i> 25	ST233/3
4529	Blood	ST180 (CC180) Allelic profile: <i>aroE</i> 7; <i>gdh</i> 15; <i>gki</i> 2; <i>recP</i> 10; <i>spi</i> 6; <i>xpt</i> 1; <i>ddl</i> 22	ST180/4
4482	Blood	ST458 (CC458) Allelic profile: <i>aroE</i> 2; <i>gdh</i> 32; <i>gki</i> 9; <i>recP</i> 47; <i>spi</i> 6; <i>xpt</i> 21; <i>ddl</i> 17	ST458/5
4499	Blood	ST233 (CC378)	ST233/6

5234	Blood	ST180 (CC180)	ST180/7
5258	Blood	ST180 (CC180)	ST180/8
5267	Blood	ST180 (CC180)	ST180/15
4483	Blood	ST458 (CC458)	ST458/20
4521	Blood	ST232 (CC378)	ST232/23
5272	Blood	ST180 (CC180)	ST180/24
5060	Blood	ST 232 (CC378)	ST 232/25
54833	Ear	ST180 (CC180)	ST180/2
57934	Ear	ST180 (CC180)	ST180/9
9706840	Ear	ST180 (CC180)	ST180/10
61887	Ear	ST232 (CC378)	ST232/11
62139	Ear	ST180 (CC180)	ST180/12
22318	Ear	ST233 (CC378)	ST233/13
75100	Ear	ST180 (CC180)	ST180/14
58497	Ear	ST180 (CC180)	ST180/16
68872	Ear	ST232 (CC378)	ST232/17
53203	Ear	ST232 (CC378)	ST232/18
79725	Ear	ST232 (CC378)	ST232/19
5069	Ear	ST180 (CC180)	ST180/21
5268	Ear	ST180 (CC180)	ST180/22

3.2.4.2 Serotype 14

A total of 18 isolates (9 blood and 9 ear) were selected for MLST typing. As seen in Table 3.10, the isolates belonged to 10 different STs. Two STs appeared to predominate: ST15 (n=5) and ST130 (n=5), both of which were similarly represented amongst blood (n=3) and ear (n=2) isolates. Other strains belonged to ST124 and ST129, or were assigned new STs by the pneumococcal MLST database curators. Each of these strains were represented by one isolate only and thus could not be matched with an isolate from the alternative niche/source. Further eBURST analysis showed that there were two distinct CCs in the collection; CC15, which comprised ST15 isolates (blood isolates 4495, 4534, 4559 and ear isolates 9-47, 51742), and CC124, which comprised ST124 (ear isolate 9-5201), ST129 (ear isolate 9-5133) and ST130 (blood isolates 4484, 4524, 4538 and ear isolates 76547, 67456). Other STs were not found to belong to a particular CC. The allelic profiles of each ST are as described below.

Table 3.10. STs and CCs of serotype 14 strains typed by MLST.

Serotype 14 isolates	Source	ST (CC)	New strain name
4534	Blood	ST15 (CC15) Allelic profile: <i>aroE</i> 1; <i>gdh</i> 5; <i>gki</i> 4; <i>recP</i> 5 <i>spi</i> 5; <i>xpt</i> 3; <i>ddl</i> 17	ST15/4534
4559	Blood	ST15 (CC15)	ST15/4559
4495	Blood	ST15 (CC15)	ST15/4495
51742	Ear	ST15 (CC15)	ST15/51742
9-47	Ear	ST15 (CC15)	ST15/9-47
4484	Blood	ST130 (CC124) Allelic profile: <i>aroE</i> 7; <i>gdh</i> 5; <i>gki</i> 1; <i>recP</i> 8; <i>spi</i> 14; <i>xpt</i> 14; <i>ddl</i> 14	ST130/4484
4524	Blood	ST130 (CC124)	ST130/4524
4538	Blood	ST130 (CC124)	ST130/4538
76547	Ear	ST130 (CC124)	ST130/76547
67456	Ear	ST130 (CC124)	ST130/67456

9-5201	Ear	ST124 (CC124) Allelic profile: <i>aroE</i> 7; <i>gdh</i> 5; <i>gki</i> 1; <i>recP</i> 8; <i>spi</i> 14; <i>xpt</i> 11; <i>ddl</i> 14	ST124/9-5201
9-5133	Ear	ST129 (CC124) Allelic profile: <i>aroE</i> 7; <i>gdh</i> 5; <i>gki</i> 1; <i>recP</i> 8; <i>spi</i> 14; <i>xpt</i> 11; <i>ddl</i> 5	ST129/9-5133
4549	Blood	ST9587 Allelic profile: <i>aroE</i> 1; <i>gdh</i> 5; <i>gki</i> 4; <i>recP</i> 5; <i>spi</i> 5; <i>xpt</i> 3; <i>ddl</i> 1	ST9587/4549
73363	Ear	ST9588 Allelic profile: <i>aroE</i> 50; <i>gdh</i> 5; <i>gki</i> 1; <i>recP</i> 8; <i>spi</i> 14; <i>xpt</i> 3; <i>ddl</i> 14	ST9588/73363
4511	Blood	ST9589 Allelic profile: <i>aroE</i> 12; <i>gdh</i> 5; <i>gki</i> 4; <i>recP</i> 5; <i>spi</i> 5; <i>xpt</i> 3; <i>ddl</i> 8	ST9589/4511
50582	Ear	ST9590 Allelic profile: <i>aroE</i> 7; <i>gdh</i> 5; <i>gki</i> 1; <i>recP</i> 5; <i>spi</i> 5; <i>xpt</i> 3; <i>ddl</i> 8	ST9590/50582
53705	Ear	ST9591 Allelic profile: <i>aroE</i> 1; <i>gdh</i> 5; <i>gki</i> 4; <i>recP</i> 5; <i>spi</i> 5; <i>xpt</i> 88; <i>ddl</i> 8	ST9591/53705
4545	Blood	ST9592 Allelic profile: <i>aroE</i> 11; <i>gdh</i> 5; <i>gki</i> 1; <i>recP</i> 5; <i>spi</i> 5; <i>xpt</i> 3; <i>ddl</i> 1	ST9592/4545

3.2.4.3 Serogroup 19

A total of 17 serogroup 19 blood and ear isolates were subjected to MLST typing. As seen in Table 3.11, serogroup 19 blood and ear isolates showed greater genetic diversity compared to serotypes 3 and 14. The 17 typed isolates comprised 14 different STs, including 3 ST177 ear isolates, 2 ST199 blood isolates and 12 other isolates each belonging to a different ST. Further detailed MLST analysis carried out via http://pubmlst.org/perl/bigssdb/bigssdb.pl?db=pubmlst_spneumoniae_seqdef&page=downloadProfiles&scheme_id=1 (Maiden *et al.*, 2013) revealed that some strains were more closely related than others. Two common clonal complexes were identified via eBURST v3 software (Feil *et al.*, 2004). Blood isolates of ST199 (5219 and 5221) and ST876 (5210) were found to belong to CC199, while ear isolates of ST177 (51862 and 61884) and ST549 (58616) belonged to CC177. Blood isolate 5239 of ST186 and ear isolate 48498 from ST2417 also comprised similar allelic profiles, but did not belong to an identified CC, while the other STs identified were classed as singletons. Generally the multiple STs found within serotype/group 3, 14 and 19 isolates in our collection showed high genetic diversity among the strains, which may have accounted for the highly variable biofilm phenotypes seen in the biofilm assays.

Table 3.11. Identified STs and CCs of serogroup 19 strains typed by MLST.

Serogroup 19 strains	Source	ST (CC)	New strain name
5210	Blood	ST876 (CC199) Allelic profile: <i>aroE</i> 8; <i>gdh</i> 13; <i>gki</i> 14; <i>recP</i> 4; <i>spi</i> 6; <i>xpt</i> 4; <i>ddl</i> 14	ST876/5210
5219	Blood	ST199 (CC199) Allelic profile: <i>aroE</i> 8; <i>gdh</i> 13; <i>gki</i> 14; <i>recP</i> 4; <i>spi</i> 17; <i>xpt</i> 4; <i>ddl</i> 14	ST199/5219
5239	Blood	ST186 Allelic profile: <i>aroE</i> 7; <i>gdh</i> 23; <i>gki</i> 1; <i>recP</i> 1; <i>spi</i> 14; <i>xpt</i> 28; <i>ddl</i> 31	ST186/5239
5221	Blood	ST199 (CC199)	ST199/5221
24190	Ear	ST1718 (CC1718) Allelic profile: <i>aroE</i> 1; <i>gdh</i> 5; <i>gki</i> 15; <i>recP</i> 5; <i>spi</i> 15; <i>xpt</i> 20; <i>ddl</i> 8	ST1718/24190
51862	Ear	ST177 (CC177) Allelic profile: <i>aroE</i> 7; <i>gdh</i> 14; <i>gki</i> 4; <i>recP</i> 12; <i>spi</i> 1; <i>xpt</i> 1; <i>ddl</i> 14	ST177/51862
53685	Ear	ST309 (CC309) Allelic profile: <i>aroE</i> 8; <i>gdh</i> 10; <i>gki</i> 2; <i>recP</i> 5; <i>spi</i> 9; <i>xpt</i> 48; <i>ddl</i> 6	ST309/53685
48498	Ear	ST2417 Allelic profile: <i>aroE</i> 7; <i>gdh</i> 13; <i>gki</i> 1; <i>recP</i> 1; <i>spi</i> 14; <i>xpt</i> 28; <i>ddl</i> 31	ST2417/48498
61884	Ear	ST177 (CC177)	ST177/61884
4514	Blood	ST43 (CC423) Allelic profile: <i>aroE</i> 1; <i>gdh</i> 10; <i>gki</i> 4; <i>recP</i> 1; <i>spi</i> 9; <i>xpt</i> 3; <i>ddl</i> 8	ST43/4514
4516	Blood	ST688 (CC426) Allelic profile: <i>aroE</i> 10; <i>gdh</i> 5; <i>gki</i> 4; <i>recP</i> 1; <i>spi</i> 15; <i>xpt</i> 1; <i>ddl</i> 6	ST688/4516
4530	Blood	ST1131 Allelic profile: <i>aroE</i> 7; <i>gdh</i> 13; <i>gki</i> 4; <i>recP</i> 6; <i>spi</i> 25; <i>xpt</i> 6; <i>ddl</i> 8	ST1131/4530
4561	Blood	ST655 Allelic profile: <i>aroE</i> 18; <i>gdh</i> 3; <i>gki</i> 4; <i>recP</i> 1; <i>spi</i> 15; <i>xpt</i> 1; <i>ddl</i> 14	ST655/4561
4562	Blood	ST462 Allelic profile: <i>aroE</i> 5; <i>gdh</i> 42; <i>gki</i> 52; <i>recP</i> 1; <i>spi</i> 9; <i>xpt</i> 1; <i>ddl</i> 11	ST462/4562

63387	Ear	ST177 (CC177)	ST177/63387
58616	Ear	ST549 (CC177) Allelic profile: <i>aroE</i> 13; <i>gdh</i> 14; <i>gki</i> 4; <i>recP</i> 12; <i>spi</i> 1; <i>xpt</i> 1; <i>ddl</i> 14	ST549/58616
60330	Ear	ST415 (CC415) Allelic profile: <i>aroE</i> 1; <i>gdh</i> 5; <i>gki</i> 12; <i>recP</i> 5; <i>spi</i> 14; <i>xpt</i> 15; <i>ddl</i> 31	ST415/60330

3.2.5 Pooled ST-typed isolate biofilm assay (CFU) analysis.

MLST typing of the isolates confirmed the unsurprising genetic diversity of the strains exhibiting variable biofilm phenotypes. It also enabled the identification of STs that included both blood and ear isolates. Examining strains belonging to the same serotype and ST might be expected to improve the chance of identifying significant effects of pH, Fe(III) supplementation and isolate source on biofilm phenotype, as the impact of differences in genetic background has been minimized. Accordingly, representative blood and ear isolates of ST232, ST233 and ST180 from serotype 3 and ST15 and ST130 from serotype 14 were selected for reanalysis of the viable count biofilm data in Sections 3.2.1.1 and 3.2.1.4, respectively. Similar analysis of serogroup 19 strains could not be undertaken, as none of the identified STs included both blood and ear isolates.

3.2.5.1 Serotype 3

CFU biofilm counts for pooled blood and pooled ear isolates within a particular ST (ST180 (7 blood and 6 ear isolates), ST232 (3 blood and 4 ear isolates) and ST233 (2 blood and 1 ear isolate)) were compared after growth in C+Y pH 7.4, C+Y pH 6.8, C+Y+Fe(III) pH 7.4 and C+Y+Fe(III) pH 6.8 to assess the influence of isolate source on biofilm formation within each ST. As seen in Figure 3.22, at pH 7.4, biofilm formation of blood isolates of ST232 and ST233 in C+Y as well as for ST232 and ST180 in C+Y+Fe(III) formed significantly greater biofilms than the respective ST-matched ear

isolates under the same conditions. Blood isolates of ST233 in C+Y+Fe(III) and ST180 in C+Y also had numerically greater biofilms than the respective ear isolates at pH 7.4, although this did not reach statistical significance. Fe(III) supplementation also significantly enhanced biofilm formation by ST232 blood isolates. In addition, ST233 blood isolates in C+Y formed significantly greater biofilms than ST232. Similarly, ST233 ear isolates in C+Y formed significantly greater biofilms than ST232 and ST180 ear isolates under the same conditions, while in C+Y+Fe(III), ST233 ear isolates also formed significantly greater biofilms than ST180 ear isolates.

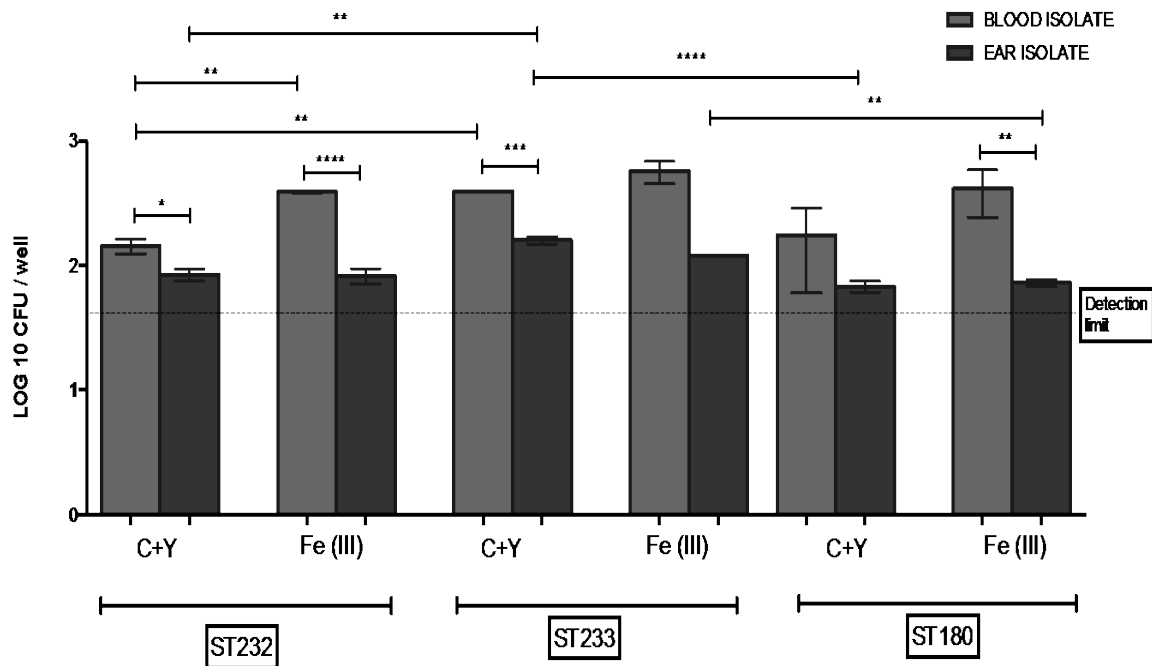


Figure 3.22. Biofilm formation by serotype 3 ST232, ST233 and ST180 blood and ear isolates at pH 7.4 (ST180 (7 blood and 6 ear isolates), ST232 (3 blood and 4 ear isolates) and ST233 (2 blood and 1 ear isolate)). Data are log₁₀ CFU per well (\pm SEM) for quadruplicate assays. Significance of differences between groups was examined using a two-tailed Student's *t*-test: *, $P < 0.05$; **, $P < 0.01$; ***, $P < 0.001$; ****, $P < 0.0001$.

At pH 6.8 (Figure 3.23) biofilm formation by ST232, ST233 and ST180 ear isolates in C+Y was significantly greater than that for the respective ST-matched blood isolates under the same conditions. Fe(III) supplementation also caused a significant reduction in biofilm formation of ear isolates for all STs. Biofilm formation by ST233 ear isolates in C+Y+Fe(III) was also significantly greater than that for ST180 and ST 232 ear isolates or ST233 blood isolates in the presence of Fe(III). Fe(III) supplementation did not significantly affect biofilm formation by blood isolates of any ST at this pH.

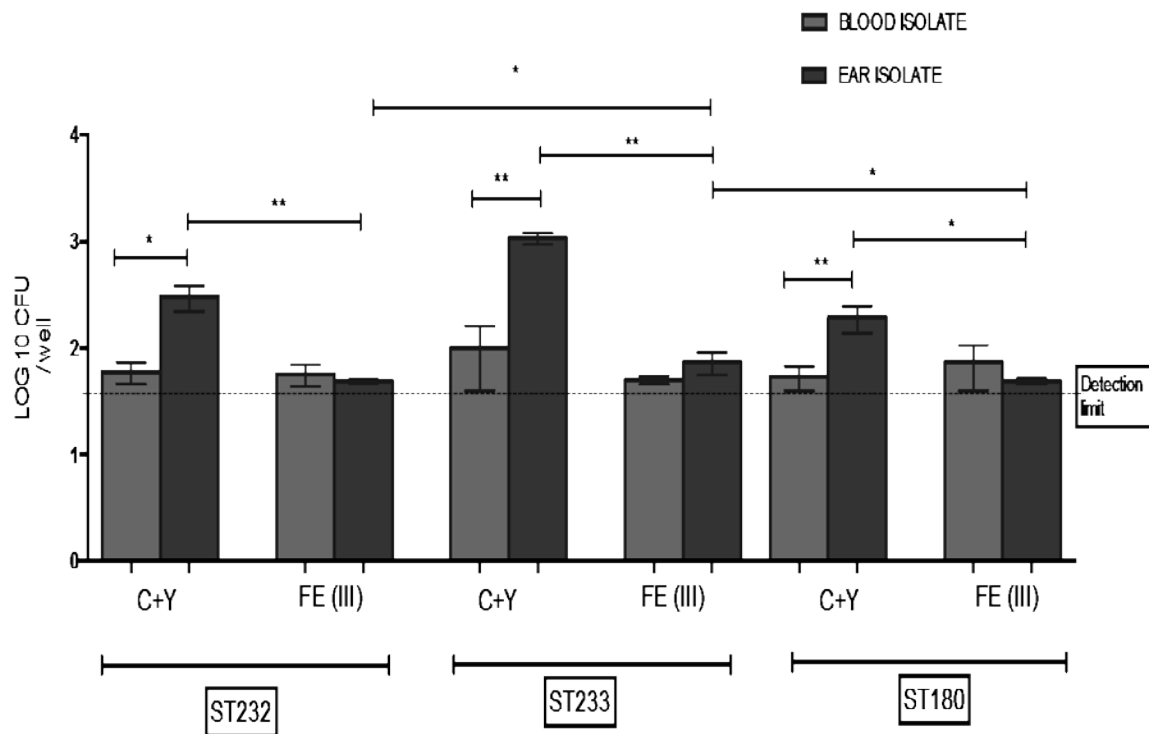


Figure 3.23. Biofilm formation by serotype 3 ST232, ST233 and ST180 blood and ear isolates at pH 6.8 (ST180 (7 blood and 6 ear isolates), ST232 (3 blood and 4 ear isolates) and ST233 (2 blood and 1 ear isolate)). Data are log₁₀ CFU per well (\pm SEM) for quadruplicate assays. Significance of differences between groups was examined using a two-tailed Student's *t*-test: *, $P < 0.05$; **, $P < 0.01$; ***, $P < 0.001$; ****, $P < 0.0001$.

3.2.5.2 Serotype 14

In C+Y pH 7.4 both blood and ear isolates of ST15 showed a significant ($P < 0.0001$) 2 log₁₀-fold increase in biofilm CFU counts compared to the ST130 clinical isolates under the same growth conditions (Figure 3.24). ST15 blood isolates in C+Y pH 7.4 showed a five-fold increase in biofilm formation compared to the respective ear isolates, although this did not reach statistical significance. At pH 7.4 ST130 ear isolates grown with or without Fe(III) supplementation showed significantly better biofilm formation than ST130 blood isolates ($P < 0.0005$). Neither ST15 nor ST130 blood isolates showed significantly higher biofilm formation than their respective ear isolates at this pH. Fe(III) supplementation significantly enhanced biofilm formation by all isolates except for ST15 blood isolates.

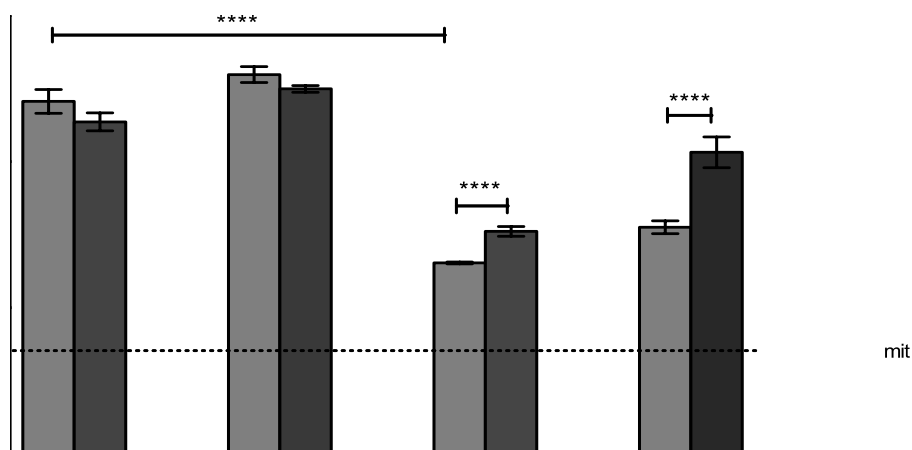


Figure 3.24 Biofilm formation by serotype 14 *S. pneumoniae* ST15 and ST130 (3 blood and 2 ear isolates for ST15 and ST130) at pH 7.4. Data are log₁₀ CFU per well (\pm SEM)

for quadruplicate assays. Significance of differences between groups was examined using a two-tailed Student's *t*-test: *, $P < 0.05$; **, $P < 0.01$; ***, $P < 0.001$; ****, $P < 0.0001$.

Similar to findings at pH 7.4, blood and ear isolates of ST15 produced significantly greater biofilms than the respective ST130 isolates (blood isolates, $P < 0.0005$; ear isolates, $P < 0.001$) at pH 6.8 (Fig. 3.25). Interestingly however, ST15 blood isolates produced significantly greater biofilms than ST15 ear isolates in both the presence and absence of Fe(III), while no significant differences were observed between ST130 blood and ear isolates. For both ST types Fe(III) supplementation at pH 6.8 did not appear to influence biofilm formation for either isolate source.

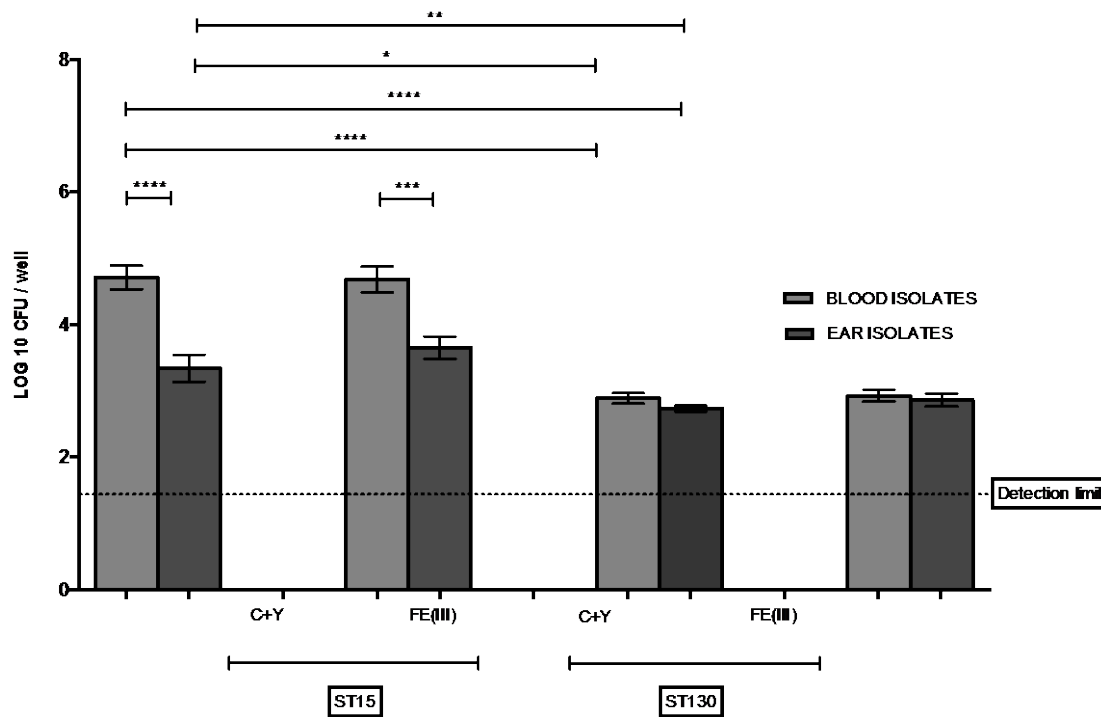


Figure 3.25. Biofilm formation by serotype 14 *S. pneumoniae* ST15 and ST130 blood and ear isolates at pH 6.8 (3 blood and 2 ear isolates for ST15 and ST130). Data are log₁₀ CFU per well (\pm SEM) for quadruplicate assays. Significance of differences between groups was examined using a two-tailed Student's *t*-test: *, $P < 0.05$; **, $P < 0.01$; ***, $P < 0.001$; ****, $P < 0.0001$.

3.3 Discussion

The formation of biofilms has been implicated in many studies as an important prerequisite for pneumococcal disease (Marks *et al.*, 2013; Moscoso *et al.*, 2006; Pettigrew *et al.*, 2014). Therefore it is important to understand the molecular determinants that regulate pneumococcal biofilm formation, particularly in the host environment, where pneumococci may encounter adverse environments such as antibiotics and host immune responses. This study aimed to investigate the role of clinical isolate source and Fe(III) supplementation in biofilm formation by 80 blood and ear isolates of *S. pneumoniae* belonging to serotypes/groups 3, 6, 9, 14 and 19, which were grown at either pH 7.4 or pH 6.8 to reflect the respective physiological conditions in the blood and ear niches.

Biofilm formation assays (Figures 3.1- 3.16) showing that most isolates formed biofilms appeared to concur with the findings of Camilli *et al.* (2011) and others (Allegrucci *et al.*, 2006; Chao *et al.*, 2014; Domenech *et al.*, 2014; Garcia-Castillo *et al.*, 2007) that biofilm formation is a common feature among pneumococcal strains. This study also found that in agreement with others (Allegrucci *et al.*, 2006; Camilli *et al.*, 2011; Domenech *et al.*, 2009; Hall-Stoodley *et al.*, 2008; Tapiainen *et al.*, 2010), serotypes 3 and 14 were the lowest and highest biofilm producers, respectively. Serotype 3 pneumococci are highly encapsulated and many studies have suggested that capsule expression interferes with biofilm formation (Allegrucci *et al.*, 2006; Domenech *et al.*, 2009; McEllistrem *et al.*, 2007; Waite *et al.*, 2001). Serogroup 6 pneumococci have also been described as significant biofilm formers, while serotype 14 are high biofilm producers (Allegrucci *et al.*, 2006; Domenech *et al.*, 2014; Domenech *et al.*, 2012).

When investigating the influence of Fe(III) supplementation on biofilm formation some strain variations were also observed, but generally biofilm formation of most blood and ear isolates was enhanced in the presence of Fe(III) at pH 7.4 for all serotypes/groups. This agreed with Trappetti *et al.* (Trappetti *et al.*, 2011) who found that biofilm formation of the type 2 strain D39 was significantly enhanced when supplemented with Fe(III) at pH 7.4. An interesting finding in this study was that at pH

6.8 Fe(III) supplementation did not result in significantly increased biofilm formation in most serotypes/groups, and actually inhibited biofilm formation in serotype 3 ear isolates. The reason for this is not clear. A possible contributing factor could be differences in the expression levels of iron transporter components PiuA (pneumococcal iron uptake) and PiaA (pneumococcal iron acquisition) when strains are grown at different pH. PiuA and PiaA transport systems are essential for iron uptake (Kadioglu *et al.*, 2008) and the possibility that these lipoproteins are expressed at lower levels at pH 6.8 warrants further investigation. Expression levels of the *luxS* gene at pH 7.4 vs pH 6.8 should also be investigated, as this system is known to impact *piuA* expression as well as biofilm formation in strain D39 (Trappetti *et al.*, 2011c).

In general, despite high strain-strain variation in biofilm formation by blood and ear isolates across all serotypes/groups, the viable count assays shown in Figures 3.1-3.8 indicated that differences in niche pH could influence biofilm formation capacity of the blood and ear isolates. Increased biofilm formation by either blood or ear isolates, where apparent, occurred primarily at their respective niche pH. That is, many blood isolates of serotypes/groups 3, 6, 9, 14 and 19 showed significant increases in biofilm formation at pH 7.4 relative to pH 6.8, while type 3 and group 19 ear isolates displayed significantly increased biofilm formation at pH 6.8. Exceptions to these generalised observations were also seen; some serogroup 6 and 9 blood and ear isolates showed variable phenotypic responses to pH, as well as the serotype 14 ear isolates which generally showed enhanced biofilm formation at pH 7.4.

A typical feature of bacterial biofilms is the extracellular matrix which provides protection and structure to the cell population within it (Moscoso *et al.*, 2009). The CV assay is a useful tool for rapid and simple assessment of biofilm formation differences between strains, as it stains the extracellular matrix as well as the aggregated bacterial cells (O'Toole 2011). The CV biofilm assays showed strain-strain variation in biofilm formation with respect to isolate source, pH and Fe(III), while some strains showed a general consistency with CFU observations. An example of this was seen for serotype 3 strains, with significant increases in biofilm formation being observed when blood and

ear isolates were grown at their respective niche pH of 7.4 and 6.8. Nevertheless, discrepancies were observed between the CFU and CV data in many cases. These are likely to be attributable to the fact that the former assay measures viable bacteria in dispersed biofilms, while the latter measures staining density of both live and dead bacteria as well as the extracellular matrix.

Similar to the CFU and CV biofilm assays, in general the microscopic images of the biofilms confirmed that biofilm formation was enhanced in most blood isolates at pH 7.4 in the presence of Fe(III), while on the other hand ear isolates showed enhanced biofilm formation at pH 6.8. Serotype 3 isolates tended to be low overall biofilm producers, while serotype 14 isolates generally showed high biofilm formation. These images also provided microscopic evidence that the presence of Fe(III) at pH 7.4 enhanced biofilm formation in most blood and ear isolates, while at pH 6.8 the influence of Fe(III) was either insignificant or inhibitory for biofilm formation.

An important challenge in this study was the occurrence in all the serotypes/groups analysed of marked variability in biofilm formation between isolates, which complicated interpretation of findings regarding the influence of clinical source, Fe(III) or pH on *in vitro* biofilm formation. Indeed, marked variation in biofilm formation capacity among individual pneumococcal strains has been demonstrated by others (Camilli *et al.*, 2011; Tapiainen *et al.*, 2010). Genetic diversity is a characteristic feature of *S. pneumoniae* with 93 different serotypes superimposed on over 5000 clonal lineages recognizable by MLST (Enright & Spratt 1998). Thus, much of the strain-strain variation in biofilm phenotype might be attributable to the presence of multiple STs within a serotype/group. MLST typing was carried out on 63 blood and ear isolates belonging to serotypes/groups 3, 14 and 19. Data presented in Tables 3.9 - 3.11 confirmed marked diversity of STs within all three serotypes/groups tested, particularly for group 19 isolates, with 14 distinct STs identified amongst the 17 tested strains. Serogroup 19 comprises several structurally-related, immuno-cross-reactive capsular types (19A, 19B, 19C and 19F), which may further contribute to genetic diversity within this group. The marked variation in biofilm formation phenotype between strains from different clinical

sources, and the variable influence of pH and Fe(III) supplementation may well be a reflection of this diversity.

Importantly, MLST typing of serotype 3 or 14 strains in this study also identified multiple examples of blood and ear isolates belonging to the same ST. This enabled analysis of the impact of isolate source, pH and Fe(III) on biofilm formation phenotype, without the complication of diversity of genetic background. At pH 7.4 (the physiological pH of the blood (Jahn, 2001)), serotype 3 ST180, ST232 and ST233 blood isolates formed significantly greater biofilms than their respective ST-matched ear isolates. Fe(III) supplementation significantly increased biofilm formation for the ST232 blood isolates, but not for any of the other strains. At pH 6.8 (the physiological pH of the middle ear cavity (Jahn, 2001)), ear isolates of all three STs tested displayed significantly better biofilm formation than the respective ST-matched blood isolates. Moreover, Fe(III) supplementation significantly reduced biofilm formation by the ear isolates, but not the blood isolates. These findings suggest that isolates from a given host niche have somehow adapted to form better biofilms at the pH commensurate with the respective niche. Between the three STs, isolates belonging to ST233 also showed significantly higher biofilm formation at both pH 7.4 and pH 6.8. This suggests that much of the strain-strain diversity in biofilm phenotype observed within a given serotype/group may indeed be attributable to diversity in genetic backgrounds therein.

For serotype 14, the ability of ST15 isolates to form biofilms was significantly (10-100-fold) greater than ST130 isolates regardless of pH or Fe(III) supplementation, confirming the impact of genetic background on biofilm phenotype. Interestingly, at pH 7.4, ST130 ear isolates formed significantly greater biofilms than blood isolates, while there was no effect of clinical isolate source for ST15 isolates. Fe(III) supplementation at pH 7.4 significantly enhanced biofilm formation for both ear and blood isolates for ST130 and ear isolates for ST15; a similar trend (albeit non-significant) was seen for ST15 blood isolates. This differs from findings for type 3 strains, where only blood isolates were stimulated by Fe(III). At pH 6.8, Fe(III) supplementation had no effect on biofilm formation by any of the type 14 strains. However, in marked contrast to findings

for type 3 strains, ST15 blood isolates produced significantly greater biofilms than ear isolates. Thus, the apparent adaptation of blood and ear isolates observed for serotype 3 ST180, ST232 and ST233 strains, whereby biofilm formation capacity is optimized at the pH of the respective physiological niche, is not seen in serotype 14 ST15 or ST130 strains.

The work described in this Chapter has identified marked discrepancies between the influence of Fe(III), pH and isolate source on biofilm phenotype in the various serotypes/groups and ST types. Importantly, however, it has also identified distinct differences in behavior in the *in vitro* biofilm assays between blood and ear isolates belonging to the same serotype/group and ST type. It is therefore important to further investigate these differences using *in vivo* models to determine whether they have relevance in terms of pathogenesis of pneumococcal disease.

Chapter 4: Influence of isolate source on virulence phenotype of serotype 3 *S. pneumoniae* clinical isolates

4.1 Introduction

The ability to form biofilms has in recent years been recognized as a necessary step in the pathogenesis of OM and other pneumococcal diseases, where strong correlations between biofilm formation and colonisation and virulence in mice have been reported in several studies (Munoz-Elias *et al.*, 2008; Oggioni *et al.*, 2006; Trappetti *et al.*, 2009). More recent studies (Marks *et al.*, 2013; Pettigrew *et al.*, 2014) have further illustrated the importance of biofilms to pneumococcal virulence. These studies demonstrated that invasive disease was triggered by bacteria from dispersed biofilms, which exhibited differential genomic expression profiles for virulence-related genes, relative to planktonic and sessile biofilm modes.

In the previous chapter, the influence of isolate type, pH and Fe(III) supplementation on biofilm formation in 25 blood and ear isolates belonging to serotype 3, a type that is frequently associated with both OM and invasive disease, was investigated (see Section 3.2.1). The primary findings in this study indicated a strong association between serotype 3 clinical isolate source and their optimal pH for biofilm formation (see Section 3.2.1.1). Microscopic examination of crystal violet-stained biofilms confirmed that robust biofilms were formed by blood isolates only at pH 7.4 and were boosted further by Fe(III), whereas ear isolates formed robust biofilms only at pH 6.8 and in the absence of Fe(III) (see Section 3.2.2). Further analysis revealed that biofilm formation between clonally related serotype 3 and serotype 14 blood and ear isolates was markedly variable; analysis of serotype 3 ST-matched isolates indicated an influence of isolate source on biofilm formation (see Section 3.2.3.1), but this was not seen for ST-matched serotype 14 isolates (see Section 3.2.3.2).

S. pneumoniae genetic diversity results in important phenotypic differences in disease potential. It has been reported that 20 of the 93 known capsular serotypes account

for 85% of pneumococcal infections (Kalin, 1998) and certain STs are more strongly associated with invasive disease than others (Brueggemann *et al.*, 2003; Hanage *et al.*, 2005). The work described in this Chapter further examines the *in vitro* and *in vivo* phenotypes of isolates belonging to the same serotype and ST, to determine whether there are any associations between isolate source, biofilm formation and capacity to cause invasive vs localized infections.

4.2 Results

4.2.1 Influence of LuxS on serotype 3 biofilm formation.

In the previous chapter a relationship between the site of isolation and ability to form biofilms under different pH and Fe(III) conditions was identified in clinical isolates belonging to serotype 3 (see Sections 3.2.1 and 3.2.2). To test whether the iron- and pH-dependent biofilm formation phenotype of serotype 3 strains is linked to the activity of the LuxS quorum sensing system, a relationship previously identified in the serotype 2 strain D39 (Trappetti *et al.*, 2011c), the level of *luxS* expression was measured using real-time RT-PCR (see Section 2.15). For this analysis, one blood isolate and one ear isolate belonging to each of the three major STs (ST180, ST232 and ST233) were selected.

The real-time RT-PCR analysis showed differences in *luxS* expression levels between the strains and growth conditions (Figure 4.1), which closely paralleled the pattern of biofilm formation previously observed for the respective strains (see Figure 3.22). In the blood isolates ST180/15, ST232/1 and ST233/3, *luxS* expression was significantly higher when cells were grown at pH 7.4 in the presence of Fe(III) compared to all other growth conditions ($P < 0.001$, $P < 0.001$, and $P < 0.01$, respectively). In contrast, for the ear isolates ST180/2, ST232/11 and ST233/13, *luxS* expression was significantly higher when cells were grown at pH 6.8 without Fe(III) supplementation, than under any of the other conditions ($P < 0.001$, $P < 0.05$, and $P < 0.01$, respectively). However, for each ST type pair, the overall level of expression of *luxS* in the ear isolate

was significantly lower than that of the corresponding blood isolate under their respective optimal conditions ($P < 0.001$, $P < 0.001$, and $P < 0.01$, for ST180, ST232 and ST233, respectively).

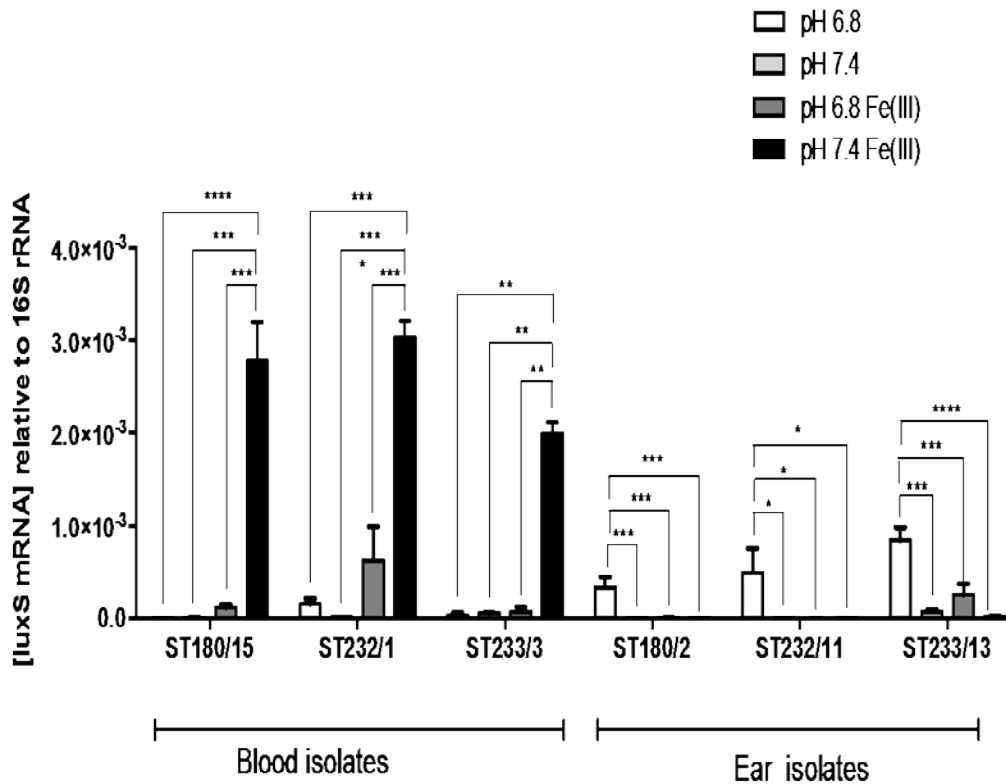


Figure 4.1. Expression of *luxS* relative to 16S rRNA in blood and ear isolates of ST180, ST233 and ST232. Expression of *luxS* relative to 16S rRNA in the indicated clinical isolates grown either at pH 7.4 or 6.8, with or without addition of 100 μ M Fe(III). Data are the mean \pm standard deviation (SD) for three independent experiments (*, $P < 0.05$; **, $P < 0.01$; ***, $P < 0.001$; 2-tailed Student's *t*-test).

To further confirm the role of *luxS* in biofilm formation by serotype 3 strains, *luxS* was deleted in the ear isolates mentioned above and the mutants were then tested for biofilm forming ability in C+Y media at pH 6.8 (see Section 2.10). Viable counts of the dispersed biofilms revealed a significant reduction in biofilm formation for the *luxS* mutants of the three ear isolates compared to the wild type when grown in C+Y at pH 6.8 ($P < 0.001$ for ST180/2 and ST233/13; $P < 0.01$ for ST232/11) (Figure 4.2). Microscopic examination after crystal violet staining confirmed the results of viable counts (Figure 4.3).

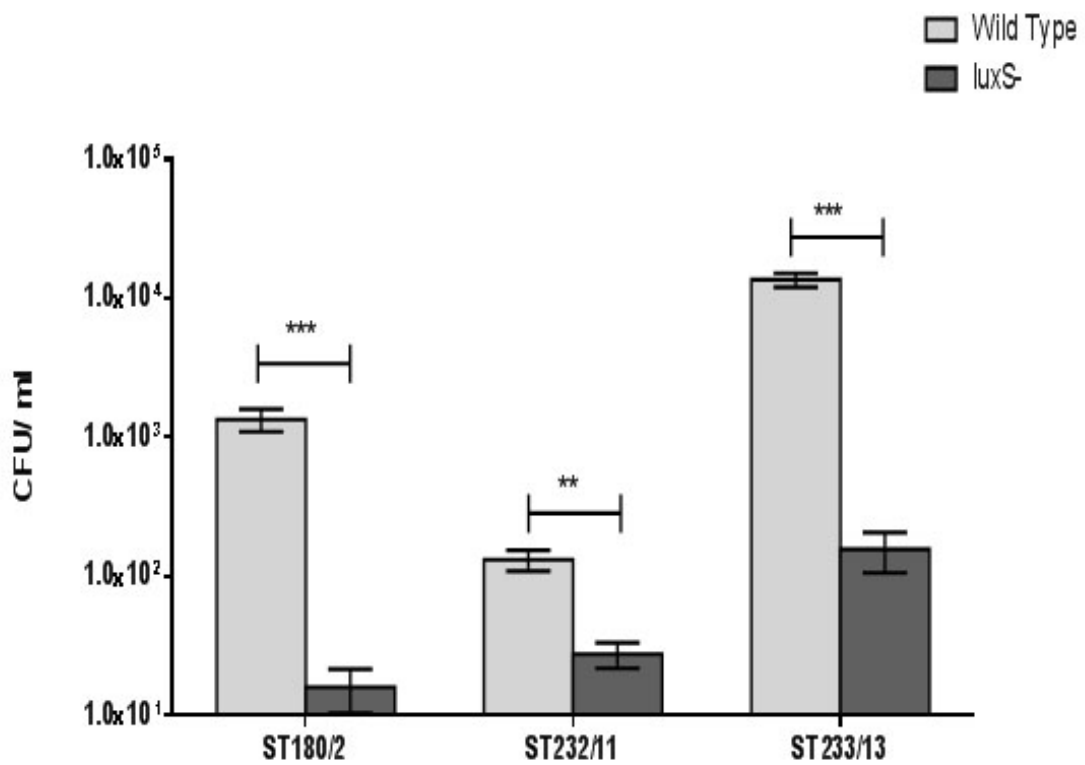


Figure 4.2. Effect of *luxS* mutation on biofilm formation by ear isolates. Effect of *luxS* mutation on biofilm formation by ear isolates, determined by viable count. Data are the mean \pm SD for three independent experiments (**, $P < 0.01$; ***, $P < 0.001$; 2-tailed Student's *t*-test)

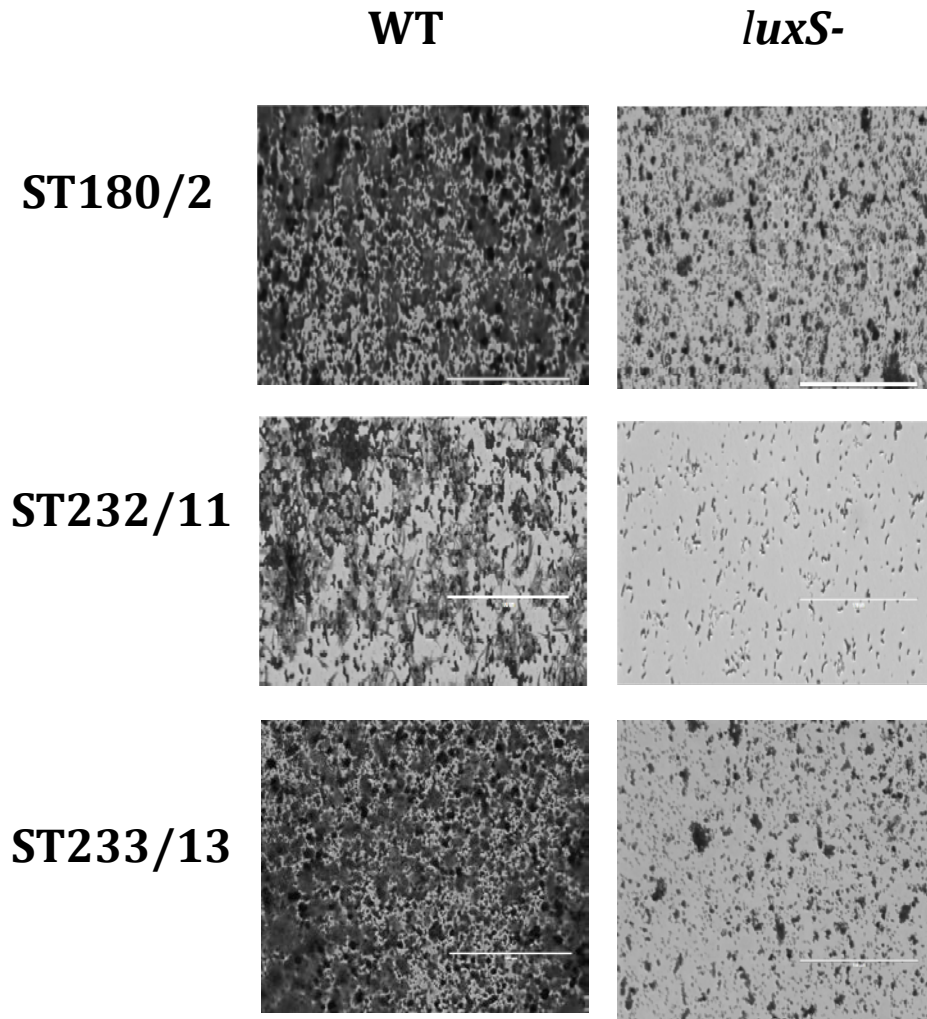


Figure 4.3. Microscopic analysis of stained biofilms. Microscopic analysis of crystal violet stained biofilms formed at pH 6.8 by ear isolates (WT=wild type) and their respective *luxS* mutants (*luxS*⁻). Microscopic examination of the dispersed biofilms revealed a significant reduction in biofilm formation for the *luxS* mutants of the three ear isolates compared to the wild type when grown in C+Y at pH 6.8 . Scale bar: 100 μ m.

4.2.2. Investigation of *piuA* expression in relation to Fe(III), pH and isolate source.

Since iron has been shown to stimulate biofilm formation in the blood isolates, but not ear isolates, the expression level of *piuA*, which encodes the major pneumococcal iron uptake system was quantified (see Section 2.15). A significantly higher level of expression of *piuA* was observed in blood isolates grown at pH 7.4 in the presence of Fe(III) compared with other growth conditions ($P < 0.01$, $P < 0.001$ and $P < 0.01$, for ST180/15, ST231/1 and ST233/3, respectively) (Figure 4.4). In contrast, *piuA* expression was very low in all the ear isolates, and there was no evidence for up-regulation of *piuA* in these isolates in the presence of iron, except for a slight increase for ST233/13 at pH 7.4 which was however insignificant.

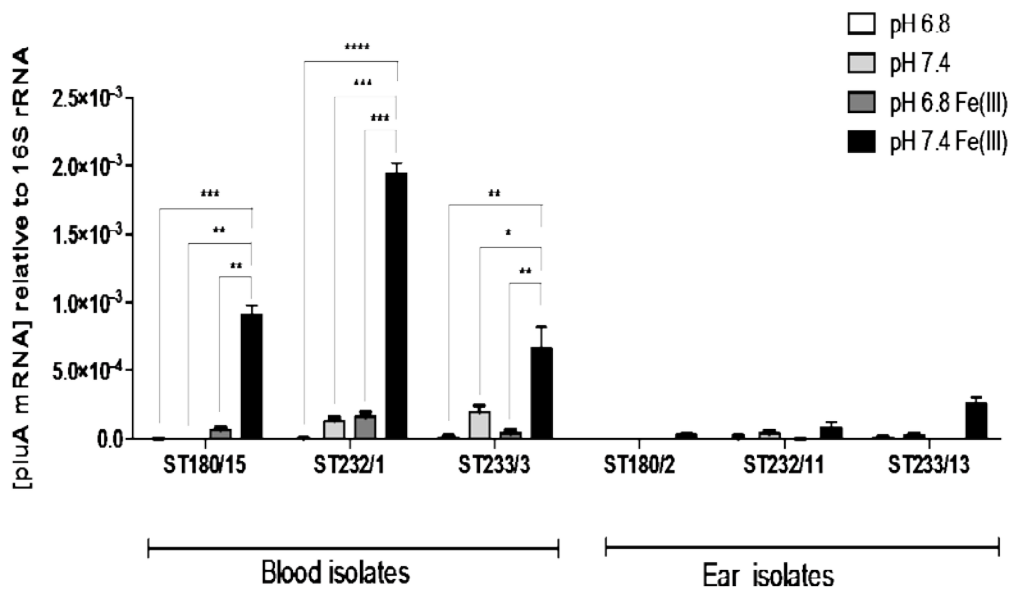


Figure 4.4. Expression of *piuA* relative to 16S rRNA in blood and ear isolates of ST180, ST233 and ST232. Expression of *piuA* relative to 16S rRNA in the indicated clinical isolates grown either at pH 7.4 or 6.8, with or without addition of 100 μ M Fe(III). Data are the mean \pm SD for three independent experiments (*, $P < 0.05$; **, $P < 0.01$; ***, $P < 0.001$; 2-tailed Student's *t*-test).

4.2.3 Investigation of transformability of serotype 3 strains.

Induction of the competence state has been shown to parallel biofilm formation in *S. pneumoniae* (Trappetti *et al.*, 2011a; Trappetti *et al.*, 2011c), and so the transformability of the six serotype 3 clinical isolates, as well as the reference invasive type 2 strain D39, was measured in planktonic cells grown at pH 7.4 and pH 6.8 (see Section 2.9), where each transformation reaction contained approximately 10^7 competent pneumococci. The transformability of the strains was found to be strongly influenced by the pH. Blood isolates exhibited a significantly greater propensity to take up external DNA at pH 7.4 ($P < 0.001$, $P < 0.001$ and $P < 0.01$ for ST180/15, ST232/1 and ST233/3, respectively), as did the reference strain D39. In contrast, the ear isolates showed higher rates of transformability at pH 6.8 ($P < 0.001$, $P < 0.001$ and $P < 0.01$ for ST180/2, ST232/11 and ST233/13, respectively) (Figure 4.5). Indeed, for the ST180 and ST232 strains, the blood isolates were completely untransformable at pH 6.8, while the ear isolates were not transformable at pH 7.4. Strains of ST233 were transformable under both conditions tested, but a significant increase in efficiency was observed for the blood isolate at pH 7.4 and ear isolate at pH 6.8.

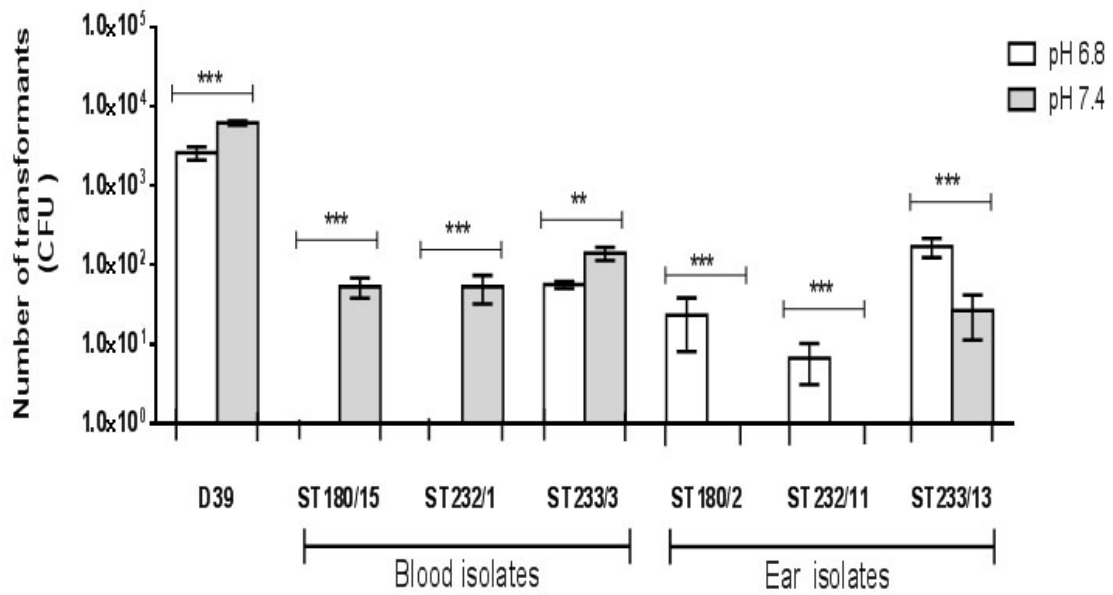


Figure 4.5. Transformability of the reference invasive strain D39 and serotype 3 blood and ear isolates. Transformability of the reference invasive strain D39 and serotype 3 blood and ear isolates grown at either pH 7.4 or 6.8. Data are the total number of transformants (mean \pm SD for three biological replicates) (**, $P < 0.01$; ***, $P < 0.001$; 2 tailed Student's t -test).

4.2.4. Capsular polysaccharide production by serotype 3 strains.

In order to investigate if phenotypic differences seen so far between the isolates within a ST were the result of differences in the amount of CPS produced, this was quantitated by uronic acid assay for blood isolates ST180/15, ST232/1 and ST233/3 and ear isolates ST180/2, ST232/11 and ST233/13 (see Section 2.12.2). As shown in Figure 4.6, CPS production was similar across all strains. Analysis of pooled CPS production data for the three blood vs three ear isolates (Figure 4.7) also showed no significant differences in CPS production between blood and ear isolates.

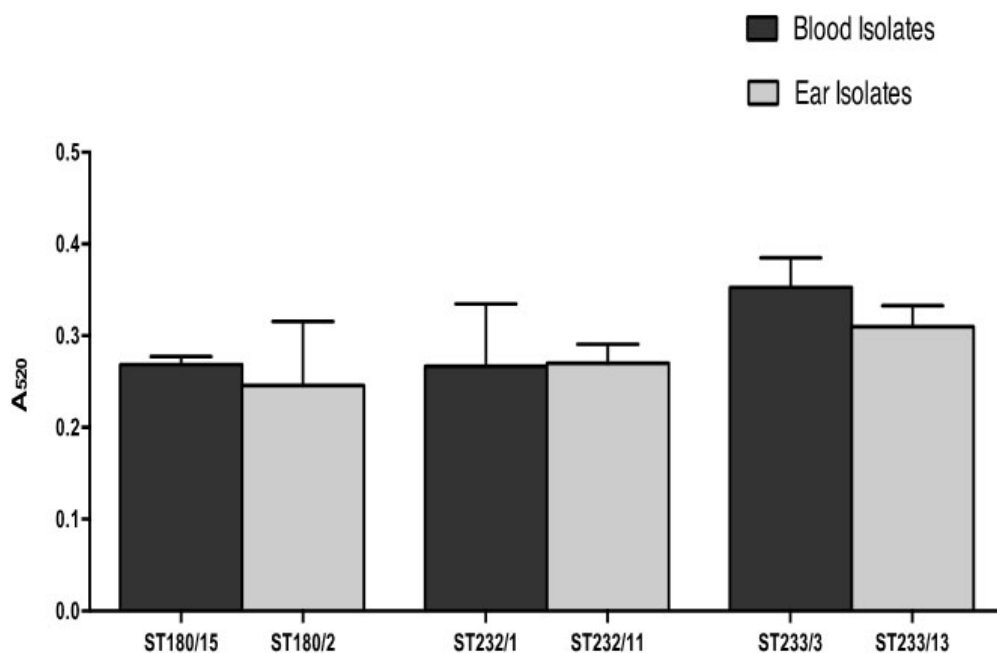


Figure 4.6. CPS production by ST180, ST232 and ST233 blood and ear isolates at pH 7.4. CPS production at pH 7.4 was determined by uronic acid assay (Section 2.12.2). Data are A₅₂₀ (mean \pm standard deviation), Significance of differences between groups was examined using a two-tailed Student's T-Test: (**, $P < 0.01$; ***, $P < 0.001$; 2 tailed Student's t -test).

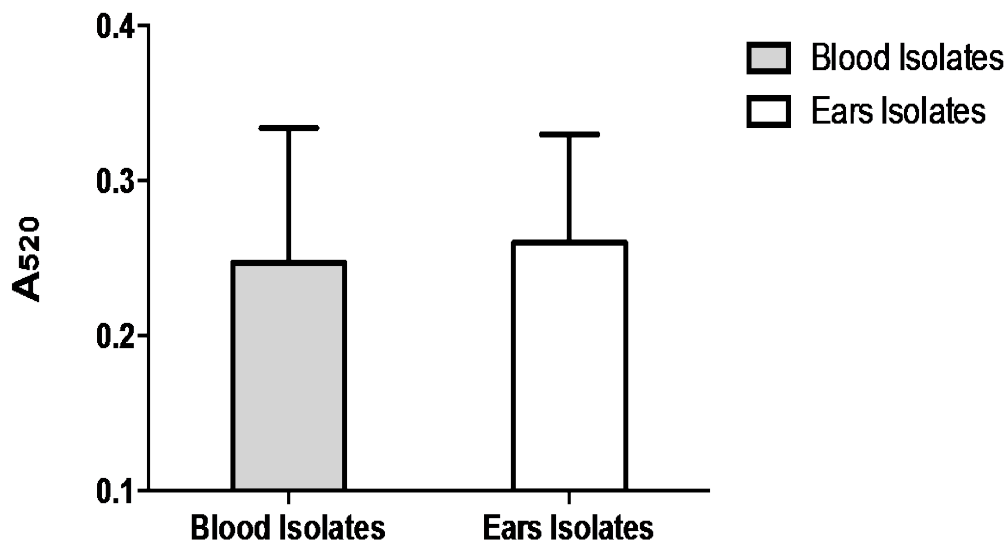


Figure 4.7. CPS production by pooled blood and ear isolates at pH 7.4. CPS production at pH 7.4 for pooled blood and ear isolates of ST180, ST232 and ST233 were quantitated by uronic acid assay. Data are A₅₂₀ (\pm SD).

4.2.5. Virulence phenotypes of serotype 3 strains.

The virulence profile of the clinical isolates was then investigated in a murine nasopharyngeal inoculation model, which mimics the natural route of infection for *S. pneumoniae* (see Section 2.18). Briefly, female outbred 5–6 week old Swiss mice were anaesthetized and inoculated intranasally with 1×10^7 CFU of *S. pneumoniae* (confirmed retrospectively by viable count) in a volume of 10 μ l. Groups of 15 mice were inoculated for each strain and five randomly selected mice from each group were euthanized by CO₂ asphyxiation at 24, 48 or 72 h post infection. Nasal wash, nasopharyngeal tissue, ear tissue, lung, brain and blood samples were collected and processed. Samples were serially diluted and plated onto blood agar plates for enumeration of viable pneumococci.

At all the time points examined (24, 48 and 72 h post infection), the majority of mice in each group infected with blood isolates (ST180/15, ST232/1 or ST233/3) showed bacteremia, whereas no bacteremia could be detected in any of the mice in groups

challenged with the ear isolates (ST180/2, ST232/11 or ST233/13) (Figure 4.8C). Collectively, the degree of bacteremia in blood isolates was significantly greater than the combined ear isolate groups at all time points ($P < 0.001$). When individual strain pairs within a ST type were compared, the level of bacteremia in the ST180/15 group was significantly greater than the ST180/2 group at all time points ($P < 0.05$), while bacteremia levels in the ST232/1 and ST233/3 groups were significantly greater than that for ST232/11 and ST233/13, respectively, at 48 h ($P < 0.05$). The situation was reversed in the nasopharyngeal tissue (Figure 4.8A), where blood isolates as a whole were inferior to ear isolates in terms of overall colonisation levels at 48 and 72 h ($P < 0.001$ in both cases). Comparing the individual ST types, ST232/11 colonized the nasopharyngeal tissue to a significantly greater extent than ST232/1 at both 48 and 72 h ($P < 0.05$ and $P < 0.01$, respectively), while ST180/2 and ST233/13 exhibited significantly higher colonisation at 72 h than the corresponding ST-matched blood isolate ($P < 0.01$ and $P < 0.05$, respectively). Bacteria were detected in ear tissue samples only in groups challenged with the ear isolates, and this difference was statistically significant ($P < 0.05$) at both 48 and 72 h (Figure 4.8B). Interestingly, at 24 h post-infection, pneumococci could not be detected in the lungs of any of the mice challenged with blood isolates, in spite of significant bacteremia in the majority of animals in each ST group (Figure 4.8F). Moreover, only 4 of the 15 mice challenged with blood isolates had evidence of pneumococci in the lungs at either 48 or 72 h. In contrast, no bacteria could be detected in the lungs of any of the mice challenged with the ear isolates. Similar findings were observed in brain tissue (Figure 4.8E). It is also interesting to note that pneumococci could not be detected in nasopharyngeal washes of any mice 24 h post infection (Figure 4.8D). At 48 h, less than half of the mice had pneumococci in nasal wash fluid, with fewer again at 72 h.

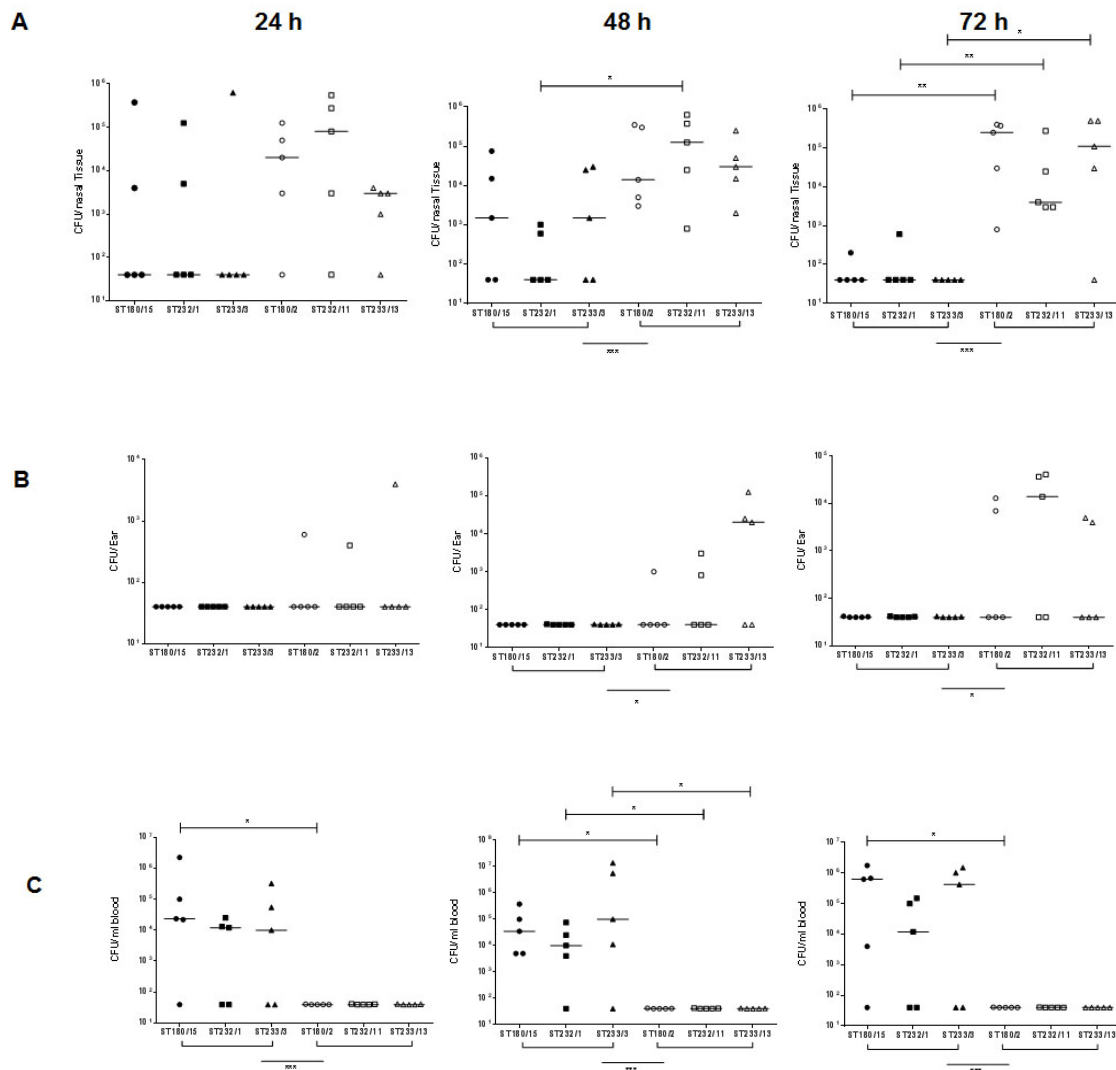


Figure 4.8A-C. Virulence phenotypes of blood and ear isolates. Groups of 15 mice were infected intranasally with 10^7 CFU of the indicated strain. At the indicated times, 5 mice from each group were euthanised and numbers of pneumococci in the indicated tissues were quantitated. (A) nasopharyngeal tissue; (B) ear; (C) blood. Viable counts are shown for each mouse at each site; horizontal bars indicate the median value for each group/time point. Blood isolates are represented by solid symbols; ear isolates are represented by open symbols. Differences between groups were analyzed by 1-tailed Mann-Whitney U test (*, $P < 0.05$; **, $P < 0.01$; ***, $P < 0.001$).

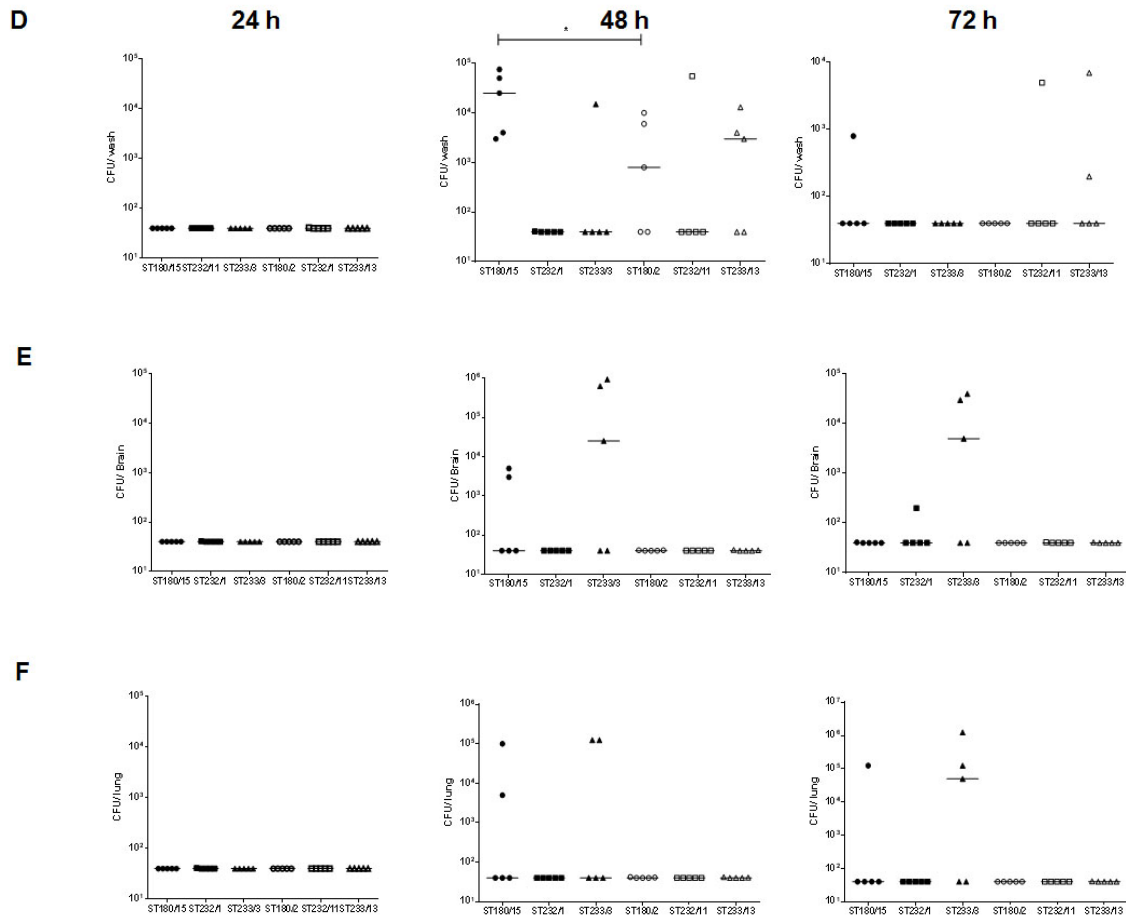


Figure 4.8D-F. Virulence phenotypes of blood and ear isolates (Continued). (D) Nasal wash; (E) brain; (F) lung. Viable counts are shown for each mouse at each site; horizontal bars indicate the median value for each group/time point. Blood isolates are represented by solid symbols; ear isolates are represented by open symbols. Differences between groups were analyzed by 1-tailed Mann-Whitney U test (*, $P < 0.05$).

4.3 Discussion

S. pneumoniae is a diverse and adaptable pathogen, capable of surviving in a range of niches within its human host. Previous studies from our laboratory have identified changes in *in vivo* transcriptional profile within a given strain that either facilitate survival in distinct host niches (nasopharynx, lungs, blood and brain), and/or aid progression from one niche to another (LeMessurier *et al.*, 2006; Mahdi *et al.*, 2008; Mahdi *et al.*, 2012; Ogunniyi *et al.*, 2012). However, genetic differences between strains may also result in pneumococci with inherent tropism for one niche over another. Studies in animal models suggest that both capsular and non-capsular loci contribute to these differences in *in vivo* phenotype (Kelly *et al.*, 1994; McAllister *et al.*, 2011), but interpretation of molecular epidemiological analyses of human isolates is complicated by the vast genetic diversity of strains. In Chapter 3, phenotypic differences between clinical isolates from either sepsis or OM (n = 12 and 13, respectively) belonging to serotype 3, an important cause of both systemic and localized pneumococcal infections, were investigated. It was demonstrated that while the blood isolates were more capable of forming biofilms at pH 7.4 than ear isolates, especially with 100 μ M Fe(III), the ear isolates were more capable of forming biofilms at pH 6.8, and at this pH, Fe(III) was inhibitory (see Section 3.3).

In this Chapter, more detailed phenotypic comparisons of matched pairs of isolates from either the blood or ear belonging to three dominant MLST types (ST180, ST232 and ST233) were conducted. It was previously reported that the LuxS quorum sensing system is a central regulator of biofilm formation in the invasive type 2 *S. pneumoniae* strain D39 (Trappetti *et al.*, 2011c), and in the present study, there was again a close parallel between expression of the *luxS* gene and biofilm formation at the permissive pH for the respective groups. The observed increased *luxS* expression in both isolate types also concurred with recent studies demonstrating that *luxS* was responsible for the regulation of pneumococcal biofilms in both human respiratory epithelial cells (HREC) and on abiotic surfaces (Vidal *et al.*, 2013). Although the level of *luxS*

expression in each of the ear isolates at pH 6.8 in the absence of Fe(III) was significantly greater than that under the other environmental conditions, they were still significantly lower than the blood isolates of the corresponding ST type under optimal conditions. The apparently lesser importance of *luxS* in biofilm formation in the ear isolates compared to the blood isolates is not understood and warrants further investigation. Given that *luxS* has been demonstrated to be important in virulence (Stroehrer *et al.*, 2003) it will be helpful to further examine this phenomenon in other clonally related pneumococci of different serotypes/serogroups. This may allow further understanding of the role of *luxS* in the virulence of pneumococci isolated from different clinical sites or environments.

Despite the decreased *luxS* expression observed in the ear isolates compared to the blood isolates, the significant reduction of biofilm formation observed through the mutagenesis of *luxS* in the ear isolates, as demonstrated by microscopy and biofilm assays, concurred with findings of Trappetti *et al.* (2011c) for D39, and validated the important role of *luxS* in biofilm formation. The link between the *luxS* system and genetic competence previously observed in D39 also held for the type 3 isolates, with maximal transformation efficiencies observed under the same environmental conditions that were most permissive for biofilm formation. This observation parallels those of Marks *et al.* (2012) who demonstrated high transformation efficiency of pneumococci in a novel biofilm model *in vitro*, which mimicked specific environmental conditions of the nasopharynx including lower temperature, limited nutrient availability and epithelial cell interaction.

The stimulatory effect of Fe(III) on biofilm formation by the blood isolates at pH 7.4 was matched by upregulated expression of *piuA*, which encodes the major pneumococcal iron transporter. In contrast, *piuA* expression was negligible in blood isolates at the non-permissive pH 6.8 or in the absence of Fe(III), and in the ear isolates under any of the conditions tested. These observations further support an association between isolate source and the optimum pH and Fe(III) level for biofilm formation.

The consistent and stark phenotypic distinction between blood and ear isolates in terms of preferred pH and requirement for Fe (III) for optimal biofilm formation suggests that there are fundamental differences between *S. pneumoniae* strains belonging to the same clonal lineage that enable adaptation to the distinct host niches from whence they were isolated. This adaptation to the human niche was closely mimicked by the behavior of the various strains in a mouse intranasal challenge model. All three blood isolates were poor colonizers of the nasopharynx, yet were able to readily spread directly to the blood in most animals, largely bypassing the lungs. Moreover, none of the blood isolates ever spread to the ear compartment. Conversely, the ear isolates were able to stably colonize the nasopharyngeal tissue of the vast majority of animals, but never spread to the blood, brain or lungs. Nearly half of the animals challenged with OM isolates had pneumococci in the ear compartment by 72 h. While the absence of ear isolates from a specific tissue might suggest that this site is bypassed during disease progression, it is also possible that bacteria were actually present in these sites at early times, but were cleared by host immune responses by 24 h. Therefore, examining host immune response gene expression patterns in mice challenged with either blood or ear isolates may provide further insights into the underlying mechanisms of tissue tropism.

The low numbers of pneumococci recovered in these studies from the nasal wash fraction despite high numbers of pneumococci present in the nasal tissue (Figure 4.8D), implies that colonizing pneumococci were very tightly adhered to the nasopharyngeal epithelium, perhaps even penetrating the mucosa. In future studies it would therefore be desirable to perform *in vitro* adherence and invasion assays of blood and ear isolates on Detroit 562 (human nasopharyngeal) cells.

The antiphagocytic polysaccharide capsule surrounding *S. pneumoniae* is a major virulence factor and within a serotype, capsule thickness is directly related to virulence (Kadioglu *et al.*, 2008). However, this cannot account for the differences in virulence phenotype between type 3 blood and ear isolates, as quantitation of CPS levels revealed no significant differences between strains from one niche vs the other. Thus, unless

relative CPS production by the various strains *in vivo* differs markedly from relative *in vitro* levels, non-capsular factors are largely responsible for the distinct virulence phenotypes.

The fact that strains belong to the same serotype and ST does not rule out genetic differences as the basis for distinct virulence profiles, particularly since clonally related strains may have acquired distinct accessory regions by horizontal gene transfer, or undergone minor DNA changes (e.g. point mutations or small insertions or deletions) outside of the housekeeping genes that determine MLST. Another possible mechanism for the distinct phenotypes may be differences in transcription patterns of otherwise similar genomes, or epigenetic effects. Manso *et al.* (2014) reported that switching of pneumococci between opacity phase variants that favour asymptomatic carriage vs invasive disease was impacted by genetic rearrangements in a Type I restriction-modification system (SpnD39III) which is ubiquitous in pneumococci. By utilizing single-molecule real-time (SMRT) methylomics, they demonstrated that the rearrangements gave rise to six alternative specificities with distinct methylation patterns. These SpnD39III variants exhibited distinct gene expression profiles and resulted in distinct virulence phenotypes in experimental infection; *in vivo* selection for switching between SpnD39III variants was also demonstrated.

This study has clearly shown that stable adaptation of pneumococci to distinct host niches occurs within clonal lineages (for journal publication of this study please refer to Appendix A). Thus, molecular epidemiological studies aimed at associating MLST type with potential to cause invasive versus non-invasive disease should be interpreted with considerable caution. It is now clear that accessory regions outside the core pneumococcal genome are major determinants of virulence phenotype in both humans and animal models. Identification of multiple ST-matched pairs of *S. pneumoniae* serotype 3 strains with distinct human tissue tropism and virulence profile in mice provides a unique opportunity to identify accessory regions or polymorphisms within the core genome common to isolates from one niche versus the other by genome sequence

analysis. This, in turn, will permit direct testing of the role of identified regions in pathogenesis by targeted mutagenesis.

Chapter 5: Influence of isolate source on virulence of serotype 14 *S. pneumoniae*

5.1 Introduction

In Chapter 3, the influence of isolate source on biofilm formation between clonally related serotype 3 and serotype 14 blood and ear isolates was found to be markedly distinct. While isolate source influenced biofilm formation capacity in ST-matched serotype 3 isolates, this was not observed for similarly matched serotype 14 isolate. Further investigations of the ST-matched serotype 3 blood and ear isolates in Chapter 4 demonstrated that the isolates differed markedly in both *in vitro* and *in vivo* phenotypes, according to clinical site of isolation, suggesting stable niche adaptation within a clonal lineage (see also Trappetti *et al.* (2013)).

Apart from the aforementioned studies of serotype 3 isolates, the relationship, if any, between clinical isolate source and pneumococcal virulence phenotype has not been fully investigated. Serotype 14 is a representative serotype with high invasive disease potential (Brueggemann *et al.*, 2003; Kronenberg *et al.*, 2006; Sleeman *et al.*, 2006), which along with serotypes 6B, 19F, 18C, 9V and 23F is responsible for over 78% of invasive infections in small children (Butler *et al.*, 1995; Sniadack *et al.*, 1995). In an experimental rabbit meningitis model, more severe inflammatory responses were observed after challenge with strains belonging to serotypes 6B, 14 and 23F, compared to the other tested serotypes (Engelhard *et al.*, 1997). Serotype 14 *S. pneumoniae* is one of the commonest etiologic agents of pneumonia in Latin America, the UK and Spain (Bewick *et al.*, 2012; Burgos *et al.*, 2013; Gentile *et al.*, 2012) and OM in children under 5 years old (Rodgers *et al.*, 2009). Serotype 14 is also one of the most highly prevalent *S. pneumoniae* serotypes in the world (Butler *et al.*, 1995; Kalin, 1998; Robbins *et al.*, 1983) including both carriage and invasive disease isolates (Sandgren *et al.*, 2004). This serotype also exhibits high rates of antimicrobial resistance and biofilm formation capacity (Hall-Stoodley *et al.*, 2008).

The work described in this chapter aimed to examine the influence of isolate

source on virulence of clonally related serotype 14 blood and ear isolates. A total of 10 (5 each for ST15 and ST130) blood and ear isolates previously investigated in Chapter 3 (see Section 3.2.3.2) were selected for this analysis.

5.2 Results

5.2.1 Effect of isolate source and ST type on expression of *luxS*.

Serotype 14 has been reported to exhibit high biofilm formation capacity in other studies (Camilli *et al.*, 2011; Tapiainen *et al.*, 2010). However, it has since been determined in Chapter 3 (see Figure 3.2.4) that biofilm phenotypes differed according to ST; biofilm formation by ST15 isolates was significantly higher than for ST130 isolates and unlike the situation with serotype 3 strains, was independent of isolate source. The pneumococcus utilizes autoinducer-2 (AI-2), the product of the LuxS enzyme, as a signaling molecule to induce biofilm formation (Trappetti *et al.*, 2011c; Vidal *et al.*, 2013). Transcription levels of the *luxS* gene were therefore investigated to determine whether this might account for differences in biofilm formation capacity between ST15 and ST130 isolates. Strains were grown at pH 7.4 without Fe(III) supplementation (see Section 2.1), in accordance to the optimal conditions observed for biofilm formation for these strains (see Section 3.2.4 and Figure 3.23); RNA was extracted and expression of *luxS* was assayed by quantitative real time RT-PCR (see Sections 2.14 and 2.15).

Figure 5.1 shows that *luxS* was transcribed at a significantly higher level (~1.5-fold) in the ST15 strains compared to the ST130 strains ($P < 0.01$). The increased *luxS* expression observed in ST15 showed a direct correlation with the relative biofilm formation capacities of ST15 and ST130 isolates, as shown in Chapter 3 (see Figure 3.24). However, no significant differences were observed in *luxS* expression between blood and ear isolates within either ST.

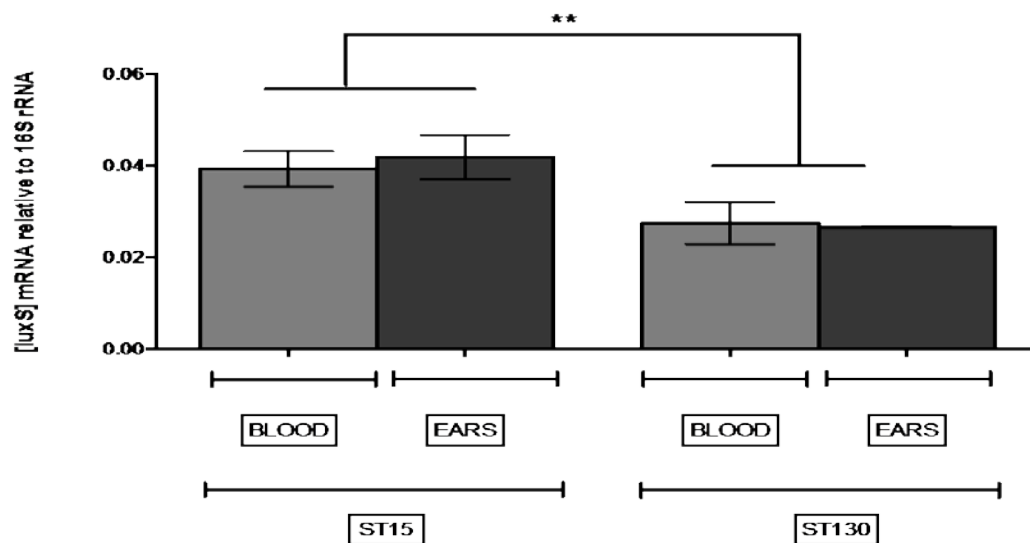


Figure 5.1. Effect of isolate source and ST type on *luxS* expression. Transcription of *luxS* relative to 16S rRNA of ST15 and ST130 blood (n=3 for each ST) and ear (n=2 for each ST) isolates, was measured by qRT-PCR, as described in Section 2.9.2. Data are means ± SEM of quadruplicate assays. Pooled data are presented for blood and ear isolates within each ST. The significance of differences between STs was determined using Student's two-tailed *t*-test (**, $P < 0.01$).

5.2.2. Virulence phenotype of ST130 blood and ear isolates.

The two dominant STs identified for the serotype 14 isolates examined in Chapter 3 were then investigated for virulence phenotype. Firstly, low biofilm forming ST130 strains were examined in the mouse intranasal challenge model (see Section 2.18). Briefly, 3 groups of 5-6 outbred 6-week old female Swiss mice were each challenged intranasally with one blood (ST130/4524) or one ear isolate (ST130/76547) (see Section 2.18). CFU counts of the respective strains were then quantitated from the nasopharynx, lungs, blood, brain and ear tissues at 24 h, 48 h and 72 h post challenge.

Blood and ear isolates colonized the nasopharynx of mice at similar levels (10^4 - 10^6 CFU) at all time points (Fig. 5.2A). At 24 h post infection, bacterial loads in the lungs were similar for blood and ear isolates, with bacteria detected in only 2/5 mice in both cases, and at levels below 10^3 CFU. At the later time points, no bacteria were detected in the lungs (Fig. 5.2B). Bacterial loads in the brain were also similar for the blood and ear isolates at all time points, and increased from 1/5 mice infected at 24 h in both cases, to

4/6 and 4/5 mice infected at 72 h for the blood and ear isolate, respectively (Fig. 5.2C). Interestingly, there was a significant difference in infection rate for the ear niche between the blood isolate ST130/4524 and the ear isolate ST130/76547 at 24 h (0/5 vs 4/5, respectively; $P < 0.05$). However, the infection rates were similar for the two strains at 48 h and 72 h (Fisher Exact test), with all mice showing infected ears at the latter time with a median bacterial load of approximately 10^3 CFU in both cases (Fig. 5.2D). Neither of the strains were detected in the blood of any of the mice at any time point (data not presented).

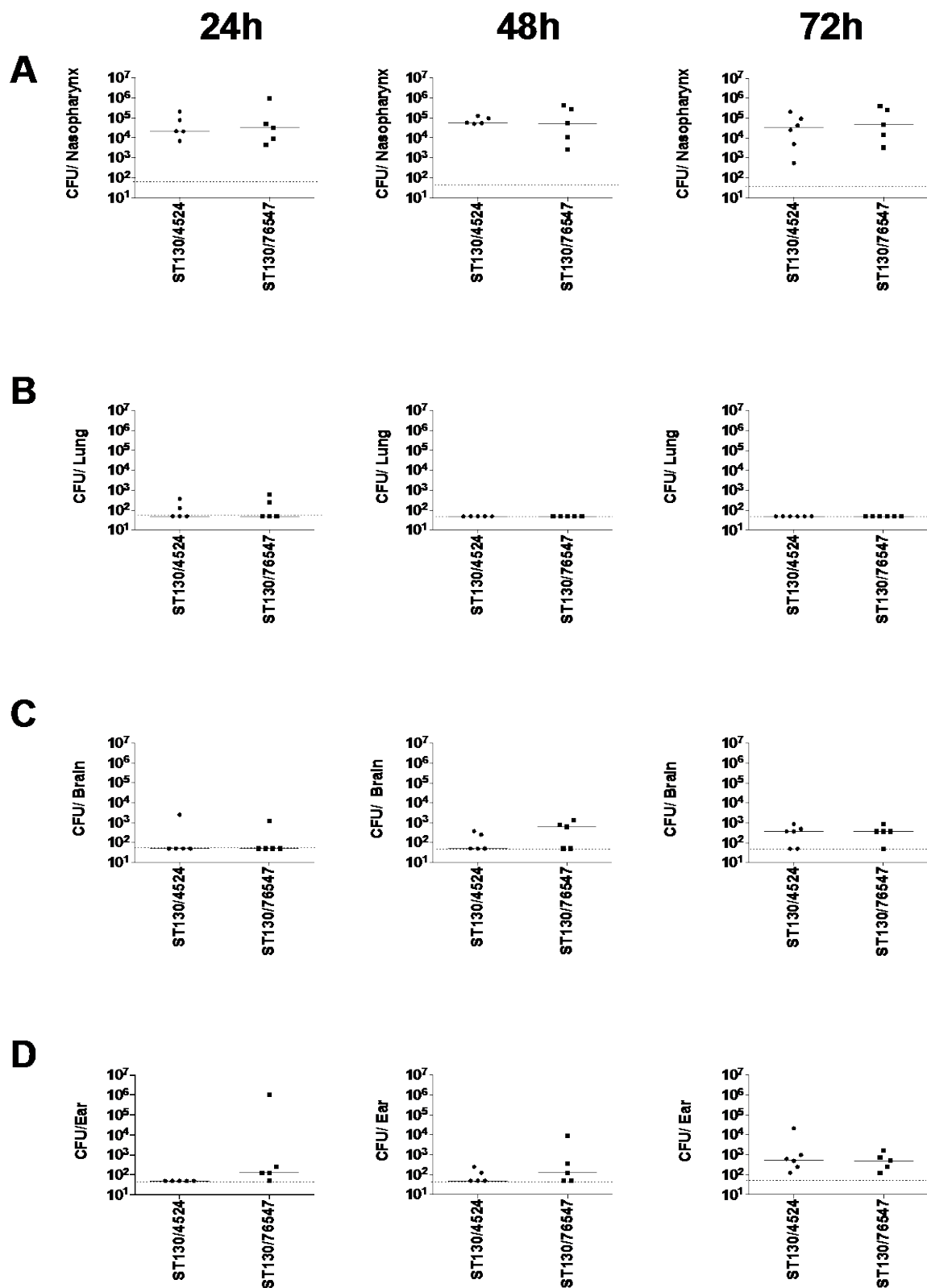


Figure 5.2. Comparative virulence of ST130 blood (ST130/4524) and ear (ST130/76547) isolates. Blood isolates are represented by round filled black symbols while ear isolates are represented by square filled black symbols. The horizontal bars denote the median CFU for each group; the dotted horizontal line indicates the lower limit of detection and symbols on the line denote no bacteria detected. No significant differences in infection rates were found (Fisher-Exact Test).

5.2.3 Virulence phenotype of ST15 blood and ear isolates.

The virulence profiles of the five ST15 strains (were also examined in the same challenge model. Group sizes at each time point (n) were 16 for one blood (ST15/4495) and one ear isolate (ST15/9-47) (both selected at random), while n = 5 at each time point for the remaining strains. Numbers of the respective strains in various host niches (nasopharynx, lungs, blood, brain and ear) were quantitated at 24 h and 72 h post-challenge (Figure 5.3). None of the strains were detected in the blood of any of the mice at either time point (data not presented). The three blood (ST15/4495, ST15/4534 and ST15/4559) and two ear isolates (ST15/9-47 and ST15/51742) all exhibited a similar capacity to colonize the nasopharynx at both 24 h and 72 h post-infection, with GM bacterial load in this niche in the range 10^4 - 10^5 CFU (Figure 5.3A). There were no significant differences in either infection rate or GM bacterial load. However, significant differences were observed between blood and ear isolates in the other host niches. Neither of the ear isolates was detectable in the lungs of any of the infected mice at either time point. In contrast, the blood isolate ST15/4495 was present in the lungs of 14/16 mice at 24 h and 8/16 at 72 h post challenge ($P < 0.0001$ and $P = 0.0032$, respectively; Fisher Exact test). A similar trend was seen for the other two blood isolates (ST15/4534 and ST15/4559), with 50% of lungs colonized at 72 h (Figure 5.3B). The opposite tropism was observed in the brain. None of the three ST15 blood isolates were detected in the brains of any of the mice at either time point. However, the ear isolate ST15/9-47 was detected in the brains of 15/16 mice and 11/16 mice at 24 h and 72 h, respectively ($P < 0.0001$ in both cases). The other ear isolate (ST15/51742) was present in the brains of 5/5 and 3/5 mice at 24 h and 72 h, respectively ($P < 0.01$ relative to any of the blood isolates at 24 h) (Figure 5.3C). In the infected mice, bacterial loads in the brain were in the range of 10^3 - 10^5 CFU. All five ST15 isolates were able to spread to the ear compartment after intranasal challenge, but the proportion of mice whose ears were infected with the ear isolate ST15/9-47 was significantly greater than that for mice challenged with the blood isolate ST15/4495 (16/16 versus 7/16 and 15/16 versus 8/16 at 24 h and 72 h, respectively; $P = 0.0008$ and $P = 0.0155$, respectively) (Figure 5.3D). The GM bacterial

load in the ears for ST15/9-47 was also significantly greater than that for ST15/4495 at both 24 h and 72 h ($P = 0.0015$ and $P = 0.0020$, respectively). Similar trends were also seen in the mice challenged with the other ST15 ear isolate and the two other blood isolates. Collectively, these results show once again that pneumococci of the same serotype and ST may exhibit distinct *in vivo* phenotypes in accordance with clinical site of isolation.

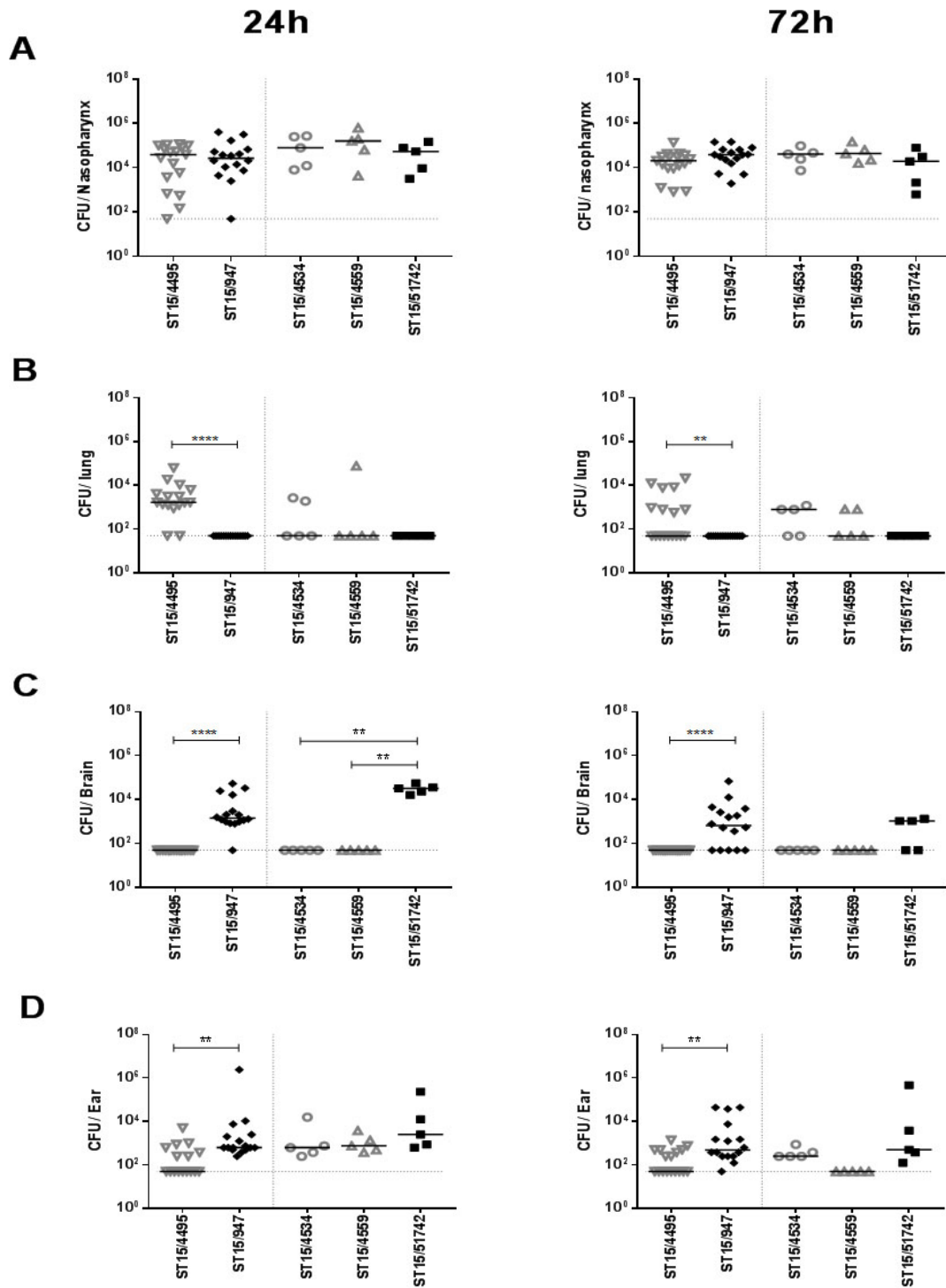


Figure 5.3. Comparative virulence of ST15 blood (ST15/4495, ST15/4534 and ST15/4559) and ST15 ear (ST15/9-47 and ST15/51742) isolates. Blood isolates are represented by hollow grey symbols while ear isolates are represented by filled black symbols. The horizontal bars denote the median CFU for each group; the dotted horizontal line indicates the lower limit of detection and symbols on the line denote no bacteria detected. Differences in infection rate (number of infected versus uninfected mice) were analyzed using the Fisher Exact test: **, $P < 0.01$; ***, $P < 0.001$; ****, $P < 0.0001$.

5.2.4 *In vivo* competition analysis of ST15 blood and ear isolates.

The distinct *in vivo* tropism observed for the ST15 ear and blood isolates could be due to differences in bacterial virulence factors, expressed either on the bacterial surface or released into the environment. It could also be attributable to differences in the nature of the host innate immune responses elicited by the respective strains, whereby the presence of a strain with superior virulence characteristics in a given niche may enhance the virulence of a “passenger” strain. To explore this, *in vivo* competition experiments were carried out (see Section 2.19) in which two groups of mice were challenged intranasally with equal numbers of ST15/4495 and ST15/9-47, and the relative numbers of each strain determined in various host niches at 24 h and 72 h post-challenge. In order to distinguish the strains, erythromycin-resistant derivatives of each strain were constructed by transformation with the plasmid pAL3 (see Section 2.8). Two competition experiments were performed with 5 mice per group for each time point. In one experiment, mice were challenged with equal numbers of ST15/4495 and ST15/9-47:pAL3; in the other, mice were challenged with equal numbers of ST15/4495:pAL3 and ST15/9-47. Tissue samples were plated on blood agar (BA) with or without erythromycin to enable calculation of the ratio of sensitive to resistant organisms, and hence the competitive index (CI). Data pooled from both experiments are shown in Figure 5.4.

In spite of the similar capacities of ST15/4495 and ST15/9-47 to colonize the murine nasopharynx when challenged in isolation (Figure 5.2), the ear isolate had a significant competitive advantage over the blood isolate in the mixed infection model in the nasopharynx at 24 h ($P < 0.001$) and at 72 h ($P < 0.0001$), by which time the median CI was approximately 10^5 (Figure 5.4B). The ear isolate also predominated in both the ear and brain compartments at both time points ($P < 0.0001$ for brain at 24 h and 72 h and ear at 24h; $P < 0.05$ for ear at 72 h). Moreover, whereas small numbers of the blood isolate were present along with the dominant ear isolate in the ears of all the infected mice, the blood isolate was never detected in brain tissue of any of the mice at either time

point. These findings are understandable, given that access to both the brain and the ear compartments occur via the nasopharynx, where the ear isolate is present at a 10^5 -fold excess over the blood isolate. A distinct scenario occurred in the lungs. Only 6/10 mice had detectable pneumococci in the lungs at either time point, and in these mice, neither strain had a significant competitive advantage overall (Figure 5.4). This is in spite of the fact that when challenged in isolation, only the blood isolate was able to persist in the lungs at either 24 h or 72 h (Figure 5.2B). In the competition experiment, the ear isolate outcompeted the blood isolate in 4/6 infected mice, whereas the blood isolate outcompeted the ear isolate in 2/6 mice (Figure 5.4). The intranasal challenge inoculum (approximately 10^6 CFU; as determined by CFU counts of the inoculum post-challenge) is instilled into the nares under general anesthesia and a proportion of the dose is aspirated directly into the lungs during the challenge. When instilled on its own, ST15/9-47 organisms entering the lung during challenge are cleared within 24 h, whereas when ST15/4495 is instilled on its own, the blood isolate is able to resist innate defenses and persist in the lung. However, in the co-infection model, significant numbers of the ear isolate are present in a proportion of the mice at both 24 h and 72 h. These findings indicate that the presence of the blood isolate ST15/4495, at least during the immediate post-challenge period, is necessary for persistence of the ear isolate ST15/9-47 in the lung compartment.

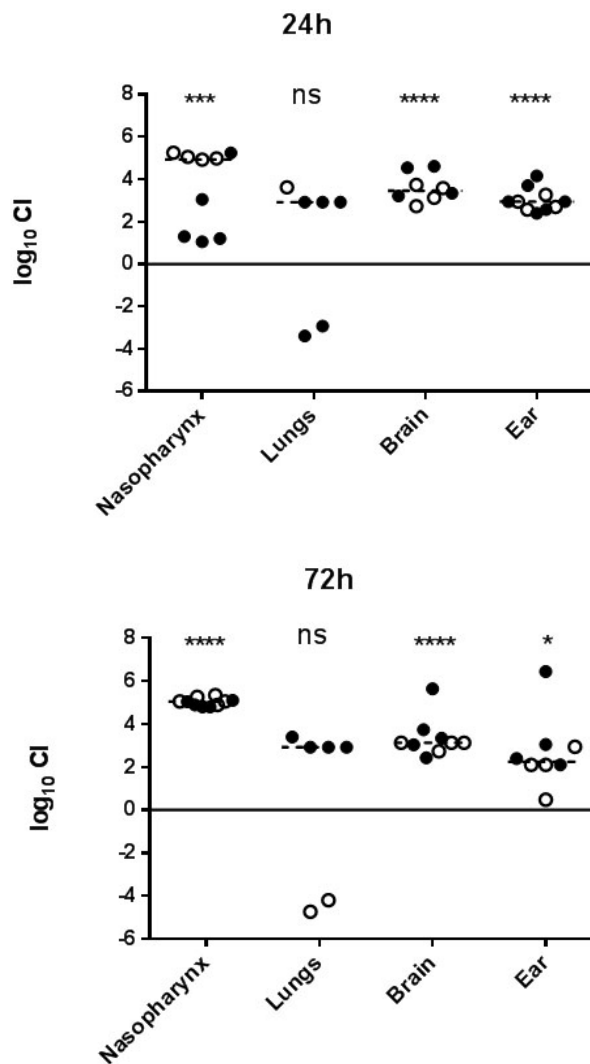


Figure 5.4. *In vivo* competition between ST15/9-47 (ear isolate) and ST15/4495 (blood isolate). Data shown are pooled from two competition experiments performed with 5 mice per group for each time point (24 h and 72 h post challenge). In one experiment, mice were challenged with equal numbers (5×10^7 CFU each) of ST15/4495 and ST15/9-47:pAL3 (hollow symbols); in the other experiment, mice were challenged with equal numbers of ST15/4495:pAL3 and ST15/9-47 (solid symbols). The competitive index (CI) has been shown as log CI for each tissue for each mouse. The horizontal dotted lines denote the geometric mean CI for each tissue. Statistical differences between the geometric mean CI and a hypothetical value of 0 (ratio of 1:1) in each niche were analyzed using the two-tailed Student's *t*-test: ns, not significant; *, $P < 0.05$; ***, $P < 0.001$; ****, $P < 0.0001$.

5.2.5 *In vitro* adherence and invasion of ST15/9-47 (ear isolate) and ST15/4495 (blood isolate).

To further explore the basis for the enhanced nasopharyngeal colonisation fitness of ST15/9-47, the adherence phenotype of all the ST15 isolates was assessed *in vitro* using Detroit 562 (human nasopharyngeal) cells (Table 5.1). There were significant differences in total *in vitro* adherence between several of the strains. Two of the blood isolates (ST15/4495 and ST15/4534) were significantly less adherent than the ear isolate ST15/9-47 ($P < 0.01$ and $P < 0.001$, respectively). The other ear isolate (ST15/51742) was even more adherent than ST15/9-47 ($P < 0.05$). The adherence of the third blood isolate (ST15/4559) was not significantly different from ST15/9-47, but it was significantly less adherent than the second ear isolate ST15/51742 ($P < 0.01$). The capacity of the ear isolate ST15/9-47 and the blood isolate ST15/4495 to invade Detroit 562 cells was also investigated (Table 5.1), but no significant difference was observed.

5.2.6 Expression of host immune response genes in infected tissues.

Although only the blood isolates are detectable in the lungs of infected mice at 24 h, ear isolates are delivered into the lungs during challenge, but are cleared by host innate defenses by 24 h. In a pilot experiment, similar bacterial loads were present in the lungs of mice challenged with either ST15/4495 or ST15/9-47 at 6 h post challenge (10^7 - 10^8 CFU in both cases). Differences in host responses during the immediate post-challenge period, which may have influenced bacterial clearance from the lungs, were therefore investigated.

Table 5.1 Adherence to and invasion of Detroit 562 cells.

Strain	Source	Adherence ^a (CFU/well ± SEM)	Invasion (CFU/well ± SEM)
ST15/9-47	Ear	7.88 ± 0.78 × 10 ⁵	3.50 ± 0.65 × 10 ³
ST15/51742	Ear	1.19 ± 0.10 × 10 ⁶ *	Not tested
ST15/4495	Blood	3.75 ± 0.56 × 10 ⁵ **	3.95 ± 0.28 × 10 ³
ST15/4534	Blood	2.85 ± 0.27 × 10 ⁵ ***	Not tested
ST15/4559	Blood	7.50 ± 0.59 × 10 ⁵	Not tested

^a Significant differences in adherence relative to that for ST15/9-47 are indicated as follows: *, $P < 0.05$; **, $P < 0.01$; ***, $P < 0.001$ (Student's *t*-test, two-tailed). (Credit: Adrienne Paton (see also Amin *et al.* (2015)).

Mice were challenged with either the blood isolate (ST15/4495) or the ear isolate (ST15/9-47), or were sham-infected (anesthetized and inoculated with 30 µl SB). Total RNA was isolated from lungs and nasopharyngeal tissue 6 h after challenge. Expression of 84 key immune response genes was then quantitated using RT-PCR arrays (see Sections 2.14 - 2.16).

When compared to levels in sham-infected samples, a total of 35 genes were induced in the lungs, as judged by a significant increase in mRNA level following challenge with at least one of the two ST15 strains (Table 5.2). Overall, the pattern of gene expression indicated a generally pro-inflammatory response in the lungs at 6 h post-challenge; genes encoding a number of pro-inflammatory cytokines were up-regulated, including IL1 α , IL1 β , IL23a, IL6 and TNF α . Other genes involved in regulating the immune response were also increased in expression. These included the chemokines CCL12, a murine homolog of (human) CCL2, and CXCL10, which is known to be induced by IFN γ , a pro-inflammatory cytokine that also showed increased expression following pneumococcal challenge. The chemokine receptor CCR5 was also elevated at the mRNA level. Genes encoding elements involved in pathogen recognition and signaling during immune responses were differentially expressed in challenged samples

compared to sham-infected samples, such as Myd88, the Toll-like receptors (TLRs) 3, 6 and 7, Nod2, Ddx58, Jak2 and Nfkbia. Other up-regulated genes included those encoding the integrin CD11b (*Itgam*), and its associated adhesion molecule ICAM1, the inflammasome component NLRP3, and granulocyte-macrophage colony stimulating factor (GM-CSF; *Csf2*). Some strain-strain differences were observed, with 8 genes showing significant differential expression in lungs following challenge with ST15/4495 compared to challenge with ST15/9-47 (Table 5.3). Of these, 6 genes were up-regulated by both strains when compared to resting samples, but to a significantly greater degree following challenge with ST15/4495. These included those encoding the pro-inflammatory cytokines TNF α and IL6, the type I interferon IFN β , the co-stimulatory molecule CD40, the transcription factor Tbet (*Tbx21*) and the chemokine CCL12. The remaining 2 genes, *Apcs* and *Il2*, were found to be up-regulated only following challenge with ST15/9-47.

Since the nasopharynx is the first host environment to which the bacteria are exposed during infection, we examined whether the blood isolate (ST15/4495) and the ear isolate (ST15/9-47) also elicited differential induction of innate immune response genes in this niche at 6 h post infection. However, no significant differences in expression were detected for any of the 84 genes analyzed between sham-infected mice and those challenged with either strain.

Table 5.2. Genes differentially expressed in infected relative to sham-infected lungs.^a

	ST15/4495 vs. sham-infected		ST15/9-47 vs. sham-infected	
Gene	Fold change	Significance	Fold change	Significance
<i>Apcs</i>	ns	ns	5.15	**
<i>C5ar1</i>	14	*	8.47	**
<i>Ccl12</i>	36.61	*	15.56	**
<i>Ccr5</i>	10.68	*	5.97	**
<i>Cd14</i>	ns	ns	61.12	**
<i>Cd40</i>	6.21	*	2.55	*

<i>Cd86</i>	3.51	*	2.51	**
<i>Csf2</i>	ns	ns	19.34	*
<i>Cxcl10</i>	ns	ns	310.55	**
<i>Ddx58</i>	ns	ns	2.36	*
<i>Icam1</i>	7.91	*	5.13	*
<i>Ifna2</i>	ns	ns	2.50	*
<i>Ifnb1</i>	96.15	***	ns	ns
<i>Ifng</i>	17.2	**	12.25	***
<i>Il10</i>	ns	ns	17.09	*
<i>Il1a</i>	29.81	**	16.64	***
<i>Il1b</i>	88.28	*	52.60	**
<i>Il1r1</i>	2.1	*	ns	ns
<i>Il2</i>	ns	ns	4.95	**
<i>Il23a</i>	40.9	**		
<i>Il6</i>	ns	ns	312.35	**
<i>Irf7</i>	4.01	*	3.80	*
<i>Itgam</i>	3.73	**		
<i>Jak2</i>	3.29	**	4.41	*
<i>Mx1</i>	152.64	*		
<i>Myd88</i>	12.3	*	5.22	*
<i>Nfkbia</i>	ns	ns	20.34	*
<i>Nlrp3</i>	36.61	***	ns	ns
<i>Nod2</i>	9	**	ns	ns
<i>Slc11a1</i>	4.26	*	5.25	*
<i>Tbx21</i>	2.4	**	ns	ns
<i>Tlr3</i>	4.8	**	ns	ns
<i>Tlr6</i>	ns	ns	3.84	**
<i>Tlr7</i>	ns	ns	4.80	**
<i>Tnf</i>	119.21	**	50.78	*

^a Data are fold-difference in gene expression for the indicated comparison. Genes up-regulated significantly after infection with both ear and blood isolates are highlighted in bold type. Statistical significance is indicated as follows: *, $P < 0.05$; **, $P < 0.01$; ***, $P < 0.001$, ns, not significant (Student's *t*-test, two-tailed).

Table 5.3. Genes differentially induced after infection with ST15/9-47 versus ST15/4495.

Gene	ST15/4495 vs sham-infected		ST15/9-47 vs sham-infected		ST15/9-47 vs ST15/4495	
	fold-change	significance	fold-change	significance	fold-change	significance
<i>Apcs</i>	-1.10	ns	5.15	**	5.67	**
<i>Il2</i>	-1.09	ns	4.95	**	5.40	*
<i>Ccl12</i>	36.61	*	15.56	**	-2.35	*
<i>Cd40</i>	6.21	*	2.55	*	-2.43	*
<i>Ifnb1</i>	96.15	***	17.84	ns	-5.39	***
<i>Il6</i>	1842.35	($P = 0.06$)	312.35	**	-5.90	*
<i>Tnf</i>	119.21	**	50.78	*	-2.35	*
<i>Tbx21</i>	2.4	**	1.02	**	-2.36	****

Statistical significance is indicated as follows: *, $P < 0.05$; **, $P < 0.01$; ***, $P < 0.001$, ****, $P < 0.0001$, ns, not significant (Student's *t*-test, two-tailed).

5.2.7 Cellular and histopathological responses to lung infection.

Blood, bronchoalveolar lavage (BAL) fluid and lung tissue from mice infected with either ST15/9-47 or ST15/4495, or sham-infected mice, were also investigated for cellular recruitment and histopathological changes (see Section 2.10.4). At 6 h post-infection, there were very few cells in the BAL and there were no significant differences in the numbers of BAL neutrophils (Ly-6G-positive cells) or monocyte/macrophages (F4/80-positive cells) between sham-infected mice and those infected with either ST15/9-47 or ST15/4495, as determined by flow cytometry (result not shown). However, similar FACS analysis of blood leukocytes showed significantly higher numbers of neutrophils (Figure 5.5A), but not monocyte/macrophages (Figure 5.5B), in ST15/4495-infected mice relative to either sham-infected or ST15/9-47-infected mice at 6 h ($P < 0.05$ in both cases for neutrophils). A similar increase in blood neutrophil count in ST15/4495-infected mice relative to either sham-infected or ST15/9-47-infected mice at 6 h was also evident from differential cell counts of blood films ($P < 0.05$ and $P < 0.01$, respectively) (Figure 5.5C).

Histological examination of HE-stained lung sections at 6 h (see Section 2.10.4) revealed early signs of tissue damage, most notably in ST15/4495-infected mice, including congested capillaries, thickened alveolar walls, swollen cuboidal epithelial cells of the bronchioles and presence of secretions in the alveolar and bronchiolar spaces (Figure 5.6A). These features were used to develop an 8-point scoring system for histopathological changes (Figure 5.6B). The mean aggregate score (\pm SE) for ST15/4495-infected mice (2.8 ± 1.3) was higher than that for either ST15/9-47-infected mice (1.4 ± 0.57), or sham-infected mice (0.5 ± 0.33), but this trend did not reach statistical significance. Finally, lung sections were examined for cellular infiltration by immunofluorescence microscopy after staining with anti-Ly-6G (Figure 5.7). This revealed patchy neutrophil infiltration in 2/5 mice infected with the blood isolate ST15/4495 and 1/5 mice infected with the ear isolate ST15/9-47, compared with 0/5 for the control mice. No differences in staining for the monocyte/macrophage marker were seen between groups.

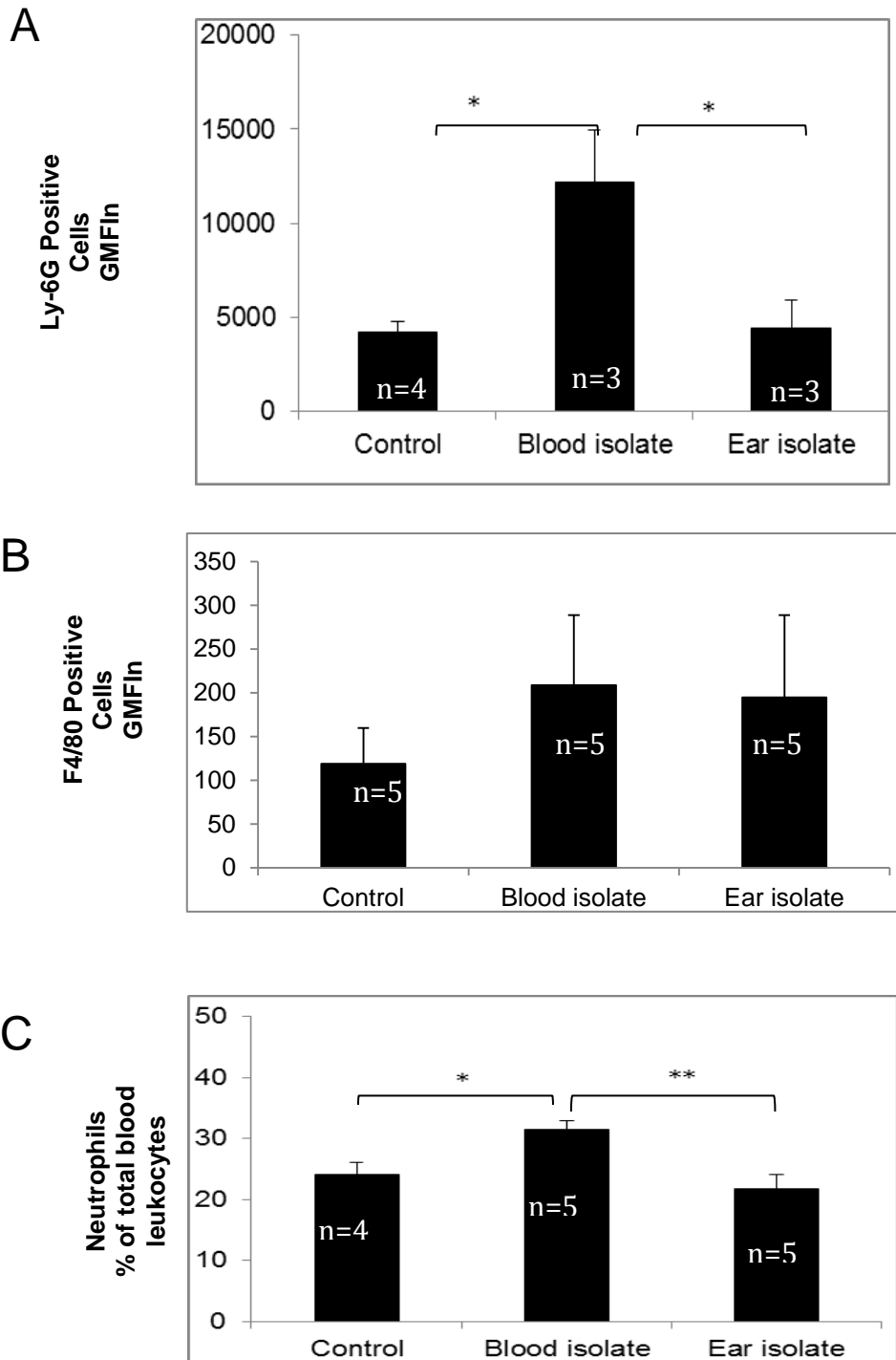


Figure 5.5. Peripheral blood leukocyte counts. Leukocytes isolated from peripheral blood collected at 6 h from control (sham-infected) mice, or those infected with the blood isolate (ST15/4495) or the ear isolate (ST15/9-47), were examined by FACS after staining with anti- Ly-6G (A) or anti F4/80 (B). Data are the product of geometric mean fluorescence intensity and the total number of positive cells (GMFI_n) for the respective marker (\pm SE). Alternatively, blood films were subjected to differential cell count and neutrophil numbers are expressed as a percentage of total leukocytes (mean \pm SE) (C). Statistical significance is indicated as follows: *, $P < 0.05$; **, $P < 0.01$ (Student's paired, two-tailed t test). (Credit: Hui Wang (see also Amin *et al.* (2015)))

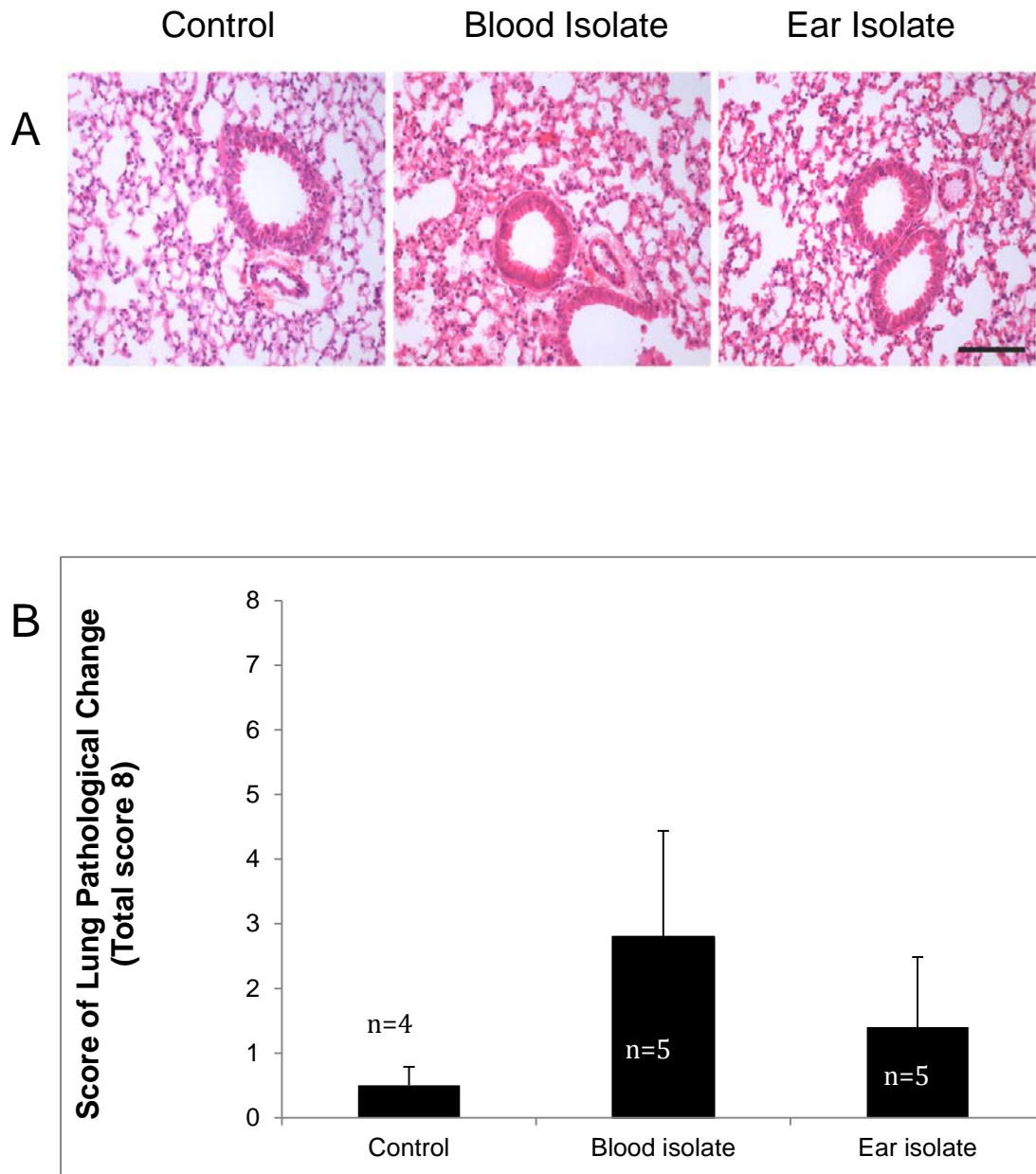


Figure 5.6. Lung histopathology. HE-stained lung sections from control (sham-infected) mice, or those infected with the blood isolate (ST15/4495) or the ear isolate (ST15/9-47) at 6 h were examined by light microscopy. Representative sections from each group are shown (A); scale bar = 0.1 mm. Slides were also scored (blind) according the following 8-point scheme: congested capillaries (fine arrows, scored 0-2); thickened alveolar wall (arrow heads, scored 0-2); swollen cuboidal epithelial cells of the bronchioles (thick arrows, scored 0-2); secretions in the alveolar and bronchiole space (hollow arrow, score 0-2). Data were examined with Student's unpaired two-tailed t test and are presented as mean \pm SE for each group (B). (Credit: Hui Wang (Amin *et al.*, 2015))

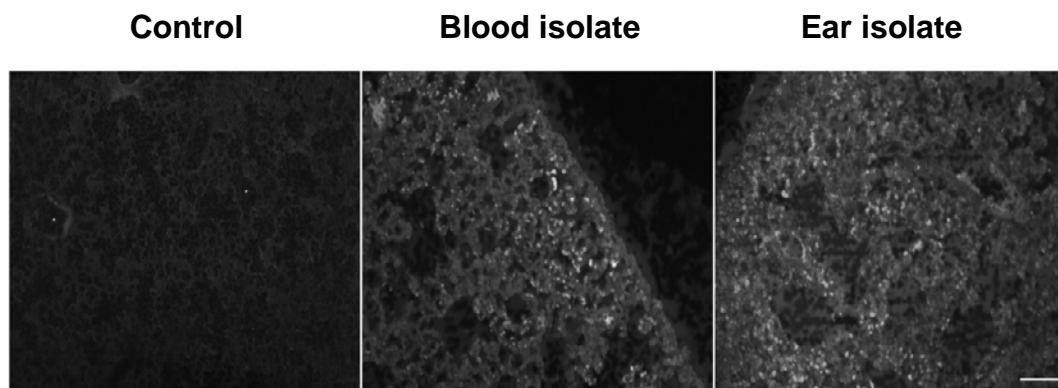


Figure 5.7. Neutrophil infiltration. Lung tissue from infected or control mice was fixed, sectioned and labelled with rat anti mouse Ly-6G or F4/80, followed by Alexa-488 conjugated anti-rat IgG and examined by fluorescence microscopy. Scale bar = 50 μ m. (Credit : Hui Wang (see also Amin *et al.* (2015)). Patchy neutrophil infiltration was observed in 2/5 mice infected with the blood isolate ST15/4495 and 1/5 mice infected with the ear isolate ST15/9-47, compared with 0/5 for the control mice

5.3 Discussion

In Chapter 4 multiple examples of serotype 3 strains belonging to the same ST, which consistently and reproducibly exhibited distinct virulence and biofilm phenotypes that directly correlated with the original site of isolation from human patients (i.e. ear vs. blood) were described (see also Trappetti *et al.* (2013)). This suggested that at least in serotype 3, pneumococci exhibit stable niche adaptation within a clonal lineage. In this Chapter, ST-matched blood and ear isolates belonging to serotype 14, a common cause of OM as well as invasive disease (Brueggemann *et al.*, 2003) were investigated for a correlation between isolate source and virulence-related phenotypes.

Previous studies in this laboratory and elsewhere show an association between *luxS* expression and biofilm formation in D39 and serotype 3 strains (Trappetti *et al.*, 2011c; Trappetti *et al.*, 2013; Vidal *et al.*, 2011; Vidal *et al.*, 2013). In this Chapter, the expression of *luxS* was significantly higher in ST15 than ST130 strains, which is consistent with the significantly higher biofilm formation capacity of the ST15 isolates at pH 7.4 (see Figure 3.24). Thus, the overall association between *luxS* expression and

biofilm formation also appears to hold for these serotype 14 strains. However, unlike the findings for the serotype 3 ST180, ST232 and ST233 lineages (see Figure 4.1), there was no significant difference in *luxS* expression between blood and ear isolates within either ST15 or ST130 (Figure 5.1). Thus, differential *luxS* expression cannot account for the significantly higher biofilm formation exhibited by ST130 ear isolates relative to ST130 blood isolates at pH 7.4 (Fig. 3.24).

Examination of the virulence phenotype of the low biofilm forming ST130/4524 blood isolate and ST130/76547 ear isolate in the mouse intranasal challenge model showed that although the ear isolate appeared to translocate more quickly to the ear compartment than the blood isolate, in general, isolate source did not appear to be associated with the overall virulence phenotype of ST130 strains. However, only one ST-matched pair of isolates was examined, which is not sufficient for a conclusive observation. Analysis of additional ST130 blood and ear isolates in the collection is clearly warranted to gain further insight into the influence of isolate source on the virulence of ST130 strains.

ST15 was the other dominant ST in the serotype 14 collection analyzed in Chapter 3 and was represented amongst clinical isolates from cases of sepsis as well as OM. ST15 blood and ear isolates were able to colonize the murine nasopharynx to roughly similar extents. However, the blood isolate (ST15/4495) was significantly better at colonisation/persistence in the lung, while the ear isolate (ST15/9-47) was significantly better able to penetrate and persist in the brain and ears. Similar preferential tropism for the brain and ear was observed for the other ST15 ear isolate (ST15/51742), while the two other ST15 blood isolates (ST15/4534 and ST15/4559) colonized the lungs in a proportion of infected mice. Significantly, neither of the ear isolates were detected in the lungs of any of the mice at either 24 or 72 h, while none of the three blood isolates were ever detected in the brain. Furthermore, none of the ST15 blood or ear isolates were detected in the blood at any time during the experiment. This is consistent with the long-known fact that mice exhibit a high degree of innate resistance to sepsis after challenge with serotype 14 *S. pneumoniae* strains (Kadioglu & Andrew 2005; Mizrachi-Nebenzahl

et al., 2003). However, these findings also suggest that the very high rate of meningitis that occurs after intranasal challenge with either of the ST15 ear isolates was not a consequence of hematogenous spread. Likely alternative routes for translocation of pneumococci from the nasopharynx to the brain include direct invasion by retrograde axonal transport along olfactory neurons into the CNS (van Ginkel *et al.*, 2004).

Collectively, the above findings provide robust evidence for the existence of distinct pathogenic profiles for serotype 14 *S. pneumoniae* strains belonging to the same ST (in this case ST15). A previous study by Silva *et al.* (2006) has shown modest differences in bacterial loads in the blood of mice 6 h after intraperitoneal challenge with three serotype 14 blood isolates belonging to ST124, although the bacteremia was transient and subclinical. However, the present study demonstrated highly significant differences in virulence and pathogenic profile between isolates belonging to the same serotype and clonal lineage as well as a close correlation between pathogenic profile in mice and the original site of isolation from human cases of pneumococcal disease. This extends the observation that was previously reported for serotype 3 strains belonging to ST180, ST232 and ST233 (Chapter 4). Thus, stable niche adaptation within a clonal lineage appears to be a more general phenomenon.

Apart from the differences in biofilm formation capacity observed in Chapter 3, differences in virulence profiles between the ST130 and ST15 strains were also observed. While ST130 strains exhibited generally similar virulence profiles between blood and ear isolates, ST15 clinical isolates showed exclusive translocation of bacteria to specific tissues in accordance with isolate source. It has been previously reported that clinical strains of the same serotype can exhibit different disease phenotypes in accordance with ST (Hanage *et al.*, 2005; Silva *et al.*, 2006). In serotype 14 strains, ST 156 was strongly associated with invasive disease; STs 482, 191, 124, and 138 were also more significantly associated with invasive disease relative to STs 485 and 62 which were more associated with carriage (Hanage *et al.*, 2005). In another study, serotype 14 isolates were found to include clones exclusively found in carriers (ST230), as well as those solely

associated with invasive disease (ST307) (Sandgren *et al.*, 2004). In serotype 14 strains the prevalence of ST types known to cause invasive disease also differs geographically, with the most prevalent being ST156 in Finland (Hanage *et al.*, 2005), ST15 in England and ST230 in Denmark (Camilli *et al.*, 2011).

Notwithstanding the above, the *in vivo* competition experiments of ST15 isolates in the present study yielded some unexpected findings. Firstly, although the ear and blood isolates are able to colonize the nasopharynx to similar levels when administered individually, the ear isolate ST15/9-47 massively out-competed the blood isolate ST15/4495 in this niche in the co-infection model. The reason for this is not clear, although production of bacteriocins by ST15/9-47 is one possibility. Regardless of underlying mechanism, it accounts for the dominance of ST15/9-47 in the brain and ear in the co-infection model, since these host niches are presumably accessed via the nasopharynx, where the ear isolate already enjoyed a 10^5 -fold numeric advantage. On the other hand, the data from the individual challenge experiments might cause one to predict that the blood isolate ST15/4495 would enjoy a competitive advantage in the lungs, but this was not the case, with neither strain predominating, a fact that mitigates against the bacteriocin hypothesis mentioned above. Similar numbers of ear and blood isolates were delivered into the lungs during challenge under general anesthesia, and bacterial loads in lung tissue at 6 h post challenge were similar. However, in the individual challenge studies, ST15/9-47 was completely cleared from the lungs of all mice by 24 h, while ST15/4495 was able to persist. There are two possible explanations for this. ST15/4495 may secrete a (yet to be defined) virulence factor that can act *in trans* and support survival of ST15/9-47 in the mixed infection model. Alternatively, differences in host innate immune responses elicited by the blood and ear isolates could account for the distinct pathogenic profiles. Clearly, host responses triggered (or inhibited) by ST15/4495 enable this strain to persist in the lung environment. However, this may create a host microenvironment that also enables persistence of co-administered strains such as ST15/9-47, which would otherwise have been cleared.

To establish if the host immune response plays a role in the distinct pathogenic profiles of the ST15 blood or ear isolates, the transcriptional responses of 84 genes representing the major pathways involved in the innate and adaptive immune response to microbial pathogens were examined. Unsurprisingly, infection with either strain induced a variety of pro-inflammatory genes. Differentially expressed genes included those encoding the cytokines IL6 and TNF α that are involved in the classical activated macrophage response to infection (Mosser, DM 2003). IL6 is induced in response to pathogen-associated molecular patterns (PAMPS) and has previously been shown to be protective in a model of pneumococcal pneumonia (van der Poll *et al.*, 1997). TNF α is a key player in induction of pro-inflammatory responses and is rapidly produced in response to injury or infection. It is primarily produced by cells of monocytic origin, such as macrophages, which in turn are highly responsive to this cytokine. Along with IL1 β , it is also known to induce up regulation of expression of adhesion molecules such as ICAM1 on endothelial cells, promoting recruitment of leukocytes such as neutrophils to sites of infection (Collins *et al.*, 1995; Mackay *et al.*, 1993). Through the induction of CCR2 ligands, including CCL12, IFN β is involved in the recruitment of “inflammatory” Ly6C high monocytes from the circulation (Lee *et al.*, 2009), and these cells then differentiate into macrophages within the infected tissue. Type I interferons have also been shown to have varying roles in the response to pneumococcal infection, with a recent study from our laboratory demonstrating a role for these cytokines in the development of invasive pneumococcal disease (Hughes *et al.*, 2014).

CD40 is expressed on a range of leukocyte subsets, including macrophages, where its expression is induced by various cytokines including IFN γ and GM-CSF (Alderson *et al.*, 1993). It is involved in macrophage activation and can, in conjunction with either IFN γ or TNF α , induce production of antimicrobials such as nitric oxide (Portillo *et al.*, 2012). *Tbx21* encodes the transcription factor T-bet, which is a hallmark of Th1 cells during adaptive immune responses. However, it is also known to be expressed by a variety of other cell types, including dendritic cells (DCs), natural killer (NK) cells and

other innate lymphoid cells (ILCs) (Lazarevic *et al.*, 2013). It has also recently been shown to be expressed by respiratory epithelium during pneumococcal infection (Woo *et al.*, 2014).

Serum amyloid P, the protein encoded by *Apcs*, is known to play a role in complement activation, and has been shown to be involved specifically in complement deposition on pneumococcus, improving phagocyte efficiency and aiding clearance of the pathogen (Yuste *et al.*, 2007), while IL2 is believed to be involved in proliferation and activation of natural killer (NK) cells and other innate lymphoid cells (ILCs), as well as proliferation and differentiation of T cells during the adaptive immune response (Gasteiger & Rudensky, 2014).

The strain-specific differences observed provide important clues as to how the immune response may vary, yielding very different patterns of infection from two clonally related strains. Six of the eight genes that were differentially expressed in response to infection with ST15/4495 relative to ST15/9-47 are up regulated in response to both strains relative to sham-infected lungs, but are induced more strongly in response to ST15/4495. This suggests that while both strains induce a broadly similar response, one of the distinguishing features between the two is the strength of the response induced at a similar bacterial load. This response included increased expression of genes encoding CCL12, IL6, TNF α , IL1 β and CD40, which points to an overall stronger macrophage response to the blood isolate than to the ear isolate. BAL fluid collected at 6 h post-infection contained very few cells and there were no significant differences between sham-infected mice and those infected with either of the isolates. However, mice infected with the blood isolate ST15/4495 exhibited significant neutropenia relative to sham-infected or ST15/9-47-infected mice at this early time point. Histopathological examination was also suggestive of increased lung damage in mice infected with ST15/4495. The above findings have parallels with a previous study from this laboratory, which compared host transcriptional responses to highly invasive and non-invasive *S. pneumoniae* strains belonging to serotype 1 in a similar intranasal challenge model. A total of 29 genes of the 84 on the array showed significant up-regulation, of which 22

were also up-regulated in the present study. Both type 1 strains were present in roughly equal numbers in the lung at 6 h, but the invasive strain triggered a much stronger type I interferon response, which facilitated invasion of the pleural cavity followed by the blood (Hughes *et al.*, 2014). In the present study we identified two genes (*Apcs* and *Il2*) that were only significantly up regulated in mice challenged with the ear isolate ST15/9-47 when compared to sham-infected mice; infection with the blood isolate had a negligible effect on their expression. Therefore, it is tempting to speculate that the expression of *Apcs* and *Il2* might contribute to the clearance of the ear isolate from the lungs. In particular, serum amyloid P, the protein encoded by *Apcs*, is known to play a role in complement deposition on the pneumococcus, improving phagocyte efficiency and aiding clearance of the pathogen (Yuste *et al.*, 2007).

In this study, we have provided further evidence that *S. pneumoniae* strains belonging to the same serotype and ST can elicit distinct host innate immune responses and cause different types of disease (for journal publication of this study please refer to Appendix B). Future comparative genomic and transcriptomic analyses of these ST-matched strain pairs with distinct virulence phenotypes should facilitate identification of specific bacterial determinants that contribute to tissue tropism. Indeed, RNA sequencing has since been carried out on ST15 isolates grown *in vitro*, and will be discussed further in Chapter 6. However, *in vivo* transcriptomic analysis of the blood and ear isolates themselves (rather than the host) during early lung infection may allow a more thorough understanding of differences between these strains that impact on virulence phenotype.

Chapter 6: Transcriptomic analysis of clonally related blood and ear isolates of Serotypes 3 and 14

6.1 Introduction

The evolution of different lineages is an important survival mechanism for the pneumococcus and has become an immense challenge in the control and treatment of pneumococcal diseases. In Chapter 5 it was observed that the serotype 14 blood isolate ST15/4495 showed a distinct virulence phenotype compared to ear isolate ST15/9-47. Further investigations of clonally related blood isolates ST15/4534, ST15/4559 and ear isolate ST15/51742 showed similar trends (see Section 5.2.3). Differential immune response gene expression patterns were also seen between mice infected with the ST15/4495 blood and ST15/9-47 ear isolates. In Chapter 4 it was also shown that serotype 3 blood and ear isolates from ST180 and ST233 also exhibited distinct virulence phenotypes in mice in accordance with clinical site of isolation.

The availability of high throughput methods to sequence and analyse whole genomes is becoming increasingly useful for probing pneumococcal genetic diversity. An extension to genome sequencing are transcriptome profiling approaches, which probe and quantitate the complete set of transcripts in the cell, including mRNAs, non-coding RNAs and small RNAs, at specific developmental stages or physiological conditions (Wang *et al.*, 2009). Two main technologies are currently used to quantify and probe the transcriptome: hybridization-based microarray analysis and the sequencing-based RNA-Seq. Whilst microarray technology is high throughput and relatively inexpensive, its main drawbacks include the requirement for prior knowledge of the genome sequence, difficulties in detecting small RNA species or those in low abundance, as well as issues with cross-hybridization. RNA-Seq has several advantages, most importantly the capacity to detect unknown transcripts, and sequence variations, thereby providing much more in-depth information. It also has very low background signals, a large dynamic range of detection at low or very high level gene expression, high levels of reproducibility and requires less RNA sample (Croucher & Thomson 2010; McClure *et al.*, 2013; Pruitt *et*

al., 2005). A further advantage is that if there are differences in genome sequence between two strains being compared (e.g. presence or absence of an AR) these will be apparent from the respective transcriptome if the genes in question are actually being expressed, thereby reducing the importance of separate genome sequence analysis.

The differences in virulence phenotype within ST lineages in accordance with isolation site observed for the serotype 3 and 14 strains in Chapters 4 and 5 suggests the possibility of differences in transcriptional profile between otherwise closely related isolates. Therefore, the aim of the work described in this chapter was to utilize RNA-Seq to compare the transcriptomes of the clonally related serotype 3 and 14 blood and ear isolates.

6.2 Results

6.2.1 Transcriptomic analysis of serotype 14 ST15 clinical isolates

For transcriptomic analysis of ST15 strains a total of 5 blood (ST15/4495, ST15/4534 and ST15/4559) and ear (ST15/9-47 and ST15/51742) isolates investigated previously in Chapter 5 were selected. Bacterial strains from frozen stock were firstly grown in serum broth in triplicates to a final OD₆₀₀ of 0.2 and RNA was extracted using the Qiagen RNeasy Mini Kit as per the manufacturer's instructions (see Section 2.14). The quantity and integrity of the RNA samples were then determined (see Section 2.18). RNA samples with a RIN (RNA Integrity Number) of ≥ 8.0 and a total amount of $\geq 3 \mu\text{g}$ were then sent to the Australian Genome and Research Facility (AGRF Melbourne, Australia) for ribosomal RNA removal using the Illumina Ribo-zero rRNA (Bacteria) removal kit, cDNA library preparation and RNA-Sequencing using the Illumina Hi-Seq 2500 sequencing platform. The number of reads produced for each of the blood (ST15/4495, ST15/4534 and ST15/4559) and ear (ST15/9-47 and ST15/51742) isolates were 26,885,011, 49,113,015, 49,936,770, 47,846,137 and 47,819,885, respectively. The per base sequence quality for the 5 samples was reported by AGRF to be excellent, with $>97\%$ bases above Q30 across all samples.

Differential gene expression analysis was performed using the publicly available serotype 14 ST15 CGSP14 genome (NC_010582.1) (Ding *et al.*, 2009) as a reference. Initial analysis to compare the group of blood isolates with the ear isolates was carried out by AGRF using the EDGE-pro (Estimated Degree of Gene Expression in PROkaryotes) pipeline (Magoc, Wood & Salzberg 2013) and R/Bioconductor-based voom and limma packages (Ritchie *et al.*, 2015). In addition to AGRF's data analysis, differential gene expression analysis was also carried out using the R/Bioconductor DESeq (v.3.2) package (Anders & Huber, 2010) to validate AGRF's analysis, as well as to carry out differential gene expression analysis between single isolates. Firstly, sequenced reads were aligned to the CGSP14 reference genome using Bowtie2 (v2.0.0.0-beta6) (Langmead & Salzberg, 2012). SAMtools (v 0.0.18) (Li *et al.*, 2009) and BEDTools (v2.24.0) (Quinlan & Hall, 2010) were then used to obtain read counts for each transcript. DESeq analysis was subsequently performed using this data. DESeq analysis applies *P*-value adjustments (*P*_{adj}) on the analysed data which account for the false discovery rate (FDR) using the Benjamini-Hochberg method (Glueck *et al.*, 2008). An FDR-adjusted *P*-value of 0.05 implies that that 5% of the tests found to be statistically significant (e.g. by *P*-value) will be false positives. A significant differential expression in DESeq refers to all *P*_{adj} values of < 1. The Basic Local Alignment Search Tool (BLAST) (Altschul *et al.*, 1990) and Kyoto Encyclopedia of Genes and Genomes (KEGG) database resource (<http://www.genome.jp/kegg/genes.html>) were used as appropriate.

6.2.1.1 Transcriptomic analysis of ST15 blood and ear isolates.

Alignment of the reads of five transcriptomes of ST15 serotype 14 blood (ST15/4495, ST15/4534, ST15/4559) and ear isolates (ST15/9-47 and ST15/51742) against the reference genome revealed a total of 2276 coding sequence (CDS) transcripts sequenced for every isolate. However, when the transcriptomes of the five ST15 clinical strains were grouped according to isolation site (ear vs blood) and compared by AGRF, no significant differences in gene expression were observed between the two groups. DESeq analysis subsequently carried out confirmed the lack of significant differences in

gene expression between the two groups as analysed by AGRF, as adjusted *P*-values (*P*_{adj}) were determined to be 1 for all genes.

As part of the aforementioned analysis, single isolates were then compared separately using DESeq. Comparison of these isolates showed variable numbers of significantly differentially expressed genes between isolates with an average of 88 genes. Ear isolate ST15/9-47 compared against blood isolate ST15/4534 showed the highest number of differences (125 genes), while ear isolate ST15/9-47 compared against blood isolate ST15/4559 showed the lowest number of significantly differentially expressed genes (52 genes). Table 6.1 summarises the number of significantly differentially expressed genes for single strain-strain comparisons.

Table 6.1. Significantly differentiated genes identified by DESeq analysis of single blood and ear isolates.

DESeq analysis of isolate pairs	Differentially expressed genes (n)^a
ST15/9-47 (ear) vs ST15/4495 (blood)	69
ST15/51742 (ear) vs ST15/4495 (blood)	116
ST15/9-47 (ear) vs ST15/4534 (blood)	125
ST15/51742 (ear) vs ST15/4534 (blood)	76
ST15/9-47 (ear) vs ST15/4559 (blood)	52
ST15/51742 (ear) vs ST15/4559 (blood)	76
ST15/9-47 (ear) vs ST15/51742(ear)	97
ST15/4495 (blood) vs ST15/4534 (blood)	77
ST15/4495 (blood) vs ST15/4559 (blood)	103
ST15/4534 (blood) vs ST15/4559 (blood)	94

^a Number of significantly differentially expressed genes (*P*_{adj} < 0.05) based on *P* value adjusted for multiple testing using Benjamini-Hochberg method in the DESeq analysis software package.

Significant differences in gene expressions observed between isolates from the same source (blood vs blood; ear vs ear) as well as between sources (ear vs blood) suggests a high background of transcriptional differences that are unrelated to isolate source or virulence profile. Therefore, further investigations on common genes that are differentially expressed between multiple ear vs multiple blood isolates were carried out to determine commonality in gene expressions within the isolate groups. To probe for significantly differentially expressed genes common to both ear isolates, parallel comparison of the two ear isolates ST15/9-47 and ST15/51742 was carried out against single blood isolates. As shown in Table 6.2, 51 significantly differentially expressed genes were found to be common in the two ear isolates when compared with blood isolate ST15/4495. As shown in Table 6.2, 27 genes were found to be significantly upregulated and 24 genes significantly downregulated in both of the ear isolates when compared with blood isolate ST15/4495.

Table 6.2. Common differentially expressed genes in ear isolates ST15/9-47 and ST15/51742 relative to blood isolate ST15/4495.

GENE ID	ST15/9-47 vs ST15/4495		ST15/51742 vs ST15/4495	
	Fold change ^a	Statistical significance (<i>P</i> _{adj} ≤ 0.05) ^b	Fold change	Statistical significance (<i>P</i> _{adj} ≤ 0.05)
SPCG_0013 (<i>comX1</i>)	52.59	**	36.98	**
SPCG_0044 (<i>comA</i>) ^c	53.54	**	19.17	***
SPCG_0045 (<i>comB</i>) ^c	55.89	**	16.44	**
SPCG_0087 (ABC transporter, permease protein)	0.01	**	0.01	****
SPCG_0088 (ABC transporter, permease protein)	0.02	**	0.01	****
SPCG_0089 (ABC transporter substrate-binding)	0.02	**	0.01	****

protein)				
SPCG_0104 (Hypothetical Protein)	58.80	**	51.51	****
SPCG_0172 (<i>rRNA methylase</i>)	0.01	****	0.01	****
SPCG_0189 (<i>ribE</i>)	0.04	*	0.05	***
SPCG_0190 (<i>ribA</i>)	0.03	*	0.05	****
SPCG_0191 (<i>ribC</i>)	0.04	*	0.05	***
SPCG_0192 (<i>ribD</i>)	0.04	*	0.06	***
SPCG_0323 (<i>kdgA</i>)	0.01	**	0.02	****
SPCG_0324 (carbohydrate kinase)	0.01	**	0.02	****
SPCG_0325 (Hypothetical Protein)	0.01	**	0.02	****
SPCG_0326 (<i>gno</i>)	0.01	**	0.03	****
SPCG_0327 (PTS system N- acetylgalactosamine- specific IIA component)	0.01	***	0.01	****
SPCG_0328 (glucuronyl hydrolase)	0.006	***	0.014	****
SPCG_0329 (PTS system, N- acetylgalactosamine- specific IIB component)	0.008	***	0.011	****
SPCG_0330 (PTS system, N- acetylgalactosamine- specific IIC component)	0.007	***	0.014	****

SPCG_0331 (PTS system, N-acetylgalactosamine-specific IID component)	0.01	***	0.015	****
SPCG_0332 (preprotein translocase)	0.01	**	0.017	****
SPCG_0333 (Hypothetical Protein)	0.01	**	0.021	****
SPCG_0413 (<i>phaB</i>)	53.38	**	33.41	****
SPCG_0417 (<i>fabK</i>)	29.26	*	26.1	****
SPCG_0423 (<i>accC</i>)	17.92	*	18.96	****
SPCG_0424 (<i>accD</i>)	17.66	*	18.72	****
SPCG_0791 (degenerate transposase)	36.36	*	35.14	**
SPCG_0807 (degenerate transposase)	37.96	**	28.69	****
SPCG_0819 (hypothetical protein)	151.61	***	150.80	****
SPCG_0888 (hypothetical protein)	37.73	*	23.09	**
SPCG_0957 (IS3-Spn1)	21.53	*	12.55	**
SPCG_0961 (hypothetical protein)	37.29	*	37.58	****
SPCG_1267 (hypothetical protein)	40.19	**	29.35	****
SPCG_1274 (site-specific recombinase)	1040.20	****	1040.20	****

SPCG_1322 (hypothetical protein)	0.01	****	0.01	****
SPCG_1323 (erythromycin ribosome methylase)	0.01	****	0.01	****
SPCG_1326 (omega2 protein)	0.01	****	0.01	****
SPCG_1327 (rRNA methylase)	0.01	****	0.01	****
SPCG_1602 (hypothetical protein)	18.32	*	18.39	***
SPCG_1603 (hypothetical protein)	130.59	***	107.98	****
SPCG_1629 (hypothetical protein)	29.50	*	27.68	***
SPCG_1856 (<i>dexS</i>)	25.78	*	42.17	****
SPCG_1857 (<i>treP</i>)	34.45	*	57.91	****
SPCG_1949 (hypothetical protein) ^c	22.23	*	9.13	•
SPCG_1950 (ABC transporter, ATP-binding protein) ^c	28.72	*	11.48	**
SPCG_1951 (immunity protein, putative) ^c	30.42	*	12.78	***
SPCG_1952 (hypothetical protein)	39.75	**	15.37	***
SPCG_2118 (arginine deiminase)	0.03	*	0.01	****
SPCG_2119 (<i>arcB</i>)	0.04	*	0.02	****
SPCG_2202 (<i>comD</i>) ^c	21.05	*	8.71	**

^a Genes up-regulated greater than 2-fold are highlighted in bold type.

^b Statistical significance is indicated as follows: *, $P_{adj} < 0.05$; **, $P_{adj} < 0.01$; ***, $P_{adj} < 0.001$; ****, $P_{adj} < 0.0001$ ($padj$ value that corresponds to p-value adjusted for multiple testing using Benjamini-Hochberg method in the DESeq analysis software).

^c Common genes in blood isolates ST15/4495 and ST15/4534 differentially expressed against the two ear isolates are highlighted in yellow.

As shown in Table 6.3 below, parallel comparisons of ST15/9-47 and ST15/51742 showed 45 common significantly differentially expressed genes when the two ear isolates were compared with blood isolate ST15/4534, with 15 genes upregulated and 27 genes downregulated in the two ear isolates. However, expression of SPCG_2152 (*glpF*), SPCG_2153 (hypothetical protein) and SPCG_2154 (*glpK*) was observed to be upregulated in ST15/9-47, while the reverse was observed in ST15/51742.

Table 6.3. Common differentially expressed genes in ear isolates ST15/9-47 and ST15/51742 relative to blood isolate ST15/4534

GENE ID	ST15/9-47 VS ST15/4534		ST15/51742 VS ST15/4534	
	Fold change ^a	Statistical significance ($P_{adj} \leq 0.05$) ^b	Fold change	Statistical significance ($P_{adj} \leq 0.05$)
SPCG_0044 (<i>comA</i>) ^c	14.35	*****	5.19	*****
SPCG_0045 (<i>comB</i>) ^c	16.13	*****	4.79	*****
SPCG_0046 (<i>purC</i>)	0.33	**	0.07	*****
SPCG_0047 (<i>purL</i>)	0.06	*****	0.03	*****
SPCG_0048 (<i>purF</i>)	0.06	*****	0.04	*****
SPCG_0049 (<i>purM</i>)	0.07	*****	0.04	*****
SPCG_0050 (<i>purN</i>)	0.08	*****	0.04	*****
SPCG_0051 (<i>vanZ</i>)	0.11	*****	0.08	*****
SPCG_0052 (<i>purH</i>)	0.13	*****	0.14	*****
SPCG_0053 (<i>purD</i>)	0.04	*****	0.09	*****

SPCG_0054 (hypothetical protein)	0.03	****	0.08	**
SPCG_0055 (<i>purE</i>)	0.04	****	0.10	****
SPCG_0056 (<i>purK</i>)	0.05	****	0.14	****
SPCG_0057 (hypothetical protein)	0.41	**	0.38	*
SPCG_153 (lipoprotein; K02073 D- methionine transport system substrate-binding protein)	0.22	****	0.19	****
SPCG_0154 (hypothetical protein)	0.28	****	0.28	***
SPCG_0300 (xanthine/uracil permease family protein)	0.11	****	0.01	****
SPCG_0301 (hypothetical protein)	0.12	****	0.10	****
SPCG_0426 (hypothetical protein)	6.32	****	2.63	*
SPCG_0462 (hypothetical protein)	0.46	**	0.39	*
SPCG_0463 (hypothetical protein)	0.45	**	0.41	*
SPCG_0491 (<i>dnaJ</i>)	2.21	***	4.51	****
SPCG_0551 (<i>metE</i>)	0.11	****	0.10	****
SPCG_0552 (<i>metF</i>)	0.11	****	0.10	****
SPCG_0641 (hypothetical protein)	3.92	***	4.40	**

SPCG_0642 (ABC transporter, ATP-binding protein)	4.42	*	6.01	*
SPCG_0841 (Type I restriction- modification system, S subunit)	0.10	****	0.15	***
SPCG_1073 (hypothetical protein)	0.16	****	0.18	****
SPCG_1509 (<i>patB</i>)	0.32	****	0.33	**
SPCG_1510 (<i>metB</i>)	0.32	****	0.33	**
SPCG_1569 (<i>oxlT</i>)	0.15	****	0.20	****
SPCG_1689 (hypothetical protein)	8.34	****	3.03	**
SPCG_1690 (ABC transporter)	9.29	****	3.40	***
SPCG_1821(<i>xpt</i>)	0.12	****	0.07	****
SPCG_1822 (xanthine permease)	0.11	****	0.08	****
SPCG_1949 (hypothetical protein) ^c	12.40	****	5.15	****
SPCG_1950 (ABC transporter) ^c	13.38	****	5.40	****
SPCG_1951 (immunity protein, putative) ^c	13.50	****	5.73	****
SPCG_1952 (hypothetical protein)	19.84	****	7.75	****
SPCG_2152 (<i>glpF</i>) ^d	3.78	****	0.30	**
SPCG_2153 (hypothetical protein) ^d	3.52	****	0.28	***

SPCG_2154 (<i>glpK</i>) ^d	3.51	****	0.29	***
SPCG_2201 (<i>comE</i>)	11.80	****	5.03	****
SPCG_2202 (<i>comD</i>) ^c	11.46	****	4.79	****
SPCG_2203 (<i>comC</i>)	12.01	****	4.54	****

^a Genes up-regulated greater than 2-fold are highlighted in bold type.

^b Statistical significance is indicated as follows: *, *P*_{adj} < 0.05; **, *P*_{adj} < 0.01; ***, *P*_{adj} < 0.001; ****, *P*_{adj} < 0.0001 (*padj* value that corresponds to p-value adjusted for multiple testing using Benjamini-Hochberg method in the DESeq analysis software).

^c Common genes in blood isolate ST15/4495 and ST15/4534 differentially expressed against the two ear isolates are highlighted in yellow.

^d Common genes in blood isolate ST15/4534 and ST15/4559 differentially expressed against the two ear isolates are highlighted in green.

As shown in Table 6.4 below, 3 significantly differentiated genes were found to be common in the two ear isolates when compared with blood isolate **ST15/4559**. However, gene expression was not similar in the two ear isolates. Similar to blood isolate ST15/4534 the expression of SPCG_2152 (*glpF*), SPCG_2153 (hypothetical protein) and SPCG_2154 (*glpK*) was observed to be upregulated in ST15/9-47 while the reverse was observed in ST15/51742.

Table 6.4. Common differentially expressed genes in ear isolates ST15/9-47 and ST15/51742 relative to blood isolate ST15/4559.

GENE ID	ST15/9-47 VS ST15/4559		ST15/51742 VS ST15/4559	
	Fold change ^a	Statistical significance (<i>P</i> _{adj} ≤ 0.05) ^b	Fold change	Statistical significance (<i>P</i> _{adj} ≤ 0.05)
SPCG_2152 (<i>glpF</i>) ^d	2.06	***	0.16	****
SPCG_2153 (HP) ^d	2.05	***	0.16	****
SPCG_2154 (<i>glpK</i>) ^d	2.02	***	0.17	****

^a Genes up-regulated greater than 2-fold change are highlighted in bold type.

^b Statistical significance is indicated as follows: *, $P_{adj} < 0.05$; **, $P_{adj} < 0.01$; ***, $P_{adj} < 0.001$; ****, $P_{adj} < 0.0001$ (p_{adj} value that corresponds to p-value adjusted for multiple testing using Benjamini-Hochberg method in the DESeq analysis software).

^d Common genes in blood isolate ST15/4534 and ST15/4559 differentially expressed against the two ear isolates are highlighted in green.

As results in Tables 6.2-6.4 showed significantly differentially expressed genes, which were common to both ear isolates when compared against a single blood isolate, further in-parallel grouped comparisons between 2 blood isolates were carried out to identify common significantly differentially expressed genes in the blood isolates against the two ear isolates. Blood isolates ST15/4495 and ST15/4534 revealed 6 common genes differentially expressed against the two ear isolates (highlighted in yellow in Tables 6.2 and 6.3) while blood isolates ST15/4559 and ST15/4534 revealed 3 common genes (highlighted in green in Tables 6.3 and 6.4). No common significantly differentially expressed genes were identified in blood isolates ST15/4495 and ST15/4559 when compared against each of the two ear isolates.

6.2.1.2 Validation of RNA-Seq data by qRT-PCR

Independent validation of RNA-Seq data is an important component of transcriptomic data analysis in order to verify differential gene expression obtained from DESeq. qRT-PCR has been shown in many studies to show strong correlation with RNA-Seq data (Croucher & Thomson, 2010; Hu *et al.*, 2015; Passalacqua *et al.*, 2009). In this study, two genes, *nanA* and *spxB*, which have previously been shown to be associated with biofilm formation (Blanchette-Cain *et al.*, 2013; Parker *et al.*, 2009) were found to be differentially expressed in ear isolate ST15/9-47 relative to blood isolates ST15/4534 and ST15/4559 by DESeq (refer to Appendix C). These were therefore selected as targets for validation of the transcriptomic data obtained from RNA-Seq.

Bacterial strains from frozen stock were firstly grown in serum broth in triplicates to a final OD₆₀₀ of 0.2 and RNA was extracted using the Qiagen RNeasy Mini Kit as per manufacturer's instructions (Section 2.14). The quantity and integrity of the RNA samples were then determined (Section 2.18). qRT-PCR was performed (Section 2.15)

using the designated primers (Section 2.1) and the relative gene expression was analyzed using the $2^{-\Delta\Delta CT}$ method (Livak & Schmittgen, 2001). Quantified gene expression data for *nanA* and *spxB* obtained from the RNA-Seq analyses were then compared with qRT-PCR data (Table 6.5). It can be seen that there was close agreement between the qRT-PCR and RNA-Seq data wherein *nanA* was upregulated in ear isolate ST15/9-47 relative to both blood isolates, while *spxB* was downregulated.

Table 6.5. Validation of RNA-Seq data for *nanA* and *spxB* by qRT-PCR.

Gene	ST15/9-47 (EAR) VS ST15/4559 (BLOOD) ^a		ST15/9-47 (EAR) VS ST15/4534 (BLOOD)	
	RNA-Seq Fold change	qRT-PCR Fold change	RNA-Seq Fold change	qRT-PCR Fold change
SPCG-1665 (<i>nanA</i>)	2.4	2.8	2.4	3.8
SPCG_0679 (<i>spxB</i>)	0.09	0.3	0.07	0.22

6.2.2 Transcriptomic analysis of serotype 3 ST180 and ST232 clinical isolates

For transcriptomic analysis of serotype 3 strains a total of 4 blood (ST180/15, ST232/1) and ear isolates (ST180/2, ST232/11) previously investigated in Chapter 4 were selected. Bacterial strains from frozen stock were firstly grown in serum broth in triplicates to a final OD₆₀₀ of 0.2 and RNA was extracted using the Qiagen RNeasy Mini Kit as per the manufacturer's instructions (Section 2.14). The quantity and integrity of the RNA samples were then determined (Section 2.18). RNA samples with a RIN integrity of ≥ 8.0 and total yield of $\geq 3 \mu\text{g}$ were then sent to the Australian Genome and Research Facility (Melbourne) for ribosomal RNA removal using the Illumina Ribo-Zero (Bacteria) kit, cDNA library preparation and RNA-Sequencing using the Illumina Hi-Seq sequencing platform. The number of reads produced for each of the blood (ST180/15, ST232/1) and ear (ST180/2 and ST232/11) isolates were 28,027,131, 29,125,338, 27,193,077 and 27,916,214, respectively.

Differential gene expression analysis between the transcriptomes of blood and ear isolates was carried out by firstly aligning the sequenced reads against the serotype 3 ST180 SPNOXC141 (NC_017592.1) (Donati *et al.*, 2010) reference genome made publicly available on KEGG (http://www.genome.jp/dbget-bin/www_bget?gn:spw) using Bowtie2 (v2.0.0.0-beta6) (Langmead & Salzberg 2012). SAMtools (v 0.0.18) (Li *et al.*, 2009) and BEDTools (v2.24.0) (Quinlan & Hall 2010) were then used to obtain read counts for each gene. Differential analysis of the transcriptomes generated from BEDTools were then carried out using the R/Bioconductor based DESeq (<http://bioconductor.org/packages/release/bioc/html/DESeq.html>) software (v.3.2) (Anders & Huber 2010). The basic local alignment search tool (BLAST) (Altschul *et al.*, 1990) and Kyoto Encyclopedia of Genes and Genomes (KEGG) database resource was used as appropriate.

Ear and blood isolates from ST180 and ST232 were selected to carry out comparison of blood and ear transcriptomes from the same sequence type as previously done for serotype 14 ST15 isolates. However, visualisation of transcripts by the Artemis genome viewer (v 16.0.11) (Carver *et al.*, 2012) revealed contamination of the ST180/2 transcriptome with another unrelated strain. As ST180/2 was found to be unusable for analysis, only ear isolate ST232/11 was subsequently used for comparison with the blood isolates ST180/15 and ST232/1.

Analysis of the ear isolate ST232/11 revealed 67 significantly differentially expressed genes when compared with blood isolate ST180/15 (refer Appendix D). and 7 genes relative to blood isolate ST232/1 (refer Appendix E). As shown in Table 6.6, 6 genes were found to be commonly upregulated in blood isolates ST232/1 and 180/15 relative to the ear isolate ST232/11.

Table 6.6. Genes commonly differentially expressed in blood isolates ST232/1 and 180/15 relative to ear isolate ST232/11.

GENE ID	ST232/11 (ear) vs ST232/1 (blood)		ST232/11 (ear) vs ST180/15 (blood)	
	Fold change	Statistical significance ^a	Fold change	Statistical significance
SPNOXC15940 (<i>trpA</i>)	93.56	**	7.92	***
SPNOXC15950 (<i>trpB</i>)	90.75	**	8.17	***
SPNOXC15960 (<i>trpF</i>)	91.32	**	9.05	**
SPNOXC15970 (<i>trpC</i>)	101.20	**	6.73	**
SPNOXC15980 (<i>trpD</i>)	125.83	**	11.05	****
SPNOXC15990 (<i>trpG</i>)	193.26	**	10.20	**

^a Statistical significance is indicated as follows: *, $P_{adj} < 0.05$; **, $P_{adj} < 0.01$; ***, $P_{adj} < 0.001$; ****, $P_{adj} < 0.0001$ ($P_{adj} = P$ value adjusted for multiple testing using Benjamini-Hochberg method in the DESeq analysis software).

6.2.2.1 RNA-Seq data validation of ST180 and ST232 isolates by RT-PCR

In order to validate the results obtained by RNA-Seq, qRT-PCR of 2 genes *trpF* and *trpG* from the common differentially expressed genes for blood isolates ST180/15 and ST232/1 against ear isolate ST232/11 (Section 2.14). qRT-PCR was performed (Section 2.15) using appropriate primers (Section 2.1) and the relative gene expression was analyzed using the $2^{-\Delta\Delta CT}$ method (Livak & Schmittgen, 2001). qRT-PCR results (Table 6.7) were then compared with RNA-Seq data (Table 6.6). However, in marked contrast to the RNA-Seq data, qRT-PCR analysis indicated that expression of *trpF* and *trpG* was not significantly different in the ear isolate relative to either of the blood isolates. Possible reasons for this stark discrepancy will be discussed further in Section 6.3.

Table 6.7. qRT-PCR validation of RNA-Seq data for *trpF* and *trpG*.

Gene	qPCR fold change	
	ST232/11 vs ST232/1	ST232/11 vs ST180/15
SPNOXC15960 (<i>trpF</i>)	0.82	0.78
SPNOXC15990 (<i>trpG</i>)	1.04	1.13

6.3 Discussion

The extreme diversity of the pneumococcus as a species has resulted in markedly variable capacities of a given strain to cause either localised or invasive disease. Molecular determinants of this variation are still poorly understood. In Chapters 4 and 5, distinct virulence phenotypes that correlated with isolate source were consistently exhibited in mice after IN challenge with ST-matched (i.e. clonally-related) serotype 3 and 14 blood and ear isolates, suggesting stable niche adaptation by these strains. Transcriptomic analyses in this Chapter aimed to identify bacterial determinants which might contribute to these distinct virulence profiles.

RNA-seq analysis revealed substantial transcriptomic variation within a clonal lineage, as evidenced by the total number of differentially expressed genes observed between individual isolates of serotype 14 ST15. Somewhat unexpectedly, there was a similar number of differentially expressed genes whether comparisons were being made between ST-matched isolates from the same niche (i.e. ear vs ear; blood vs blood) or from different niches (ear vs blood). For the four strain-strain comparisons from the same niche, the number of differentially expressed genes ranged from 77 to 103 (mean 93), while for the six cross-niche comparisons, the range was 52-125 (mean 86) (Table 6.1). Thus, identification of transcriptional differences that might be associated with distinct virulence phenotypes is complicated by a high background of unrelated interstrain transcriptional variation.

To minimise the impact of the above variability, transcriptomic comparisons were made between the two ear isolates ST15/9-47 and ST15/51742 and each of the blood

isolates ST15/4495 and ST15/4534 to identify common differentially expressed genes (Tables 6.2 and 6.3). This identified 51 and 45 differentially expressed genes common to both ear isolates relative to ST15/4495 and ST15/4534, respectively.

However, of these, only 6 genes were differentially expressed in both ear isolates relative to both blood isolates. These 6 genes were all upregulated in the ear isolates and included competence genes *comA*, *comB* and *comD*. These genes are important components of the competence regulon, which mediates horizontal gene transfer that drives pneumococcal genome plasticity. Other competence-related genes, notably *comC*, *comE* and *comX1*, were also significantly upregulated in both ear isolates relative to either of the two blood isolates. The competence genes have been increasingly linked with virulence in recent years. For example, a study by Lau *et al.* (2001) reported that the ability of *S. pneumoniae* to cause pneumonia and bacteraemia in mice is attenuated in *comB* and *comD* mutants. ComB, and ComA are components of the ABC transporter required for the export of CSP (the competence stimulating peptide encoded by *comC*), while *comD* and *comE* respectively encode the histidine kinase and response regulator of the two-component signal transduction system that senses and responds to extracellular CSP.

Several other recent studies have also confirmed the role of competence in increasing virulence of pneumococci (Ibrahim *et al.*, 2004; Lin *et al.*, 2016; Zhu *et al.*, 2015). Zhu *et al.* (2015) demonstrated the importance of 14 of the ComX-regulated late competence genes in virulence, as deletion of these genes attenuated pneumococcal fitness during host infection to the same level in both wild-type and ComX-null genetic backgrounds; suggesting that the constitutive baseline expression of these genes was important for bacterial fitness (Zhu *et al.*, 2015). Ibrahim *et al.* (2004) also demonstrated the importance of the CiaR/H two-component system, involved in regulating pneumococcal virulence and competence; deletion of *CiaR* caused pneumococcal strains to become much less virulent in mouse models, less able to grow at higher temperatures, and more sensitive to oxidative stress. The expression of the CiaR/H-regulated HtrA,

implicated in the ability of the pneumococcus to colonize the nasopharynx of infant rats, was also reduced in a *ciaR*-null mutant (Ibrahim *et al.*, 2004).

It is notable, however, that in the present study, higher *com* regulon expression was observed in the two ear isolates relative to the blood isolates ST15/4495 and ST15/4534, even though the latter were better able to cause lung infection in the mouse model. It should, of course, be remembered that in the present study, even the blood isolates are still expressing *com* genes, albeit to a lesser extent than the ear isolates, whereas the various *com* mutants described in previous studies would lack the respective transcripts altogether. A further complicating factor is that when the transcriptomes of the two ST15 ear isolates were compared with the third ST15 blood isolate (ST15/4559), no *com* genes were differentially expressed. Thus, differences in expression of this regulon cannot account for the distinct virulence profiles of ST15 blood and ear isolates. Moreover, it remains a possibility that the observed differences in *com* expression were fortuitous, and related to slight variations in growth phase (*com* expression is influenced by cell density, i.e. quorum sensing (Cvitkovitch *et al.*, 2003)) at the time of RNA extraction for the various strains.

Three more genes found to be commonly differentially expressed in blood isolates ST15/4495 and ST15/4534 relative to the two ear isolates are SPCG_1949, SPCG_1950 and SPCG_1951. SPCG_1949 and SPCG_1951 are hypothetical and putative proteins with unknown functions, while SPCG_1950, is identified as an ABC transporter (ATP binding protein). ABC transporters are an important class of transmembrane transporters involved in the import and export of a wide variety of substrates, and many of these systems contribute to pneumococcal virulence as demonstrated in various studies (Kadioglu *et al.*, 2008; Lau *et al.*, 2001; Whalan *et al.*, 2006). Nonetheless, the expression of SPCG_1950 was not found to be significantly different in the blood isolate ST15/4559 when compared against the two ear isolates.

The differential expression of SPCG_2152 (*glpF*), SPCG_2153 (hypothetical protein) and SPCG_2154 (*glpK*) was also seen in blood isolates ST15/4559 and ST15/4534 relative to the ear isolates. Glycerol uptake facilitator protein (*glpF*) and

glycerol kinase (*glpK*) are involved as transporters in pneumococcal glycerol uptake. *glpF* has also been implicated in pneumococcal opacity variation (Saluja & Weiser 1995). However, the expression of *glpO* (glycerol oxidase), an important virulence factor preferentially expressed during meningitis in a mouse model (Mahdi *et al.*, 2012), was not significantly upregulated in the ear isolates. This was rather surprising, as the ability to cause meningitis was exclusively observed in the ST15 ear isolates, as shown in Chapter 5 (Figure 5.3).

Transcriptomic analysis of serotype 3 isolates revealed a high number of differentially expressed genes between ear isolate ST232/11 and blood isolate ST180/15. In contrast, only 7 genes were differentially expressed between ear isolate ST232/11 and blood isolate ST232/1 (see Appendix E). Interestingly, the 6 genes that were significantly upregulated in the ear isolate ST232/11 compared to both blood isolates ST232/1 and ST180/15 were all from a single operon: the tryptophan biosynthesis pathway genes *trpA*, *trpB*, *trpC*, *trpD*, *trpF* and *trpG*. However, it remains to be determined whether this differential expression of the *trp* operon directly contributes to the distinct virulence profiles of the serotype 3 ear and blood isolates.

Although qRT-PCR was able to validate RNA-Seq differential gene expression analysis (DEG) of the ST15 isolates, the same was not observed for serotype 3 isolates. qRT-PCR analysis did not detect any significant differential expression of *trpF* or *trpG* between the ear isolate ST232/11 and either of the blood isolates ST232/1 or ST180/15, compared with approximately 94-fold and 8-fold upregulation respectively as determined by RNAseq analysis. One possible explanation is that the *trp* operon is known to be repressed whenever tryptophan is present in the environment (Merino *et al.*, 2008). Thus, since RNAseq and qRT-PCR analyses were conducted on RNA extracted from bacterial cultures grown on different occasions, using different batches of serum broth as the growth medium, slight differences in residual tryptophan concentration in the medium at the time of harvest could have impacted the findings. This might also account for the roughly 10-fold differences in relative expression of the various *trp* genes observed

between the two blood isolates observed by RNAseq analysis (Table 6.6).

The transcriptomic analyses of both serotype 3 and serotype 14 isolates described in this Chapter failed to detect any genes that were consistently differentially expressed between the blood and ear isolates of a given ST. This is in spite of the consistent differences in virulence profiles observed in mice between serotype- and ST-matched blood and ear isolates. A probable explanation for these seemingly discordant findings could be that relative expression of key virulence-related genes *in vivo* may be markedly different from that observed in *in vitro* cultures from which the bacterial RNA was extracted in the present study. Indeed, several previous studies from this laboratory have shown differential virulence gene expression patterns between *in vitro* batch culture and *in vivo* derived RNA extracts, but also between bacterial RNA extracts from distinct host niches (e.g. nasopharynx vs blood vs brain) (Harvey *et al.*, 2011; Mahdi *et al.*, 2008; Ogunniyi *et al.*, 2009). These studies employed either qRT-PCR analysis of known virulence-related genes, or transcriptomic microarray analysis, which lacks the resolving power of more modern RNAseq approaches. Clearly, comparative transcriptomic analyses of the various serotype/ST-matched ear and blood isolates using RNA extracted from infected mouse tissues may provide a more meaningful indication of differential virulence gene expression patterns. However, the purity of bacterial RNA required for RNAseq analyses is somewhat greater than that needed for microarray studies. In the present study, total bacterial numbers in several of the key host niches under investigation were very low at critical times (particularly the first 24 h) of the disease process ($<10^3$ - 10^4 CFU per mouse in some niches [e.g. see Fig. 4.8 and 5.3]). To date, bacterial RNA yields in extracts from these samples have not been sufficient for RNAseq analysis.

As mentioned previously, Manso *et al.*, (2014) have identified a type I restriction-modification (RM) system (SpnIII) in *S. pneumoniae* strain D39, which can spontaneously rearrange to generate six SpnIII variants with distinct genomic methylation patterns (Manso *et al.*, 2014). Each SpnD39III variant exhibited distinct virulence profiles in experimental infection and there was evidence of *in vivo* selection for switching

between SpnD39III variants. Importantly, while the relative frequencies of the six alleles in a given culture was relatively stable during *in vitro* culture, the proportions varied significantly upon injection into mice. This finding suggests that regulation of virulence by epigenetic switching occurs *in vivo*. Whether such epigenetic switching contributes to the distinct virulence profiles of the serotype/ST-matched ear and blood isolates studied here is uncertain. Manso *et al.* described a PCR-amplification/restriction fragment assay for accurate quantitation of SpnIII allele frequencies. This technique could be used in future studies to determine whether there are differences in these frequencies between the various paired isolates, using DNA extracted from both *in vitro* and *in vivo* cultures. The fact that the first step of the assay involves PCR amplification of a region of DNA spanning the *spnIII* locus should enable accurate data to be obtained even when bacterial CFU counts in a given tissue are very low.

Chapter 7: Final Discussion

7.1 Introduction

S. pneumoniae is a preeminent human respiratory pathogen responsible for massive global morbidity and mortality. Its ability to survive in, and adapt to, distinct ecological niches within the human host results in capacity to cause a wide spectrum of invasive and localized infections. Its extremely diverse and plastic genome makes the pneumococcus highly adaptable to various selective pressures (Chaguza *et al.*, 2015). *S. pneumoniae* strains differ markedly in their capacity to cause either invasive or localized infections, and both serotype and genetic background influence virulence profile (Blomberg *et al.*, 2009; Sandgren *et al.*, 2005). The existence of over 93 CPS serotypes superimposed on over 5000 clonal lineages is a reflection of species diversity which underlies profound differences in disease potential. Due to this diversity, attempts to associate a given clonal lineage or serotype with propensity to cause disease are problematic. More importantly, these marked variations have frustrated attempts to identify specific molecular determinants of the distinct virulence phenotypes.

Formation of biofilms is an important step in pneumococcal pathogenesis, as they serve as reservoirs of infection and organisms within biofilms are resistant to antimicrobials and host immune defences. Biofilms also significantly impact on pneumococcal genetic diversity, as this environment favours horizontal gene transfer between cells (Marks *et al.*, 2012) and biofilm formation capacity has also been found to vary among clinical isolates (Moscoso *et al.*, 2009; Allegrucci *et al.*, 2006; Tapiainen *et al.*, 2010). This study initially examined the influence of three parameters, namely isolate source, pH and Fe(III) supplementation, on the formation of biofilms by a group of clinical isolates (Section 3.2). Previous studies have identified multiple molecular determinants of biofilm formation in clinical isolates (Tapiainen *et al.*, 2010; Trappetti *et al.*, 2011). However, this is the first study which has explored the association between clinical isolate source, biofilm formation capacity and virulence phenotype. This study focused on blood and ear isolates (from cases of sepsis and OM, respectively), as the

strain collection available to us had greater numbers of isolates from these sources rather than, for example, from CSF, ensuring a wide selection of serotypes and STs.

7.1.1 Biofilm formation of blood and ear clinical isolates of serotypes/serogroups 3, 6, 9, 14 and 19.

The initial assessment of blood and ear clinical isolates of serotypes/serogroups 3, 6, 9, 14 and 19 revealed profound inconsistencies in the influence of Fe(III), pH and isolate type on biofilm formation capacity. However after MLST typing, distinct biofilm phenotypes were identified between blood and ear isolates belonging to the same serotype/group and ST type. The suppressive effect of Fe(III) in biofilm formation when the strains were grown at pH 6.8 was also demonstrated. Additionally, the importance of LuxS and Fe(III) for biofilm formation capacity previously reported by Trappetti *et al.* (2011) also held true in this study.

7.1.2. Influence of clinical isolate source on virulence profiles of ST-matched serotype 3 and 14 isolates.

The stark differences in phenotypes observed between serotype 3 blood and ear isolates with respect to physiological conditions for optimal biofilm formation prompted questions as to whether the influence of source of clinical isolate might also be reflected in virulence phenotype. ST typing carried out in Chapter 3 allowed the selection of representative clonally related (ST-matched) blood and ear isolates from serotype 3 (ST180, ST233 and ST232) and serotype 14 (ST15 and ST130) for investigation of the influence of isolate source on virulence phenotype in Chapters 4 and 5.

Further *in vivo* investigations on blood and ear isolates belonging to serotype 3 ST180, ST232, and ST233, and serotype 14 ST15 revealed distinct pathogenic profiles. None of the blood isolates were found in the ear compartment after intranasal challenge, whereas the ear isolates were never recovered from the lung tissue at 24 h post infection. This showed a consistently stark distinction in virulence profiles *in vivo*, which clearly demonstrated the adaptation of the strains to their respective niches. This was further

supported by the exclusive detection of only serotype 14 ST15 ear isolates being recovered from the brain tissue over the time of the experiments. However, the *in vivo* co-infection experiment with ST15 isolates showed that ear isolates could also persist in the lungs when co-infected with the blood isolate. This suggested the possibilities of differential host immune responses to ear versus blood isolates, or the secretion of a virulence factor by the blood isolate that enabled the survival of the ear isolate over the course of the experiment.

7.1.3. Early lung immune response of mice to infection with blood and ear isolates.

The investigation of early immune response in the lungs of mice challenged by blood and ear isolates (Section 5.2.6), revealed an unsurprising induction of 35 pro-inflammatory genes in response to pneumococcal infection. However, strain-specific differences in gene expression were also observed, with 8 genes showing significant differential expression in lung tissue following challenge with blood isolate ST15/4495 compared to that in mice challenged with ear isolate ST15/9-47. Six genes showed a significantly greater degree of upregulation following challenge with the blood isolate. Two more genes, *Apcs* and *Il2*, were found to be up-regulated only following challenge with the ear isolate. These findings provided insight into how the host immune response may vary from strain to strain, resulting in distinct patterns of infection from two closely related strains.

7.1.4. Transcriptomic analysis of blood and ear isolate *in vitro*.

The consistent differences in pathogenic profiles of pneumococcal strains within a clonal lineage seen in Chapters 4 and 5 was consistent with stable niche adaptation by these strains in accordance with their original site of isolation. This suggested the existence of fundamental genomic, methylomic, transcriptomic, proteomic or metabolomic differences between clonally-related blood and ear isolates, which allows them to adapt and survive in distinct host niches. A comprehensive combined “omics” analysis of the various strains, preferably using *in vivo*-derived samples, would be

required to identify the underlying molecular basis for our observations. This is a major and costly undertaking, well beyond the scope of this thesis. Nevertheless, available resources were sufficient to commence transcriptomic analysis of the ST180, ST232 and ST15 strains using RNA-Sequencing.

Despite the observed differences in virulence profiles between serotype- and ST-matched blood and ear isolates, the transcriptomic analyses of both serotype 3 and serotype 14 isolates did not identify any genes that were consistently differentially expressed between the blood and ear isolates of a given ST. A probable explanation is that there may be differences in expression patterns of key virulence-related genes even between bacteria growing in different *in vivo* niches, let alone between *in vivo* niches and the *in vitro* cultures from which the bacterial RNA was extracted in the present study. Thus, future studies need to be focused on examining patterns of gene transcription in *in vivo*-derived bacterial RNA samples.

Concluding remarks and future directions

The findings of this study constitute a significant paradigm shift, in that we have found multiple examples of clonally-related strains that consistently and reproducibly exhibit distinct virulence phenotypes in mice that directly correlate with the original site of isolation from human patients (in this case, ear vs blood). Thus, strains within a clonal lineage can exhibit stable niche adaptation. Moreover, our data suggest differential capacity to trigger early host innate immune responses may, at least in part, underpin this adaptation and influence the course of disease. These findings provide a robust platform for future studies aimed at identifying critical bacterial and host determinants of pneumococcal virulence phenotype. Specific questions that can be addressed in these studies include the following:-

- *What bacterial features (genomic, methylomic, transcriptomic, proteomic or metabolomic) determine virulence/pathogenic phenotype?*

Comprehensive comparative “omics” analyses of the type 3 strains ST180/2 and ST180/15, and type 14 strains ST15/9-47 and ST15/4559 are currently in progress as part

of a nation-wide collaborative study. This will provide a comprehensive list of candidate genes/proteins/pathways whose level of expression or activity is associated with virulence phenotype. The contribution of individual components could then be tested, for example by mutagenesis or manipulation of expression of a candidate gene, and determining the impact on pathogenic profile of ear or blood isolates. Techniques for construction and analysis of in-frame deletion mutants of *S. pneumoniae*, or strains over-expressing genes as a consequence of ectopic expression from multi-copy plasmids, are well established in this laboratory. Alternatively, the course of disease induced by challenge with ear vs blood isolates could be followed in mice that have been immunized against one or more candidate proteins.

- *Which host factors/responses have the greatest influence on disease course?*

Studies in Chapter 5 identified several host genes which were differentially induced in mice during the early stages of infection with serotype- and ST-matched blood vs ear isolates. These factors can now be targeted to determine their individual contribution to disease progression. Experiments could include *in vivo* blockade by administration of appropriate factor-specific neutralizing monoclonal antibodies immediately before and after challenge with the respective strains, and determining the impact on disease progression. Alternatively, the pathogenic profile of ear and blood isolates could be compared in wild type vs gene knock-out mice (e.g. *Icam-1*^{-/-}, *Ifn-β1*^{-/-} and *IfnAR1*^{-/-} mice are available in the C57BL/6 background).

Management of pneumococcal disease is being hampered by increasing rates of antibiotic resistance and the limited serotype coverage and other shortcomings of existing vaccines. Future studies such as those outlined above, will provide important new information on the molecular basis for the range of pathogenic phenotypes displayed by *S. pneumoniae* strains. This will inform future development of novel vaccines capable of protecting against the full spectrum of pneumococcal infections, and identification of novel bacterial and host targets for therapeutic intervention.

References

- Alderson MR, Armitage RJ, Tough TW, Strockbine L, Fanslow WC & Spriggs MK. 1993.** CD40 expression by human monocytes: regulation by cytokines and activation of monocytes by the ligand for CD40. *J Exp Med*, **178**, 669-674.
- Alhamdi Y, Neill DR, Abrams ST, Malak HA, Yahya R, Barrett-Jolley R, Wang G, Kadioglu A & Toh CH. 2015.** Circulating pneumolysin is a potent inducer of cardiac injury during pneumococcal infection. *PLoS Pathog*, **11**, e1004836.
- Allegrucci M, Hu FZ, Shen K, Hayes J, Ehrlich, GD Post, JC & Sauer K. 2006.** Phenotypic characterization of *Streptococcus pneumoniae* biofilm development. *J Bacteriol*, **188**, 2325-2335.
- Altschul SF, Gish W, Miller W, Myers EW & Lipman DJ. 1990.** Basic local alignment search tool. *J Mol Biol*, **215**, 403-410.
- Amin Z, Harvey RM, Wang H, Hughes CE, Paton AW, Paton JC & Trappetti C .2015.** Isolation site influences virulence phenotype of serotype 14 *Streptococcus pneumoniae* strains belonging to multilocus sequence type 15. *Infect Immun*, **83**(, 4781-4790.
- Anderl JN, Franklin MJ & Stewart PS. 2000.** Role of antibiotic penetration limitation in *Klebsiella pneumoniae* biofilm resistance to ampicillin and ciprofloxacin. *Antimicrob Agents Chemother*, **44**, 1818-1824.
- Anderl JN, Zahller J, Roe F & Stewart PS. 2003.** Role of nutrient limitation and stationary-phase existence in *Klebsiella pneumoniae* biofilm resistance to ampicillin and ciprofloxacin. *Antimicrob Agents Chemother*, **47**, 1251-1256.
- Anders S & Huber W. 2010.** Differential expression analysis for sequence count data. *Genome Biol*, **11**,106.
- Andersson B, Dahmen J, Frejd T, Leffler H, Magnusson G, Noori G & Eden CS. 1983.** Identification of an active disaccharide unit of a glycoconjugate receptor for pneumococci attaching to human pharyngeal epithelial cells. *J Exp Med*, **158**, 559-570.
- Berry AM & Paton JC. 2000.** Additive attenuation of virulence of *Streptococcus pneumoniae* by mutation of the genes encoding pneumolysin and other putative pneumococcal virulence proteins. *Infect Immun*, **68**, 133-140.

- Berry AM, Paton JC & Hansman D. 1992.** Effect of insertional inactivation of the genes encoding pneumolysin and autolysin on the virulence of *Streptococcus pneumoniae* type 3. *Microb Pathog*, **12**, 87-93.
- Berry AM, Yother J, Briles DE, Hansman D & Paton JC. 1989.** Reduced virulence of a defined pneumolysin-negative mutant of *Streptococcus pneumoniae*. *Infect Immun*, **57**, 2037-2042.
- Berry AM, Lock RA, Paton JC. 1996.** Cloning and characterization of nanB, a second *Streptococcus pneumoniae* neuraminidase gene, and purification of the NanB enzyme from recombinant *Escherichia coli*. *J Bacteriol*. **178**, 4854-4860.
- Bewick T, Sheppard C, Greenwood S, Slack M, Trotter C, George R & Lim WS. 2012.** Serotype prevalence in adults hospitalised with pneumococcal non-invasive community-acquired pneumonia. *Thorax*, **67**, 540-545.
- Bewley MA, Naughton M, Preston J, Mitchell A, Holmes A, Marriott HM, Read RC, Mitchell TJ, Whyte MK & Dockrell DH. 2014.** Pneumolysin activates macrophage lysosomal membrane permeabilization and executes apoptosis by distinct mechanisms without membrane pore formation. *MBio*, **5**, e01710-01714.
- Biswas I, Jha JK, Fromm N. 2008.** Shuttle expression plasmids for genetic studies in *Streptococcus mutans*, *Microbiology*, **154**, 2275-2282.
- Blanchette-Cain K, Hinojosa CA, Akula Suresh Babu R, Lizcano A, Gonzalez-Juarbe, N, Munoz-Almagro, C, Sanchez, CJ, Bergman, MA & Orihuela, CJ. 2013.** *Streptococcus pneumoniae* biofilm formation is strain dependent, multifactorial, and associated with reduced invasiveness and immunoreactivity during colonisation. *MBio*, **4**, e00745-00713.
- Blomberg C, Dagerhamn J, Dahlberg S, Browall S, Fernebro J, Albiger B, Morfeldt, E, Normark S & Henriques-Normark B. 2009.** Pattern of accessory regions and invasive disease potential in *Streptococcus pneumoniae*. *J Infect Dis*, **199**, 1032-1042.
- Bodor AM, Jansch L, Wissing J & Wagner-Dobler I . 2011.** The luxS mutation causes loosely-bound biofilms in *Shewanella oneidensis*. *BMC Res Notes*, **4**, 180.
- Bogaert D, De Groot R & Hermans PW. 2004.** *Streptococcus pneumoniae* colonisation: the key to pneumococcal disease. *Lancet Infect Dis*, **4**,144-154.
- Branger J, Knapp S, Weijer S, Leemans JC, Pater JM, Speelman P, Florquin S & van der Poll T. 2004.** Role of Toll-like receptor 4 in gram-positive and gram-negative pneumonia in mice. *Infect Immun*, **72**, 788-794.

- Brown JS, Gilliland SM & Holden DW. 2001.** A *Streptococcus pneumoniae* pathogenicity island encoding an ABC transporter involved in iron uptake and virulence. *Mol Microbiol*, **40**, 572-585.
- Brown JS, Hussell T, Gilliland SM, Holden DW, Paton JC, Ehrenstein MR, Walport MJ & Botto M. 2002.** The classical pathway is the dominant complement pathway required for innate immunity to *Streptococcus pneumoniae* infection in mice. *Proc Natl Acad Sci U S A*, **99**, 16969-16974.
- Brueggemann AB, Griffiths DT, Meats E, Peto T, Crook DW & Spratt BG. 2003.** Clonal relationships between invasive and carriage *Streptococcus pneumoniae* and serotype- and clone-specific differences in invasive disease potential. *J Infect Dis*, **187**, 1424-1432.
- Burgos J, Falco V, Borrego A, Sorde R, Larrosa MN, Martinez X, Planes AM, Sanchez A, Palomar M, Rello J & Pahissa A. 2013.** Impact of the emergence of non-vaccine pneumococcal serotypes on the clinical presentation and outcome of adults with invasive pneumococcal pneumonia. *Clin Microbiol Infect*, **19**, 385-391.
- Burnaugh AM, Frantz LJ, King SJ. 2008.** Growth of *Streptococcus pneumoniae* on human glycoconjugates is dependent upon the sequential activity of bacterial exoglycosidases. *J Bacteriol*, **190**, 221-230.
- Butler JC, Breiman RF, Lipman HB, Hofmann J & Facklam RR. 1995.** Serotype distribution of *Streptococcus pneumoniae* infections among preschool children in the United States, 1978-1994: implications for development of a conjugate vaccine. *J Infect Dis*, **171**, 885-889.
- Cámara M, Boulnois G.J, Andrew P.W, Mitchell T.J. 1994.** A neuraminidase from *Streptococcus pneumoniae* has the features of a surface protein. *Infect. Immun.* **62**, 3688–3695.
- Camilli R, Pantosti A & Baldassarri L. 2011.** Contribution of serotype and genetic background to biofilm formation by *Streptococcus pneumoniae*. *Eur J Clin Microbiol Infect Dis*, **30**, 97-102.
- Canvin JR, Marvin AP, Sivakumaran M, Paton JC, Boulnois GJ, Andrew PW & Mitchell TJ. 1995.** The role of pneumolysin and autolysin in the pathology of pneumonia and septicemia in mice infected with a type 2 pneumococcus. *J Infect Dis*, **172**, 119-123.

- Cappelli G, Tetta C & Canaud B. 2005.** Is biofilm a cause of silent chronic inflammation in haemodialysis patients? A fascinating working hypothesis. *Nephrol Dial Transplant*, **20**, 266-270.
- Carver T, Harris SR, Berriman M, Parkhill J & McQuillan, JA. 2012.** Artemis: an integrated platform for visualization and analysis of high-throughput sequence-based experimental data. *Bioinformatics*, **28**, 464-469.
- Ceri H, Olson ME, Stremick C, Read RR, Morck D & Buret A. 1999.** The Calgary Biofilm Device: new technology for rapid determination of antibiotic susceptibilities of bacterial biofilms. *J Clin Microbiol*, **37**, 1771-1776.
- Chaguza C, Cornick JE & Everett DB. 2015.** Mechanisms and impact of genetic recombination in the evolution of *Streptococcus pneumoniae*. *Comput Struct Biotechnol J*, **13**, 241-247.
- Chao Y, Marks LR, Pettigrew MM & Hakansson AP. 2014.** *Streptococcus pneumoniae* biofilm formation and dispersion during colonisation and disease. *Front Cell Infect Microbiol*, **4**, 194.
- Chen X, Schauder S, Potier N, Van Dorsselaer A, Pelczer I, Bassler BL & Hughson FM. 2002.** Structural identification of a bacterial quorum-sensing signal containing boron. *Nature*, **415(6871)**, 545-549.
- Coffey TJ, Enright MC, Daniels M, Morona JK, Morona R, Hryniewicz W, Paton JC & Spratt BG. 1998.** Recombinational exchanges at the capsular polysaccharide biosynthetic locus lead to frequent serotype changes among natural isolates of *Streptococcus pneumoniae*. *Mol Microbiol*, **27(1)**, 73-83.
- Collins T, Read MA, Neish AS, Whitley MZ, Thanos D & Maniatis T. 1995.** Transcriptional regulation of endothelial cell adhesion molecules: NF-kappa B and cytokine-inducible enhancers. *FASEB J*, **9(10)**, 899-909.
- Costerton JW. 1999.** Introduction to biofilm. *Int J Antimicrob Agents*, **11(3-4)**, 217-221.
- Costerton JW, Lewandowski Z, Caldwell DE, Korber DR & Lappin-Scott HM. 1995.** Microbial biofilms. *Annu Rev Microbiol*, **49**, 711-745.
- Costerton JW, Stewart PS & Greenberg EP. 1999.** Bacterial biofilms: a common cause of persistent infections. *Science*, **284**, 131-1322.
- Costerton W, Veeh R, Shirtliff M, Pasmore M, Post C & Ehrlich G. 2003.** The application of biofilm science to the study and control of chronic bacterial infections. *J Clin Invest*, **112**, 1466-1477.

- Crook DW, Brueggemann AB, Sleeman KL, Peto TEA, Tuomanen EI. 2004.** Pneumococcal carriage. *The Pneumococcus. Washington Press*, 136-147
- Croucher NJ & Thomson NR. 2010.** Studying bacterial transcriptomes using RNA-seq. *Curr Opin Microbiol*, **13**, 619-624.
- Cundell DR, Gerard NP, Gerard C, Idanpaan-Heikkila I & Tuomanen EI. 1995.** *Streptococcus pneumoniae* anchor to activated human cells by the receptor for platelet-activating factor. *Nature*, **377**, 435-438.
- Cundell DR, Weiser JN, Shen J, Young A & Tuomanen EI. 1995.** Relationship between colonial morphology and adherence of *Streptococcus pneumoniae*. *Infect Immun*, **63**, 757-761.
- Currie AJ, Davidson DJ, Reid GS, Bharya S, MacDonald KL, Devon RS & Speert DP. 2004.** Primary immunodeficiency to pneumococcal infection due to a defect in Toll-like receptor signaling. *J Pediatr*, **144**, 512-518.
- Cvitkovitch DG, Li YH & Ellen RP. 2003.** Quorum sensing and biofilm formation in Streptococcal infections. *J Clin Invest*, **112**, 1626-1632.
- Dalia AB, Standish AJ & Weiser JN. 2010.** Three surface exoglycosidases from *Streptococcus pneumoniae*, NanA, BgaA, and StrH, promote resistance to opsonophagocytic killing by human neutrophils. *Infect Immun*, **78**, 2108-2116.
- Dave S, Carmicle S, Hammerschmidt S, Pangburn MK & McDaniel LS. 2004a.** Dual roles of PspC, a surface protein of *Streptococcus pneumoniae*, in binding human secretory IgA and factor H. *J Immunol*, **173**, J471-477.
- Dave S, Pangburn MK, Pruitt C & McDaniel LS. 2004b.** Interaction of human factor H with PspC of *Streptococcus pneumoniae*. *Indian J Med Res*, **119**, 66-73.
- Dawid S, Roche AM & Weiser JN. 2007.** The blp bacteriocins of *Streptococcus pneumoniae* mediate intraspecies competition both in vitro and in vivo. *Infect Immun*, **75**, 443-451.
- Dawid S, Sebert ME & Weiser JN. 2009.** Bacteriocin activity of *Streptococcus pneumoniae* is controlled by the serine protease HtrA via posttranscriptional regulation. *J Bacteriol*, **191**, 509-1518.
- De Araujo C, Balestrino D, Roth L, Charbonnel N & Forestier C. 2010.** Quorum sensing affects biofilm formation through lipopolysaccharide synthesis in *Klebsiella pneumoniae*. *Res Microbiol*, **161**, 595-603.

- Ding F, Tang P, Hsu MH, Cui P, Hu S, Yu J & Chiu CH. 2009.** Genome evolution driven by host adaptations results in a more virulent and antimicrobial-resistant *Streptococcus pneumoniae* serotype 14. *BMC Genomics*, **10**, 158.
- Domenech M, Araujo-Bazan L, Garcia E & Moscoso M 2014.** In vitro biofilm formation by *Streptococcus pneumoniae* as a predictor of post-vaccination emerging serotypes colonizing the human nasopharynx. *Environ Microbiol*, **16**, 1193-1201.
- Domenech M, Garcia E & Moscoso M 2009.** Versatility of the capsular genes during biofilm formation by *Streptococcus pneumoniae*. *Environ Microbiol*, **11**, 2542-2555.
- Domenech M, Garcia E & Moscoso M. 2012.** Biofilm formation in *Streptococcus pneumoniae*. *Microb Biotechnol*, **5**, 455-465.
- Domenech M, Garcia E, Prieto A & Moscoso M. 2013.** Insight into the composition of the intercellular matrix of *Streptococcus pneumoniae* biofilms. *Environ Microbiol*, **15**, 502-516.
- Donati C, Hiller NL, Tettelin H, Muzzi A, Croucher NJ, Angiuoli SV, Oggioni M, Dunning Hotopp JC, Hu FZ, Riley DR, Covacci A, Mitchell TJ, Bentley SD, Kilian M, Ehrlich GD, Rappuoli R, Moxon ER & Masignani V . 2010.** Structure and dynamics of the pan-genome of *Streptococcus pneumoniae* and closely related species. *Genome Biol*, **11**, R107.
- Donlan RM. 2002.** Biofilms: microbial life on surfaces. *Emerg Infect Dis*, **8**, 881-890.
- Douglas RM, Paton JC, Duncan SJ & Hansman DJ. 1983.** Antibody response to pneumococcal vaccination in children younger than five years of age. *J Infect Dis*, **148**, 131-137.
- Durack DT & Beeson PB. 1972.** Experimental bacterial endocarditis. II. Survival of a bacteria in endocardial vegetations. *Br J Exp Pathol*, **53**, 50-53.
- Ehrlich GD, Veeh R, Wang X, Costerton JW, Hayes JD, Hu FZ, Daigle BJ, Ehrlich MD & Post JC. 2002.** Mucosal biofilm formation on middle-ear mucosa in the chinchilla model of otitis media. *JAMA*, **287**,1710-1715.
- Eldholm V, Johnsborg O, Haugen K, Ohnstad HS & Havarstein LS 2009,** Fratricide in *Streptococcus pneumoniae*: contributions and role of the cell wall hydrolases CbpD, LytA and LytC. *Microbiology*, **155**, 2223-2234.

- Eng RH, Padberg FT, Smith SM, Tan EN & Cherubin CE 1991.** Bactericidal effects of antibiotics on slowly growing and nongrowing bacteria. *Antimicrob Agents Chemother*, **35**, 1824-1828.
- Engelhard D, Pomeranz S, Gallily R, Strauss N & Tuomanen E 1997.** Serotype-related differences in inflammatory response to *Streptococcus pneumoniae* in experimental meningitis. *J Infect Dis*, **175**, 79-982.
- Enright MC & Spratt BG. 1998.** A multilocus sequence typing scheme for *Streptococcus pneumoniae*: identification of clones associated with serious invasive disease. *Microbiology*, **144**, 3049-3060.
- Enright MC & Spratt BG. 1999.** Multilocus sequence typing. *Trends Microbiol*, **7**, 482-487.
- Feil EJ, Li BC, Aanensen DM, Hanage WP & Spratt BG. 2004.** eBURST: inferring patterns of evolutionary descent among clusters of related bacterial genotypes from multilocus sequence typing data. *J Bacteriol*, **186**, 1518-1530.
- Fernebro J, Andersson I, Sublett J, Morfeldt, E, Novak R, Tuomanen E, Normark S & Normark BH. 2004.** Capsular expression in *Streptococcus pneumoniae* negatively affects spontaneous and antibiotic-induced lysis and contributes to antibiotic tolerance. *J Infect Dis*, **189**, 328-338.
- Forbes ML, Horsey E, Hiller NL, Buchinsky FJ, Hayes JD, Compliment JM, Hillman T, Ezzo S, Shen K, Keefe R, Barbadora K, Post JC, Hu, FZ & Ehrlich, GD. 2008.** Strain-specific virulence phenotypes of *Streptococcus pneumoniae* assessed using the Chinchilla laniger model of otitis media *PLoS ONE*, **3**, e1969.
- Freeman JA & Bassler BL. 1999.** A genetic analysis of the function of LuxO, a two-component response regulator involved in quorum sensing in *Vibrio harveyi*. *Mol Microbiol*, **31**, 665-677.
- Frolet C, Beniazza M, Roux L, Gallet B, Noirclerc-Savoie M, Vernet T & Di Guilmi, AM. 2010.** New adhesin functions of surface-exposed pneumococcal proteins. *BMC Microbiol*, **10**, 190.
- Fux CA, Stoodley P, Hall-Stoodley L & Costerton JW. 2003.** Bacterial biofilms: a diagnostic and therapeutic challenge. *Expert Rev Anti Infect Ther*, **1**, 667-683.
- Fux CA, Wilson S & Stoodley P. 2004.** Detachment characteristics and oxacillin resistance of *Staphylococcus aureus* biofilm emboli in an in vitro catheter infection model. *J Bacteriol*, **186**, 4486-4491.

- Garcia-Castillo M, Morosini MI, Valverde A, Almaraz F, Baquero F, Canton R & del Campo R. 2007.** Differences in biofilm development and antibiotic susceptibility among *Streptococcus pneumoniae* isolates from cystic fibrosis samples and blood cultures. *J Antimicrob Chemother*, **59**, 301-304.
- Gasteiger G & Rudensky AY. 2014.** Interactions between innate and adaptive lymphocytes', *Nat Rev Immunol*, **14**, 631-639.
- Gaviria-Agudelo CL, Jordan-Villegas A, Garcia C & McCracken GH, Jr. 2016.** The Effect of 13-Valent Pneumococcal Conjugate Vaccine on the Serotype Distribution and Antibiotic Resistance Profiles in Children With Invasive Pneumococcal Disease. *J Pediatric Infect Dis Soc.*(EPub)
- Gentile A, Bardach A, Ciapponi A, Garcia-Marti S, Aruj P, Glujovsky D, Calcagno JI, Mazzoni A & Colindres RE 2012.** Epidemiology of community-acquired pneumonia in children of Latin America and the Caribbean: a systematic review and meta-analysis. *Int J Infect Dis*, **16**, e5-15.
- Gibson H, Taylor JH, Hall KE & Holah JT. 1999.** Effectiveness of cleaning techniques used in the food industry in terms of the removal of bacterial biofilms. *J Appl Microbiol*, **87**, 41-48.
- Gilmore KS, Srinivas P, Akins DR, Hatter KL & Gilmore MS. 2003.** Growth, development, and gene expression in a persistent *Streptococcus gordonii* biofilm. *Infect Immun*, **71**, 4759-4766.
- Glueck DH, Mandel J, Karimpour-Fard A, Hunter L, Muller KE. 2008.** Exact calculations of average power for the Benjamini-Hochberg procedure. *Int J Biostat*, **4**, doi: 10.2202/1557-4679.1103.
- Gogarten JP & Townsend JP. 2005.** Horizontal gene transfer, genome innovation and evolution. *Nat Rev Microbiol*, **3**, 679-687.
- Gonzalez MR, Bischofberger M, Pernet L, van der Goot FG & Freche B. 2008.** Bacterial pore-forming toxins: the (w)hole story?. *Cell Mol Life Sci*, **65**, 493-507.
- Gosink KK, Mann ER, Guglielmo C, Tuomanen EI & Masure HR. 2000.** Role of novel choline binding proteins in virulence of *Streptococcus pneumoniae*. *Infect Immun*, **68**, 5690-5695.
- Hale BG, Randall RE, Ortin J & Jackson D. 2008.** The multifunctional NS1 protein of influenza A viruses. *J Gen Virol*, **89**, 2359-2376.
- Hall-Stoodley L, Costerton JW & Stoodley P. 2004.** Bacterial biofilms: from the natural environment to infectious diseases. *Nat Rev Microbiol*, **2**, 95-108.

- Hall-Stoodley L, Hu FZ, Gieseke A, Nistico L, Nguyen D, Hayes J, Forbes M, Greenberg DP, Dice B, Burrows A, Wackym PA, Stoodley P, Post JC, Ehrlich GD & Kerschner JE. 2006.** Direct detection of bacterial biofilms on the middle-ear mucosa of children with chronic otitis media. *JAMA*, **296**, 202-211.
- Hall-Stoodley L, Nistico L, Sambanthamoorthy K, Dice B, Nguyen D, Mershon WJ, Johnson C, Hu FZ, Stoodley P, Ehrlich GD & Post JC. 2008.** Characterization of biofilm matrix, degradation by DNase treatment and evidence of capsule downregulation in *Streptococcus pneumoniae* clinical isolates *BMC Microbiol*, **8**, 173.
- Hall-Stoodley L & Stoodley P. 2002.** Developmental regulation of microbial biofilms. *Curr Opin Biotechnol*, **13**, 228-233.
- Hall-Stoodley L & Stoodley P. 2005.** Biofilm formation and dispersal and the transmission of human pathogens. *Trends Microbiol*, **13**, 7-10.
- Hammerschmidt S, Talay SR, Brandtzaeg P & Chhatwal GS. 1997.** SpsA, a novel pneumococcal surface protein with specific binding to secretory immunoglobulin A and secretory component. *Mol Microbiol*, **25**, 1113-1124.
- Hammerschmidt S, Wolff S, Hocke A, Rosseau S, Muller E & Rohde M. 2005.** Illustration of pneumococcal polysaccharide capsule during adherence and invasion of epithelial cells. *Infect Immun*, **73**, 4653-4667.
- Hanage WP, Kaijalainen TH, Syrjanen RK, Auranen K, Leinonen M, Makela PH & Spratt BG. 2005.** Invasiveness of serotypes and clones of *Streptococcus pneumoniae* among children in Finland. *Infect Immun*, **73**, 431-435.
- Harvey RM, Strocher UH, Ogunniyi AD, Smith-Vaughan HC, Leach AJ & Paton JC. 2011.** A variable region within the genome of *Streptococcus pneumoniae* contributes to strain-strain variation in virulence. *PLoS ONE*, **6(5)**, e19650.
- Havarstein LS, Coomaraswamy G & Morrison DA. 1995.** An unmodified heptadecapeptide pheromone induces competence for genetic transformation in *Streptococcus pneumoniae*. *Proc Natl Acad Sci U S A*, **92**, 11140-11144.
- Hiller NL, Ahmed A, Powell E, Martin DP, Eutsey R, Earl J, Janto B, Boissy RJ, Hogg J, Barbadora K, Sampath R, Lonergan S, Post JC, Hu, FZ. & Ehrlich GD. 2010.** Generation of genic diversity among *Streptococcus pneumoniae* strains via horizontal gene transfer during a chronic polyclonal pediatric infection. *PLoS Pathog*, **6**, e1001108.

- Hiller NL, Janto B, Hogg JS, Boissy R, Yu S, Powell E, Keefe R, Ehrlich NE, Shen K, Hayes J, Barbadora K, Klimke W, Dernovoy D, Tatusova,T, Parkhill J, Bentley SD, Post JC, Ehrlich GD & Hu FZ. 2007. Comparative genomic analyses of seventeen *Streptococcus pneumoniae* strains: insights into the pneumococcal supragenome. *J Bacteriol*, **189**, 8186-8195.
- Hoang M, Syamal M, Schaeffer MA, Sachdeva L, Berk R & Coticchia J. 2010. Biofilms and chronic otitis media: an initial exploration into the role of biofilms in the pathogenesis of chronic otitis media. *Am J Otolaryngol*, **31**, 241-245.
- Hoge CW, Reichler MR, Dominguez EA, Bremer JC, Mastro TD, Hendricks KA, Musher DM, Elliott JA, Facklam RR & Breiman RF. 1994. An epidemic of pneumococcal disease in an overcrowded, inadequately ventilated jail. *N Engl J Med*, **331**, 643-648.
- Houldsworth S, Andrew PW & Mitchell TJ. 1994. Pneumolysin stimulates production of tumor necrosis factor alpha and interleukin-1 beta by human mononuclear phagocytes. *Infect Immun*, **62**, 1501-1503.
- Hoyle BD & Costerton JW. 1991. Bacterial resistance to antibiotics: the role of biofilms. *Prog Drug Res*, **37**, 91-105.
- Hu L, Li H, Chen L, Lou Y, Amombo E & Fu J. 2015. RNA-seq for gene identification and transcript profiling in relation to root growth of bermudagrass (*Cynodon dactylon*) under salinity stress. *BMC Genomics*, **16**, 575.
- Hughes CE, Harvey RM, Plumptre CD & Paton JC. 2014. Development of primary invasive pneumococcal disease caused by serotype 1 pneumococci is driven by early increased type I interferon response in the lung. *Infect Immun*, **82**, 3919-3926.
- Hyams C, Camberlein E, Cohen JM, Bax K & Brown JS. 2010. The *Streptococcus pneumoniae* capsule inhibits complement activity and neutrophil phagocytosis by multiple mechanisms. *Infect Immun*, **78**, 704-715.
- Hyams C, Opel S, Hanage W, Yuste J, Bax K, Henriques-Normark B, Spratt BG & Brown JS. 2011. Effects of *Streptococcus pneumoniae* strain background on complement resistance. *PLoS ONE*, **6**, e24581.
- Ibrahim YM, Kerr AR, McCluskey J & Mitchell TJ. 2004. Control of virulence by the two-component system CiaR/H is mediated via HtrA, a major virulence factor of *Streptococcus pneumoniae*. *J Bacteriol*, **186**, 5258-5266.

- Jensen ET, Kharazmi A, Garred P, Kronborg G, Fomsgaard A, Mollnes TE & Hoiby N. 1993.** Complement activation by *Pseudomonas aeruginosa* biofilms. *Microb Pathog*, **15**, 377-388.
- Jesaitis AJ, Franklin MJ, Berglund D, Sasaki M, Lord CI, Bleazard JB, Duffy JE, Beyenal H & Lewandowski Z. 2003.** Compromised host defense on *Pseudomonas aeruginosa* biofilms: characterization of neutrophil and biofilm interactions. *J Immunol*, **171**, 4329-4339.
- Joyce EA, Kawale A, Censini S, Kim CC, Covacci A & Falkow S. 2004.** LuxS is required for persistent pneumococcal carriage and expression of virulence and biosynthesis genes. *Infect Immun*, **72**, 964-2975.
- Kadioglu A & Andrew PW. 2005.** Susceptibility and resistance to pneumococcal disease in mice. *Brief Funct Genomic Proteomic*, **4**, 241-247.
- Kadioglu A, Weiser JN, Paton JC & Andrew PW. 2008.** The role of *Streptococcus pneumoniae* virulence factors in host respiratory colonisation and disease. *Nat Rev Microbiol*, **6**, 288-301.
- Kalin M. 1998.** Pneumococcal serotypes and their clinical relevance. *Thorax*, vol. **53**, 159-162.
- Kelly T, Dillard JP & Yother J. 1994.** Effect of genetic switching of capsular type on virulence of *Streptococcus pneumoniae*. *Infect Immun*, **62**, 1813-1819.
- Kharazmi A & Nielsen H. 1991.** Inhibition of human monocyte chemotaxis and chemiluminescence by *Pseudomonas aeruginosa* elastase. *APMIS*, **9**, 93-95.
- Kilian M, Poulsen K, Blomqvist T, Havarstein LS, Bek-Thomsen M, Tettelin H & Sorensen UB. 2008.** Evolution of *Streptococcus pneumoniae* and its close commensal relatives. *PLoS ONE*, **3**, e2683.
- Kim JO & Weiser JN. 1998.** Association of intrastain phase variation in quantity of capsular polysaccharide and teichoic acid with the virulence of *Streptococcus pneumoniae*. *J Infect Dis*, **177**, 368-377.
- Kim SH, Song JH, Chung DR, Thamlikitkul V, Yang Y, Wang H, Lu M, So TM, Hsueh PR, Yasin RM, Carlos CC, Pham HV, Lalitha MK, Shimono N, Perera J, Shibl AM, Baek JY, Kang CI, Ko KS, Peck KR; ANSORP Study Group. 2012.** Changing trends in antimicrobial resistance of *Streptococcus pneumoniae* isolates in Asian countries: an Asian Network for Surveillance of Resistant Pathogens (ANSORP) study. *Antimicrob Agents Chemother*. **56**, 1418-1426.

- King SJ, Hippe KR, Gould JM, Bae D, Peterson S, Cline RT, Fasching C, Janoff EN & Weiser JN. 2004.** Phase variable desialylation of host proteins that bind to *Streptococcus pneumoniae* in vivo and protect the airway, *Mol Microbiol*, **54**, 159-171.
- King SJ, Whatmore AM & Dowson CG. 2005.** NanA, a neuraminidase from *Streptococcus pneumoniae*, shows high levels of sequence diversity, at least in part through recombination with *Streptococcus oralis*. *J Bacteriol*, **187**, 5376-5386.
- King S.J, Hippe K.R, Weiser J.N. 2006.** Deglycosylation of human glycoconjugates by the sequential activities of exoglycosidases expressed by *Streptococcus pneumoniae*. *Mol. Microbiol.* **59**, 961–974.
- Klein JO. 2000.** The burden of otitis media. *Vaccine*, **19**, S2-8.
- Koch R. 1880.** Investigations into the etiology of traumatic infective diseases. The New Sydenham Society, Volume LXXXVIII.
- Konig C, Schwank S & Blaser J. 2001.** Factors compromising antibiotic activity against biofilms of *Staphylococcus epidermidis*. *Eur J Clin Microbiol Infect Dis*, **20**, 20-26.
- Kronenberg A, Zucs P, Droz S & Muhlemann K. 2006.** Distribution and invasiveness of *Streptococcus pneumoniae* serotypes in Switzerland, a country with low antibiotic selection pressure, from 2001 to 2004. *J Clin Microbiol*, **44**, 2032-2038.
- Langmead B & Salzberg SL. 2012.** Fast gapped-read alignment with Bowtie 2. *Nat Methods*, **9**, 357-359.
- Lau GW, Haataja S, Lonetto M, Kensit SE, Marra A, Bryant AP, McDevitt D, Morrison DA & Holden DW. 2001.** A functional genomic analysis of type 3 *Streptococcus pneumoniae* virulence. *Mol Microbiol*, **40**, 555-571.
- Lazarevic V, Glimcher LH & Lord GM. 2013.** T-bet: a bridge between innate and adaptive immunity. *Nat Rev Immunol*, **13**, 777-789.
- Leach AJ, Boswell JB, Asche V, Nienhuys TG & Mathews JD. 1994.** Bacterial colonisation of the nasopharynx predicts very early onset and persistence of otitis media in Australian aboriginal infants. *Pediatr Infect Dis J*, **13**, 983-989.
- Lee PY, Li Y, Kumagai Y, Xu Y, Weinstein JS, Kellner ES, Nacionales DC, Butfiloski EJ, van Rooijen N, Akira S, Sobel ES, Satoh M & Reeves WH.**

2009. Type I interferon modulates monocyte recruitment and maturation in chronic inflammation. *Am J Pathol*, **175**, 2023-2033.
- Lehmann D, Willis J, Moore HC, Giele C, Murphy D, Keil AD, Harrison C, Bayley K, Watson M & Richmond P. 2010.** The changing epidemiology of invasive pneumococcal disease in aboriginal and non-aboriginal western Australians from 1997 through 2007 and emergence of nonvaccine serotypes. *Clin Infect Dis*, **50**, 1477-1486.
- LeMessurier KS, Ogunniyi AD & Paton JC. 2006.** Differential expression of key pneumococcal virulence genes in vivo. *Microbiology*, **152**, 305-311.
- Levine OS, Farley M, Harrison LH, Lefkowitz L, McGeer A & Schwartz B. 1999.** Risk factors for invasive pneumococcal disease in children: a population-based case-control study in North America, *Pediatrics*, **103**, E28.
- Li H, Handsaker B, Wysoker A, Fennell T, Ruan J, Homer N, Marth G, Abecasis G, Durbin R & Genome Project Data Processing Subgroup. 2009.** The Sequence Alignment/Map format and SAMtools, *Bioinformatics*, **25**, 2078-2079.
- Lin J, Zhu L & Lau GW. 2016.** Disentangling competence for genetic transformation and virulence in *Streptococcus pneumoniae*. *Curr Genet*, **62**, 97-103.
- Linder TE, Daniels RL, Lim DJ & DeMaria TF. 1994.** Effect of intranasal inoculation of *Streptococcus pneumoniae* on the structure of the surface carbohydrates of the chinchilla eustachian tube and middle ear mucosa. *Microb Pathog*, **16**, 435-441.
- Lizcano A, Chin T, Sauer K, Tuomanen EI & Orihuela CJ. 2010.** Early biofilm formation on microtiter plates is not correlated with the invasive disease potential of *Streptococcus pneumoniae*. *Microb Pathog*, **48**, 124-130.
- Lock R.A, Paton J.C, Hansman D. 1988.** Purification and immunological characterization of neuraminidase produced by *Streptococcus pneumoniae*. *Microb. Pathog.* **4**, 33-43.
- Loo CY, Corliss DA & Ganeshkumar N. 2000.** *Streptococcus gordonii* biofilm formation: identification of genes that code for biofilm phenotypes. *J Bacteriol*, **182**, 1374-1382.
- Lopez R, Ronda-Lain C, Tapia A, Waks SB & Tomasz A. 1976.** Suppression of the lytic and bactericidal effects of cell wallinhibitory antibiotics. *Antimicrob Agents Chemother*, **10**, 697-706.
- Mackay F, Loetscher H, Stueber D, Gehr G & Lesslauer W. 1993.** Tumor necrosis factor alpha (TNF-alpha)-induced cell adhesion to human endothelial cells is

- under dominant control of one TNF receptor type, TNF-R55. *J Exp Med*, **177**, 1277-1286.
- Magoc T, Wood D & Salzberg SL. 2013.** EDGE-pro: Estimated Degree of Gene Expression in Prokaryotic Genomes. *Evol Bioinform Online*, **9**, 127-136.
- Mahdi LK, Ogunniyi AD, LeMessurier KS & Paton JC. 2008.** Pneumococcal virulence gene expression and host cytokine profiles during pathogenesis of invasive disease. *Infect Immun*, **76**, 646-657.
- Mahdi LK, Wang H, Van der Hoek MB, Paton JC & Ogunniyi AD. 2012.** Identification of a novel pneumococcal vaccine antigen preferentially expressed during meningitis in mice. *J Clin Invest*, **122**, 2208-2220.
- Mai-Prochnow A, Lucas-Elio P, Egan S, Thomas T, Webb JS, Sanchez-Amat A & Kjelleberg S. 2008.** Hydrogen peroxide linked to lysine oxidase activity facilitates biofilm differentiation and dispersal in several gram-negative bacteria. *J Bacteriol*, **190**, 5493-5501.
- Maiden MC, Jansen van Rensburg MJ, Bray JE, Earle SG, Ford SA, Jolley KA & McCarthy ND. 2013,** MLST revisited: the gene-by-gene approach to bacterial genomics. *Nat Rev Microbiol*, **11**, 728-736.
- Manco S, Hernon F, Yesilkaya H, Paton JC, Andrew PW & Kadioglu A. 2006.** Pneumococcal neuraminidases A and B both have essential roles during infection of the respiratory tract and sepsis. *Infect Immun*, **74**, 4014-4020.
- Mandigers CM, Diepersloot RJ, Dessens M, Mol SJ & van Klingeren B. 1994.** A hospital outbreak of penicillin-resistant pneumococci in The Netherlands. *Eur Respir J*, **7**, 1635-1639.
- Manso AS, Chai MH, Atack JM, Furi L, De Ste Croix M, Haigh R, Trappetti C, Ogunniyi AD, Shewell LK, Boitano M, Clark TA, Korlach J, Blades M, Mirkes E, Gorban AN, Paton JC, Jennings MP & Oggioni MR. 2014.** A random six-phase switch regulates pneumococcal virulence via global epigenetic changes. *Nat Commun*, **5**, 5055.
- Marion C, Stewart JM, Tazi MF, Burnaugh AM, Linke CM, Woodiga SA & King SJ. 2012.** *Streptococcus pneumoniae* can utilize multiple sources of hyaluronic acid for growth. *Infect Immun*, **80**, 1390-1398.
- Marks LR, Davidson BA, Knight PR & Hakansson AP. 2013.** Interkingdom signaling induces *Streptococcus pneumoniae* biofilm dispersion and transition from asymptomatic colonisation to disease. *MBio*, **4**, 4.

- Marks LR, Parameswaran GI & Hakansson AP. 2012.** Pneumococcal interactions with epithelial cells are crucial for optimal biofilm formation and colonisation in vitro and in vivo. *Infect Immun*, **80**, 2744-2760.
- Marks LR, Reddinger RM & Hakansson AP. 2012.** High levels of genetic recombination during nasopharyngeal carriage and biofilm formation in *Streptococcus pneumoniae*, *MBio*, **3**, 5.
- Maukonen J, Matto J, Wirtanen G, Raaska L, Mattila-Sandholm T & Saarela M. 2003.** Methodologies for the characterization of microbes in industrial environments: a review. *J Ind Microbiol Biotechnol*, **30**, 327-356.
- McAllister LJ, Ogunniyi AD, Stroehner UH, Leach AJ & Paton JC. 2011.** Contribution of serotype and genetic background to virulence of serotype 3 and serogroup 11 pneumococcal isolates. *Infect Immun*, **79**, 4839-4849.
- McAllister LJ, Tseng HJ, Ogunniyi AD, Jennings MP, McEwan AG & Paton JC. 2004.** Molecular analysis of the psa permease complex of *Streptococcus pneumoniae*. *Mol Microbiol*, **53**, 889-901.
- McClure R, Balasubramanian D, Sun Y, Bobrovskyy M, Sumbly P, Genco CA, Vanderpool CK & Tjaden B. 2013.** Computational analysis of bacterial RNA-Seq data. *Nucleic Acids Res*, **41**, e140.
- McCullers JA & Bartmess KC. 2003.** Role of neuraminidase in lethal synergism between influenza virus and *Streptococcus pneumoniae*. *J Infect Dis*, **187**, 1000-1009.
- McCullers, JA & Tuomanen, EI. 2001.** Molecular pathogenesis of pneumococcal pneumonia. *Front Biosci*, **6**, 877-889.
- McDevitt CA, Ogunniyi AD, Valkov E, Lawrence MC, Kobe B, McEwan AG & Paton JC. 2011.** A molecular mechanism for bacterial susceptibility to zinc, *PLoS Pathog*, **7**, e1002357.
- McEllistrem MC, Adams JM, Shutt K, Sanza LT, Facklam RR, Whitney CG, Jorgensen JH & Harrison LH. 2005.** Erythromycin-nonsusceptible *Streptococcus pneumoniae* in children, 1999-2001. *Emerg Infect Dis*, **11**, 969-972.
- McEllistrem MC, Ransford JV & Khan SA. 2007.** Characterization of in vitro biofilm-associated pneumococcal phase variants of a clinically relevant serotype 3 clone. *J Clin Microbiol*, **45**, 97-101.
- Merino E, Jensen RA & Yanofsky C. 2008.** Evolution of bacterial trp operons and their regulation. *Curr Opin Microbiol*, **11**, 78-86.

- Merritt J, Kreth J, Shi W & Qi F. 2005.** LuxS controls bacteriocin production in *Streptococcus mutans* through a novel regulatory component. *Mol Microbiol*, **57**, 960-969.
- Miller E, Andrews NJ, Waight PA, Slack MP & George RC. 2011.** Herd immunity and serotype replacement 4 years after seven-valent pneumococcal conjugate vaccination in England and Wales: an observational cohort study. *Lancet Infect Dis*, **11**, 760-768.
- Miller MB & Bassler BL. 2001.** Quorum sensing in bacteria. *Annu Rev Microbiol*, **55**, 165-199.
- Mitchell TJ, Andrew PW, Saunders FK, Smith AN & Boulnois GJ. 1991.** Complement activation and antibody binding by pneumolysin via a region of the toxin homologous to a human acute-phase protein. *Mol Microbiol*, **5**, 1883-1888.
- Mizrachi-Nebenzahl Y, Lifshitz S, Teitelbaum R, Novick S, Levi A, Benharroch D, Ling E & Dagan R. 2003.** Differential activation of the immune system by virulent *Streptococcus pneumoniae* strains determines recovery or death of the host'. *Clin Exp Immunol*, **134**, 23-31.
- Morens DM, Taubenberger JK & Fauci AS. 2008.** Predominant role of bacterial pneumonia as a cause of death in pandemic influenza: implications for pandemic influenza preparedness. *J Infect Dis*, **198**, 962-970.
- Morris PS, Leach AJ, Silberberg P, Mellon G, Wilson C, Hamilton E & Beissbarth J. 2005.** Otitis media in young Aboriginal children from remote communities in Northern and Central Australia: a cross-sectional survey. *BMC Pediatr*, **5**, 27.
- Moscoso M, Garcia E & Lopez R. 2006.** Biofilm formation by *Streptococcus pneumoniae*: role of choline, extracellular DNA, and capsular polysaccharide in microbial accretion. *J Bacteriol*, **188**, 7785-7795.
- Moscoso M, Garcia E & Lopez R. 2009.** Pneumococcal biofilms. *Int Microbiol*, **12**, 77-85.
- Mosser DM. 2003.** The many faces of macrophage activation. *J Leukoc Biol*, **73**, 209-212.
- Mosser JL & Tomasz A. 1970.** Choline-containing teichoic acid as a structural component of pneumococcal cell wall and its role in sensitivity to lysis by an autolytic enzyme. *J Biol Chem*, **245**, 287-298.

- Munoz-Elias EJ, Marcano J & Camilli A. 2008.** Isolation of *Streptococcus pneumoniae* biofilm mutants and their characterization during nasopharyngeal colonisation. *Infect Immun*, **76**, 5049-5061.
- Naucler P, Darenberg J, Morfeldt E, Ortqvist A & Henriques Normark B. 2013.** Contribution of host, bacterial factors and antibiotic treatment to mortality in adult patients with bacteraemic pneumococcal pneumonia. *Thorax*, **68**, 571-579.
- Nelson AL, Roche AM, Gould JM, Chim K, Ratner AJ & Weiser JN. 2007.** Capsule enhances pneumococcal colonisation by limiting mucus-mediated clearance, *Infect Immun*, **75**, 83-90.
- O'Brien KL, Wolfson LJ, Watt JP, Henkle E, Deloria-Knoll M, McCall N, Lee E, Mulholland K, Levine OS & Cherian T. 2009.** Burden of disease caused by *Streptococcus pneumoniae* in children younger than 5 years: global estimates. *Lancet*, **374**, 893-902.
- O'Toole GA. 2011.** Microtiter dish biofilm formation assay. *J Vis Exp*, **47**.
- Obaro SK, Adegbola RA, Banya WA & Greenwood BM. 1996.** Carriage of pneumococci after pneumococcal vaccination. *Lancet*, **348(9022)**, 271-272.
- Oggioni MR, Trappetti C, Kadioglu A, Cassone M, Iannelli F, Ricci S, Andrew PW & Pozzi G. 2006.** Switch from planktonic to sessile life: a major event in pneumococcal pathogenesis. *Mol Microbiol*, **61**, 1196-1210.
- Ogunniyi AD, Grabowicz M, Mahdi LK, Cook J, Gordon DL, Sadlon TA & Paton JC. 2009.** Pneumococcal histidine triad proteins are regulated by the Zn²⁺-dependent repressor AdcR and inhibit complement deposition through the recruitment of complement factor H. *FASEB J*, **23**, 731-738.
- Ogunniyi AD, Mahdi LK, Trappetti C, Verhoeven N, Mermans D, Van der Hoek MB, Plumtre CD & Paton JC. 2012.** Identification of genes that contribute to the pathogenesis of invasive pneumococcal disease by in vivo transcriptomic analysis. *Infect Immun*, **80**, 3268-3278.
- Opitz B, van Laak V, Eitel J & Suttorp N. 2010.** Innate immune recognition in infectious and noninfectious diseases of the lung. *Am J Respir Crit Care Med*, **181**, 1294-1309.
- Orihuela CJ, Mahdavi J, Thornton J, Mann B, Wooldridge KG, Abouseada N, Oldfield NJ, Self T, Ala'Aldeen DA & Tuomanen EI. 2009.** Laminin receptor initiates bacterial contact with the blood brain barrier in experimental meningitis models. *J Clin Invest*, **119**, 1638-1646.

- Parker D, Soong G, Planet P, Brower J, Ratner AJ & Prince A. 2009.** The NanA neuraminidase of *Streptococcus pneumoniae* is involved in biofilm formation. *Infect Immun*, **77**, 3722-3730.
- Parveen A, Smith G, Salisbury V & Nelson SM. 2001.** Biofilm culture of *Pseudomonas aeruginosa* expressing lux genes as a model to study susceptibility to antimicrobials. *FEMS Microbiol Lett*, **199**, 115-118.
- Passalacqua KD, Varadarajan A, Ondov BD, Okou DT, Zwick ME & Bergman NH. 2009.** Structure and complexity of a bacterial transcriptome. *J Bacteriol*, vol. **191**, 3203-3211.
- Pastor P, Medley F & Murphy TV. 1998.** Invasive pneumococcal disease in Dallas County, Texas: results from population-based surveillance in 1995. *Clin Infect Dis*, **26**, 590-595.
- Paton JC, Rowan-Kelly B & Ferrante A. 1984.** Activation of human complement by the pneumococcal toxin pneumolysin. *Infect Immun*, **43**, 1085-1087.
- Pessoa D, Hoti F, Syrjanen R, Sa-Leao R, Kaijalainen T, Gomes MG & Auranen K. 2013.** Comparative analysis of *Streptococcus pneumoniae* transmission in Portuguese and Finnish day-care centres. *BMC Infect Dis*, **13**, 180.
- Pettigrew MM, Fennie KP, York MP, Daniels J & Ghaffar F. 2006.** Variation in the presence of neuraminidase genes among *Streptococcus pneumoniae* isolates with identical sequence types. *Infect Immun*, **74**, 3360-3365.
- Pettigrew MM, Marks LR, Kong Y, Gent JF, Roche-Hakansson H & Hakansson AP. 2014.** Dynamic changes in the *Streptococcus pneumoniae* transcriptome during transition from biofilm formation to invasive disease upon influenza A virus infection. *Infect Immun*, **82**, 4607-4619.
- Platt, TG & Fuqua C. 2010.** What's in a name? The semantics of quorum sensing. *Trends Microbiol*, **18**, 383-387.
- Pneumococcal vaccines WHO position paper - 2012 - recommendations.** 2012, *Vaccine*, **30**, 4717-4718.
- Pneumococcal vaccines WHO position paper--2012.** 2012, *Wkly Epidemiol Rec*, vol. **87**, 129-144.
- Portillo, JA, Feliciano, LM, Okenka, G, Heinzl, F, Subauste, MC & Subauste, CS. 2012.** CD40 and tumour necrosis factor-alpha co-operate to up-regulate inducible nitric oxide synthase expression in macrophages. *Immunology*, **135**, 140-150.

- Post JC, Stoodley P, Hall-Stoodley, L & Ehrlich, GD. 2004.** The role of biofilms in otolaryngologic infections. *Curr Opin Otolaryngol Head Neck Surg*, **12**, 185-190.
- Pruitt KD, Tatusova T & Maglott DR. 2005.** NCBI Reference Sequence (RefSeq): a curated non-redundant sequence database of genomes, transcripts and proteins. *Nucleic Acids Res*, **33**, D501-504.
- Quinlan AR & Hall IM. 2010.** BEDTools: a flexible suite of utilities for comparing genomic features. *Bioinformatics*, **26**, 841-842.
- Rajam G, Anderton JM, Carlone GM, Sampson JS & Ades EW. 2008.** Pneumococcal surface adhesin A (PsaA): a review. *Crit Rev Microbiol*, **34**, 131-142.
- Reading NC & Sperandio V. 2006.** Quorum sensing: the many languages of bacteria. *FEMS Microbiol Lett*, **254**, 1-11.
- Reid SD, Hong W, Dew KE, Winn DR, Pang B, Watt J, Glover DT, Hollingshead SK & Swords WE. 2009.** *Streptococcus pneumoniae* forms surface-attached communities in the middle ear of experimentally infected chinchillas. *J Infect Dis*, **199**, 786-794.
- Ren B, Szalai AJ, Thomas, O, Hollingshead, SK & Briles, DE. 2003.** Both family 1 and family 2 PspA proteins can inhibit complement deposition and confer virulence to a capsular serotype 3 strain of *Streptococcus pneumoniae*. *Infect Immun*, **71**, 75-85.
- Ritchie ME, Phipson B, Wu D, Hu Y, Law CW, Shi W & Smyth GK. 2015.** limma powers differential expression analyses for RNA-sequencing and microarray studies, *Nucleic Acids Res*, **43**, e47.
- Robbins JB, Austrian R, Lee CJ, Rastogi SC, Schiffman G, Henrichsen J, Makela PH, Broome CV, Facklam RR, Tiesjema RH & et al., 1983.** Considerations for formulating the second-generation pneumococcal capsular polysaccharide vaccine with emphasis on the cross-reactive types within groups. *J Infect Dis*, **148**, 1136-1159.
- Rodgers GL, Arguedas A, Cohen R & Dagan R. 2009.** Global serotype distribution among *Streptococcus pneumoniae* isolates causing otitis media in children: potential implications for pneumococcal conjugate vaccines. *Vaccine*, **27**, 3802-3810.
- Rosenow C, Ryan P, Weiser JN, Johnson S, Fontan P, Ortqvist A & Masure HR. 1997.** Contribution of novel choline-binding proteins to adherence, colonisation and immunogenicity of *Streptococcus pneumoniae*. *Mol Microbiol*, **25**, 819-829.

- Rubins JB, Charboneau D, Paton JC, Mitchell TJ, Andrew PW & Janoff EN. 1995.** Dual function of pneumolysin in the early pathogenesis of murine pneumococcal pneumonia. *J Clin Invest*, **95**, 142-150.
- Rutebemberwa E, Mpeka B, Pariyo G, Peterson S, Mworzi E, Bwanga F, Källander K. 2015.** High prevalence of antibiotic resistance in nasopharyngeal bacterial isolates from healthy children in rural Uganda: A cross-sectional study. *Ups J Med Sci*, **120**, 249-256.
- Saluja SK & Weiser JN. 1995.** The genetic basis of colony opacity in *Streptococcus pneumoniae*: evidence for the effect of box elements on the frequency of phenotypic variation. *Mol Microbiol*, **16**, 215-227.
- Sanchez CJ, Hurtgen BJ, Lizcano A, Shivshankar P, Cole GT & Orihuela CJ. 2011.** Biofilm and planktonic pneumococci demonstrate disparate immunoreactivity to human convalescent sera. *BMC Microbiol*, **11**, 245.
- Sanchez CJ, Kumar N, Lizcano A, Shivshankar P, Dunning Hotopp JC, Jorgensen JH, Tettelin H & Orihuela CJ. 2011.** *Streptococcus pneumoniae* in biofilms are unable to cause invasive disease due to altered virulence determinant production. *PLoS ONE*, **6**, e28738.
- Sanchez CJ, Shivshankar P, Stol K, Trakhtenbroit S, Sullam PM, Sauer K, Hermans PW & Orihuela CJ. 2010.** The pneumococcal serine-rich repeat protein is an intra-species bacterial adhesin that promotes bacterial aggregation in vivo and in biofilms. *PLoS Pathog*, **6**, e1001044.
- Sandgren A, Albiger B, Orihuela CJ, Tuomanen E, Normark S & Henriques-Normark B. 2005.** Virulence in mice of pneumococcal clonal types with known invasive disease potential in humans. *J Infect Dis*, **192**, 791-800.
- Sandgren A, Sjoström K, Olsson-Liljequist B, Christensson B, Samuelsson A, Kronvall G & Henriques Normark B. 2004.** Effect of clonal and serotype-specific properties on the invasive capacity of *Streptococcus pneumoniae*. *J Infect Dis*, **189**, 785-796.
- Serrano I, Melo-Cristino J & Ramirez M. 2006.** Heterogeneity of pneumococcal phase variants in invasive human infections. *BMC Microbiol*, **6**, 67.

- Shak JR, Ludewick HP, Howery KE, Sakai F, Yi H, Harvey RM, Paton JC, Klugman KP & Vidal JE. 2013.** Novel role for the *Streptococcus pneumoniae* toxin pneumolysin in the assembly of biofilms. *MBio*, **4**, e00655-00613.
- Shaper M, Hollingshead SK, Benjamin WH, Jr. & Briles DE. 2004.** PspA protects *Streptococcus pneumoniae* from killing by apolactoferrin, and antibody to PspA enhances killing of pneumococci by apolactoferrin [corrected]. *Infect Immun*, **72**, 5031-5040.
- Shewell LK, Harvey RM, Higgins MA, Day CJ, Hartley-Tassell LE, Chen AY, Gillen CM, James DBA, Alonzo F, Torres VJ, Walker MJ, Paton AW, Paton JC & Jennings MP. 2014.** The cholesterol-dependent cytolysins pneumolysin and streptolysin O require binding to red blood cell glycans for hemolytic activity. *Proc Natl Acad Sci U S A*, **111**, E5312-E5320.
- Shiri, T, Nunes MC, Adrian PV, Van Niekerk N, Klugman KP & Madhi SA. 2013.** Interrelationship of *Streptococcus pneumoniae*, *Haemophilus influenzae* and *Staphylococcus aureus* colonisation within and between pneumococcal-vaccine naive mother-child dyads. *BMC Infect Dis*, **13**, 483.
- Shrestha S, Foxman B, Weinberger DM, Steiner C, Viboud, C & Rohani P. 2013.** Identifying the interaction between influenza and pneumococcal pneumonia using incidence data. *Sci Transl Med*, **5**, 91-184.
- Siegel SJ, Roche AM & Weiser JN. 2014.** Influenza promotes pneumococcal growth during coinfection by providing host sialylated substrates as a nutrient source. *Cell Host Microbe*, **16**, 55-67.
- Sihorkar V & Vyas SP. 2001.** Biofilm consortia on biomedical and biological surfaces: delivery and targeting strategies. *Pharm Res*, **18**, 1247-1254.
- Silva,NA, McCluskey J, Jefferies JM, Hinds J, Smith A, Clarke SC, Mitchell TJ & Paterson GK. 2006.** Genomic diversity between strains of the same serotype and multilocus sequence type among pneumococcal clinical isolates. *Infect Immun*, **74**, 3513-3518.
- Sjöström K, Spindler C, Ortqvist A, Kalin M, Sandgren A, Kühlmann-Berenzon S, Henriques-Normark B.** Clonal and capsular types will decide whether pneumococci will act as a primary or opportunistic pathogen. *Clin Infect Dis*. **42**, 451-9.
- Sleeman KL, Griffiths D, Shackley F, Diggle L, Gupta S, Maiden MC, Moxon ER, Crook DW & Peto TE. 2006.** Capsular serotype-specific attack rates and

- duration of carriage of *Streptococcus pneumoniae* in a population of children. *J Infect Dis*, **194**, 682-688.
- Sniadack DH, Schwartz B, Lipman H, Bogaerts J, Butler JC, Dagan R, Echaniz-Aviles G, Lloyd-Evans N, Fenoll A, Girgis NI & et al., 1995.** Potential interventions for the prevention of childhood pneumonia: geographic and temporal differences in serotype and serogroup distribution of sterile site pneumococcal isolates from children--implications for vaccine strategies. *Pediatr Infect Dis J*, **14**, 503-510.
- Souli M & Giamarellou H. 1998.** Effects of slime produced by clinical isolates of coagulase-negative staphylococci on activities of various antimicrobial agents, *Antimicrob Agents Chemother*, **42**, 939-941.
- Stoodley LH, Costerton JW, Stoodley P. 2004.** Bacterial biofilms: from the Natural environment to infectious diseases. *Nat Rev Microb*, **2**, 95-108.
- Stroher UH, Paton AW, Ogunniyi AD & Paton JC. 2003.** Mutation of luxS of *Streptococcus pneumoniae* affects virulence in a mouse model. *Infect Immun*, **71**, 3206-3212.
- Swanson J. 1982.** Colony opacity and protein II compositions of gonococci. *Infect Immun*, **37**, 359-368.
- Swiatlo E, Champlin FR, Holman SC, Wilson WW & Watt JM. 2002.** Contribution of choline-binding proteins to cell surface properties of *Streptococcus pneumoniae*. *Infect Immun*, **70**, 412-415.
- Taga ME, Semmelhack JL & Bassler BL. 2001.** The LuxS-dependent autoinducer AI-2 controls the expression of an ABC transporter that functions in AI-2 uptake in *Salmonella typhimurium*. *Mol Microbiol*, **42**, 777-793.
- Takala AK, Jero, J, Kela, E, Ronnberg, PR, Koskenniemi, E & Eskola, J. 1995.** Risk factors for primary invasive pneumococcal disease among children in Finland. *JAMA*, **273**, 859-864.
- Talekar SJ, Chochua S, Nelson K, Klugman KP, Quave CL & Vidal JE. 2014.** 220D-F2 from *Rubus ulmifolius* kills *Streptococcus pneumoniae* planktonic cells and pneumococcal biofilms. *PLoS ONE*, **9**, e97314.
- Tapiainen T, Kujala T, Kaijalainen T, Ikaheimo I, Saukkoriipi A, Renko M, Salo J, Leinonen M & Uhari M. 2010.** Biofilm formation by *Streptococcus pneumoniae* isolates from paediatric patients. *APMIS*, **118**, 255-260.

- Tasher D, Stein M, Simoes EA, Shohat T, Bromberg M & Somekh E. 2011.** Invasive bacterial infections in relation to influenza outbreaks, 2006-2010, *Clin Infect Dis*, **53**, 1199-1207.
- Taylor, G. 1996.** Sialidases: structures, biological significance and therapeutic potential. *Curr Opin Struct Biol*, **6**, 830-837.
- Tomasz A, Jamieson JD & Ottolenghi E. 1964.** The Fine Structure of Diplococcus Pneumoniae. *J Cell Biol*, **22**, 453-467.
- Tomasz A & Waks S. 1975.** Mechanism of action of penicillin: triggering of the pneumococcal autolytic enzyme by inhibitors of cell wall synthesis. *Proc Natl Acad Sci U S A*, **72**, 4162-4166.
- Tong HH, Blue LE, James MA & DeMaria TF. 2000.** Evaluation of the virulence of a *Streptococcus pneumoniae* neuraminidase-deficient mutant in nasopharyngeal colonisation and development of otitis media in the chinchilla model. *Infect Immun*, **68**,921-924.
- Tong HH, Grants I, Liu X & DeMaria TF. 2002.** Comparison of alteration of cell surface carbohydrates of the chinchilla tubotympanum and colonial opacity phenotype of *Streptococcus pneumoniae* during experimental pneumococcal otitis media with or without an antecedent influenza A virus infection. *Infect Immun*, **70**, 4292-4301.
- Torzillo PJ, Morey F, Gratten M, Murphy D, Matters R & Dixon, J. 2007.** Changing epidemiology of invasive pneumococcal disease in central Australia prior to conjugate vaccine: a 16-year study. *Vaccine*, **25**, 2375-2378.
- Trappetti C, Gualdi L, Di Meola L, Jain P, Korir CC, Edmonds P, Iannelli F, Ricci S, Pozzi G & Oggioni MR. 2011a.** The impact of the competence quorum sensing system on *Streptococcus pneumoniae* biofilms varies depending on the experimental model. *BMC Microbiol*, **11**, 75.
- Trappetti C, Kadioglu A, Carter M, Hayre J, Iannelli F, Pozzi G, Andrew PW & Oggioni MR. 2009.** Sialic acid: a preventable signal for pneumococcal biofilm formation, colonisation, and invasion of the host. *J Infect Dis*, **199**, 1497-1505.
- Trappetti C, Ogunniyi AD, Oggioni MR & Paton JC. 2011b.** Extracellular matrix formation enhances the ability of *Streptococcus pneumoniae* to cause invasive disease. *PLoS ONE*, **6**, e19844.

- Trappetti C, Potter AJ, Paton AW, Oggioni MR & Paton JC. 2011c.** LuxS mediates iron-dependent biofilm formation, competence, and fratricide in *Streptococcus pneumoniae*. *Infect Immun*, **79**, 4550-4558.
- Trappetti C, van der Maten E, Amin Z, Potter AJ, Chen AY, van Mourik PM, Lawrence AJ, Paton AW & Paton, JC. 2013.** Site of isolation determines biofilm formation and virulence phenotypes of *Streptococcus pneumoniae* serotype 3 clinical isolates. *Infect Immun*, **81**, 505-513.
- Tu AH, Fulgham RL, McCrory MA, Briles DE & Szalai AJ. 1999.** Pneumococcal surface protein A inhibits complement activation by *Streptococcus pneumoniae*. *Infect Immun*, **67**, 4720-4724.
- Tyrrell GJ. 2011.** The changing epidemiology of *Streptococcus pneumoniae* serogroup 19A clonal complexes. *J Infect Dis*, **203**, 1345-1347.
- van der Poll T, Keogh CV, Guirao X, Buurman WA, Kopf M & Lowry SF. 1997.** Interleukin-6 gene-deficient mice show impaired defense against pneumococcal pneumonia. *J Infect Dis*, **176**, 439-444.
- Vandecasteele SJ, Peetermans, WE Merckx R & Van Eldere J. 2003.** Expression of biofilm-associated genes in *Staphylococcus epidermidis* during in vitro and in vivo foreign body infections. *J Infect Dis*, **188**, 730-737.
- van Ginkel FW, McGhee JR, Watt JM, Campos-Torres A, Parish LA, Briles DE. 2004.** Pneumococcal carriage results in ganglioside-mediated olfactory tissue infection. *Proc Natl Acad Sci USA*. **100**, 14363-14367.
- Vidal JE, Howery KE, Ludewick HP, Nava P & Klugman KP. 2013.** Quorum-sensing systems LuxS/autoinducer 2 and Com regulate *Streptococcus pneumoniae* biofilms in a bioreactor with living cultures of human respiratory cells. *Infect Immun*, **81**, 1341-1353.
- Vidal JE, Ludewick HP, Kunkel RM, Zahner D & Klugman KP. 2011.** The LuxS-dependent quorum-sensing system regulates early biofilm formation by *Streptococcus pneumoniae* strain D39. *Infect Immun*, **79**, 4050-4060.
- Waite RD, Struthers JK & Dowson CG. 2001.** Spontaneous sequence duplication within an open reading frame of the pneumococcal type 3 capsule locus causes high-frequency phase variation. *Mol Microbiol*, **42**, 1223-1232.
- Walker CL, Rudan I, Liu L, Nair H, Theodoratou E, Bhutta ZA, O'Brien KL, Campbell H & Black RE. 2013.** Global burden of childhood pneumonia and diarrhoea. *Lancet*, **81**, 1405-1416.

- Walters MC, Roe F, Bugnicourt A, Franklin MJ & Stewart PS. 2003.** Contributions of antibiotic penetration, oxygen limitation, and low metabolic activity to tolerance of *Pseudomonas aeruginosa* biofilms to ciprofloxacin and tobramycin. *Antimicrob Agents Chemother*, **47**,17-323.
- Wang Y, Zhang W, Wu Z, Zhu X & Lu C. 2011.** Functional analysis of luxS in *Streptococcus suis* reveals a key role in biofilm formation and virulence. *Vet Microbiol*, **152**, 151-160.
- Wang Z, Gerstein, M & Snyder, M. 2009.** RNA-Seq: a revolutionary tool for transcriptomics. *Nat Rev Genet*, **10**, 57-63.
- Weinberger DM, Harboe ZB, Flasche S, Scott JA & Lipsitch M. 2011.** Prediction of serotypes causing invasive pneumococcal disease in unvaccinated and vaccinated populations. *Epidemiology*, **22**, 199-207.
- Weiser JN. 2010.** The pneumococcus: why a commensal misbehaves. *J Mol Med (Berl)*, **88**, 97-102.
- Weiser JN, Austrian R, Sreenivasan PK & Masure HR. 1994.** Phase variation in pneumococcal opacity: relationship between colonial morphology and nasopharyngeal colonisation. *Infect Immun*, **62**, 2582-2589.
- Weiser JN, Markiewicz Z, Tuomanen EI & Wani JH. 1996.** Relationship between phase variation in colony morphology, intrastain variation in cell wall physiology, and nasopharyngeal colonisation by *Streptococcus pneumoniae*. *Infect Immun*, **64**, 2240-2245.
- Weiser JN, Williams A & Moxon ER. 1990.** Phase-variable lipopolysaccharide structures enhance the invasive capacity of *Haemophilus influenzae*. *Infect Immun*, **58**, 3455-3457.
- Whalan RH, Funnell SG, Bowler LD, Hudson MJ, Robinson A & Dowson CG. 2006.** Distribution and genetic diversity of the ABC transporter lipoproteins PiuA and PiaA within *Streptococcus pneumoniae* and related streptococci. *J Bacteriol*, **188**, 1031-1038.
- White RT. 1988.** Pneumococcal vaccine. *Thorax*, **43**, 345-348.
- Williams I, Venables WA, Lloyd D, Paul F & Critchley I. 1997.** The effects of adherence to silicone surfaces on antibiotic susceptibility in *Staphylococcus aureus*. *Microbiology*, **143**, 2407-2413.

- Woo CH, Shin SG, Koh SH & Lim JH. 2014.** TBX21 participates in innate immune response by regulating Toll-like receptor 2 expression in *Streptococcus pneumoniae* infections. *Mol Oral Microbiol*, **29**, 233-243.
- Xavier KB & Bassler BL. 2005.** Regulation of uptake and processing of the quorum-sensing autoinducer AI-2 in *Escherichia coli*. *J Bacteriol*, **187**, 238-248.
- Xu KD, Franklin MJ, Park CH, McFeters GA & Stewart PS. 2001.** Gene expression and protein levels of the stationary phase sigma factor, RpoS, in continuously-fed *Pseudomonas aeruginosa* biofilms. *FEMS Microbiol Lett*, **199**, 67-71.
- Xu Q & Pichichero ME. 2014.** Co-colonisation by *Haemophilus influenzae* with *Streptococcus pneumoniae* enhances pneumococcal-specific antibody response in young children. *Vaccine*, vol. **32**, 706-711.
- Yadav MK, Chae SW, Park K & Song JJ. 2013.** Hyaluronic Acid Derived from Other Streptococci Supports *Streptococcus pneumoniae* In Vitro Biofilm Formation. *Biomed Res Int*, **2013**, 690217.
- Yadav MK, Kwon SK, Cho CG, Park SW, Chae SW & Song JJ. 2012.** Gene expression profile of early in vitro biofilms of *Streptococcus pneumoniae*. *Microbiol Immunol*, **56**, 621-629.
- Yuste J, Botto M, Bottoms SE & Brown JS. 2007.** Serum amyloid P aids complement-mediated immunity to *Streptococcus pneumoniae*. *PLoS Pathog*, **3**, 1208-1219.
- Yuste J, Botto M, Paton JC, Holden DW & Brown JS. 2005.** Additive inhibition of complement deposition by pneumolysin and PspA facilitates *Streptococcus pneumoniae* septicemia. *J Immunol*, **175**, 1813-1819.
- Yuste J, Khandavilli S, Ansari N, Muttardi K, Ismail L, Hyams C, Weiser J, Mitchell T & Brown JS. 2010.** The effects of PspC on complement-mediated immunity to *Streptococcus pneumoniae* vary with strain background and capsular serotype. *Infect Immun*, **78**, 283-292.
- Zhang JR, Mostov KE, Lamm ME, Nanno M, Shimida S, Ohwaki M & Tuomanen E. 2000.** The polymeric immunoglobulin receptor translocates pneumococci across human nasopharyngeal epithelial cells. *Cell*, **102**, 827-837.
- Zhu L, Lin J, Kuang Z, Vidal JE & Lau GW. 2015.** Deletion analysis of *Streptococcus pneumoniae* late competence genes distinguishes virulence determinants that are dependent or independent of competence induction. *Mol Microbiol*, **97**, 151-165.
- Zobell CE. 1943.** The effect of solid surfaces upon bacterial activity. *J Bacteriol*, **46**, 39-56.

APPENDICES

APPENDIX A



Site of Isolation Determines Biofilm Formation and Virulence Phenotypes of *Streptococcus pneumoniae* Serotype 3 Clinical Isolates

Claudia Trappetti,^a Erika van der Maten,^a Zarina Amin,^a Adam J. Potter,^a Austen Y. Chen,^a Paula M. van Mourik,^a Andrew J. Lawrence,^b Adrienne W. Paton,^a James C. Paton^a

Research Centre for Infectious Diseases, School of Molecular and Biomedical Science, University of Adelaide, South Australia, Australia^a; SA Pathology, Women's and Children's Hospital, North Adelaide, South Australia, Australia^b

Streptococcus pneumoniae is a diverse species causing invasive as well as localized infections that result in massive global morbidity and mortality. Strains vary markedly in pathogenic potential, but the molecular basis is obscured by the diversity and plasticity of the pneumococcal genome. In the present study, *S. pneumoniae* serotype 3 blood ($n = 12$) or ear ($n = 13$) isolates were multilocus sequence typed (MLST) and assessed for biofilm formation and virulence phenotype. Blood and ear isolates exhibited similar MLST distributions but differed markedly in phenotype. Blood isolates formed robust biofilms only at pH 7.4, which were enhanced in Fe(III)-supplemented medium. Conversely, ear isolates formed biofilms only at pH 6.8, and Fe(III) was inhibitory. Biofilm formation paralleled *luxS* expression and genetic competence. In a mouse intranasal challenge model, blood isolates did not stably colonize the nasopharynx but spread to the blood; none spread to the ear. Ear isolates colonized the nasopharynx at higher levels and also spread to the ear compartment in a significant proportion of animals; none caused bacteremia. Thus, pneumococci of the same serotype and MLST exhibit distinct phenotypes in accordance with clinical site of isolation, indicative of stable niche adaptation within a clonal lineage.

Streptococcus pneumoniae (the pneumococcus) is responsible for massive global morbidity and mortality. It is a major cause of pneumonia, meningitis, and sepsis, especially in young children and the elderly. *S. pneumoniae* also causes less serious but highly prevalent infections such as otitis media (OM) and sinusitis (1–5). The World Health Organization estimates that 1.6 million people, of whom 0.7 to 1 million are under the age of 5, die of pneumococcal diseases each year, with the highest incidence in developing countries. Indeed, *S. pneumoniae* accounts for more deaths worldwide than any other single pathogen (6, 7). In spite of this mortality, *S. pneumoniae* is part of the commensal nasopharyngeal flora of humans. Most colonized individuals are asymptomatic, and carriers are the principal reservoirs for transmission of *S. pneumoniae* in the community. In a small proportion of carriers, which nevertheless translates into globally significant total case numbers, *S. pneumoniae* invades from its nasopharyngeal beachhead to cause disease. This may occur, for example, by aspiration into the lungs to cause pneumonia, by direct invasion of the blood, or by ascension of the Eustachian tube to access the middle ear and cause OM (1, 8, 9). However, the mechanisms whereby pneumococci transition from commensal to pathogen are poorly understood. OM is one of the most common pediatric diagnoses (10), and although not usually life-threatening, it has a massive socioeconomic impact (11).

The capacity to form biofilms is increasingly being recognized as a critical event in the pathogenesis of OM and other pneumococcal diseases, and several studies have shown a strong correlation between biofilm formation *in vitro* and colonization and lung infection in mice (12–15). Pneumococcal OM is also frequently associated with previous viral respiratory infections that lead to stasis, congestion, and blockade of the normal mucosal ciliary function, as well as Eustachian tube obstruction in very young children, thereby predisposing to secondary bacterial infection (10, 16–18).

It has recently been demonstrated that pneumococcal S-ribo-

syhomocysteine lyase, encoded by *luxS*, plays an important role in biofilm formation (19, 20). This enzyme is involved in the S-adenosylhomocysteine pathway that synthesizes autoinducer 2 (AI-2), a molecule involved in bacterial quorum sensing. In this case, extracellular AI-2 recognized by the pneumococcus has an effect on the transcription of genes involved in biofilm formation. Most recently, we have characterized the impact of exogenous Fe(III), as well as the LuxS-mediated AI-2 quorum sensing system, on biofilm formation by *S. pneumoniae* D39 (19). Fe(III) strongly enhanced biofilm formation, while Fe(III) chelation with deferoxamine was inhibitory. Importantly, Fe(III) also upregulated expression of *luxS* and *piuA* (encoding the major iron transporter) in wild-type D39. Similarly, genetic competence, as measured by transformation frequency, as well as expression of competence genes *comD*, *comX*, *comW*, *cglA*, and *dltA*, and the murein hydrolase *cbpD* gene associated with fratricide-dependent DNA release, were all directly related to *luxS* expression levels and further upregulated by Fe(III).

S. pneumoniae is a genetically plastic and diverse species, comprising 93 capsular serotypes superimposed on over 5,000 clonal groups recognizable by multilocus sequence typing (MLST) (21). Capsule switching experiments also show that both serotype and genetic background influence virulence (22, 23). This strain complexity has complicated attempts to examine whether there is any association between a given clonal lineage or serotype and pro-

Received 25 September 2012 Returned for modification 8 November 2012

Accepted 24 November 2012

Published ahead of print 3 December 2012

Editor: A. Camilli

Address correspondence to James C. Paton, james.paton@adelaide.edu.au.

Copyright © 2013, American Society for Microbiology. All Rights Reserved.

doi:10.1128/IAI.01033-12

TABLE 1 *S. pneumoniae* serotype 3 isolates used in this study^a

Strain	MLST	Source
ST232/1	ST232	Blood
ST233/3	ST233	Blood
ST180/4	ST180	Blood
ST458/5	ST458	Blood
ST233/6	ST233	Blood
ST180/7	ST180	Blood
ST180/8	ST180	Blood
ST180/15	ST180	Blood
ST458/20	ST458	Blood
ST232/23	ST232	Blood
ST180/24	ST180	Blood
ST232/25	ST232	Blood
ST180/2	ST180	Ear
ST180/9	ST180	Ear
ST180/10	ST180	Ear
ST232/11	ST232	Ear
ST180/12	ST180	Ear
ST233/13	ST233	Ear
ST180/14	ST180	Ear
ST180/16	ST180	Ear
ST232/17	ST232	Ear
ST232/18	ST232	Ear
ST232/19	ST232	Ear
ST180/21	ST180	Ear
ST180/22	ST180	Ear

^a Strains were isolated between 1988 and 1996 from patients at either the Women's and Children's Hospital, North Adelaide, South Australia, or the Alice Springs Hospital, Northern Territory, Australia. Similar proportions of OM and blood isolates were derived from each site.

density to cause invasive rather than localized infections, and whether biofilm formation capacity can account for differences in virulence phenotype. In the current study, we have simplified the analysis by confining our examination to *S. pneumoniae* serotype 3 clinical isolates from cases of sepsis or OM. We present evidence for a strong association between clinical site of isolation, pH-dependent biofilm formation capacity, *luxS* expression, and virulence phenotype in a murine model.

MATERIALS AND METHODS

Bacterial strains and growth conditions. *S. pneumoniae* strains used in this study are listed in Table 1. Cells were grown in a casein-based semi-synthetic liquid medium (C+Y) (24) and on Columbia agar supplemented with 5% (vol/vol) horse blood (blood agar [BA]) at 37°C in a CO₂-enriched atmosphere. Bacterial stocks were prepared from mid-log-phase cultures and stored at -80°C in 10% glycerol.

MLST. For MLST analysis, the *aroE*, *gdh*, *gki*, *recP*, *spi*, *xpt*, and *ddl* genes of the *S. pneumoniae* strains were PCR amplified and sequenced, as described by Spratt (25). The sequence types (ST) of strains were determined from the MLST database (<http://www.mlst.net>) based on the resulting allelic profiles.

Biofilm assays. Static biofilm assays were performed by growing bacteria in 24- or 96-well flat-bottom polystyrene plates as described previously (19). Briefly, cells were grown in C+Y medium, adjusted to either pH 7.4 or 6.8, and supplemented with 100 μM Fe(III) nitrate where indicated for 24 h at 37°C in a CO₂-enriched atmosphere. Microscopic examination of biofilms was performed by washing wells three times with PBS, desiccation at 50°C, staining with 1% crystal violet for 30 min, and photomicrography under transmitted light. Quantification of bacteria attached to the plastic substratum was performed by washing unstained plates three times, filling wells with 0.1 ml of fresh C+Y medium, detach-

ing cells using a sonicating water bath, and plating serial dilutions onto blood agar. Statistical analysis was performed using 2-tailed Student's *t* test.

RNA extraction and quantitative real-time RT-PCR. Selected clinical isolates were grown in C+Y with or without additional Fe(III) (100 μM) for 24 h in a static biofilm model and total RNA was extracted as previously described (26). The level of gene expression relative to that of 16S rRNA was determined using a one-step reverse transcriptase PCR (RT-PCR) kit and a LC480 real-time cyclor (Roche) as described previously (19). Statistical analysis was performed using 2-tailed Student's *t* test.

Mutagenesis of *luxS*. The *luxS* gene was deleted from various type 3 strains using overlap extension PCR and transformation as described previously (19).

Infection of mice. Animal experiments were approved by the University of Adelaide Animal Ethics Committee. Female outbred 5- to 6-week-old CD-1 (Swiss) mice were inoculated intranasally with 1×10^7 CFU of *S. pneumoniae* (confirmed retrospectively by viable count) in a volume of 10 μl. Groups of 15 mice were inoculated for each strain, and 5 randomly selected mice from each group were euthanized by CO₂ asphyxiation at 24, 48, or 72 h postinfection. Nasal wash, nasopharyngeal tissue, ear tissue, lung, brain, and blood samples were collected and processed as previously described (27, 28). Samples were serially diluted and plated onto BA plates for enumeration of viable pneumococci. Statistical analyses were done using the Mann-Whitney *U* test.

RESULTS

Serotype 3 biofilm formation is pH dependent. It has been reported that certain serotypes and STs of *S. pneumoniae* have a greater potential to cause invasive disease in humans than others; likewise, strains differ in their propensities to cause OM (29, 30). This suggests that strains may differ in their capacity to adapt to and survive or proliferate within distinct host microenvironments. This further implies that clinical isolates from cases of otitis media may exhibit *in vitro* and *in vivo* phenotypes distinct from those of blood isolates.

Two conditions that vary significantly between different niches of the human body are metal ion concentrations (31) and pH; the pH of the blood is typically around 7.4, while in the (uninfected) ear cavity it is in the range of 6.5 to 6.8 (32). We first examined whether a relationship exists between the site of isolation and ability to form biofilms under different pH and [Fe(III)] conditions. We tested 12 blood isolates and 13 ear isolates belonging to serotype 3, a type that is frequently associated with both OM and invasive disease. Interestingly, the two groups contained representatives of the same four STs in similar proportions (ST180, ST232, ST233, and ST458, in order of prevalence) (Table 1). All 25 strains were in the opaque phase, as judged by opacity phenotype when grown on THY-catalase plates (28), and there was no significant difference in the level of type 3 capsular polysaccharide production, as determined by uronic acid assay (33) (results not presented). In the first instance, strains were grown in C+Y medium (pH 7.4) with or without supplementation with 100 μM Fe(III) nitrate and were tested in the static biofilm assay. Pneumococcal growth rates were not significantly different in the presence of this Fe(III) concentration compared with rates in standard C+Y medium, which contains 0.8 μM total Fe, as measured by inductively coupled plasma mass spectrometry (ICPMS) (data not shown). After 24 h of incubation, a marked increase in biofilm density in the presence of Fe(III) was observed in strains isolated from the blood compared with strains isolated from the ear, as judged by viable counts of dispersed, unstained biofilms ($P < 0.001$) (Fig. 1A). The biofilm density was also significantly greater in blood

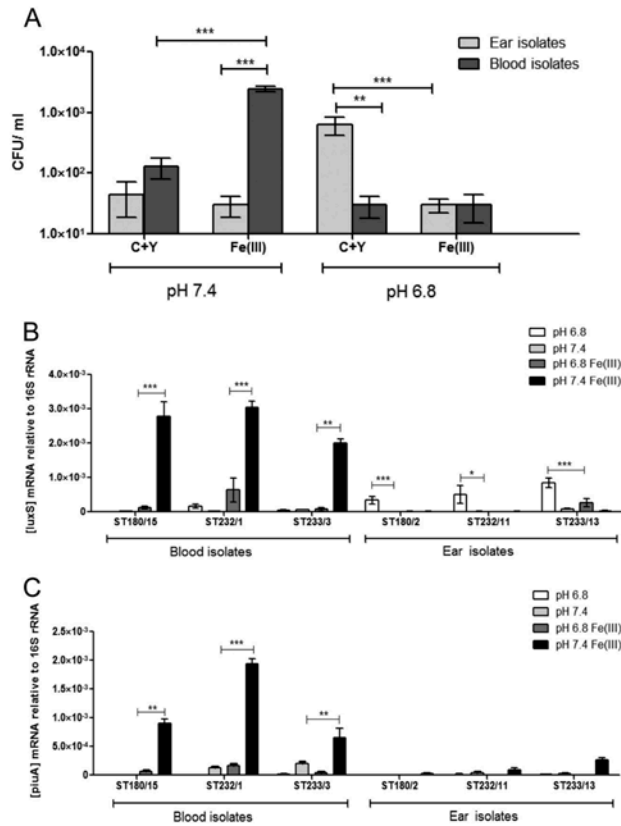


FIG 1 Biofilm formation and gene expression. (A) Biofilm formation by clinical isolates (12 from blood and 13 from ear) after 24 h of growth at either pH 7.4 or 6.8, with or without 100 μ M Fe(III), determined by viable count. Data are the means \pm standard deviations for three independent experiments (*, $P < 0.05$; **, $P < 0.01$; and ***, $P < 0.001$; 2-tailed Student's t test). (B and C) Expression of *luxS* (B) and *piuA* (C) relative to 16S rRNA in the indicated clinical isolates grown either at pH 7.4 or 6.8, with or without addition of 100 μ M Fe(III). Data are the means \pm standard deviations for three independent experiments (*, $P < 0.05$; **, $P < 0.01$; and ***, $P < 0.001$; 2-tailed Student's t test).

isolates in the presence of Fe(III) than in standard C+Y medium ($P < 0.001$) (Fig. 1A), consistent with our previous observation for the type 2 laboratory strain D39 (19). However, the presence of Fe(III) had no significant effect on the low level of biofilm formation by the type 3 ear isolates at pH 7.4 (Fig. 1A). In marked contrast, when biofilm formation assays were performed using C+Y medium with the pH adjusted to 6.8 (a level within the range found in the ear cavity), the biofilm density of the ear isolates was significantly greater than that of the blood isolates ($P < 0.01$). Interestingly, supplementation of C+Y (pH 6.8) medium with Fe(III) abolished the ability of ear isolates to form biofilms ($P < 0.001$) and did not increase the low level of biofilm formation by blood isolates at the lower pH (Fig. 1A). Microscopic examination of crystal violet-stained biofilm assay plates confirmed that robust biofilms were formed by blood isolates only at pH 7.4 and were

boosted further by Fe(III), whereas ear isolates formed robust biofilms only at pH 6.8 and in the absence of Fe(III) (Fig. 2).

LuxS is involved in serotype 3 biofilm formation. To test whether the iron- and pH-dependent biofilm formation of serotype 3 strains is linked to the activity of the LuxS quorum sensing system, a relationship previously identified in strain D39 serotype 2 (19), the level of *luxS* and *piuA* expression was measured using real-time RT-PCR. For this analysis, one blood isolate and one ear isolate belonging to each of the three major STs (ST180, ST232, and ST233) were selected. The difference in *luxS* expression levels (Fig. 1B) between strains and growth conditions closely paralleled the pattern of biofilm formation (Fig. 1A). In the blood isolates ST180/15, ST232/1, and ST233/3, *luxS* expression was significantly higher when cells were grown at pH 7.4 in the presence of Fe(III) than under other growth conditions ($P < 0.001$ for

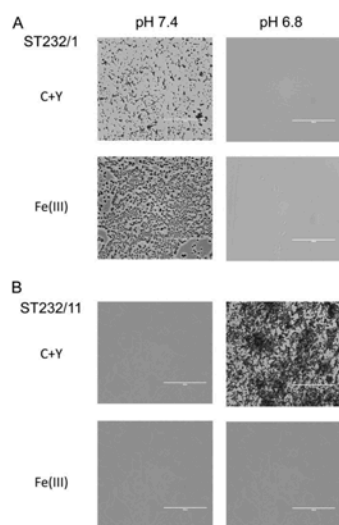


FIG 2 Microscopic analysis of crystal violet-stained 24-h biofilms of the blood isolate ST232/1 (A) and the ear isolate ST232/11 (B) grown at pH 7.4 or 6.8 in the presence or absence of 100 μ M Fe(III). Scale bar, 100 μ m.

ST180/15 and ST232/1; $P < 0.01$ for ST233/3). In contrast, for the ear isolates ST180/2, ST232/11, and ST233/13, *luxS* expression was significantly higher when cells were grown at pH 6.8 in the absence of Fe(III) than under any of the other conditions ($P < 0.001$ for ST180/2 and ST233/13; $P < 0.05$ for ST232/11). However, for each ST pair, the overall level of expression of *luxS* of the ear isolate was lower than that of the corresponding blood isolate under their respective optimal conditions ($P < 0.001$ for ST180 and ST232; $P < 0.01$ for ST233) (Fig. 1B).

Since iron has been shown to stimulate biofilm formation in the blood isolates, we also quantified the expression level of *piuA*, which encodes the major pneumococcal iron uptake system (34). A significantly higher level of expression of *piuA* was observed in blood isolates grown at pH 7.4 in the presence of Fe(III) than under other growth conditions ($P < 0.01$ for ST180/15 and ST233/3; $P < 0.001$ for ST232/1) (Fig. 1C). In contrast, *piuA* expression was very low in all the ear isolates, and there was no evidence for upregulation of *piuA* in these isolates in the presence of iron, except for ST233/13 at pH 7.4 (Fig. 1C).

***luxS* mutation reduces the ability of serotype 3 clinical isolates to form biofilms.** To further confirm the role of *luxS* in biofilm formation by serotype 3 strains, *luxS* was deleted in all 6 clinical isolates mentioned above and the mutants were then tested for biofilm forming ability. Viable counts of the dispersed biofilms revealed a significant reduction in biofilm formation for the *luxS* mutants of the three ear isolates compared to the wild type when grown in C+Y (pH 6.8) medium ($P < 0.001$ for ST180/2 and ST233/13; $P < 0.01$ for ST232/11) (Fig. 3A). Microscopic examination after crystal violet staining confirmed the results of viable counts (Fig. 4). A similar finding was also observed

for the *luxS* mutants of all three blood isolates grown at pH 7.4 in the presence of Fe(III) (data not shown).

Transformability is pH dependent in serotype 3 strains. Induction of the competence state has been shown to parallel biofilm formation in *S. pneumoniae* (13, 19), and so the transformability of the six serotype 3 clinical isolates, as well as the reference invasive type 2 strain D39, was measured in planktonic cells grown at pH 7.4 and pH 6.8, as described previously (19). The transformability of the strains was found to be strongly influenced by the pH; blood isolates exhibited a significantly greater propensity to take up external DNA at pH 7.4 ($P < 0.001$ for ST180/15 and ST232/1; $P < 0.01$ for ST233/3), as did the reference strain D39. In contrast, the ear isolates showed higher rates of transformability at pH 6.8 ($P < 0.001$ for ST180/2 and ST232/11; $P < 0.01$ for ST233/13) (Fig. 3B). Indeed, for the ST180 and ST232 strains, the blood isolates were completely untransformable at pH 6.8, while the ear isolates were not transformable at pH 7.4. Strains of ST233 were transformable under both conditions tested, but a significant increase in efficiency was observed for the blood isolate at pH 7.4 and ear isolate at pH 6.8.

Clinical isolation site corresponds with virulence phenotype in mice. To investigate the virulence profile of the clinical isolates, we used a murine nasopharyngeal inoculation model, which mimics the natural route of infection for *S. pneumoniae*. At all the time points examined (24, 48, and 72 h postinfection), the majority of mice in each group infected with blood isolates (ST180/15, ST232/1, or ST233/3) showed bacteremia, whereas no bacteremia could be detected in any of the mice in groups challenged with the ear isolates (ST180/2, ST232/11, or ST233/13) (Fig. 5C). Collectively, the degree of bacteremia for blood isolates was significantly greater than that for the combined ear isolate groups at all time points ($P < 0.001$). When individual groups within an ST were compared, the bacteremia level for the ST180/15 group was significantly greater than that for the ST180/2 group at all time points ($P < 0.05$), while bacteremia levels in the ST232/1 and ST233/3 groups were significantly greater than those for ST232/11 and ST233/13, respectively, at 48 h ($P < 0.05$). The situation was reversed in the nasopharyngeal tissue (Fig. 5A), where blood isolates as a whole were inferior to ear isolates in terms of overall colonization levels at 48 and 72 h ($P < 0.001$ in both cases). Comparing the individual STs, ST232/11 colonized the nasopharyngeal tissue to a significantly greater extent than ST232/1 at both 48 and 72 h ($P < 0.05$ and $P < 0.01$, respectively), while ST180/2 and ST233/13 exhibited significantly higher rates of colonization at 72 h than the corresponding ST-matched blood isolate ($P < 0.01$ and $P < 0.05$, respectively). Bacteria in ear tissue samples were detected only in groups challenged with the ear isolates, and this difference was statistically significant ($P < 0.05$) at both 48 and 72 h (Fig. 5B).

Interestingly, at 24 h postinfection, pneumococci could not be detected in the lungs of any of the mice challenged with blood isolates, in spite of significant bacteremia in the majority of animals in each ST group (Fig. 6C). Moreover, only 4 of the 15 mice challenged with blood isolates had evidence of pneumococci in the lungs at either 48 or 72 h. In contrast, no bacteria could be detected in the lungs of any of the mice challenged with the ear isolates. Similar findings were observed in brain tissue (Fig. 6B). It is also interesting to note that pneumococci could not be detected in nasopharyngeal washes of any mice 24 h postinfection

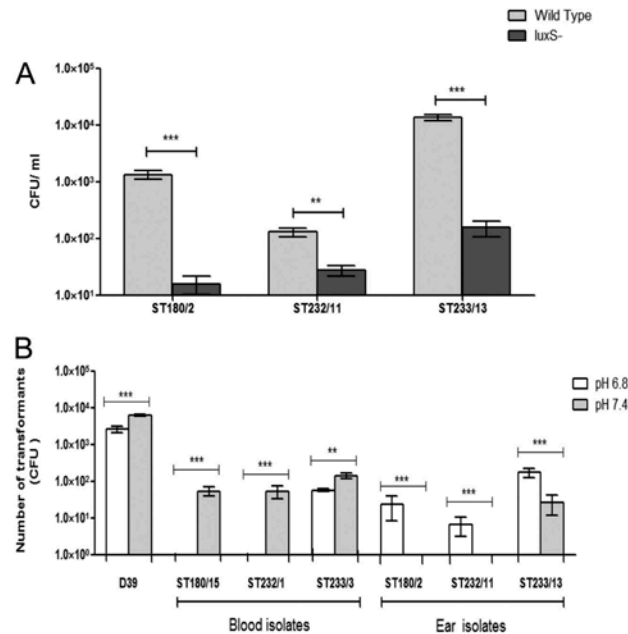


FIG 3 (A) Effect of *luxS* mutation on biofilm formation by ear isolates, determined by viable count. Data are the means \pm standard deviations for three independent experiments (**, $P < 0.01$, and ***, $P < 0.001$; 2-tailed Student's *t* test). (B) Transformability of the reference invasive type 2 strain D39 and the type 3 clinical isolates (from blood or ear) grown at either pH 7.4 or 6.8. Data are the total numbers of transformants (means \pm standard deviations for three independent experiments (**, $P < 0.01$, and ***, $P < 0.001$; 2-tailed Student's *t* test). Each transformation reaction mixture contained approximately 10^7 competent pneumococci.

(Fig. 6A). At 48 h, less than half of the mice had pneumococci in nasal wash fluid, with fewer again at 72 h.

DISCUSSION

S. pneumoniae is a diverse and adaptable pathogen, capable of surviving in a range of niches within its human host. Previous studies from our laboratory have identified changes in *in vivo* transcriptional profile within a given strain that facilitate survival in distinct host niches (nasopharynx, lungs, blood, and brain) and/or aid progression from one niche to another (26, 27, 35, 36). However, genetic differences between strains also result in pneumococci with inherent tropism for one niche over another. Studies in animal models suggest that both capsular and noncapsular loci contribute to these differences in *in vivo* phenotype (22, 23, 37–40), but interpretation of molecular epidemiological analyses of human isolates is complicated by the vast genetic diversity of strains.

In the present study, we have examined phenotypic differences between clinical isolates from either sepsis or OM ($n = 12$ and 13, respectively), focusing on strains belonging to serotype 3, an important cause of both systemic and localized pneumococcal infections. All 25 strains were in the opaque phase and produced similar amounts of type 3 capsular polysaccharide. Moreover, the groups of blood and ear isolates comprised the same four MLST

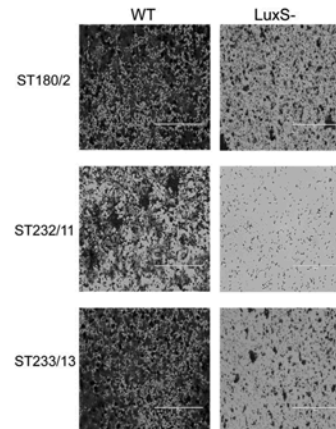


FIG 4 Microscopic analysis of crystal violet-stained biofilms formed at pH 6.8 by ear isolates and their respective *luxS* mutant derivatives. WT, wild type. Scale bar, 100 μ m.

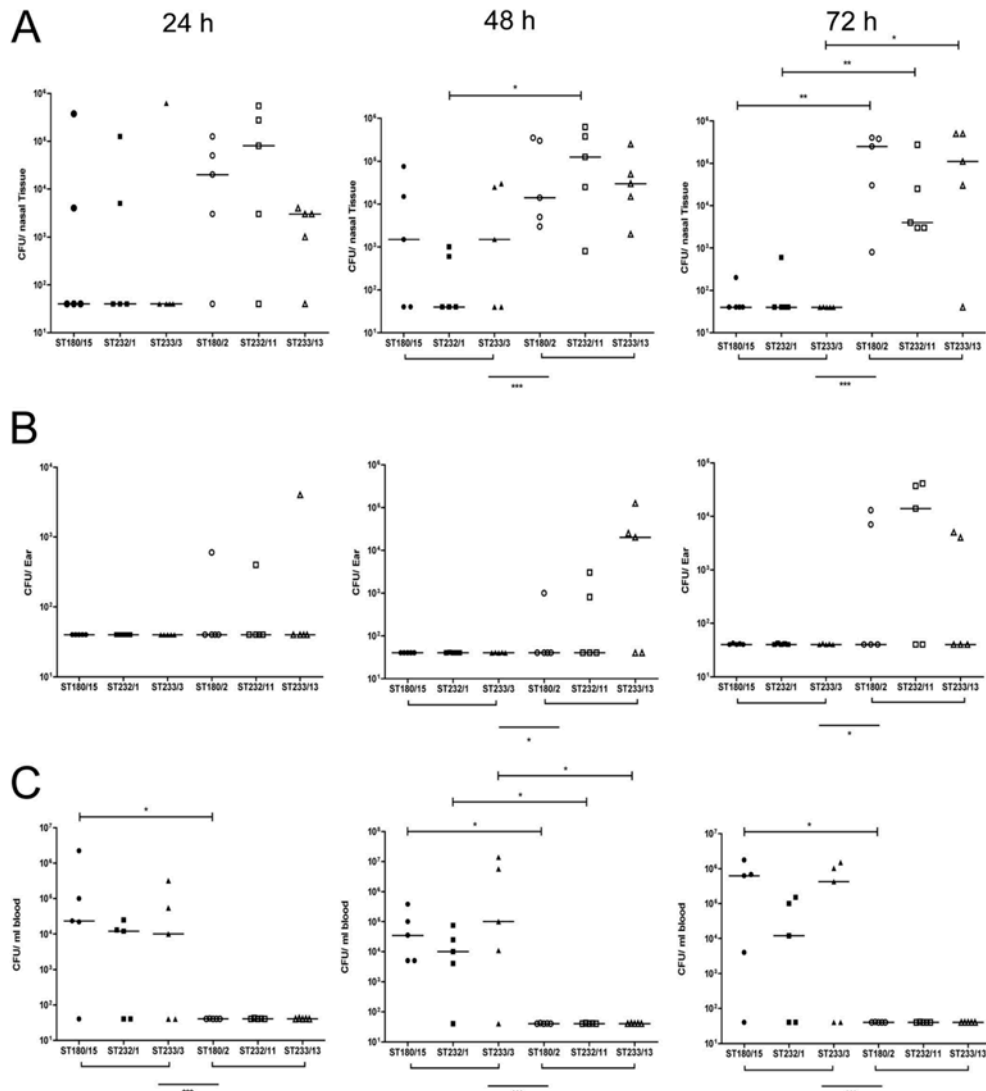


FIG 5 Virulence phenotypes of blood and ear isolates. Groups of 15 mice were infected intranasally with 10^7 CFU of the indicated strain. At the indicated times, 5 mice from each group were euthanized and numbers of pneumococci in the indicated tissues were quantitated. (A) Nasopharyngeal tissue; (B) ear; (C) blood. Viable counts are shown for each mouse at each site; horizontal bars indicate the median value for each group/time point. Blood isolates are represented by solid symbols; ear isolates are represented by open symbols. Differences between groups were analyzed by 1-tailed Mann-Whitney *U* test (*, $P < 0.05$; **, $P < 0.01$; and ***, $P < 0.001$).

in similar proportions. Surprisingly, however, the *in vitro* and *in vivo* phenotypes of the two groups were strikingly different. Only the blood isolates were capable of forming *in vitro* biofilms at pH 7.4, and this property was significantly augmented by supplement-

ation of the medium with Fe(III). On the other hand, only the ear isolates were capable of forming biofilms at pH 6.8, and at this pH, Fe(III) was inhibitory.

We then conducted more detailed phenotypic comparisons of

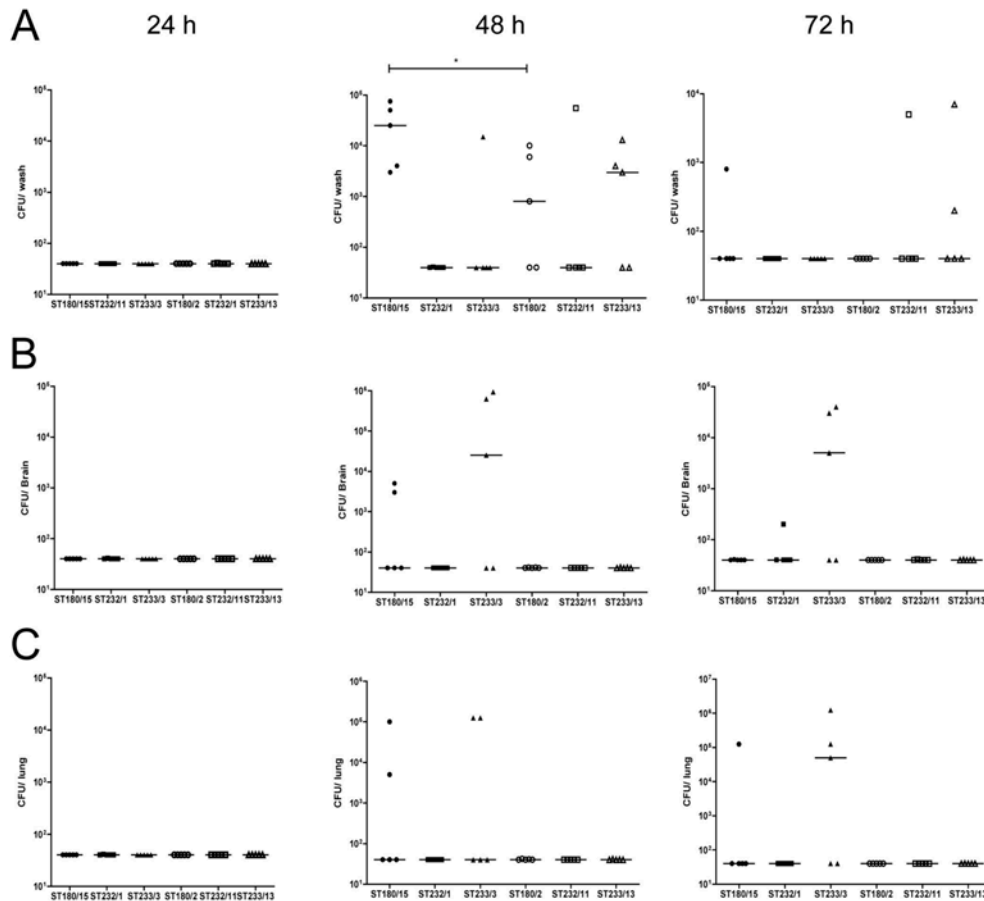


FIG 6 Virulence phenotypes of blood and ear isolates. Groups of 15 mice were infected intranasally with 10^7 CFU of the indicated strain. At the indicated times, 5 mice from each group were euthanized and numbers of pneumococci in the indicated tissues were quantitated. (A) Nasal wash; (B) brain; (C) lungs. Viable counts are shown for each mouse at each site; horizontal bars indicate the median value for each group and time point. Blood isolates are represented by solid symbols; ear isolates are represented by open symbols. Differences between groups were analyzed by 1-tailed Mann-Whitney U test (*, $P < 0.05$).

matched pairs of isolates from either the blood or ear belonging to the dominant MLSTs (ST180, ST232, and ST233). We have previously reported that the LuxS quorum sensing system is a central regulator of biofilm formation in the invasive type 2 *S. pneumoniae* strain D39, and in the present study, there was again a close parallel between expression of the *luxS* gene and biofilm formation at the permissive pH for the respective groups. Moreover, the stimulatory effect of Fe(III) on biofilm formation by the blood isolates at pH 7.4 was matched by upregulated expression of *piuA*, which encodes the major pneumococcal iron transporter. In contrast, *piuA* expression was negligible in blood isolates at the nonpermissive pH of 6.8 or in the absence of Fe(III), and in the ear isolates under any of the conditions tested.

Although the level of *luxS* expression in each of the ear isolates at pH 6.8 in the absence of Fe(III) was significantly greater than that under the other environmental conditions, *luxS* expression in each of the ear isolates was significantly lower than that in the blood isolate of the corresponding ST under its optimal conditions. This suggested that *luxS* might play a less important role in biofilm formation by ear isolates relative to blood isolates. Nevertheless, mutagenesis of *luxS* significantly reduced biofilm formation, regardless of the source of the isolate. The link between the *luxS* system and genetic competence previously observed in D39 also held for the type 3 isolates, with maximal transformation efficiencies observed under the same environmental conditions as were permissive for biofilm formation.

The consistent and stark phenotypic distinction between blood and ear isolates in terms of preferred pH and requirement for Fe(III) for optimal biofilm formation suggests that there are fundamental genetic differences between *S. pneumoniae* strains belonging to the same clonal lineage that enable adaptation to the distinct host niches from whence they were isolated. This adaptation to the human niche was closely mimicked by the behavior of the various strains in a mouse intranasal challenge model. All three blood isolates were poor colonizers of the nasopharynx, yet they were able to readily spread directly to the blood in most animals, largely bypassing the lungs. Moreover, none of the blood isolates ever spread to the ear compartment. On the other hand, the ear isolates were able to stably colonize the nasopharyngeal tissue of the vast majority of animals, but they never spread to the blood, brain, or lungs. Nearly half of the animals challenged with OM isolates had pneumococci in the ear compartment by 72 h.

In this study, we have provided compelling evidence that stable adaptation of pneumococci to distinct host niches occurs within clonal lineages. Thus, molecular epidemiological studies aimed at associating MLST with potential to cause invasive versus noninvasive disease should be interpreted with considerable caution. It is now clear that accessory regions outside the core pneumococcal genome are major determinants of virulence phenotype in both humans and animal models. Identification of multiple ST-matched pairs of *S. pneumoniae* serotype 3 strains with distinct human tissue tropism and virulence profile provides a unique opportunity to identify accessory regions or polymorphisms within the core genome common to isolates from one niche versus the other by genome sequence analysis. This, in turn, will permit direct testing of the role of identified regions in pathogenesis by targeted mutagenesis.

ACKNOWLEDGMENTS

This work was supported by the National Health and Medical Research Council (NHMRC) of Australia (Program Grant 565526 to J.C.P. and A.W.P. and NHMRC Australia Fellowship to J.C.P.), the Australian Research Council (DORA Fellowship to A.W.P.), and the Garnett Passe and Rodney Williams Memorial Foundation (Training Fellowship to C.T.).

REFERENCES

- Gray BM, Converse GM, III, Dillon HC, Jr. 1980. Epidemiologic studies of *Streptococcus pneumoniae* in infants: acquisition, carriage, and infection during the first 24 months of life. *J. Infect. Dis.* 142:923–933.
- Ispahani P, Slack RC, Donald FE, Weston VC, Rutter N. 2004. Twenty year surveillance of invasive pneumococcal disease in Nottingham: serogroups responsible and implications for immunisation. *Arch. Dis. Child.* 89:757–762.
- Hussain M, Melegaro A, Pebody RG, George R, Edmunds WJ, Talukdar R, Martin SA, Efstratiou A, Miller E. 2005. A longitudinal household study of *Streptococcus pneumoniae* nasopharyngeal carriage in a UK setting. *Epidemiol. Infect.* 133:891–898.
- Kadioglu A, Weiser JN, Paton JC, Andrew PW. 2008. The role of *Streptococcus pneumoniae* virulence factors in host respiratory colonization and disease. *Nat. Rev. Microbiol.* 6:288–301.
- Varon E, Mainardi JL, Gutmann L. 2010. *Streptococcus pneumoniae*: still a major pathogen. *Clin. Microbiol. Infect.* 16:401.
- WHO. 2007. Pneumococcal conjugate vaccine for childhood immunization—WHO position paper. *Wkly. Epidemiol. Rec.* 82:93–104.
- Mulholland K. 2003. Global burden of acute respiratory infections in children: implications for interventions. *Pediatr. Pulmonol.* 36:469–474.
- Brueggemann AB, Peto TE, Crook DW, Butler JC, Kristinsson KG, Spratt BG. 2004. Temporal and geographic stability of the serogroup-specific invasive disease potential of *Streptococcus pneumoniae* in children. *J. Infect. Dis.* 190:1203–1211.
- Sleeman KL, Griffiths D, Shackley F, Diggle L, Gupta S, Maiden MC, Moxon ER, Crook DW, Peto TE. 2006. Capsular serotype-specific attack rates and duration of carriage of *Streptococcus pneumoniae* in a population of children. *J. Infect. Dis.* 194:682–688.
- Parsons DS, Wald ER. 1996. Otitis media and sinusitis: similar diseases. *Otolaryngol. Clin. North Am.* 29:11–25.
- Teele DW, Klein JO, Rosner B. 1989. Epidemiology of otitis media during the first seven years of life in children in greater Boston: a prospective, cohort study. *J. Infect. Dis.* 160:83–94.
- Oggioni MR, Trappetti C, Kadioglu A, Cassone M, Iannelli F, Ricci S, Andrew PW, Pozzi G. 2006. Switch from planktonic to sessile life: a major event in pneumococcal pathogenesis. *Mol. Microbiol.* 61:1196–1210.
- Trappetti C, Gualdi L, Di Meola L, Jain P, Korir CC, Edmunds P, Iannelli F, Ricci S, Pozzi G, Oggioni MR. 2011. The impact of the competence quorum sensing system on *Streptococcus pneumoniae* biofilms varies depending on the experimental model. *BMC Microbiol.* 11:75.
- Muñoz-Elias EJ, Marcano J, Camilli A. 2008. Isolation of *Streptococcus pneumoniae* biofilm mutants and their characterization during nasopharyngeal colonization. *Infect. Immun.* 76:5049–5061.
- Trappetti C, Kadioglu A, Carter M, Hayre J, Iannelli F, Pozzi G, Andrew PW, Oggioni MR. 2009. Sialic acid: a preventable signal for pneumococcal biofilm formation, colonization, and invasion of the host. *J. Infect. Dis.* 199:1497–1505.
- Brook I. 2011. Microbiology of sinusitis. *Proc. Am. Thorac. Soc.* 8:90–100.
- Del Beccaro MA, Mendelman PM, Inglis AF, Richardson MA, Duncan NO, Clausen CR, Stull TL. 1992. Bacteriology of acute otitis media: a new perspective. *J. Pediatr.* 120:81–84.
- Faden H, Stanievich J, Brodsky L, Bernstein J, Ogra PL. 1990. Changes in nasopharyngeal flora during otitis media of childhood. *Pediatr. Infect. Dis. J.* 9:623–626.
- Trappetti C, Potter AJ, Paton AW, Oggioni MR, Paton JC. 2011. LuxS mediates iron-dependent biofilm formation, competence, and fratricide in *Streptococcus pneumoniae*. *Infect. Immun.* 79:4550–4558.
- Vidal JE, Ludewick HP, Kunkel RM, Zahner D, Klugman KP. 2011. The LuxS-dependent quorum-sensing system regulates early biofilm formation by *Streptococcus pneumoniae* strain D39. *Infect. Immun.* 79:4050–4060.
- Enright MC, Spratt BG. 1998. A multilocus sequence typing scheme for *Streptococcus pneumoniae*: identification of clones associated with serious invasive disease. *Microbiology* 144:3049–3060.
- Kelly T, Dillard JP, Yother J. 1994. Effect of genetic switching of capsular type on virulence of *Streptococcus pneumoniae*. *Infect. Immun.* 62:1813–1819.
- McAllister LJ, Ogunniyi AD, Stroehrer UH, Leach AJ, Paton JC. 2011. Contribution of serotype and genetic background to virulence of serotype 3 and serogroup 11 pneumococcal isolates. *Infect. Immun.* 79:4839–4849.
- Lacks S, Hotchkiss RD. 1960. A study of the genetic material determining an enzyme in *Pneumococcus*. *Biochim. Acta* 39:508–518.
- Spratt BG. 1999. Multilocus sequence typing: molecular typing of bacterial pathogens in an era of rapid DNA sequencing and the internet. *Curr. Opin. Microbiol.* 2:312–316.
- Mahdi LK, Ogunniyi AD, LeMessurier KS, Paton JC. 2008. Pneumococcal virulence gene expression and host cytokine profiles during pathogenesis of invasive disease. *Infect. Immun.* 76:646–657.
- LeMessurier KS, Ogunniyi AD, Paton JC. 2006. Differential expression of key pneumococcal virulence genes in vivo. *Microbiology* 152:305–311.
- Trappetti C, Ogunniyi AD, Oggioni MR, Paton JC. 2011. Extracellular matrix formation enhances the ability of *Streptococcus pneumoniae* to cause invasive disease. *PLoS One* 6:e19844.
- Forbes ML, Horsey E, Hiller NL, Buchinsky FJ, Hayes JD, Compliment JM, Hillman T, Ezzo S, Shen K, Keefe R, Barbadora K, Post JC, Hu FZ, Ehrlich GD. 2008. Strain-specific virulence phenotypes of *Streptococcus pneumoniae* assessed using the *Chinchilla laniger* model of otitis media. *PLoS One* 3:e1969.
- Hanage WP, Kajjalainen TH, Syrjanen RK, Auranen K, Leinonen M, Mäkelä PH, Spratt BG. 2005. Invasiveness of serotypes and clones of *Streptococcus pneumoniae* among children in Finland. *Infect. Immun.* 73:431–435.
- McDevitt CA, Ogunniyi AD, Valkov E, Lawrence MC, Kobe B, McEwan AG, Paton JC. 2011. A molecular mechanism for bacterial susceptibility to zinc. *PLoS Pathog.* 7:e1002357.
- Jahn AF. 2001. Bone physiology of the ear, p. 59–74. *In* Jahn AF, Santos-

- Sacchi J (ed), Physiology of the ear, 2nd ed. Singular, Thomson Learning, San Diego, CA.
33. Blumenkrantz N, Asboe-Hansen G. 1973. New method for quantitative determination of uronic acids. *Anal. Biochem.* 54:484–489.
 34. Brown JS, Ogunniyi AD, Woodrow MC, Holden DW, Paton JC. 2001. Immunization with components of two iron uptake ABC transporters protects mice against systemic *Streptococcus pneumoniae* infection. *Infect. Immun.* 69:6702–6706.
 35. Mahdi LK, Wang H, Van der Hoek MB, Paton JC, Ogunniyi AD. 2012. Identification of a novel pneumococcal vaccine antigen preferentially expressed during meningitis in mice. *J. Clin. Invest.* 122:2208–2220.
 36. Ogunniyi AD, Mahdi LK, Trappetti C, et al, Verhoeven N, Mermans D, Van der Hoek MB, Plumtre CD, Paton JC. 2012. Identification of genes that contribute to pathogenesis of invasive pneumococcal disease by in vivo transcriptomic analysis. *Infect. Immun.* 80:3268–3278.
 37. Böttig P, Hathaway LJ, Hofer S, Muhlemann K. 2006. Serotype-specific invasiveness and colonization prevalence in *Streptococcus pneumoniae* correlate with the lag phase during in vitro growth. *Microbes Infect.* 8:2612–2617.
 38. Sjöström K, Spindler C, Ortqvist A, Kalin M, Sandgren A, Köhlmann-Berenzon S, Henriques-Normark B. 2006. Clonal and capsular types decide whether pneumococci will act as a primary or opportunistic pathogen. *Clin. Infect. Dis.* 42:451–459.
 39. Inverarity D, Lamb K, Diggle M, Robertson C, Greenhalgh D, Mitchell TJ, Smith A, Jefferies JM, Clarke SC, McMenamin J, Edwards GF. 2011. Death or survival from invasive pneumococcal disease in Scotland: associations with serogroups and multilocus sequence types. *J. Med. Microbiol.* 60:793–802.
 40. Sandgren A, Albiger B, Orihuela CJ, Tuomanen E, Normark S, Henriques-Normark B. 2005. Virulence in mice of pneumococcal clonal types with known invasive disease potential in humans. *J. Infect. Dis.* 192:791–800.

APPENDIX B



Isolation Site Influences Virulence Phenotype of Serotype 14 *Streptococcus pneumoniae* Strains Belonging to Multilocus Sequence Type 15

Zarina Amin, Richard M. Harvey, Hui Wang, Catherine E. Hughes, Adrienne W. Paton, James C. Paton, Claudia Trappetti

Research Centre for Infectious Diseases, Department of Molecular and Cellular Biology, School of Biological Sciences, University of Adelaide, Adelaide, South Australia, Australia

Streptococcus pneumoniae is a diverse species causing invasive as well as localized infections that result in massive global morbidity and mortality. Strains vary markedly in pathogenic potential, but the molecular basis is obscured by the diversity and plasticity of the pneumococcal genome. We have previously reported that *S. pneumoniae* serotype 3 isolates belonging to the same multilocus sequence type (MLST) differed markedly in *in vitro* and *in vivo* phenotypes, in accordance with the clinical site of isolation, suggesting stable niche adaptation within a clonal lineage. In the present study, we have extended our analysis to serotype 14 clinical isolates from cases of sepsis or otitis media that belong to the same MLST (ST15). In a murine intranasal challenge model, five ST15 isolates (three from blood and two from ears) colonized the nasopharynx to similar extents. However, blood and ear isolates exhibited significant differences in bacterial loads in other host niches (lungs, ear, and brain) at both 24 and 72 h postchallenge. In spite of these differences, blood and ear isolates were present in the lungs at similar levels at 6 h postchallenge, suggesting that early immune responses may underpin the distinct virulence phenotypes. Transcriptional analysis of lung tissue from mice infected for 6 h with blood isolates versus ear isolates revealed 8 differentially expressed genes. Two of these were exclusively expressed in response to infection with the ear isolate. These results suggest a link between the differential capacities to elicit early innate immune responses and the distinct virulence phenotypes of clonally related *S. pneumoniae* strains.

Streptococcus pneumoniae (pneumococcus) is one of the foremost bacterial pathogens in terms of global morbidity and mortality. Its disease spectrum includes life-threatening infections such as pneumonia, meningitis, and bacteremia as well as less-serious but highly prevalent infections, including otitis media (OM) and sinusitis. Young children and the elderly are at highest risk, with global estimates of pneumococcal deaths in children under 5 years of age approaching 1 million per year (1). Despite this mortality, *S. pneumoniae* is a component of the normal microflora of the human nasopharynx. It is estimated that at any given time, approximately 10 to 15% of adults and 25 to 40% of healthy children may be asymptomatically colonized with *S. pneumoniae* (2). Although only a small fraction of carriers progress to invasive or localized pneumococcal disease, the scale of the denominator results in massive global disease burden.

S. pneumoniae is a diverse, genetically plastic species, and the 93 known capsular serotypes are superimposed on >5,000 sequence types (ST) recognizable by multilocus sequence type (MLST) analysis (3). It has a core genome of roughly 1,500 genes common to all strains, with the remaining 30% of the genome comprising accessory regions (AR) present in some but not all clonal lineages. Individual *S. pneumoniae* strains differ markedly in their capacity to cause either invasive or localized infections, and both serotype and genetic background influence virulence profile (4, 5). However, the vast heterogeneity has frustrated attempts to identify any association between a given clonal lineage or serotype and the propensity to cause invasive rather than localized infections. Indeed, large molecular epidemiological studies have not yielded consistent findings (6, 7).

We recently identified a link between human tissue tropism, as judged by the source of a clinical isolate (blood versus ear), and

virulence profile in a mouse model by comparing multiple ST-matched pairs of *S. pneumoniae* serotype 3 strains. In the murine intranasal challenge model, only blood isolates caused sepsis, while only otitis media isolates spread to the ear. These findings were indicative of stable niche adaptation within a clonal lineage (8). To further examine the nexus between the clinical source of isolates and their respective virulence-related phenotypes, we have now conducted similar studies in *S. pneumoniae* serotype 14 strains. Type 14 is a representative serotype conferring high invasive disease potential (9–11). It is also one of the most common etiologic agents of pneumonia in Latin America, the United Kingdom, and Spain and of otitis media in children under 5 years old (12–14). To further understand the basis for the distinct virulence profiles, we have also examined the nature of host innate immune responses elicited by these clinical isolates during the early stages of infection.

MATERIALS AND METHODS

Bacterial strains and growth conditions. *S. pneumoniae* strains used in this study are listed in Table 1. Cells were grown in a casein-based, semi-

Received 20 August 2015 Accepted 25 September 2015

Accepted manuscript posted online 28 September 2015

Citation Amin Z, Harvey RM, Wang H, Hughes CE, Paton AW, Paton JC, Trappetti C. 2015. Isolation site influences virulence phenotype of serotype 14 *Streptococcus pneumoniae* strains belonging to multilocus sequence type 15. *Infect Immun* 83:4781–4790. doi:10.1128/IAI.01081-15.

Editor: L. Pirofski

Address correspondence to Claudia Trappetti, claudia.trappetti@adelaide.edu.au.

Copyright © 2015, American Society for Microbiology. All Rights Reserved.

TABLE 1 *S. pneumoniae* serotype 14 isolates used in this study

Strain ^a	MLST	Source
ST15/9-47	ST15	Ear
ST15/51742	ST15	Ear
ST15/4495	ST15	Blood
ST15/4534	ST15	Blood
ST15/4559	ST15	Blood

^a Strains were isolated between 1988 and 1996 from patients at either the Women's and Children's Hospital, North Adelaide, South Australia, or the Alice Springs Hospital, Northern Territory, Australia. The MLST of each strain was determined as described in Materials and Methods.

synthetic liquid medium (C+Y) or in serum broth (SB), as required (8), or on Columbia agar supplemented with 5% (vol/vol) horse blood (BA) at 37°C in a CO₂-enriched atmosphere. Bacterial stocks were prepared from mid-log-phase cultures and stored at -80°C in 20% glycerol.

MLST. For MLST analysis, the *aroE*, *gdh*, *gki*, *recP*, *xpt*, and *ddl* genes were PCR amplified and sequenced as described by Spratt (15). The sequence types (ST) of the strains were determined from the MLST database (<http://www.pubmlst.org>) based on the resulting allelic profiles.

ELISA for CPS quantitation. Total capsular polysaccharide (CPS) produced by strains was quantified by enzyme-linked immunosorbent assay (ELISA) using a modification of the method described previously (16). Briefly, serial 2-fold dilutions of either purified type 14 CPS standard (American Type Culture Collection, USA) at a starting concentration of 10 µg/ml or total CPS preparations of the strains included in this study were coated on poly-L-lysine-treated Nunc MaxiSorp flat-bottom 96-well plates overnight at 4°C. After blocking with 1% fetal calf serum was performed, the samples were reacted with a 1:10,000 dilution of group 14 typing sera (Statens Seruminstitut, Copenhagen, Denmark) for 2 h. The plates were washed five times in wash buffer (0.05% Tween 20-phosphate-buffered saline [PBS]) and then reacted with a 1:20,000 dilution of goat anti-rabbit IgG alkaline phosphatase conjugate (Sigma-Aldrich) overnight at 4°C. After extensive washing, the plates were developed using alkaline phosphatase substrate (Sigma) in diethanolamine buffer, and the absorbance at 405 nm was read in a Spectramax M2 spectrometer (Molecular Devices, CA, USA).

Animal studies. Animal experiments were approved by the University of Adelaide Animal Ethics Committee. For each test strain, two groups of five outbred 6-week-old female Swiss mice were anesthetized by intraperitoneal injection of pentobarbital sodium (Nembutal; Rhone-Merieux) at a dose of 66 µg per g of body weight. They were then intranasally challenged with 30 µl of bacterial suspension containing approximately 1 × 10⁸ CFU in SB. The challenge dose was confirmed retrospectively by serial dilution and plating on BA. Groups of five mice were euthanized by CO₂ asphyxiation at either 24 or 72 h. Blood and tissue samples (lungs, nasopharynx, brain, and ear) were harvested and pneumococci enumerated in blood or tissue homogenates as described previously (8, 16). For *in vivo* competition experiments, groups of mice were challenged intranasally with a mixed inoculum comprising approximately 5 × 10⁷ CFU of each strain, as previously described (17). The competitive index (CI) within nasopharyngeal, ear, lung, and brain samples was determined at 24 h and 72 h postchallenge by plating on selective and nonselective media and calculating the ratio of ear isolates to blood isolates relative to the input ratio. For the purposes of CI calculation, when a given strain was not detected in a particular niche, it was assigned a CFU value equivalent to 50% of the detection threshold.

Detroit 562 adherence and invasion assays. Detroit 562 (human nasopharyngeal carcinoma) cells were grown in a 1:1 mix of Dulbecco's modified Eagle medium (Gibco) and Ham's F-12 nutrient mixture (Gibco) supplemented with 5% fetal bovine serum, 2 mM L-glutamine, 50 IU of penicillin, and 50 µg/ml streptomycin. Confluent monolayers in 24-well plates were washed with PBS and infected with pneumococci (approximately 5 × 10⁵ CFU per well) in a 1:1 mixture of the culture medium

described above (without antibiotics) and C+Y (pH 7.4). Plates were centrifuged at 500 × g for 5 min and then incubated at 37°C in 5% CO₂ for 2.5 h. Monolayers were washed 3 times in PBS, and adherent bacteria were released by treatment with 100 µl trypsin-EDTA followed by 400 µl 0.025% Triton X-100. Lysates were serially diluted and plated on BA to enumerate adherent bacteria. Invasion assays were carried out essentially as described above, except that after the postadherence washing step, cultures were incubated for 1 h in fresh medium supplemented with 200 µg gentamicin and 10 µg benzylpenicillin per ml to kill extracellular bacteria, after which monolayers were again washed, lysed, serially diluted, and plated on BA, as described above.

PCR arrays. At 6 h postinfection, lung and nasopharyngeal tissue was harvested from infected or sham-infected mice and homogenized. RNA was extracted using a PureLink RNA minikit (Life Technologies), including on-column DNase digestion, according to the manufacturer's instructions. cDNA synthesis was carried out using a RT² First Strand kit (Qiagen). RNA was analyzed on a LightCycler 480 II system (Roche) by quantitative reverse transcriptase PCR (qRT-PCR) using a RT² Profiler PCR array mouse innate and adaptive immune responses kit (Qiagen), according to the manufacturer's instructions (18). Data were analyzed using PCR Array data analysis software provided by the manufacturer.

Fluorescence-activated cell sorter (FACS) detection of Ly-6G- and F4/80-positive cells in blood and BAL fluid. Blood was collected from infected and uninfected mice into heparin tubes by cardiac puncture. Blood leukocytes were extracted by lysing the red blood cells (RBC) with a hypotonic shock. Bronchoalveolar lavage (BAL) was performed using 1 ml of ice-cold PBS.

The blood leukocytes or BAL fluid cells were washed in ice-cold PBS and fixed in 1% paraformaldehyde-PBS over night at 4°C. Before immunofluorescence labeling, the leukocytes were washed with PBS and permeabilized with 0.1 ml of 0.1% Triton X100-PBS for 30 s. The cells were then washed again with PBS and were then incubated with monoclonal rat anti-mouse Ly-6G (BD Biosciences; 551459) or monoclonal rat anti-mouse F4/80 (Santa Cruz Biotechnology; SC-52664) at room temperature for 1 h. Ly-6G (neutrophil marker) or F4/80 (monocyte/macrophage marker) was detected by incubation with Alexa 488-conjugated donkey anti-rat Ig (Invitrogen; A21208) at room temperature for 1 h. Fluorescence data were acquired by the use of a BD FACSCanto system (serial no. V0130) or a BD LSR II system with a high-throughput sampler (serial no. H1169) plus BD FACSDiva software (version 5.0.3) and were analyzed with WEASLE v2.6 software. The fluorescence intensity of Alexa 488 was proportional to the expression level of Ly-6G or F4/80. The data are reported as the product of geometric mean (GM) fluorescence intensity and the total number of Ly-6G- or F4/80-positive cells. The data are presented as means and standard errors (SE), and differences were analyzed using Student's *t* test.

Examination of lung tissue with HE staining or immunofluorescence labeling. After the blood and BAL fluid were collected, the lungs of infected and uninfected mice were removed and fixed in 4% formaldehyde overnight at 4°C, embedded in paraffin, sectioned, stained with hematoxylin-eosin (HE), and examined by light microscopy. Alternatively, sections were labeled with rat anti-mouse Ly-6G or F4/80 followed by Alexa-488-conjugated anti-rat IgG and examined by fluorescence microscopy (AX 70; Olympus).

RESULTS

Initial characterization of serotype 14 clinical isolates. The purpose of this study was to compare pneumococci belonging to the same serotype and clonal lineage derived from distinct host niches. Therefore, we carried out MLST analysis on 18 serotype 14 strains, comprising 9 blood and 9 ear isolates. The two predominant STs were ST15 (*n* = 5) and ST130 (*n* = 5). Of the other strains, two belonged to ST124 and ST129, while the others were all assigned to new STs by <http://pubmlst.org> but were not further investigated. We focused on ST15 because three isolates origi-

nated from blood and two from ears (Table 1). All ST15 strains were in the opaque phase, as judged by the opacity phenotype seen during growth on Todd-Hewitt broth supplemented with yeast extract (THY)-catalase plates (16), and the total capsular polysaccharide production levels were similar for all strains, as judged by ELISA (data not shown).

Virulence phenotype of ST15 blood and ear isolates. The virulence profiles of the various ST15 strains were then examined in a murine intranasal challenge model. Group sizes were 16 each for one blood (ST15/4495) and one ear isolate (ST15/9-47) (both selected at random) and $n = 5$ for the remaining strains. Numbers of the respective strains in various host niches (nasopharynx, lungs, blood, brain, and ear) were quantitated at 24 h and 72 h postchallenge (Fig. 1). None of the strains were detected in the blood of any of the mice at either time point (data not presented). The three blood isolates (ST15/4495, ST15/4534, and ST15/4559) and the two ear isolates (ST15/9-47 and ST15/51742) all exhibited similar capacities to colonize the nasopharynx at both 24 h and 72 h postinfection, with the GM bacterial load in this niche in the range of 10^4 to 10^5 CFU (Fig. 1A). There were no significant differences in either infection rates or GM bacterial loads. However, significant differences between blood and ear isolates were observed in the other host niches. Neither of the ear isolate strains was detectable in the lungs of any of the infected mice at either time point. In contrast, the ST15/4495 blood isolate strain was present in the lungs of 14/16 mice at 24 h and 8/16 at 72 h postchallenge ($P < 0.0001$ and $P = 0.0032$, respectively; Fisher exact test). A similar trend was seen for the other two blood isolates (ST15/4534 and ST15/4559), with 50% of lungs colonized at 72 h (Fig. 1B). The opposite tropism was observed in the brain. None of the three ST15 blood isolates were detected in the brains of any of the mice at either time point. However, the ST15/9-47 ear isolate was detected in the brains of 15/16 mice and 11/16 mice at 24 h and 72 h, respectively ($P < 0.0001$ in both cases). The other ear isolate (ST15/51742) was present in the brains of 5/5 and 3/5 mice at 24 h and 72 h, respectively ($P < 0.01$ relative to any of the blood isolates at 24 h) (Fig. 1C). In the infected mice, bacterial loads in the brain were in the range of 10^3 to 10^5 CFU. All five ST15 isolates were able to spread to the ear compartment after intranasal challenge, but the proportion of mice whose ears were infected with the ST15/9-47 ear isolate was significantly greater than that of mice challenged with the ST15/4495 blood isolate (16/16 versus 7/16 and 15/16 versus 8/16 at 24 h and 72 h, respectively; $P = 0.0008$ and $P = 0.0155$, respectively) (Fig. 1D). The GM bacterial load in the ears for ST15/9-47 was also significantly greater than that for ST15/4495 at both 24 h and 72 h ($P = 0.0015$ and $P = 0.0020$, respectively). Similar trends were also seen in the mice challenged with the other ST15 ear isolate and the two other blood isolates. Collectively, these results show that pneumococci of the same serotype and ST exhibit distinct *in vivo* phenotypes in accordance with the clinical site of isolation.

***In vivo* competition between ST15/4495 and ST15/9-47.** The distinct *in vivo* tropism observed for the ST15 ear and blood isolates could be attributable to differences in expression of bacterial virulence factors on the bacterial surface or released into the environment and/or to differences in the nature of the host innate immune responses elicited by the respective strains. Thus, the presence of a strain with superior virulence characteristics in a given niche may enhance the virulence of a “passenger” strain. To explore this, we conducted *in vivo* competition experiments in

which two groups of mice were challenged with equal numbers of ST15/4496 and ST15/9-47, and the relative numbers of each strain were determined in various host niches at 24 h and 72 h postchallenge. In order to distinguish the strains, it was necessary to construct erythromycin-resistant derivatives of each strain by transformation with plasmid pAL3 (19). Introduction of the plasmid had no effect on the bacterial growth rate of either strain (data not shown).

Two competition experiments were performed with 5 mice per group for each time point. In one experiment, mice were challenged with equal numbers of ST15/4496 and ST15/9-47:pAL3; in the other experiment, mice were challenged with equal numbers of ST15/4496:pAL3 and ST15/9-47. Tissue samples were plated on BA or BA plus erythromycin to enable calculation of the ratio of sensitive organisms to resistant organisms and hence of the competitive index (CI). Data pooled from the two experiments are shown in Fig. 2. In spite of the similar capacities of ST15/4495 and ST15/9-47 to colonize the murine nasopharynx when challenged in isolation (Fig. 1A), the ear isolate had a significant competitive advantage over the blood isolate in the mixed-infection model in the nasopharynx at 24 h ($P < 0.001$) and at 72 h ($P < 0.0001$), by which time the median CI was approximately 10^5 (Fig. 2). The ear isolate also predominated in both the ear and brain compartments at both time points ($P < 0.0001$ for brain at 24 h and 72 h and for ear at 24 h; $P < 0.05$ for ear at 72 h). Moreover, whereas small numbers of the blood isolate were present along with the dominant ear isolate in the ears of all the infected mice, the blood isolate was never detected in brain tissue of any of the mice at either time point. These findings are understandable, given that access to both the brain and the ear compartments occurs via the nasopharynx, where the ear isolate was present at a 10^5 -fold excess over the blood isolate. A distinct scenario occurred in the lungs. Only 6/10 mice had detectable pneumococci in the lungs at either time point, and in these mice, neither strain had a significant competitive advantage overall (Fig. 2). This was the case in spite of the fact that, when used in isolation for the challenge, only the blood isolate was able to persist in the lungs at either 24 h or 72 h (Fig. 1B). In the competition experiment, the ear isolate outcompeted the blood isolate in 4/6 infected mice, whereas the blood isolate outcompeted the ear isolate in 2/6 mice (Fig. 2). The intranasal challenge inoculum was instilled into the nares under general anesthesia, and a proportion of the dose was aspirated directly into the lungs during the challenge (approximately 10^6 CFU). When instilled on their own, ST15/9-47 organisms entering the lung during challenge were cleared within 24 h, whereas when ST15/4495 organisms were instilled on their own, the blood isolate was able to resist innate defenses and persist in the lung. However, in the coinfection model, significant numbers of the ear isolate were present in a proportion of the mice at both 24 h and 72 h. These findings indicate that the presence of the ST15/4495 blood isolate, at least during the immediate postchallenge period, is necessary for persistence of the ST15/9-47 ear isolate in the lung compartment.

***In vitro* adherence and invasion.** To further explore the basis for the enhanced nasopharyngeal colonization fitness of ST15/9-47, the adherence phenotype of all the ST15 isolates was assessed *in vitro* using Detroit 562 (human nasopharyngeal) cells (Table 2). There were significant differences between several of the strains in total *in vitro* adherence. Two of the blood isolates (ST15/4495 and ST15/4534) were significantly less adherent than the ST15/9-47 ear isolate ($P < 0.01$ and $P < 0.001$, respectively). The other ear

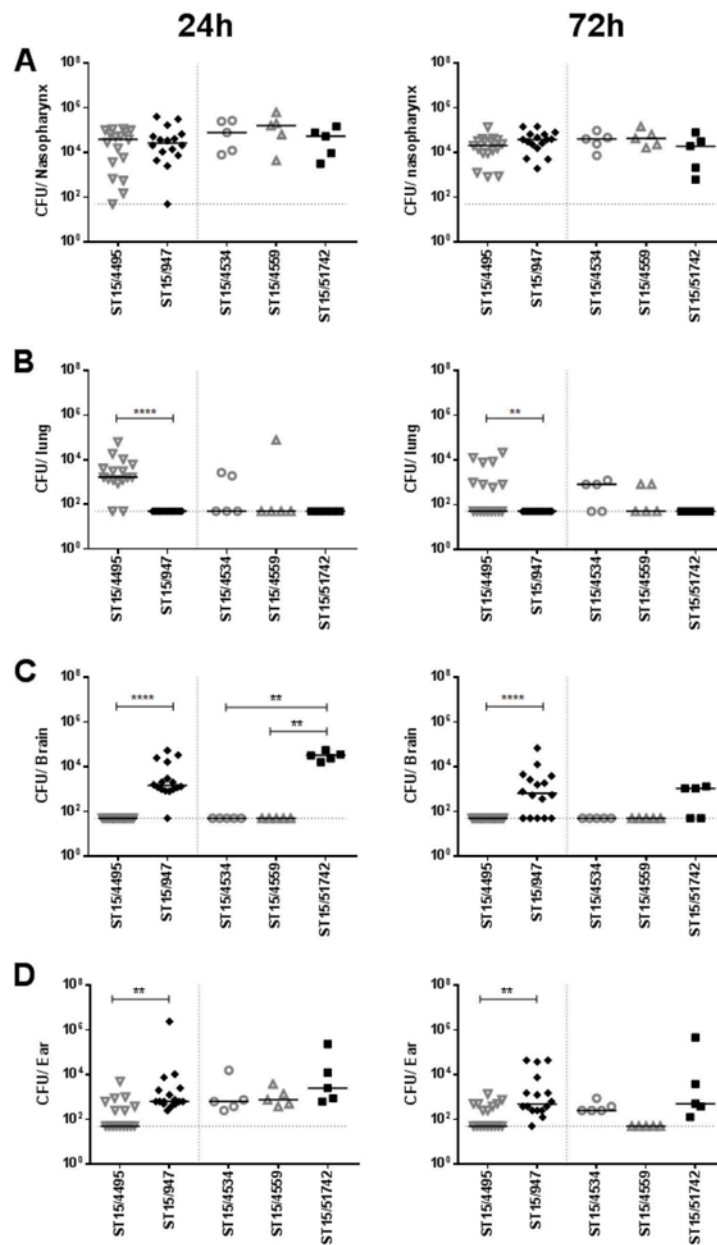


FIG 1 Comparative virulence of ST15 blood and ear isolates. Groups of mice were challenged intranasally with the three blood isolates (ST15/4495, ST15/4534, and ST15/4559) and the two ear isolates (ST15/9-47 and ST15/51742), and numbers of pneumococci in the nasopharynx, lungs, brain, and ear at either 24 h or 72 h postchallenge were determined. For ST15/4495 and ST15/9-47, 16 challenged mice were examined at each time point compared with 5 mice at each time point for the remaining strains. Blood isolates are represented by open gray symbols; ear isolates are represented by filled black symbols. The horizontal bars denote the median CFU for each group; the dotted horizontal lines indicate the lower limit of detection, and symbols on the lines denote that no bacteria were detected. Differences in infection rates (number of infected versus number of uninfected mice) were analyzed using the Fisher exact test. **, $P < 0.01$; ****, $P < 0.0001$.

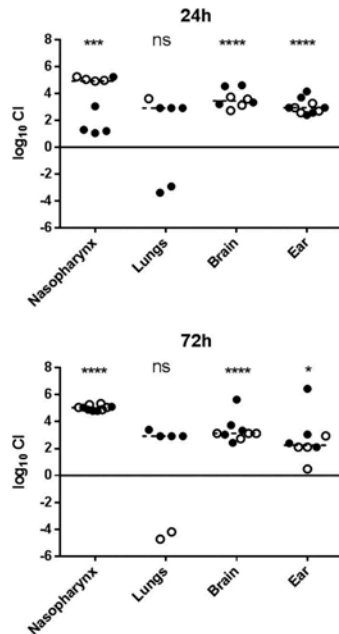


FIG 2 *In vivo* competition between ST15/9-47 (ear isolate) and ST15/4495 (blood isolate). Data shown are pooled from two competition experiments performed with 5 mice per group for each time point (24 h and 72 h postchallenge). In one experiment, mice were challenged with equal numbers (5×10^7 CFU each) of ST15/4495 and ST15/9-47:pAL3 (open symbols); in the other experiment, mice were challenged with equal numbers of ST15/4495:pAL3 and ST15/9-47 (solid symbols). The competitive index (CI) is shown as log₁₀ CI for each tissue of each mouse. The horizontal dotted lines denote the geometric mean CI for each tissue. Statistical differences between the log-transformed geometric mean CI and a hypothetical value of 0 (ratio of 1:1) in each niche were analyzed using the two-tailed Student's *t* test. ns, not significant; *, $P < 0.05$; **, $P < 0.01$; ***, $P < 0.001$; ****, $P < 0.0001$.

isolate (ST15/51742) was even more adherent than ST15/9-47 ($P < 0.05$). The adherence of the third blood isolate (ST15/4559) was not significantly different from that of ST15/9-47, but that isolate was significantly less adherent than the second ear isolate, ST15/51742 ($P < 0.01$). The capacity of the ST15/9-47 ear isolate and the ST15/4495 blood isolate to invade Detroit cells was also investigated (Table 2), but no significant difference was observed.

TABLE 2 Adherence to and invasion of Detroit 562 cells

Strain	Source	Adherence ^a (CFU/well \pm SEM)	Invasion (CFU/well \pm SEM)
ST15/9-47	Ear	$7.88 \times 10^5 \pm 0.78 \times 10^5$	$3.50 \times 10^5 \pm 0.65 \times 10^5$
ST15/51742	Ear	$1.19 \times 10^5 \pm 0.10 \times 10^6$ *	Not tested
ST15/4495	Blood	$3.75 \times 10^5 \pm 0.56 \times 10^6$ **	$3.95 \times 10^5 \pm 0.28 \times 10^5$
ST15/4534	Blood	$2.85 \times 10^5 \pm 0.27 \times 10^5$ ****	Not tested
ST15/4559	Blood	$7.50 \times 10^5 \pm 0.59 \times 10^5$	Not tested

^a Significant differences in adherence relative to that of ST15/9-47 are indicated as follows: *, $P < 0.05$; **, $P < 0.01$; ***, $P < 0.001$ (Student's *t* test, two-tailed).

Transcriptional analysis of host innate responses. Although only the blood isolates are detectable in the lungs at 24 h, ear isolates are delivered into the lungs during challenge but are cleared by host innate defenses by 24 h. In a pilot experiment, we found similar bacterial loads in the lungs of mice challenged with either ST15/4495 or ST15/9-47 at 6 h postchallenge (10^7 to 10^8 CFU in both cases; result not shown). We therefore investigated whether differences in host responses during the immediate post-challenge period might have influenced bacterial clearance from the lungs. Mice were challenged with either the blood isolate (ST15/4495) or the ear isolate (ST15/9-47) or were sham infected (anesthetized and inoculated with 30 μ l SB). Total RNA was isolated from lungs and nasopharyngeal tissue 6 h after challenge. Expression of 84 key immune response genes was then quantitated using RT-PCR arrays. Compared to levels in sham-infected samples, a total of 35 genes were induced in the lungs, as judged by a significant increase in the mRNA level following challenge with at least one of the two ST15 strains (Table 3). Overall, the pattern of gene expression indicated a generally proinflammatory response in the lungs at 6 h postchallenge; genes encoding a number of proinflammatory cytokines, including interleukin-1 α (IL-1 α), IL-1 β , IL-23a, IL-6, and tumor necrosis factor alpha (TNF- α), were upregulated. Other genes involved in regulating the immune response were also increased in expression. These included genes encoding the chemokines CCL12, a murine homolog of (human) CCL2, and CXCL10, which is known to be induced by gamma interferon (IFN- γ), a proinflammatory cytokine that also showed increased expression following pneumococcal challenge. Expression of the CCR5 chemokine receptor was also elevated at the mRNA level. Genes encoding elements involved in pathogen recognition and signaling during immune responses, such as Myd88, Toll-like receptor 3 (TLR3), TLR6, TLR7, Nod2, Ddx58, JAK2, and NF- κ B α , were differentially expressed in challenged samples compared to sham-infected samples. Other upregulated genes included those encoding the CD11b integrin (ITGAM) and the associated adhesion molecule ICAM1, inflammasome component NLRP3, and granulocyte-macrophage colony-stimulating factor (GM-CSF) CSF2.

Some strain-strain differences were observed, with 8 genes showing significant differential levels of expression in lungs following challenge with ST15/4495 compared to challenge with ST15/9-47 (Table 4). Of these, 6 genes were upregulated by both challenge strains compared to resting samples but to a significantly greater degree following challenge with ST15/4495. These included those encoding the proinflammatory cytokines TNF- α and IL-6, the type I interferon IFN- β , the costimulatory molecule CD40, the transcription factor Tbet (TBX21), and the chemokine CCL12. The remaining 2 genes, encoding APCS and IL-2, were found to be upregulated only following challenge with ST15/9-47.

TABLE 3 Genes significantly upregulated in infected relative to sham-infected lung tissue^a

Gene product	ST15/4495 infected vs sham infected		ST15/9-47 infected vs sham infected	
	Fold gene expression change	Significance	Fold gene expression change	Significance
APCS			5.15	**
CSar1	14	*	8.47	**
CCL12	36.61	*	15.56	**
CCR5	10.68	*	5.97	**
CD14			61.12	**
CD40	6.21	*	2.55	*
CD86	3.51	*	2.51	**
CSF2			19.34	*
CXCL10			310.55	**
Ddx58			2.36	*
ICAM1	7.91	*	5.13	*
IFN- α 2			2.50	*
IFN- β 1	96.15	***		
IFN-γ	17.2	**	12.25	***
IL-10			17.09	*
IL-1α	29.81	**	16.64	***
IL-1β	88.28	*	52.60	**
IL-1r1	2.1	*		
IL-2			4.95	**
IL-23 α	40.9	**		
IL-6			312.35	**
IRF7	4.01	*	3.80	*
ITGAM	3.73	**		
JAK2	3.29	**	4.41	*
Mx1	152.64	*		
Myd88	12.3	*	5.22	*
NF- κ B α			20.34	*
NLRP3	36.61	***		
Nod2	9	**		
SLC11α1	4.26	*	5.25	*
TBX21	2.4	**		
TLR3	4.8	**		
TLR6			3.84	**
TLR7			4.80	**
TNF	119.21	**	50.78	*
IL-1r1	2.1	*		

^a Data for genes upregulated significantly after infection with both ear and blood isolates are highlighted in bold type. Statistical significance is indicated as follows: *, $P < 0.05$; **, $P < 0.01$; ***, $P < 0.001$ (Student's *t*-test, two-tailed).

Since the nasopharynx is the first host environment to which the bacteria are exposed during infection, we examined whether the blood isolate (ST15/4495) and the ear isolate (ST15/9-47) also elicited differential levels of induction of innate immune response genes in this niche at 6 h postinfection. However, we found no significant differences between sham-infected mice and those challenged with either strain in expression of any of the 84 genes analyzed (data not shown).

Cellular and histopathological responses to lung infection. We also examined blood, BAL fluid, and lung tissue for cellular recruitment and histopathological changes. At 6 h postinfection, there were very few cells in the BAL fluid and there were no significant differences between sham-infected mice and those infected with either ST15/9-47 or ST15/4495 in the numbers of BAL fluid neutrophils (Ly-6G-positive cells) or monocyte/macrophages (F4/80-positive cells), as determined by flow cytometry (result not shown). However, a similar FACS analysis of blood leukocytes showed numbers of neutrophils (Fig. 3A), but not monocyte/macrophages (Fig. 3B), in ST15/4495-infected mice that were significantly higher than those seen with either sham-infected or ST15/9-47-infected mice at 6 h ($P < 0.05$ in both cases). A similar increase in the blood neutrophil count in ST15/4495-infected mice relative to either sham-infected or ST15/9-47-infected mice at 6 h was also evident from differential cell counts of blood films ($P < 0.05$ and $P < 0.01$, respectively) (Fig. 3C).

Examination of HE-stained lung sections at 6 h revealed early signs of tissue damage, including congested capillaries, thickened alveolar walls, swollen cuboidal epithelial cells of the bronchioles, and the presence of secretions in the alveolar and bronchiolar spaces, most notably in ST15/4495-infected mice (Fig. 4A). These features were used to develop an 8-point system for scoring histopathological changes (Fig. 4B). The mean aggregate score (\pm SE) for ST15/4495-infected mice (2.8 ± 1.3) was higher than that for either the ST15/9-47-infected mice (1.4 ± 0.57) or the sham-infected mice (0.5 ± 0.33), but this trend did not reach statistical significance.

Finally, we examined lung sections for cellular infiltration by immunofluorescence microscopy after staining with anti-Ly-6G (Fig. 5) or anti-F4/80 (not shown). This revealed patchy neutrophil infiltration in 2/5 mice infected with the ST15/4495 blood isolate and 1/5 mice infected with the ST15/9-47 ear isolate, compared with 0/5 for the control mice. No differences between groups in staining for the monocyte/macrophage marker were seen.

TABLE 4 Genes differentially induced by infection with ST15/9-47 versus ST15/4495^a

Gene product	ST15/4495 vs sham infected		ST15/9-47 vs sham infected		ST15/9-47 vs ST15/4495	
	Fold gene expression change	Significance	Fold gene expression change	Significance	Fold gene expression change	Significance
APCS	-1.10	ns	5.15	**	5.67	**
IL-2	-1.09	ns	4.95	**	5.40	*
CCL12	36.61	*	15.56	**	-2.35	*
CD40	6.21	*	2.55	*	-2.43	*
IFN- β 1	96.15	***	17.84	ns	-5.39	***
IL-6	1,842.35	$P = 0.06$	312.35	**	-5.90	*
TNF	119.21	**	50.78	*	-2.35	*
TBX21	2.4	**	1.02	ns	-2.36	****

^a Statistical significance is indicated as follows: ns, not significant; *, $P < 0.05$; **, $P < 0.01$; ***, $P < 0.001$; ****, $P < 0.0001$ (Student's *t*-test, two-tailed).

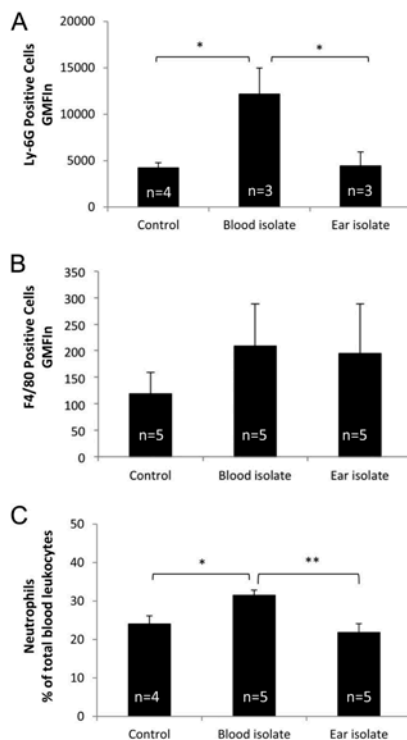


FIG 3 Peripheral blood leukocyte counts. (A and B) Leukocytes isolated from peripheral blood collected at 6 h from control (sham-infected) mice or from those infected with the blood isolate (ST15/4495) or the ear isolate (ST15/9-47) were examined by FACS analysis after staining with anti-Ly-6G (A) or anti-F4/80 (B), as described in Materials and Methods. Data are presented as the product of geometric mean fluorescence intensity and the total number of positive cells (GMFln) for the respective marker (\pm SE). (C) Alternatively, blood films were subjected to differential cell counts, and neutrophil numbers are expressed as a percentage of total leukocyte levels (mean \pm SE). Statistical significance is indicated as follows: *, $P < 0.05$; **, $P < 0.01$ (Student's paired, two-tailed t test).

DISCUSSION

S. pneumoniae is a genetically diverse pathogen, and individual isolates vary markedly in their capacity to progress from asymptomatic nasopharyngeal carriage to causing either localized or systemic disease. The plethora of capsular serotypes and clonal lineages (MLST types) no doubt contribute to their adaptability in different host microenvironments, but they have also complicated previous attempts to unequivocally associate particular serotypes or clonal groups with specific virulence attributes (6, 7). However, we have previously described multiple examples of serotype 3 strains belonging to the same ST that consistently and reproducibly exhibit distinct virulence phenotypes in mice that directly correlate with the original site of isolation from human patients (i.e., ear versus blood) (8). This suggested that, at least in serotype

3, pneumococci exhibit stable niche adaptation within a clonal lineage.

In the present study, we investigated blood and ear isolates belonging to serotype 14, a common cause of OM as well as of invasive disease worldwide (11). This serotype also exhibits high rates of antimicrobial resistance (20). ST15 was one of the dominant STs in our collection and was represented among clinical isolates from cases of sepsis and OM. ST15 blood and ear isolates were able to colonize the murine nasopharynx to roughly similar extents. However, the blood isolate (ST15/4495) was significantly better at colonization and persistence in the lung, while the ear isolate (ST15/9-47) was significantly better able to penetrate and persist in the brain and ears. Similar preferential tropism results for the brain and ear were observed for the other ST15 ear isolate (ST15/51742), while the two other ST15 blood isolates (ST15/4534 and ST15/4559) colonized the lungs in a proportion of infected mice. Significantly, neither of the ear isolates was detected in the lungs of any of the mice at either 24 or 72 h, while none of the three blood isolates were ever detected in the brain. Furthermore, none of the ST15 blood or ear isolates were detected in the blood at any time during the experiment. This is consistent with the long-known fact that mice exhibit a high degree of innate resistance to sepsis after challenge with serotype 14 *S. pneumoniae* strains. However, these findings also suggest that the very high rate of meningitis that occurs after intranasal challenge with either of the ST15 ear isolates was not a consequence of hematogenous spread. Likely alternative routes for pneumococci from the nasopharynx to the brain include direct invasion by retrograde axonal transport along olfactory neurons into the central nervous system (CNS) (21). Collectively, the findings reported above provide robust evidence for the existence of distinct pathogenic profiles for serotype 14 *S. pneumoniae* strains belonging to the same ST (in this case, ST15). In a previous study (22), modest differences in bacterial loads in the blood of mice 6 h after intraperitoneal challenge with three serotype 14 blood isolates belonging to ST124 were detected, although the bacteremia was transient and subclinical. However, in the present study, we not only observed highly significant differences in virulence and pathogenic profiles between isolates belonging to the same serotype and clonal lineage but also found a close correlation between pathogenic profiles in mice and the original sites of isolation from human cases of pneumococcal disease. This extends an observation that we have previously reported for serotype 3 strains belonging to ST180, ST232, and ST233 (8). Thus, stable niche adaptation within a clonal lineage appears to be a general phenomenon.

Notwithstanding the conclusions presented above, the *in vivo* competition experiments in the present study yielded some unexpected findings. First, although the ear and blood isolates were able to colonize the nasopharynx to similar levels when administered individually, the ST15/9-47 ear isolate massively outcompeted the ST15/4495 blood isolate in this niche in the coinfection model. The reason for this is not clear. Neither strain predominated when the two were cocultured *in vitro*, and the two strains express the same bacteriocin genes (data not presented). Nevertheless, this finding accounts for the dominance of ST15/9-47 in the brain and ear in the coinfection model, since these host niches are presumably accessed via the nasopharynx, where the ear isolate already enjoyed a 10^5 -fold numeric advantage. On the other hand, the data from the individual challenge experiments might lead one to predict that the ST15/4495 blood isolate would enjoy a

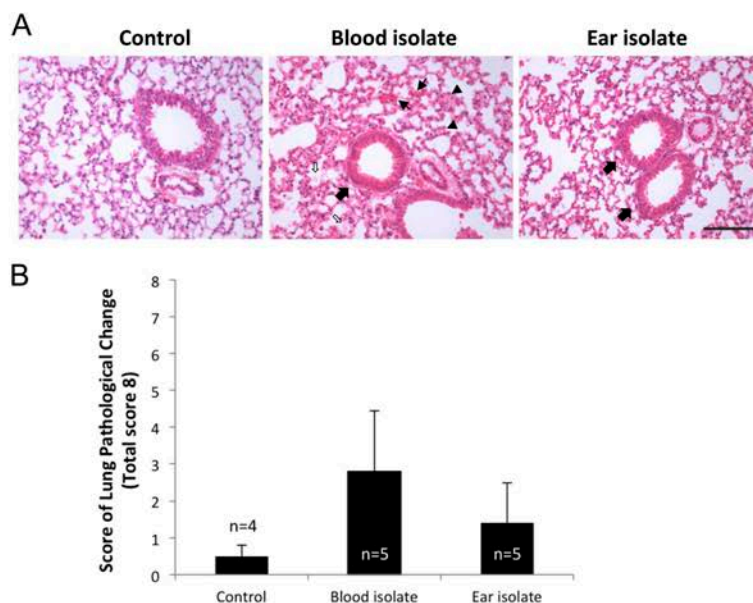


FIG 4 Lung histopathology. HE-stained lung sections from control (sham-infected) mice or from those infected with the blood isolate (ST15/4495) or the ear isolate (ST15/9-47) at 6 h were examined by light microscopy. (A) Representative sections from each group are shown. Bar, 0.1 mm. Slides were also scored (blind) according to the following 8-point scheme: congested capillaries (fine arrows) were scored 0 to 2; thickened alveolar wall (arrowheads) were scored 0 to 2; swollen cuboidal epithelial cells of the bronchioles (thick arrows) were scored 0 to 2; and secretions in the alveolar and bronchiole space (open arrows) were scored 0 to 2. (B) Data were examined with Student's unpaired two-tailed *t* test and are presented as mean \pm SE for each group.

competitive advantage in the lungs, but this was not the case, with neither strain predominating. Similar numbers of ear and blood isolates were delivered into the lungs during challenge under general anesthesia, and bacterial loads in lung tissue at 6 h postchallenge were similar. However, in the individual challenge studies, ST15/9-47 was completely cleared from the lungs of all mice by 24 h, while ST15/4495 was able to persist. There are two possible explanations for this. ST15/4495 may secrete a (yet to be identified) virulence factor that can act *in trans* and support survival of ST15/9-47 in the mixed-infection model. Alternatively, differences in host innate immune responses elicited by the blood and

ear isolates could account for the distinct pathogenic profiles. Clearly, responses triggered by ST15/4495 enable this strain to persist in the lung environment. However, this may create a host microenvironment that also enables persistence of coadministered strains such as ST15/9-47 which would otherwise have been cleared.

To establish if the host immune response could play a role in the distinct pathogenic profiles of the ST15 blood or ear isolates, we examined the transcriptional responses of 84 genes representing the major pathways involved in the innate and adaptive immune response to microbial pathogens. Unsurprisingly, infection

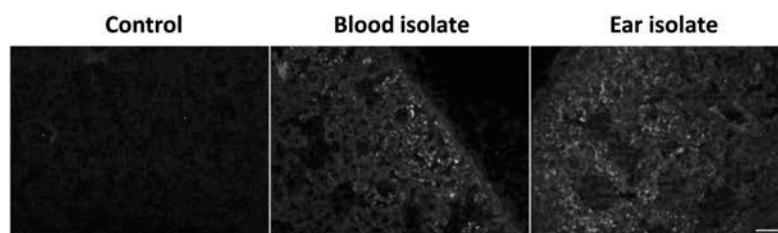


FIG 5 Neutrophil infiltration. Lung tissue from infected or control mice was fixed, sectioned, and labeled with rat anti-mouse Ly-6G or F4/80, followed by Alexa-488-conjugated anti-rat IgG and examined by fluorescence microscopy. Bar, 50 μ m.

with either strain induced a variety of proinflammatory genes. However, the strain-specific differences observed provide us with important clues as to how the immune response may vary, yielding very different patterns of infection from two clonally related strains. Six of the eight genes that were differentially expressed in response to infection with ST15/4495 relative to ST15/9-47 are upregulated in response to both strains relative to sham-infected lungs but are induced more strongly in response to ST15/4495. This suggests that while both strains induce a broadly similar response, one of the features distinguishing the two is the strength of the responses induced at similar bacterial loads. Those responses included increased expression of genes encoding CCL12, IL-6, TNF- α , IL-1 β , and CD40, which points to an overall stronger macrophage response to the blood isolate than to the ear isolate (23–29). BAL fluid collected at 6 h postinfection contained very few cells, and there were no significant differences between sham-infected mice and those infected with either of the isolates in this regard. However, mice infected with the ST15/4495 blood isolate exhibited significant neutropenia relative to sham-infected or ST15/9-47-infected mice at this early time point. Results of a histopathological examination were also suggestive of increased lung damage in mice infected with ST15/4495.

The findings presented above have parallels with those from a previous study in which we compared host transcriptional responses to highly invasive and noninvasive *S. pneumoniae* strains belonging to serotype 1 in a similar intranasal challenge model. We showed that a total of 29 genes of the 84 on the array showed significant upregulation; of those, 22 were also upregulated in the present study. The two type 1 strains were present in roughly equal numbers in the lung at 6 h, but the invasive strain triggered a much stronger type 1 interferon response, which facilitated invasion of the pleural cavity followed by the blood (18).

In the present study, we identified two genes (encoding APCS and IL-2) that were significantly upregulated only in the mice challenged with the ST15/9-47 ear isolate compared to the sham-infected mice; infection with the blood isolate had a negligible effect on their expression. Therefore, it is tempting to speculate that expression of the genes encoding APCS and IL-2 might contribute to the clearance of the ear isolate from the lungs. In particular, serum amyloid P, the protein encoded by the APCS gene, is known to play a role in complement deposition on the pneumococcus, improving phagocyte efficiency and aiding clearance of the pathogen (30).

In this study, we have provided further evidence that *S. pneumoniae* strains belonging to the same serotype and ST can elicit distinct host innate immune responses and cause different types of disease. Future comparative genomic and transcriptomic analyses of these ST-matched strain pairs with distinct virulence phenotypes should enable identification of specific bacterial determinants of tissue tropism. This knowledge may, in turn, provide opportunities to develop improved vaccine formulations capable of eliciting protection against the full spectrum of pneumococcal disease.

ACKNOWLEDGMENTS

This work was supported by Program Grants 565526 and 1071659 from the National Health and Medical Research Council of Australia (NHMRC). A.W.P. is an Australian Research Council (ARC) DORA Fellow; J.C.P. is a NHMRC Senior Principal Research Fellow; C.T. is an ARC DECRA Fellow.

We thank Layla Mahdi for assistance with animal experiments.

REFERENCES

- O'Brien KL, Wolfson LJ, Watt JP, Henkle E, Deloria-Knoll M, McCall N, Lee E, Mulholland K, Levine OS, Cheria T, Hib and Pneumococcal Global Burden of Disease Study Team. 2009. Burden of disease caused by *Streptococcus pneumoniae* in children younger than 5 years: global estimates. *Lancet* 374:893–902. [http://dx.doi.org/10.1016/S0140-6736\(09\)61204-6](http://dx.doi.org/10.1016/S0140-6736(09)61204-6).
- Crook DW, Brueggemann AB, Sleeman KL, Peto TEA. 2004. Pneumococcal carriage, p 136–147. In Tuomanen EI, Mitchell TJ, Morrison DA (ed), *The pneumococcus*. ASM Press, Washington, DC.
- Enright MC, Spratt BG. 1998. A multilocus sequence typing scheme for *Streptococcus pneumoniae*: identification of clones associated with serious invasive disease. *Microbiology* 144:3049–3060. <http://dx.doi.org/10.1099/00221287-144-11-3049>.
- Kelly T, Dillard JP, Yother J. 1994. Effect of genetic switching of capsular type on virulence of *Streptococcus pneumoniae*. *Infect Immun* 62:1813–1819.
- McAllister LJ, Ogunniyi AD, Stroehrer UH, Leach AJ, Paton JC. 2011. Contribution of serotype and genetic background to virulence of serotype 3 and serogroup 11 pneumococcal isolates. *Infect Immun* 79:4839–4849. <http://dx.doi.org/10.1128/IAI.05663-11>.
- Sjöström K, Spindler C, Ortvist A, Kalin M, Sandgren A, Kühmann-Berenzon S, Henriques-Normark B. 2006. Clonal and capsular types decide whether pneumococci will act as a primary or opportunistic pathogen. *Clin Infect Dis* 42:451–459. <http://dx.doi.org/10.1086/499242>.
- Sandgren A, Sjöström K, Olsson-Liljequist B, Christensson B, Samuelsson A, Kronvall G, Henriques Normark B. 2004. Effect of clonal and serotype-specific properties on the invasive capacity of *Streptococcus pneumoniae*. *J Infect Dis* 189:785–796. <http://dx.doi.org/10.1086/381686>.
- Trappetti C, van der Maten E, Amin Z, Potter AJ, Chen AY, van Mourik PM, Lawrence AJ, Paton AW, Paton JC. 2013. Site of isolation determines biofilm formation and virulence phenotypes of *Streptococcus pneumoniae* serotype 3 clinical isolates. *Infect Immun* 81:505–513. <http://dx.doi.org/10.1128/IAI.01033-12>.
- Sleeman KL, Griffiths D, Shackley F, Diggle L, Gupta S, Maiden MC, Moxon ER, Crook DW, Peto TE. 2006. Capsular serotype-specific attack rates and duration of carriage of *Streptococcus pneumoniae* in a population of children. *J Infect Dis* 194:682–688. <http://dx.doi.org/10.1086/505710>.
- Kronenberg A, Zucs P, Droz S, Mühleemann K. 2006. Distribution and invasiveness of *Streptococcus pneumoniae* serotypes in Switzerland, a country with low antibiotic selection pressure, from 2001 to 2004. *J Clin Microbiol* 44:2032–2038. <http://dx.doi.org/10.1128/JCM.00275-06>.
- Brueggemann AB, Griffiths DT, Meats E, Peto T, Crook DW, Spratt BG. 2003. Clonal relationships between invasive and carriage *Streptococcus pneumoniae* and serotype- and clone-specific differences in invasive disease potential. *J Infect Dis* 187:1424–1432. <http://dx.doi.org/10.1086/374624>.
- Burgos J, Falcó V, Borrego A, Sordé R, Larrosa MN, Martínez X, Planes AM, Sánchez A, Palomar M, Rello J, Pahissa A. 2013. Impact of the emergence of non-vaccine pneumococcal serotypes on the clinical presentation and outcome of adults with invasive pneumococcal pneumonia. *Clin Microbiol Infect* 19:385–391. <http://dx.doi.org/10.1111/j.1469-0691.2012.03895.x>.
- Bewick T, Sheppard C, Greenwood S, Slack M, Trotter C, George R, Lim WS. 2012. Serotype prevalence in adults hospitalised with pneumococcal non-invasive community-acquired pneumonia. *Thorax* 67:540–545. <http://dx.doi.org/10.1136/thoraxjnl-2011-201092>.
- Gentile A, Bardach A, Ciapponi A, Garcia-Marti S, Aruj P, Glujovsky D, Calcagno JI, Mazzoni A, Colindres RE. 2012. Epidemiology of community-acquired pneumonia in children of Latin America and the Caribbean: a systematic review and meta-analysis. *Int J Infect Dis* 16:e5–e15. <http://dx.doi.org/10.1016/j.ijid.2011.09.013>.
- Spratt BG. 1999. Multilocus sequence typing: molecular typing of bacterial pathogens in an era of rapid DNA sequencing and the internet. *Curr Opin Microbiol* 2:312–316. [http://dx.doi.org/10.1016/S1369-5274\(99\)80054-X](http://dx.doi.org/10.1016/S1369-5274(99)80054-X).
- Trappetti C, Ogunniyi AD, Oggioni MR, Paton JC. 2011. Extracellular matrix formation enhances the ability of *Streptococcus pneumoniae* to cause invasive disease. *PLoS One* 6:e19844. <http://dx.doi.org/10.1371/journal.pone.0019844>.
- Harvey RM, Stroehrer UH, Ogunniyi AD, Smith-Vaughan HC, Leach AJ, Paton JC. 2011. A variable region within the genome of *Streptococcus*

- pneumoniae* contributes to strain-strain variation in virulence. *PLoS One* 6:e19650. <http://dx.doi.org/10.1371/journal.pone.0019650>.
18. Hughes CE, Harvey RM, Plumpré CD, Paton JC. 2014. Development of primary invasive pneumococcal disease caused by serotype 1 pneumococci is driven by early increased type I interferon response in the lung. *Infect Immun* 82:3919–3926. <http://dx.doi.org/10.1128/IAI.02067-14>.
 19. Macrina FL, Tobian JA, Jones KR, Evans RP, Clewell DB. 1982. A cloning vector able to replicate in *Escherichia coli* and *Streptococcus sanguis*. *Gene* 19:345–353. [http://dx.doi.org/10.1016/0378-1119\(82\)90025-7](http://dx.doi.org/10.1016/0378-1119(82)90025-7).
 20. Hall-Stoodley L, Nistico L, Sambanthamoorthy K, Dice B, Nguyen D, Mershon WJ, Johnson C, Hu FZ, Stoodley P, Ehrlich GD, Post JC. 2008. Characterization of biofilm matrix, degradation by DNase treatment and evidence of capsule downregulation in *Streptococcus pneumoniae* clinical isolates. *BMC Microbiol* 8:173. <http://dx.doi.org/10.1186/1471-2180-8-173>.
 21. van Ginkel FW, McGhee JR, Watt JM, Campos-Torres A, Parish LA, Briles DE. 2003. Pneumococcal carriage results in ganglioside-mediated olfactory tissue infection. *Proc Natl Acad Sci U S A* 100:14363–14367.
 22. Silva NA, McCluskey J, Jefferies JM, Hinds J, Smith A, Clarke SC, Mitchell TJ, Paterson GK. 2006. Genomic diversity between strains of the same serotype and multilocus sequence type among pneumococcal clinical isolates. *Infect Immun* 74:3513–3518. <http://dx.doi.org/10.1128/IAI.00079-06>.
 23. Mosser DM. 2003. The many faces of macrophage activation. *J Leukoc Biol* 73:209–212. <http://dx.doi.org/10.1189/jlb.0602325>.
 24. van der Poll T, Keogh CV, Guirao X, Buurman WA, Kopf M, Lowry SF. 1997. Interleukin-6 gene-deficient mice show impaired defense against pneumococcal pneumonia. *J Infect Dis* 176:439–444.
 25. Mackay F, Loetscher H, Stueber D, Gehr G, Lesslauer W. 1993. Tumor necrosis factor alpha (TNF-alpha)-induced cell adhesion to human endothelial cells is under dominant control of one TNF receptor type, TNF-R55. *J Exp Med* 177:1277–1286. <http://dx.doi.org/10.1084/jem.177.5.1277>.
 26. Collins T, Read MA, Neish AS, Whitley MZ, Thanos D, Maniatis T. 1995. Transcriptional regulation of endothelial cell adhesion molecules: NF-kappa B and cytokine-inducible enhancers. *FASEB J* 9:899–909.
 27. Lee PY, Li Y, Kumagai Y, Xu Y, Weinstein JS, Kellner ES, Nacionales DC, Butfiloski EJ, van Rooijen N, Akira S, Sobel ES, Satoh M, Reeves WH. 2009. Type I interferon modulates monocyte recruitment and maturation in chronic inflammation. *Am J Pathol* 175:2023–2033. <http://dx.doi.org/10.2353/ajpath.2009.090328>.
 28. Alderson MR, Armitage RJ, Tough TW, Strockbine L, Fanslow WC, Spriggs MK. 1993. CD40 expression by human monocytes: regulation by cytokines and activation of monocytes by the ligand for CD40. *J Exp Med* 178:669–674. <http://dx.doi.org/10.1084/jem.178.2.669>.
 29. Portillo JA, Feliciano LM, Okenka G, Heinzl F, Subauste MC, Subauste CS. 2012. CD40 and tumour necrosis factor-alpha co-operate to up-regulate inducible nitric oxide synthase expression in macrophages. *Immunology* 135:140–150. <http://dx.doi.org/10.1111/j.1365-2567.2011.03519.x>.
 30. Yuste J, Botto M, Bottoms SE, Brown JS. 2007. Serum amyloid P aids complement-mediated immunity to *Streptococcus pneumoniae*. *PLoS Pathog* 3:1208–1219.

APPENDIX C

Significantly differentiated genes identified by DESeq analysis of ST15/947 ear isolate against blood isolates ST15/4559 and ST15/4534.

Blood Isolate	Gene Name	Gene ID	log2FoldChange	pval	padj
ST15/4559	<i>spxB</i>	SPCG_0679	-3.39	1.08E-46	2.35E-43
	<i>nanA</i>	SPCG_1665	1.26	1.12E-06	7.14E-05
ST15/4534	<i>spxB</i>	SPCG_0679	-3.66	4.05E-35	1.46E-32
	<i>nanA</i>	SPCG_1665	1.26	7.12E-05	0.0016

APPENDIX D

67 significantly differentiated genes identified by DESeq analysis of ST 232/11 ear isolate against blood isolate ST180/15.

	Gene ID	baseMean	foldChange	log2Fold Change	pval	padj
1	18	6228.650114	0.0000854	-13.51534761	3.03E-23	5.69E-20
2	19	3641.708552	0.00014608	-12.74095601	2.22E-16	1.39E-13
3	20	1723.592906	0.000308696	-11.66152506	2.89E-09	0.000000905
4	21	1299.580926	0	NA	6.54E-08	0.0000112
5	27	1256.8718	0.000423374	-11.20577811	0.000000375	0.0000504
6	42	1178.379932	0.000451588	-11.11270469	0.000000886	0.0000925
7	44	791.9688466	0	NA	0.0000269	0.001684408
8	46	783.0386341	0	NA	0.0000301	0.001765716
9	54	1064.105323	0	NA	0.000000987	0.0000976
10	56	1436.069843	0.001112398	-9.812110735	0.00000026	0.0000407
11	125	6665.375848	5.686144864	2.507450855	0.001107587	0.034117299
12	150	13983.98134	0.245080505	-2.028672364	0.001624346	0.045554426
13	169	58105.26845	7.170871695	2.842148504	0.000000675	0.0000746
14	207	6154.970899	0.15929277	-2.650247312	0.000792862	0.027087033
15	279	44051.12444	5.573863105	2.47867757	0.0000155	0.001076942
16	362	45510.01627	11.28463811	3.496288248	4.83E-09	0.00000113
17	421	8392.212622	0.15598515	-2.68051941	0.000245293	0.009686162
18	426	670.9535251	0.00318111	-8.296253935	0.001074907	0.033662492
19	427	500.5619119	0	NA	0.001149558	0.034839011
20	428	906.8372489	0.001762741	-9.147963476	0.0000609	0.003177756
21	430	932.1559618	0.001142534	-9.773547154	0.0000281	0.001702636
22	436	5615.285517	0.0000947	-13.365774	7.98E-22	7.49E-19
23	448	2145.006433	0.063559746	-3.975742838	0.000922387	0.030915679
24	477	1818.438305	0.013338292	-6.22828228	0.0000134	0.000969648
25	518	6340.299349	6.621286774	2.727111616	0.000520374	0.019172213
26	561	5501.730843	6.225636876	2.638221431	0.00120449	0.035924402
27	662	652.8455359	0	NA	0.000156945	0.006702249
28	688	12228.81068	4.374535624	2.129129877	0.001289841	0.03672138
29	730	968.6930521	0	NA	0.00000308	0.000262891
30	731	1705.732481	0.000311929	-11.64649273	3.46E-09	0.000000928
31	732	680.5761958	0	NA	0.000109961	0.00480505
32	873	894.9012961	0	NA	0.00000754	0.000589969
33	874	617.594697	0	NA	0.000247438	0.009686162
34	875	555.1451005	0.000959051	-10.02610513	0.001245053	0.036553977
35	886	541.452885	0	NA	0.00066926	0.024183444
36	895	7695.491882	5.433397777	2.44185467	0.000956964	0.031002339
37	913	4369.160419	7.599319868	2.925870304	0.000937836	0.030915679

38	952	11337.73164	0.152906334	-2.709279925	0.0000786	0.003989468
39	953	16969.1098	0.118070972	-3.082273775	0.00000214	0.000191102
40	954	9726.296282	0.123012696	-3.023120875	0.000025	0.00162191
41	955	8945.271328	0.131310662	-2.928944031	0.000057	0.003061955
42	956	9293.287758	0.141664192	-2.819452958	0.0000866	0.004284108
43	975	7434.85257	0.112722201	-3.149156405	0.0000408	0.002324363
44	976	5793.438074	0.151010426	-2.727279936	0.000712814	0.0248051
45	1048	4291.785365	0.113430182	-3.140123527	0.000468413	0.017602944
46	1068	2207.828209	0.000723272	-10.43317361	1.95E-10	7.32E-08
47	1163	17347.32352	4.962571993	2.311088032	0.000235023	0.009600162
48	1164	13724.28108	4.590638169	2.198694724	0.000712866	0.0248051
49	1379	5585.036336	0.062859861	-3.991717098	0.00000355	0.000290111
50	1380	3682.609516	0.073161613	-3.772769304	0.000102902	0.004603632
51	1459	13555.36806	7.917910418	2.985119745	0.00000876	0.000658529
52	1460	19093.50874	8.172165258	3.030718379	0.00000203	0.000190561
53	1461	8500.687096	9.053439622	3.178466011	0.0000194	0.001303794
54	1462	8135.227103	6.733950818	2.751453184	0.00019446	0.008119777
55	1463	14125.02924	11.04510562	3.46533531	0.000000359	0.0000504
56	1464	5894.369888	10.19724472	3.350107485	0.0000473	0.002612199
57	1465	11716.58411	11.43307188	3.515141179	0.000000635	0.0000746
58	1636	290759.1824	4.189083986	2.066634809	0.0000981	0.004494175
59	1663	229336.2727	4.245064977	2.085786636	0.0000899	0.004331528
60	1677	18528.09069	11.72861848	3.551961183	6.01E-08	0.0000112
61	1739	6003.419977	0.111366051	-3.166618586	0.0000976	0.004494175
62	1784	24034.28075	0.23432342	-2.093426941	0.000458937	0.017598829
63	1795	12835.97118	4.324610465	2.112570189	0.001266048	0.036598538
64	1799	37594.80616	22.49795704	4.491722096	1.45E-12	6.83E-10
65	1818	2996.276481	0.017705082	-5.819692642	0.000000439	0.0000549
66	1819	4767.765706	0.022471621	-5.475752	1.59E-08	0.00000332
67	1820	2820.632316	0.090929384	-3.459109617	0.001025532	0.032660584

APPENDIX E

7 significantly differentiated genes identified by DESeq analysis of ST232/11 ear isolate against blood isolate ST232/1.

	Gene ID	baseMean	foldChange	log2FoldChange	pval	padj
1	1458(15930)	12014.663	72.168	6.173	5.68E-05	0.015
2	1459(15940)	16929.487	93.576	6.548	2.64E-05	0.009
3	1460(15950)	7620.592	90.750	6.504	3.02E-05	0.009
4	1461(15960)	7050.898	91.319	6.513	2.98E-05	0.009
5	1462(15970)	12879.388	101.202	6.661	2.13E-05	0.009
6	1463(15980)	5327.498	125.826	6.975	1.23E-05	0.009
7	1464(15990)	10663.586	193.256	7.594	3.30E-06	0.006

CONFERENCES ATTENDED

1. 6TH ASM CONFERENCE ON BIOFILMS, Sept 29-Oct 4 2012, Miami Florida USA

POSTER ABSTRACTS

cal isolates using real-time reverse-transcription PCR (qRT-PCR) shows *luxS* expression and biofilm forming phenotype are directly proportional. Clearly, an association between biofilm formation, *luxS* expression and tropism for the middle ear exists *in vivo*.

■ 209B

SITE OF ISOLATION AND ENVIRONMENTAL CONDITIONS AFFECT BIOFILM DEVELOPMENT IN *STREPTOCOCCUS PNEUMONIAE*

C. Trappetti¹, Z. Amin¹, A. J. Potter¹, A. J. Lawrence², A. W. Paton¹, J. C. Paton¹;

¹University of Adelaide, Adelaide, AUSTRALIA, ²Women's and Children's Hospital, Adelaide, AUSTRALIA.

Otitis media (OM) is a significant human health concern, accounting for more antibiotic prescriptions than any other infection. The most common organism responsible for causing OM in children and adults is *Streptococcus pneumoniae*, which also causes invasive diseases (meningitis, pneumonia and sepsis) that kill over 1 million children each year. The presence of pneumococcal biofilms has been demonstrated on the middle ear mucosa of children with chronic OM, indicating a role for biofilm formation in the disease process. Under physiological conditions the middle ear cavity has a pH of 6.6, whereas the pH of blood is 7.4. Thus the bacteria must adapt to these distinct environmental niches. In this study we aimed to compare the biofilm formation capacity of *S. pneumoniae* isolates from OM cases, relative to strains associated with more invasive diseases, under different pH conditions. Since widespread introduction of the seven-valent pneumococcal conjugate vaccine, cases of acute OM caused by *S. pneumoniae* serotype 3 strains have been increasing in young children, a phenomenon known as serotype replacement. Accordingly, we studied 40 *S. pneumoniae* serotype 3 clinical isolates, representing 20 isolates from OM and 20 from blood. We found 100% of the OM isolates

form robust biofilms *in vitro* under environmental conditions that mimic the middle ear cavity (pH 6.6). Under these conditions, none of the type 3 isolates from the blood were able to form biofilms. Conversely, at pH 7.4, all of the blood isolates, but none of the OM isolates formed biofilms.

S. pneumoniae possesses a quorum-sensing regulatory system, mediated by the enzyme LuxS that we have previously shown to be directly involved in regulation of pneumococcal biofilm formation. In the current work we demonstrated a direct correlation between biofilm formation and *luxS* expression levels in 6 selected strains (3 blood isolates and 3 ear isolates) by quantifying *luxS* mRNA levels at pH 6.6 and pH 7.4 using qRT-PCR. Furthermore, we found that the low biofilm formation capacity at the non-permissive pH could be increased to levels similar to that seen at the permissive pH by increasing *luxS* expression through transformation with a plasmid carrying a cloned copy of *luxS* under the control of a constitutive promoter. Conversely, deleting *luxS* in the highest biofilm forming strains abolished biofilm formation even at the optimal pH. We conclude that serotype 3 *S. pneumoniae* strains exhibit distinct pH-dependent biofilm formation phenotypes in accordance with host tissue tropism and *luxS* expression.

■ 210B


MULTIPLE FACTORS MODULATE BIOFILM FORMATION BY THE ANAEROBIC PATHOGEN *CLOSTRIDIUM DIFFICILE*

T. Dapa¹, R. Leuzzi¹, Y. K. Ng², S. T. Boban², S. A. Kuehne², M. Scarselli¹, N. P. Minton², D. Serruto¹, M. Unnikrishnan¹;

¹Novartis Vaccines and Diagnostics, Siena, ITALY, ²Clostridia Research Group, School of Molecular Medical Sciences, Centre for Biomolecular Sciences, University of Nottingham, Nottingham, UNITED KINGDOM.

Clostridium difficile is an obligate anaerobic, Gram-positive, endospore-forming bacterium. Although an opportunistic pathogen, it is

2. 12th European Meeting on the Molecular Biology of the Pneumococcus (EuroPneumo 2015), 7th-10th July 2015, St. Catherine's College, Oxford United Kingdom.



Stable niche adaptation within clonal lineages of *S. pneumoniae*

Zarina Amin, Bart A. Eijkelkamp, Richard M. Harvey, Catherine E. Hughes, Christopher A. McDevitt, Adrienne W. Paton, James C. Paton, Claudia Trappetti

Research Centre for Infectious Diseases, School of Biological Sciences, University of Adelaide, Adelaide, S.A., 5005, Australia

INTRODUCTION

- Individual *S. pneumoniae* strains differ markedly in their virulence phenotypes.
- Genetic heterogeneity has complicated attempts to identify any association between a given clonal lineage and propensity to cause a particular disease type.
- Serotype 3 isolates belonging to the same multi-locus sequence type were previously reported to differ markedly in *in vitro* and *in vivo* phenotype, in accordance with clinical site of isolation.

OBJECTIVES

Investigation of serotype 14 blood and ear isolates of the same ST type for pathogenic phenotype.

RESEARCH FINDINGS

1. Biofilm formation by serotype 14 pneumococci is influenced by ST type.

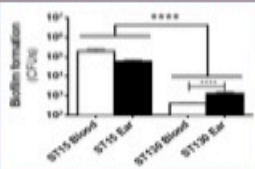


FIG 1. Biofilm formation by serotype 14 *S. pneumoniae* ST15 and ST130 isolates. Three blood and two ear isolates from each ST were assessed for biofilm formation after 18 h growth in C+Y medium at 37°C. Data are log₁₀ CFU per well (± SEM) for quadruplicate assays. Significance of differences between groups was examined using a two-tailed Student's *t*-test. ****, *P* < 0.0001.

ST15 isolates are vastly superior biofilm formers compared to ST130.

2. ST15 clinical isolates exhibit distinct *in vivo* phenotypes in accordance with site of isolation.

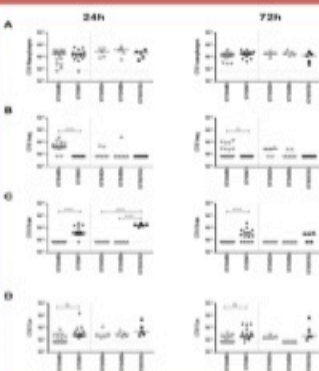


FIG 2. Comparative virulence of ST15 blood and ear isolates. Mice were challenged intranasally with the three blood (ST154495, ST154534 and ST154559) and two ear isolates (ST159-47 and ST1551742) and numbers of pneumococci in A) nasopharynx, B) lungs, C) brain and D) ear at either 24 h or 72 h post challenge were determined. Blood isolates are represented by filled black symbols, ear isolates are represented by hollow grey symbols. Differences in bacterial load between groups were analyzed using a two-tailed Student's *t*-test. **, *P* < 0.01. ****, *P* < 0.0001.

ST15 ear isolates target the brain and ears. ST15 blood isolates target lungs.

3. Ear isolate ST15/9-47 displays significant competitive advantage over blood isolate ST15/4495 in nasopharynx, brain and ear.

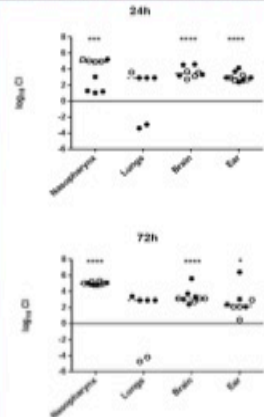


FIG 3 *In vivo* competition between ST15/9-47 (ear isolate) and ST15/4495 (blood isolate). Data shown are pooled from two competition experiments performed with 5 mice per group for each time point (24 h and 72 h post challenge). In one experiment, mice were challenged with equal numbers (10⁷ CFU each) of ST15/4495 and ST15/9-47:pAL3 (hollow symbols). In the other experiment, mice were challenged with equal numbers of ST15/4495:pAL3 and ST15/9-47 (solid symbols). The competitive index (CI) of ear blood has been shown as log₁₀ CI for each tissue of each mouse. The horizontal dotted lines denote the geometric mean CI for each tissue. Statistical differences between the log₁₀-transformed geometric mean CI and a hypothetical value of 0 (ratio of 1:1) in each niche were analyzed using the two-tailed Student's *t*-test. ns, not significant; *, *P* < 0.05; **, *P* < 0.01; ****, *P* < 0.0001.

Ear isolate ST15/9-47 has significant competitive advantage in host nasopharynx, brain and ear tissues. Neither strain has competitive advantage in host lung in competition model.

4. Strain-specific differences observed in host immune response

Ear (ST159-47) V Blood (ST154495) isolate		
Gene symbol	Fold-change	<i>P</i>
<i>Apex</i>	6.67	<0.01
<i>Iti</i>	5.40	<0.01
<i>Ccl12</i>	-3.38	<0.01
<i>Gad6</i>	-2.43	<0.01
<i>Iti1</i>	-5.39	<0.001
<i>Iti</i>	-5.30	<0.01
<i>Tnf</i>	-3.33	<0.01
<i>Tbx21</i>	-2.24	<0.001

FIGURE 3. Differences in induction of immune response genes in lungs of ear (ST15/9-47) and blood (ST15/4495) isolates at 6h post challenge. RNA from lungs infected for 6h with ST15/9-47 or ST15/4495 was investigated using the RT² Profiler[™] PCR Array Mouse Innate & Adaptive Immune Responses (Qiagen).

Out of 84 immune genes tested, significant differences were observed in 8.

CONCLUSION

We have provided further evidence that *S. pneumoniae* strains belonging to the same serotype and ST can elicit distinct host innate immune responses and cause different types of disease. Blood isolate elicits enhanced macrophage response, while upregulated *Apex* may enhance clearance of ear isolate from lungs. In the co-infection model the innate response to blood isolate enhances survival of ear isolate in the lung.